THE EFFECT OF INFLAMMATORY AGENTS

ON THE BLOOD-RETINAL BARRIER

SIMON DAVID BAMFORTH

A thesis submitted for the degree of

Doctor of Philosophy

May 1996

Division of Clinical Science
Department of Clinical Ophthalmology
Institute of Ophthalmology
University College London

ProQuest Number: 10105727

ProQuest 10105727

ACKNOWLEDGEMENTS

2

ABSTRACT

The blood-retinal barrier (BRB), like that of the blood-brain barrier (BBB), forms a selective interface between the blood and the neural parenchyma. During inflammatory diseases of the retina there is a large scale increase in leucocyte infiltration and breakdown of the BRB. It is not entirely clear, however, what the causative factors are in BRB disruption, but recently cytokines have been implicated. An understanding of the role of cytokines within retinal inflammatory diseases, such as posterior uveitis where BRB breakdown leads to macular oedema and impaired vision, may lead to improved therapies and disease control.

Cytokines have been detected within the eyes of patients with uveitis. Also, the injection of cytokines to experimental animals has been shown to cause leucocyte recruitment and an increase in vascular permeability. However, it is not known whether cytokines have a direct effect on increasing vascular permeability, if they induce the release of vasoactive mediators, or if they exert their effects through leucocyte recruitment. It was therefore hypothesised that the injection of a proinflammatory cytokine to the vitreous of the Lewis rat will induce a leucocytic infiltration to the retina and breakdown of the BRB. Inhibitor studies may then identify the mechanism by which BRB dysfunction is occurring.

The effect of the proinflammatory cytokines interleukin-1ß (IL-1ß), tumour necrosis factor-α (TNF-α) and interleukin-6 (IL-6) upon the Lewis rat BRB were investigated. Following an intravitreal injection of cytokine the structural integrity of the retina was evaluated using both light and electron microscopy. The permeability of the BRB was assessed by either introducing the small molecular weight tracer [^{14}C]-mannitol, or the large molecular weight tracer horseradish peroxidase, into the circulation.

Following administration of IL-1ß a biphasic opening of the BRB was found, as determined by increased [^{14}C]-mannitol extravasation. The initial breakdown occurred at 4 hr post injection (PI), corresponding to the appearance of leucocytes within the retinal vessels and adhering to the endothelium. The BRB permeability then decreased although this did not correspond to a reduction in the number of infiltrating leucocytes. A second, larger, and more prolonged increase in barrier permeability was detected at 24 to 48 hr

PI which coincided with peak infiltration of leucocytes. Inhibitor and leucocyte depletion studies indicated that the IL-1ß-induced breakdown of the BRB was mediated by histamine and cyclooxygenase metabolites (prostaglandins and thromboxanes), and associated with leucocyte infiltration to the retina.

Following the intravitreal injection of TNF-α a monophasic and reversible opening of the BRB occurred but without the accompanying large scale cellular infiltrate. Immunohistochemical studies revealed the upregulation of major histocompatibility complex (MHC) class II molecules within the retina of TNF-α injected eyes. It was also demonstrated that there was an opening of the BRB of the non-injected contralateral eye which may be due to a neuronal reflex arc mechanism.

Administration of IL-6 caused a minimal inflammatory cell infiltrate, but did not increase the permeability of the BRB at the dose examined.

The intravitreal injection of the cytokines examined in this study exhibited different effects on the retina and BRB of the Lewis rat. IL-1ß caused a biphasic breakdown of the BRB that appeared to be the consequence of classic inflammatory mediators and dependent on leucocyte infiltration, whereas TNF-α caused a monophasic increase in BRB permeability which appeared to be independent of leucocytic involvement. IL-6 had no effect on barrier integrity. Therefore, it appears that, *in vivo*, proinflammatory cytokines differ in their ability to induce leucocyte recruitment and cause increased vascular permeability. The mechanism by which TNF-α caused BRB breakdown is unknown, but the IL-1ß-induced biphasic breakdown of the BRB is dependent on the presence of leucocytes recruited to the retina and the release of vasoactive mediators such as histamine.

TABLE OF CONTENTS

LIST OF FIGURES

LIST OF TABLES

ABBREVIATIONS

AA	arachidonic acid
Ab	antibody
AEC	3-amino-9-ethylcarbazole
Ag	antigen
APC	antigen presenting cell
APES	3-amino propyl tri-ethoxy silane
BAB	blood-aqueous barrier
BBB	blood-brain barrier
BRB	blood-retinal barrier
BSA	bovine serum albumin
Cox	cyclooxygenase
CNS	central nervous system
CSF	cerebrospinal fluid
DAB	diaminobenzidine
DMSO	dimethyl sulfoxide
EAAU	experimental autoimmune anterior uveitis
EAE	experimental autoimmune encephalomyelitis
EAU	experimental autoimmune uveoretinitis
EC	endothelial cell
ECGS	endothelial cell growth supplement
EIU	endotoxin induced uveitis
EM	electron microscopy
FCS	foetal calf serum
FITC	fluoroscein isothiocyanate
HBSS	Hank's balanced salt solution
H_2O_2	hydrogen peroxide
HRP	horseradish peroxidase
HUVEC	human umbilical vein endothelial cell
ICE	IL-1-converting enzyme

IL	interleukin
IOP	intraocular pressure
IP	intraperitoneally
kDa	kilo-Dalton
LFA-1	lymphocyte-function associated antigen-1
LPS	lipopolysaccharide
LT	leukotriene
MHC	major histocompatibility complex
MIP	macrophage inflammatory protein
MMP	matrix metalloproteinase
MN	mononuclear
mRNA	messenger ribonucleic acid
MS	multiple sclerosis
% O_2	percent oxygen saturation
PAF	platelet-activating factor
pCO_2	partial pressure of carbon dioxide
pO_2	partial pressure of oxygen
PDS	plasma derived serum
PECAM-1	platelet endothelial cell adhesion molecule-1
PI	post injection
PGI_2	prostacyclin
PG	prostaglandin
PMN	polymorphonuclear
PNS	peripheral nervous system
REC	retinal endothelial cell
RANTES	regulated upon activation, normal T cell expressed and secreted
RIA	radio immunoassay
RPE	retinal pigment epithelium
SEM	scanning electron microscope
TEM	transmission electron micrograph
TNF	tumour necrosis factor
Tx	thromboxane

CHAPTER ONE

INTRODUCTION

1.1 STRUCTURES OF THE EYE

The eye (*Fig 1.1*) is a highly specialised organ of photoreception, a process which involves the conversion of different quanta of light energy into nerve action potentials by the retina. The eye consists of three main layers: the outer coat, comprising the cornea and sclera; the middle vascular layer, known as the uvea, which consists of the choroid, ciliary body and iris; and the inner layer which is represented by the retina.
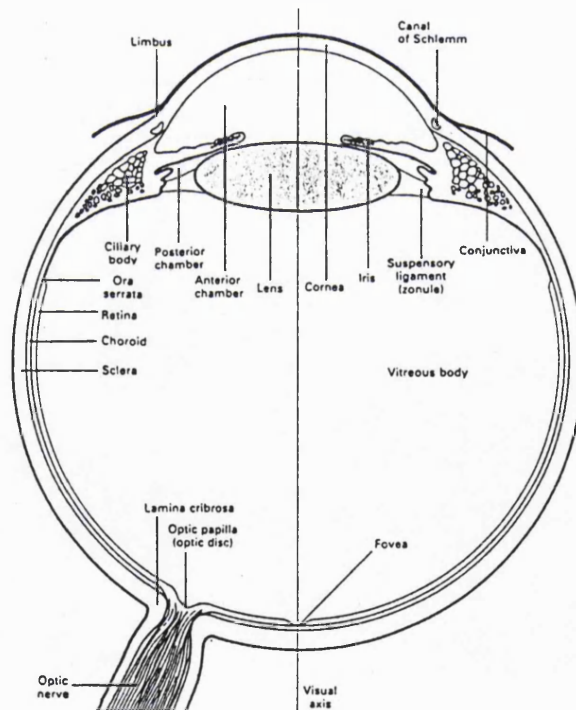
Figure 1.1. *Diagrammatic section of the eye* (From Wheater *et al,.* 1987).

1.1.1 The Retina

The retina in man is a vascularised sheet of tissue situated at the posterior of the eye cup, inside the choroid and posterior to the ora serrata (*Fig. 1.1*). The retina is considered to be an extension of the central nervous system (CNS) as retinal vessels share a common neuroectodermal origin with cerebral vessels. During embryo development, the structure that will form the neural retina derives from the retinal disc, the thickened portion of the optic vesicle. The optic vesicle is formed from an evagination of the optic sulci, which appear as shallow grooves in the inner aspect of the neural folds that develop into the diencephalon region of the forebrain vesicle. The thinner, outermost layer of the optic vesicle forms the retinal pigment epithelium (RPE). The retina remains connected to the brain by the axons of ganglion cells, which form the nerve fibre layer, and travel down the optic nerve. It is the retina that is responsible for the processing of light information to the visual area of the cerebral cortex of the brain for image formation.

At the anterior aspect of the retina (*Fig. 1.2*) is the inner limiting membrane. This is comprised of the basal lamina (basement membrane) of the Müller cells, which are the major glial elements of the retina, and is a continuous glycoprotein coating identical to the basal lamina of epithelia or endothelia. The inner limiting membrane, which separates the base of the Müller cells from the vitreous body, has permeability properties identical to those of endothelial basal laminae, which retain particulate substances but are permeable up to the size of ferritin (400,000 kDa) (Raviola, 1977). The intercellular clefts between the Müller cell processes that border on the inner limiting membrane are open and lack specialised intercellular junctions. If the haemeprotein tracer horseradish peroxidase (HRP) is injected directly into the vitreous of experimental animals it is able to freely diffuse through the inner limiting membrane into the retina (Peyman & Apple, 1972) and penetrate the outer segments of the photoreceptor layer, where its further passage is restricted by the tight junctions of the RPE (Peyman *et al.*, 1971). The external limiting membrane, which separates the rod outer segments from the outer nuclear layer, is composed entirely of zonula adherens types of intercellular junctions which serve to mechanically join adjacent cells together and therefore provides no diffusion barrier to intravitreal peroxidase.

VITREOUS
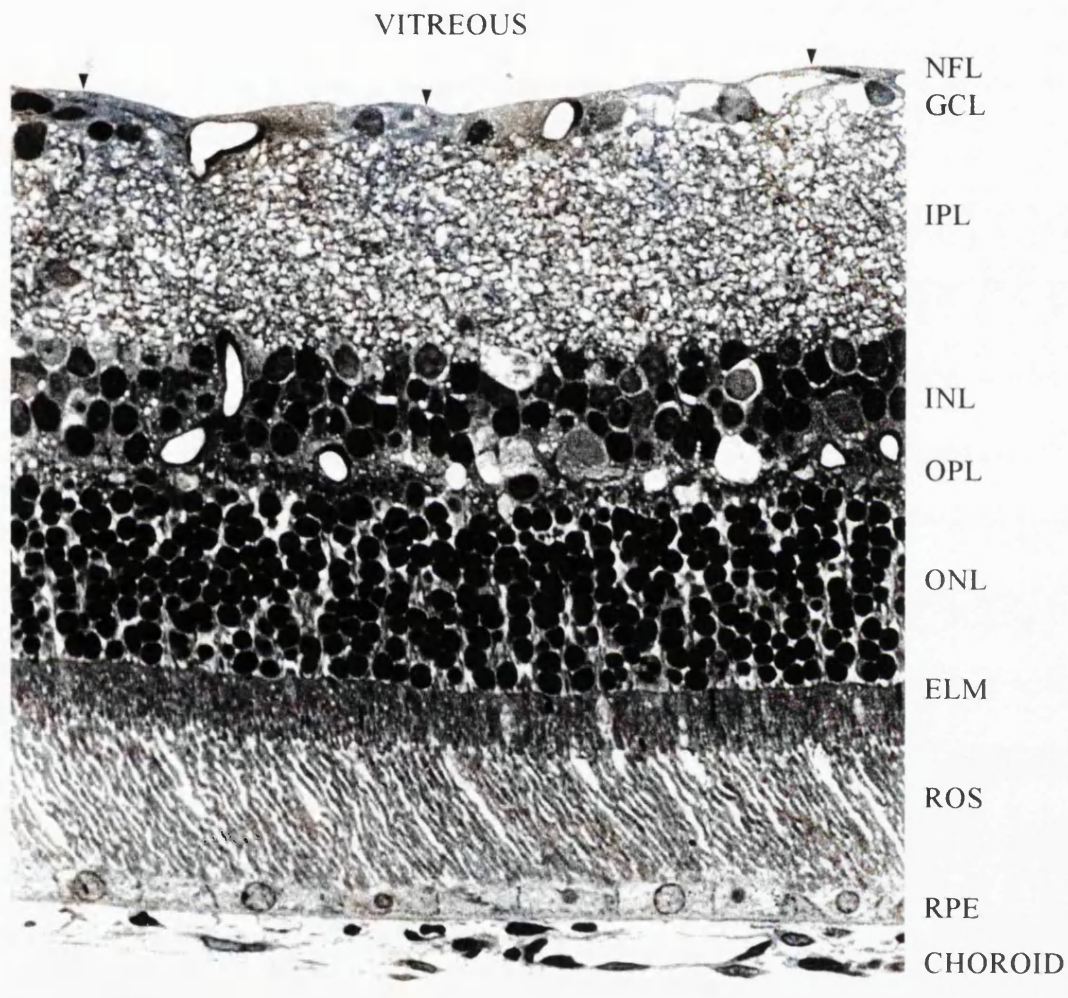
Figure 1.2. *Toluidine blue stained resin section of a normal Lewis rat retina. The inner limiting membrane is situated at the anterior of the retina* (arrow heads); **NFL:** *nerve fibre layer;* **GCL:** *ganglion cell layer;* **IPL:** *inner plexiform layer;* **INL:** *inner nuclear layer;* **OPL:** *outer plexiform layer;* **ONL:** *outer nuclear layer;* **ELM:** *external limiting membrane;* **ROS:** *rod outer segments;* **RPE:** *retinal pigment epithelium.* (Bar = 25μM)

The inner plexiform layer is the region of synapse between the bipolar and ganglion cells and contains the ramifications of the axonal processes of the nerve cells, the horizontal and amacrine cells. The cell bodies of these cells are contained within the inner nuclear layer which is formed by the cell bodies of the bipolar cells. The outer nuclear layer contains the cell bodies and the nuclei of the rods and cones. The outer segments of photoreceptors, below the external limiting membrane and which rest on the RPE, contain the light sensitive pigment, rhodopsin. At the other end is the synaptic body and it is through this that the effects of light on the receptor are transmitted to the bipolar or horizontal cells.

The human rod is $2\mu m$ thick and $60\mu m$ long. The cones vary greatly in size and shape with their position in the retina, becoming long and thin and not easily distinguished from rods in the macula at the most central position.

Blood supply to the inner retina is provided by the central retinal artery which branches from the ophthalmic artery. This artery, along with its accompanying vein, enters the centre of the optic nerve and is subdivided into inferior and superior branches at the optic disc. Further divisions create arterioles which extend capillary networks to the nerve fibre-ganglion cell and inner plexiform layers, the inner vascular plexus, and the inner nuclear and outer plexiform layers of the retina, the outer vascular plexus. The avascular outer retina is provided with nutrients from the blood supply of the choroid.

1.1.2 The Retinal Pigment Epithelium

The RPE, along with the outer nuclear layer, is avascular, and is therefore not in direct contact with the bloodstream, unlike the endothelium of the retinal blood vessels. Nutrients from the choroidal circulation pass through the fenestrated endothelium of the choriocapillaris and Bruch's membrane to reach the base of the RPE. The basal plasmalemma of the RPE cells develop numerous infoldings to facilitate transport function. The RPE cells are joined to each other by zonula occludens, zonula adherens and macula adherens types of cell junctions, which collectively form a junctional complex (Zinn & Benjamin-Henkind, 1979). Physiologically, while the vascular endothelial cells (ECs) are specialised for transport function, the RPE serves as the metabolic warehouse for the retina. It provides support for the photoreceptor cells, and phagocytoses photoreceptor cell outer segments as they are continually shed and renewed, in addition

to its function as the blood-retinal barrier (BRB) for the outer retina.

Both retinal ECs and the RPE are non-mitotic cells under normal conditions, that is, there is no proliferation or replacement of cells in the normal physiologic state. Mitosis is rarely, if ever, seen in the normal retina (Tso, 1980).

1.1.3 Bruch's Membrane

Bruch's membrane is a transparent layer separating the RPE from the choriocapillaris. It is composed of a pair of basement membranes belonging to the choroid and RPE, and separated by a layer of collagen which is itself divided by a thin elastic layer. The main components are collagen and glycosaminoglycans, which consist of proteoglycans (ie. complexes with proteins). Bruch's membrane, like most other vascular basement membranes, acts as a diffusion barrier only to molecules of large molecular size and does not obstruct the passage of tracers such as HRP (Shiose, 1970).

1.1.4 The Choroid

The endothelium of the capillaries of the choroid, the choriocapillaris, display numerous fenestrations, which occur particularly in the region of the vessel wall that border Bruch's membrane, and are permeable to the macromolecules ferritin (Bernstein & Hollenberg, 1965) and HRP (Shiose, 1970). The choriocapillaris plays a major role in providing nutrition to the retina due to its extensive covering of the retina with vessels that possess relatively large lumens, yielding a considerable cross-sectional area with a low velocity of flow (Bernstein & Hollenberg, 1965).

The choroid in man is dark in colouration, due to the pigment melanin, and lines most of the internal surface of the sclera. Any light that is not absorbed by the pigments in the photoreceptor cells is absorbed by the melanin contained within choroidal melanocytes. This restricts internal reflection of light on the choroid layer, which may subsequently activate photoreceptors elsewhere in the retina.

1.1.5 The Ciliary Body

Aqueous humour is secreted into the posterior chamber (the region between the iris and the front of the lens) by the ciliary processes from where it flows through the pupil into the anterior chamber and leaves the eye by bulk flow at the chamber angle by the

trabecular or uveoscleral routes. There are diffusional solute exchanges between aqueous humour and surrounding tissues, the posterior chamber, and the vitreous compartment.

The ciliary epithelium consists of two layers, the non-pigmented and the pigmented epithelium (Raviola, 1977). The bases of the non-pigmented cells line the posterior chamber whereas the bases of the pigmented cells rest on the ciliary body stroma. The pigmented layer is continuous posteriorly with the RPE and anteriorly with the anterior epithelium of the iris. The non-pigmented layer is continuous with the neuroretina at the ora serrata and anteriorly merges with the posterior epithelium of the iris.

The Blood Aqueous Barrier

The blood capillaries of the ciliary body are large and exhibit fenestrations that occupy the entire circumference of the endothelium. Capillaries with fenestrations are found to be highly permeable to all solutes, so that even plasma proteins escape into the stroma and tend to build up a high colloid osmotic pressure (Bill, 1975). Restraint must therefore be provided by the non-pigmented epithelium of the ciliary body to maintain the composition of the intraocular fluids. It is this non-pigmented epithelia, along with the epithelium covering the iris in the posterior chamber, that forms the majority of the functional blood-aqueous barrier (BAB). The BAB is also formed by the ECs of the vessels of the iris, which are tight to the intravenously injected haemepeptide microperoxidase (Smith & Rudt, 1975).

HRP injected into the circulation of the monkey was found to rapidly fill the stroma of the ciliary body and the intercellular spaces of the pigmented layer, but was stopped at the non-pigmented layer, passing along the intercellular clefts only to a restricted extent and was prevented from passing further by junctional complexes, thus demonstrating the presence of a BAB (Raviola, 1974). This was also found to be true for the smaller molecular weight tracer microperoxidase (Smith & Rudt, 1975). Similar findings have been described in the rabbit (Uusitalo et al., 1973) and in the mouse (Shiose, 1970).

1.1.6 The Vitreous

The majority of the vitreous (99%) is comprised of water and dissolved salts. The mucopolysaccharide hyaluronic acid gives the solution a high viscosity due to its high molecular weight and highly asymmetrical molecules. In addition, there is a small percentage of soluble proteins, some of which are specific for the vitreous and others that are identical to plasma proteins (Laurent *et al.*, 1962). In particular, the glycoproteins, containing sialic acid, are in much higher concentration than in plasma. Vitrosin, hyaluronic acid and soluble proteins are present in such small quantities that the colloidal material constitutes only 0.1% of the total vitreous body. The protein of the vitreous exists as very fine randomly orientated fibrils which are anchored to the inner limiting membrane of the retina (Snowden & Swann, 1980). Attachment plaques (hemidesmosomes) attach the vitreous to the adjacent Müller cells except at the posterior zone close to the optic disc (Foos, 1972).

1.2 IMMUNE PRIVILEGE OF THE EYE

It has been recognised for over a century that some sites in the body are immunologically privileged. The classic example of an immune-privileged site is one where a non-syngeneic tissue graft will have a prolonged survival rate compared to other areas. Thus, these sites have been defined as regions in the body where the immune response appears to be attenuated, and include the brain (Head & Griffin, 1985), testis (Maddocks & Setchell, 1990), and the eye (Tompsett *et al.*, 1990; Streilein *et al.*, 1992). Features that are thought to allow these regions to function as immune-privileged sites include the absence of efferent lymphatics and direct drainage of tissue fluid into the blood, the presence of structural barriers with extensive tight junctions, eg. the blood-ocular barriers, and a reduced expression of major histocompatibility complex (MHC) class I and II molecules.

The presentation of antigen to the immune system via the anterior chamber leads to a unique pattern of immunity, termed anterior chamber-associated immune deviation (ACAID) (Streilein *et al.*, 1992). This involves the processing of antigen within the anterior chamber of the eye by local antigen presenting cells (APC) in an unconventional

manner. These cells leave the eye via the trabecular meshwork and enter the blood stream and migrate to the spleen. In the spleen, interactions with antigen-specific lymphocytes result in the production of the unique set of effector characteristics that are found in ACAID. These include primed cytotoxic T cells, B cells that secrete non-complement fixing antibodies, and afferent and efferent suppressor T cells that down-regulate activation and expression of delayed hypersensitivity. Therefore, the usual mediators of immunogenic inflammation, such as delayed hypersensitivity T cells and complement-fixing antibodies, are diminished.

The retina and brain are not as immunologically privileged sites as once thought. This is due to CNS-resident cells, such as bone marrow-derived perivascular microglial cells (Hickey & Kimura, 1988; Sedgwick *et al.*, 1991), being implicated as immunocompetent APCs which resemble professional macrophages outside of the CNS. Furthermore, there is now strong evidence that a direct drainage route exists from cranial cerebrospinal fluid (CSF) to the cervical lymph nodes via the nasal lymphatics (Kida *et al.*, 1993). A possible lymphatic drainage route is also thought to exist along the subarachnoid space of the optic nerve (De La Motte, 1978).

1.3 OCULAR INFLAMMATORY CONDITIONS

Ocular inflammation is a common clinical problem that may involve any part of the eye. The inflammatory conditions seen are usually named after the parts of the eye that they particularly affect, for example, scleritis, choroiditis, conjunctivitis and uveitis. The uvea, along with the retina, is often seriously affected during ocular inflammatory diseases.

1.3.1 Uveitis

Uveitis is a relatively common clinical disorder occurring at a yearly rate of about 20/100,000 of the population (Forrester *et al.*, 1990). It is characterised by acute, recurrent or persistent inflammation that may affect the anterior or posterior uvea. Immunohistochemical studies have demonstrated a predominance of CD4^{+} T cells within the retina of uveitic eyes, and an increase in MHC class II expression (Lightman & Chan, 1990). Very few B cells or neutrophils are observed, however.

Posterior uveitis, which particularly affects the retina and choroid, is a significant cause of irreversible visual loss in man. This condition may occur in association with systemic disorders such as sarcoidosis and Behçets disease, or as an organ specific autoimmune condition as in sympathetic ophthalmia (Lightman & Chan, 1990). Most forms of the ocular-specific autoimmune disease have several features in common such as retinal vasculitis, macular oedema and vitreous inflammatory cells. The disease usually runs a chronic relapsing course that may be difficult to manage clinically and can lead to extensive retinal damage and visual loss.

Retinal oedema can be observed and recorded using fluorescein angiography. The oedema, which is generally associated with breakdown of either the vascular or RPE blood-retinal barriers, is the major cause of the devastating effect posterior uveitis has on visual acuity. When retinal oedema occurs there are specific anatomic regions where the oedema appears to be most prominent, particularly the macula, which becomes thickened. Retinal oedema is predominantly extracellular, although intracellular swelling of neurons and glia may occur secondarily. Acute vascular occlusion also gives rise to retinal oedema through vascular sheathing of the arteries or veins, which is usually caused by infiltration of inflammatory cells around the blood vessels.

1.4 EXPERIMENTAL MODELS OF UVEITIS

In humans suffering from uveitis it is not usually feasible for chorioretinal biopsies to be taken to identify the inflammatory cells present. Examination of eyes usually takes place if enucleation becomes necessary due to complications of the disease, which is usually at its end stage (Lightman & Towler, 1992). Therefore it is necessary to employ animal models to study the pathogenesis of intraocular inflammation.

1.4.1 Experimental Autoimmune Uveoretinitis

The animal model of posterior uveitis is experimental autoimmune uveoretinitis (EAU) and can be induced in the rat, guinea pig, rabbit and mouse. Susceptible strains of the animal are injected with an antigen extracted from the retina as an emulsion in complete Freund's adjuvant, at a site distant from the target organ. This process was first achieved by Wacker & Lipton (1968). EAU can be induced by systemic immunisation

with soluble retinal antigen (S-antigen) (de Kozak *et al.*, 1978; de Kozak *et al.*, 1981), retinal photoreceptor cell proteins such as rhodopsin (Schalken *et al.*, 1988) or phosducin (Dua *et al.*, 1992), or interphotoreceptor retinoid-binding protein (IRBP) (Harper *et al.*, 1992). Alternatively, the disease can be adoptively transferred by systemic administration of *in vitro* activated T cells specific for a retinal antigen (Mochizuki *et al.*, 1985; Caspi *et al.*, 1986) which demonstrates the central role played by T cells in the disease. Following immunisation of Lewis rats with S-antigen the disease becomes clinically detectable by day 10 to 14 (de Kozak *et al.*, 1978; de Kozak *et al.*, 1981; Lightman & Greenwood, 1992) with uveal inflammation often occurring before that in the retina, as determined by histological examination. Infiltrating leucocytes are found cuffing the retinal vessels and within the photoreceptor layer (de Kozak *et al.*, 1981; Lin *et al.*, 1991; Lightman & Greenwood, 1992). As the disease progresses, considerable extravasation of inflammatory cells from the choroid occurs with damage to the RPE, retinal detachment and formation of a subretinal exudate (de Kozak *et al.*, 1978; de Kozak *et al.*, 1981). However in tracer studies virtually no increase in the permeability of the RPE was detected (Lin *et al.*, 1991; Lightman & Greenwood, 1992; Greenwood *et al.*, 1994).

EAU has many similarities to the experimental model of multiple sclerosis (MS), experimental autoimmune encephalomyelitis (EAE) (Calder & Lightman, 1992; Calder & Greenwood, 1995).

1.4.2 Anterior Uveitis

Ocular inflammation of the ciliary body and iris is termed anterior uveitis, and can be induced experimentally in a number of ways. The systemic immunisation of rats with bovine iris-ciliary body antigen (Bora *et al.*, 1995) results in an inflammatory response which resembles the human clinical condition and is termed experimental autoimmune anterior uveitis (EAAU). Anterior uveitis can also be induced by lipopolysaccharide (LPS), which is also known as endotoxin. This is a component of the gram-negative bacterial cell wall and is one of the most potent inflammatory agents known. An anterior ocular inflammatory response can be induced by injecting LPS into the vitreous (Forrester *et al.*, 1980; Csukas *et al.*, 1990; Howes *et al.*, 1994), or by administrating LPS via a systemic route by injecting into the footpad (Bhattacherjee *et al.*, 1983; Herbort *et al.*, 1988; McMenamin & Crewe, 1995), intraperitoneally (Cousins *et al.*, 1984),

subcutaneously (Planck *et al.*, 1994) or intravenously (Rosenbaum *et al.*, 1980). An acute inflammatory response occurs, primarily within the anterior chamber of the eye, which typically peaks at 24 hr and is resolved by 3-7 days post inoculation. The inflammation, which is termed endotoxin induced uveitis (EIU), is usually accompanied by breakdown of the BAB, and this is generally measured by increased protein concentrations within the aqueous humour.

Anterior uveitis has also been induced in the rat by the intravitreal injection of the cytokine interleukin-8 (IL-8). This caused a significant influx of neutrophils into the anterior chamber of Fischer rats, which began at 4 hr post-injection (PI), and peaked between 10 and 24 hr PI (Ferrick *et al.*, 1991). However, there was no significant increase in protein concentration within the aqueous, indicating that no breakdown of the blood-ocular barriers had occurred.

1.4.3 Lens-Induced Uveitis

The term endophthalmitis phaco-anaphylactica was used by Verhoeff & Lemoine (1922) to describe a certain type of intraocular inflammation following cataract surgery. It was believed that some patients were sensitive to lens proteins. Experimental lens-induced granulomatous endophthalmitis can be induced, following lens injury, in animals previously sensitised to heterologous lens protein (Marak *et al.*, 1977; Till *et al.*, 1992). Animals can also be immunised against their own lens proteins, thus supporting the idea that auto-immunisation may lead to intraocular inflammation (Rahi *et al.*, 1977). However, sensitisation is not a necessary prerequisite for inducing lens-induced inflammation as it has been shown that if the lens is damaged by puncturing with a needle, inflammatory cells are present within the lumen of retinal vessels after 42 hr (Deem *et al.*, 1974).

1.5 THE BLOOD-BRAIN BARRIER

During embryonic development, brain ECs from permeable capillaries of the perineural vascular plexus are stimulated by angiogenic factors to invade the neural tissue, a process known as angiogenesis. These ECs form the BBB, relatively late in embryonic development, at day 13 in the chick embryo (Wakai & Hirokawa, 1978). Transplantation studies have shown that cerebral ECs are not predetermined by lineage and the brain has

the capacity to induce BBB characteristics in possibly any vascular EC (Stewart & Wiley, 1981). There is evidence that astroglial cells may play a role as astrocytes are capable of inducing BBB properties in non-neural EC *in vivo* (Janzer & Raff, 1987), but also cell-cell contact (DeBault & Cancilla, 1980) and soluble factors (Rubin *et al.*, 1991) have been implicated.

The existence of a blood-brain barrier (BBB) was originally described by Ehrlich (1885) and further elicited through the work of Goldman (1913), Spatz (1934), and Broman (1949), among others (reviewed by Dermietzel & Krause, 1991). It was discovered that if the acid dye trypan blue is injected into animals, the dye penetrates into all the tissues of the body and subsequently stains them. However, the brain and spinal cord remain completely unstained, although some parts of the brain do take up the blue dye, for example, the pia mater and the pituitary body. It was also noticed that if trypan blue was introduced via the CSF, it penetrated the CNS, but not the other tissues of the body. The barrier that prevents the passage of dye from the blood to the CNS was found to be localised anatomically at the ECs of the blood vessels, as no dye was observed passing beyond the CNS ECs, unlike other vascular beds. If, however the endothelium of a vessel from the CNS is damaged, then the dye is able to pass through and thus enter the surrounding tissue. Davson (1959) confirmed that the impermeability of the BBB was due to a true barrier formed by the ECs, and not to the lack of extracellular space.

The ultrastructural correlate of the barrier is the presence of successive belts of tight junctions between adjacent ECs, which are considered to be identical to the zonula occludens described for the tight junctions between epithelial cells (Farquhar & Palade, 1963). Additionally, there is a low level of vesicular transport of endocytosed protein from the luminal to abluminal surface of these ECs. This limits the transvascular permeability of endogenous molecules, as well as tracers such as HRP, so they do not cross normal cerebral vessels (Reese & Karnovsky, 1967). This is in direct contrast to capillaries in the heart and skeletal muscle, where endogenous molecules and the vascular tracers HRP and lanthanum are freely able to permeate the EC junctions (Karnovsky, 1967). Unlike the tight cerebral junctions these junctions consist of macula occludens (Karnovsky, 1967), as opposed to the tight junction zonula occludens, as they possess small gaps through which molecules may pass.

1.5.1 The Blood-CSF Barrier

As mentioned above, the intravenous injection of trypan blue was found not to stain the spinal cord, as well as the brain, and this was discovered to be due to the blood-CSF barrier. The blood-CSF barrier is sited inside the cerebral ventricles at the choroid plexus which consists of a typical secretory epithelium with a core of highly vascularised connective tissue. The choroid plexus is the primary site for CSF secretion. In adult animals the epithelium has many features in common with the RPE. It is a single layer of cuboidal cells connected by tight junctions at the apical intercellular regions, the cells possess complex infoldings in the basolateral intercellular region, and numerous microvilli on the apical surface. The cytoplasm also contains mitochondria and other organelles indicative of high metabolic activity.

The permeability characteristics of the blood-CSF barrier appear to be similar to those of the BBB (Davson *et al.*, 1987).

1.5.2 The Blood-Nerve Barrier

The blood-brain and the blood-CSF barriers of the CNS therefore separate the brain and the CSF from the blood, and regulate exchange of various substances between blood and brain and the CSF.

In the peripheral nervous system (PNS), the micro-environment of nerve fibres and their supporting cells, the endoneurial space, is also enclosed and separated from the blood by the blood-nerve barrier (BNB). The BNB consists of endoneurial blood vessels, similar in morphology to cerebral capillaries, and the epineural sheath, that forms a loose cylindrical coat, consisting of layers of collagen fibres and fibroblasts, with tight junctions between the cell layers. The epineurium is continuous with the dura mater which surrounds the spinal cord, and the leptomeninges of the CNS. The BNB and BBB have similar transport selectivity for positively charged macromolecules. The passive permeability characteristics of the BNB to many substances thus resembles those of the BBB (Wadhwani & Rapoport, 1994).

1.6 THE BLOOD-RETINAL BARRIER

The neuroretina of the eye is separated from the blood by the BRB, which performs a similar role to that of the BBB in that it forms a selective interface between the blood and the neural parenchyma (Ashton, 1965; Cunha-Vaz *et al.*, 1966; Bradbury & Lightman, 1990).

The BRB is comprised of two anatomically distinct components, the retinal vascular endothelia (*Fig. 1.3*) and the RPE (*Fig. 1.4*), forming the anterior and posterior barriers respectively. The anterior aspect of the BRB is formed by the highly specialised ECs of the retinal vasculature, which are structurally and functionally similar to those ECs that form the BBB. The posterior aspect of the BRB, however, is formed by the RPE situated at the base of the retina and inside Bruch's membrane. These cells possess tight apical junctions, and are analogous to the tight epithelial cells which also overlie the highly fenestrated vascular endothelial bed of the choroid plexus and which are responsible for the blood-CSF barrier.

Together, these cellular barriers control the passage of molecules and cells into and out of the retinal parenchyma and are instrumental in maintaining homeostasis of the neural environment. This is especially important within the CNS where small fluctuations in extracellular fluid composition may, among other deleterious actions, seriously affect the sensitivity of synaptic signalling (Abbott, 1992).

1.6.1 Permeability of the BRB

Retinal vessels have a higher density of interendothelial junctions and endothelial vesicles than brain vessels which suggests that they possess a greater vascular permeability (Vinores, 1995). Indeed, it has been reported that the permeability of the normal BRB is approximately four times greater than for the BBB to sucrose (Ennis & Betz, 1986) and to the small molecular weight neutral amino acid, α-amino isobutyric acid (Stewart & Tuor, 1994). However, a contradictory report stated that the BRB has the same permeability properties of the BBB to sucrose and mannitol (Lightman *et al.*, 1987a).
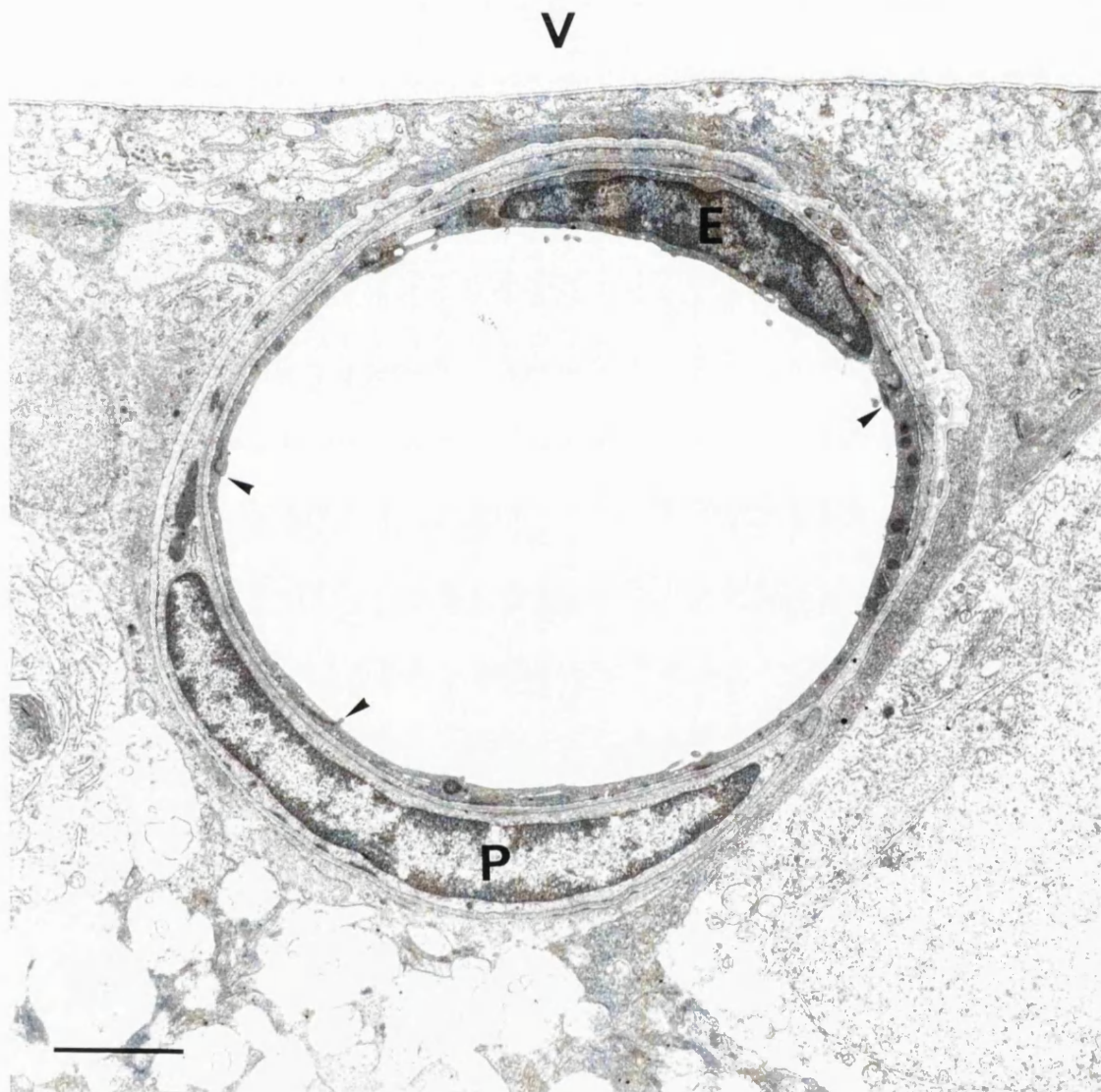
Figure 1.3. *Transmission electron micrograph (TEM) of a blood vessel from the normal Lewis rat retina. E = EC nucleus, P = pericyte, arrow heads = tight junctions, V = vitreous.* (Bar = 2μM).
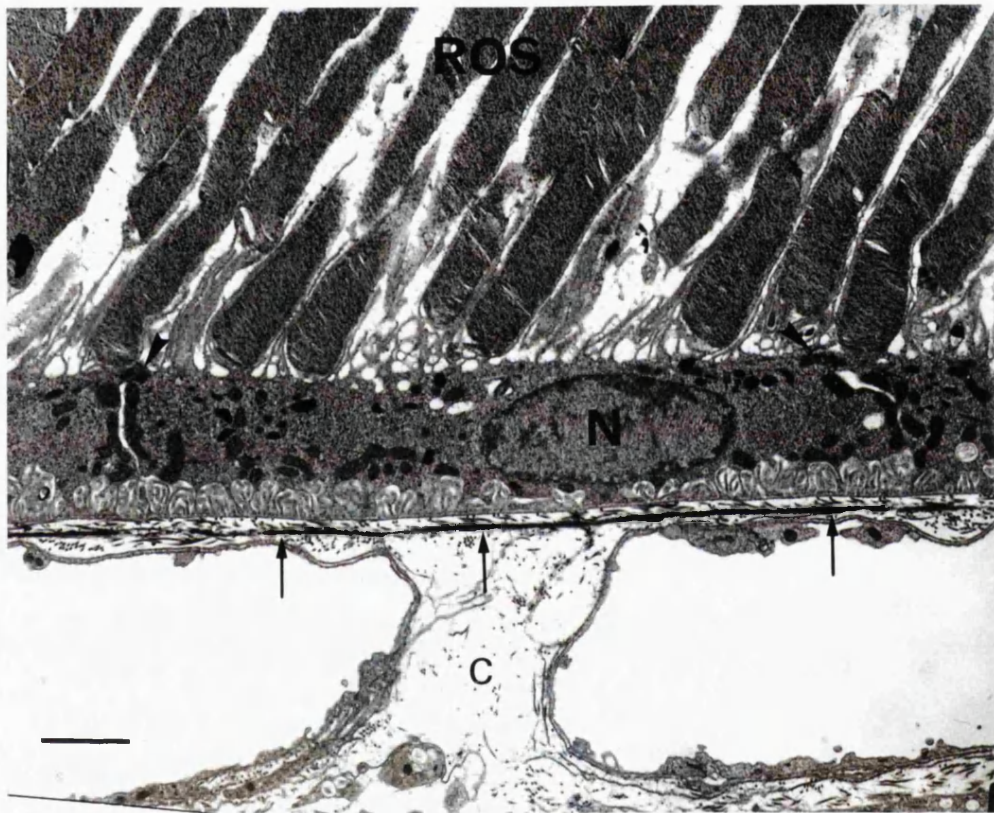
Figure 1.4. TEM of the RPE from a normal Lewis rat retina. N = RPE cell nucleus, arrow heads = tight junction of junctional complex, C = choroid, ROS = rod outer segments, arrows = Bruch's membrane   (Bar = 2μM).

Pericytes, which lie within the basement membrane of blood vessels, are approximately four times as numerous in the retina than in the brain, and it has been suggested that they compensate for the more permeable retinal endothelial barrier (Stewart & Tuor, 1994). This is supported by the observation that following intravenous HRP administration in normal mice, HRP reaction product was detected within cerebral pericytes, indicating that these cells may serve as the first line of defence when the barrier is breached (Broadwell & Salcman, 1981). Furthermore, the greater apparent permeability of the BRB may be due to the BRB possessing a significantly higher surface area for exchange than the BBB provided by the basal infoldings of the RPE (Gratton et al., 1992).

The existence of a BRB was revealed through similar studies that identified the BBB. Palm (1947) injected large quantities of trypan blue intravenously into rabbits and noticed that although there was intense blue staining in a great majority of tissues, the retina remained completely unstained (along with the areas of brain previously described). It was also noticed that although the choroid was stained blue, the outer part of the retina fed by the choroid was unstained. It was concluded that another factor must be acting as a barrier, which was later confirmed to be the RPE which forms the posterior aspect of the BRB.

1.6.2 Retinal Endothelial Cells

The ECs that comprise the vascular BRB, and indeed the BBB, have tight, impermeable junctions, are devoid of fenestrations and transcapillary channels, and express a very low rate of pinocytotic activity and vesicular transport. It is these structural characteristics that allow the ECs to form a selective interface between the blood and the neural parenchyma.

The structure of these CNS microvessels result in them exhibiting very high transvascular resistances with low ion permeability (Towler et al., 1994; Butt et al., 1990).

Control over the movement of essential molecules and cells into and out of the retina is provided by the presence of specific transport systems and receptor molecules at the BRB, which are essentially the same as those that exist in the EC of the BBB. A constant supply of blood-borne glucose is vital to CNS metabolism and therefore effective transport of glucose across the blood-CNS barriers is essential. The glucose transporter, GLUT-1, is a molecule that is concentrated on cells that form tight junctions, including

the capillary ECs of the retina and RPE (Takata *et al.*, 1992). GLUT-1 molecules are localised at both the apical and basolateral plasma membranes of RPE cells, and the luminal and abluminal plasma membranes of the ECs, where they are likely to serve as the machinery for glucose transport across the BRB.

CNS ECs have at least three different amino acid carrier systems (reviewed by Dermietzel & Krause, 1991). The L-system transports large neutral amino acids, such as phenylalanine, isoleucine and valine, which provide the essential basis for synthesis of neurotransmitters and peptides. The other transport systems exist for the basic (lysine, arginine and ornithine) and acidic (glutamate and aspartate) amino acids. Select smaller amino acids are synthesised within the CNS and act as inhibitory neurotransmitters, eg. glycine and γ-aminobutyric acid, so their concentration must be constantly controlled. In the abluminal EC membrane a carrier system exists for transporting the small amino acids out of the extracellular space where they are delivered to the blood by transport systems localised at the luminal EC membranes. Vitamins are transported across the CNS ECs by a variety of mechanisms including passive diffusion and by carrier-mediated transport (reviewed by Pratt, 1992).

Retinal capillaries generally share the same molecular characteristics as brain capillaries with the exception of γ-glutamyl-transpeptidase (γ-GTP), which is apparently absent in retinal, but expressed in brain capillaries (Holash & Stewart, 1993). γ-GTP is a major part of the amino acid transport system and catalyses the transfer of the γ-glutamyl residue of glutathione to amino acids.

Macromolecules are also able to enter the CNS tissue from the blood. A system is present in the ECs for the transport of transferrin into the CNS by receptor mediated endocytosis. CNS cells, including neurons and glial cells, require a constant supply of iron to maintain their normal function. This endocytosis may use an intercellular target such as the Golgi complex to overcome the barrier to direct transcytosis (Broadwell, 1989).

The ionic homeostasis of the retina, brain and CSF, can only be maintained if specific transport systems exist for electrolyte transfer between the blood and CNS compartments. Since CNS ECs display high resistance, due to the presence of tight junctions, its permeability for ions is minimised. The concentrations of sodium and potassium ions in the CNS have been found to be controlled by sodium-potassium ATPase localised in the abluminal EC membrane of CNS capillaries (Betz *et al.*, 1980). The

luminal and abluminal membranes of CNS capillaries are biochemically and functionally different and it is believed that this polarity permits active transport across the ECs of the BRB and BBB.

The product of the multidrug resistancy gene, P-glycoprotein, is expressed on ECs of the BRB and BBB (Greenwood, 1992a). At the BBB it has been suggested that P-glycoprotein actively pumps hydrophobic xenobiotics, that diffuse into the endothelium, back into the circulation. It has been shown that disruption of the P-glycoprotein gene leads to elevated drug levels in tissues and decreased drug elimination (Schinkel et al., 1994).

Electron microscopical observations made by Cunha-Vaz et al. (1966) of the retinal vessels of adult cats, rabbits and rats, showed that their structure is very similar to that of brain capillaries. These vessels are formed by a continuous layer of thick ECs, held together by constant and conspicuously dense junctional complexes, with abundant organelles in their cytoplasm, such as membrane-bound vesicles, mitochondria and occasional pigment granules. The endothelial lining was observed to be resting upon a thick basement membrane which engulfed the intramural pericytes and was in direct contact with the glial tissue, which in the retina are predominantly Müller cells.

Cunha-Vaz et al. (1966) reported that one of the sites of the BRB was situated at the retinal vascular endothelium and its junctions. This was concluded from studies in the immature retinal vessels of the kitten which lie in a compact glial tissue with thick endothelium displaying well defined attachment structures. The basement membrane however was tenuous and incomplete and was therefore eliminated as the structural barrier to trypan blue. In the young rabbit the retinal vessels consisted solely of simple tubes of ECs with dense and constant junctional complexes, but were entirely devoid of basement membrane or perivascular glia. Therefore, from these studies it was concluded that the site of the BRB to trypan blue must be at the EC and the attachments between them.

In further ultrastructural studies it was demonstrated that in both immature and mature retinal vessels there was a consistent occurrence of a certain type of junctional complex (Shakib & Cunha-Vaz, 1966). This complex was characterised by a combination of a well defined and extensive zonula occludens with some features of a desmosome (or macula adherens), junctional features that had been described for various epithelial cells (Farquhar & Palade, 1963). The presence of extensive zonula occludens was seen as proof

that they are continuous in a three-dimensional plane and completely seal the interendothelial spaces of the retinal vessels.

Further experimental evidence demonstrating the efficiency of the retinal tight junctions was provided by tracer studies. Following the intravenous injection of thorium dioxide (Shakib & Cunha-Vaz, 1966), HRP (Shiose, 1970), microperoxidase (Smith & Rudt, 1975), or lanthanum (Pederson, 1979), the progress of the tracer along the clefts between the EC of retinal capillaries was found to be blocked by tight junctions. These zonula occludens tight junctions also block the movement of macromolecular tracers from the interstitial spaces to the lumen of the retinal vessels. When HRP was injected directly into the vitreous it freely penetrated the intercellular spaces of the retina but was prevented from reaching the vessel lumen by the tight junctions (Peyman & Apple, 1972).

Other cellular aspects of retinal ECs include the presence of lysosomes which are thought to play a role in constituting the BRB because they block the transendothelial transport of proteins (Lin & Essner, 1987).

1.6.3 The Retinal Pigment Epithelium

The posterior aspect of the BRB is formed by the junctional complex between the epithelial cells of the RPE, which resemble the junctional complexes described for most other epithelia (Farquhar & Palade, 1963). In most tissues, epithelia are joined together by a junctional complex formed by zonula occludens, the intermediate junction or zonula adherens, and the desmosome or macula adherens. The zonula occludens, closest to the apices of the cells, form continuous belt-like attachments around the cells which are fused so no intercellular space exists. Below the tight junction is the zonula adherens, which is characterised by an intercellular space, and the macula adherens, which is a discontinuous button-like, rather than belt-like, structure. The latter two junctions act as mechanical attachment devices and do not act as a barrier to diffusion. However, the junctional complex of the RPE cells in certain species (eg. the frog) appears to include another specialised membrane contact termed the gap junction, which lies at the apical end of the complex (Hudspeth & Yee, 1973). Additionally in these species, the desmosome is absent and the zonula occludens overlap the zonula adherens which modifies the cleavage properties of the junction and provides a novel freeze-fracture pattern (Hudspeth & Yee, 1973).

When the tracer HRP was injected intravenously, it was able to freely diffuse through the choroid, through Bruch's membrane, and between the junctional complexes of the RPE cells up to the zonula occludens, where its further passage was prevented (Shiose, 1970). Shiose (1970) termed this region, where the tracer was apprehended, as the terminal bar. When HRP was injected into the vitreous it freely diffused through the retinal layers but its passage through the RPE was blocked by the zonula occludens tight junctions (Peyman et al., 1971).

Disruption of the RPE barrier, however, allows tracer material to infiltrate the retina (Tso, 1980). Intravenously injected HRP passes through the RPE cells or their cell junctions, and extends into the subretinal space. Some tracer material is temporarily apprehended by the zonulae adherens of the external limiting membrane, but even though these cell junctions are not tight, they are capable of impeding diffusion of the HRP (Tso, 1980).

1.6.4 Molecular Organisation of BRB and BBB Tight Junctions

A number of tight junction proteins have been identified in epithelial and ECs, but the molecular organisation of these proteins within the tight junction is unclear (Citi, 1993). The first specific tight junction associated protein identified in mammalian epithelial cells was ZO-1 (named after zonula occludens), a 220 kDa peripheral membrane polypeptide tightly associated with the cytoplasmic surface (Stevenson et al., 1986) and located at the inter-endothelial junctions of cerebral microvessels of the BBB (Watson et al., 1991). ZO-1 is known to interact with other tight junction specific proteins, such as spectrin (Itoh et al., 1991) and ZO-2 (Gumbiner et al., 1991). Cingulin (140 kDa) is localised in the apical zone of the terminal web, at the endofacial surfaces of the zonula occludens, and is not an integral membrane component (Citi et al., 1988). Occludin is an integral membrane 65 kDa protein exclusively localised at tight junctions of both epithelial and ECs (Furuse et al., 1993) and is expressed at the tight junctions of the RPE (Konari et al., 1995).

Other important junctional proteins found in endothelial and epithelial cells, which may be important in the formation and regulation of BRB and BBB tight junctions, include platelet endothelial cell adhesion molecule-1 (PECAM-1; also known as CD31), (Albelda et al., 1991), and the cadherins, a family of transmembrane cell surface

glycoproteins that mediate calcium dependent cell-cell adhesion (Takeichi, 1991). The cadherins locally anchor the microfilament system to the plasma membrane in tight junctions (Gumbiner & Simons, 1986). The cadherins are tightly associated with several intercellular proteins, known as catenins (α-catenin, ß-catenin and plakoglobin), which link them to the cytoskeleton.

1.7 ROLE OF THE BLOOD-CNS BARRIERS IN DISEASE

Breakdown of the BRB and BBB occurs as a consequence of a variety of diseases that affect the CNS, and in many, this breakdown plays an important role in the pathogenesis of the disease. For example, BRB dysfunction occurs during posterior uveitis, and BBB breakdown is a factor in the pathogenesis of MS.

BBB dysfunction is a major consequence of cerebral ischaemia (reviewed by Davson et al., 1987; Wimalaratna & Capildeo, 1989). Ischaemic brain oedema is of two major types, cytotoxic and vasogenic. The cytotoxic mechanism involves an acute fall in ATP levels immediately following ischaemia, which causes inactivation of the sodium pump. This results in failure to pump sodium across cell membranes and leads to inflow and retention of water, causing swelling of the cell, and subsequently a reduction of the extracellular space. It is the concomitant breakdown of the BBB to serum proteins that gives rise to vasogenic oedema.

Breakdown of the BBB is also associated with intracerebral tumours (reviewed by Dermietzel & Krause, 1991; Luthert, 1992). It appears that the degree of barrier dysfunction correlates with the malignancy of the tumour. The blood vessels within the tumour lose the tightness of their interendothelial junctions, resulting in increased permeability to proteins, which may be accompanied by the appearance of collagen-filled perivascular spaces. An increase in vesicular activity and fenestrations are also apparent in the ECs.

The BRB plays a major role in the pathogenesis of the retinopathy associated with diabetes mellitus (Cunha-Vaz et al., 1975). Disruption of the integrity of the barrier leads to the development of macula oedema and impaired vision. BRB breakdown has been detected in streptozocin-induced diabetic rats, but only between 7 and 13 months of chronic hyperglycaemia (Lightman et al., 1990), and does not appear to occur before 20

weeks post induction of diabetes (Ennis & Betz, 1986). Barrier breakdown is not thought to occur at the site of the endothelial tight junctions in diabetic rats as their structure remains normal (Caldwell & Slapnick, 1992).

Immunologically-mediated diseases that affect the blood-CNS barriers include EAE and EAU. The experimental model of MS, EAE, can be induced in animals, among other methods, by inoculation with spinal cord homogenate (Raine, 1984). During the course of the disease, inflammatory cells enter the brain and the myelin sheath of neurons is destroyed and phagocytosed by macrophages, and this progressive demyelination leads to paralysis. Another major feature of EAE is breakdown in the integrity of the BBB, as demonstrated by HRP extravasation (Lossinsky *et al.*, 1989; Claudio *et al.*, 1989; Claudio *et al.*, 1990).

Breakdown of the BRB occurs during the course of posterior uveitis. BRB dysfunction has been demonstrated in the experimental model of posterior uveitis, EAU, to the small molecular weight tracer sucrose, but only in association with lymphocytic infiltration, and is not apparent prior to this event (Lightman & Greenwood, 1992). In the later stages of EAU, however, the barrier becomes permeable to the larger molecular weight tracers, HRP and ^{125}I-albumin, when gross destruction of the retina develops (Lin *et al.*, 1991; Lightman & Greenwood, 1992).

1.8 EXPERIMENTAL MANIPULATION OF THE BLOOD-CNS BARRIERS

The BRB and BBB can be manipulated experimentally in order to ascertain the factors responsible for pathological disruption, as well as to develop therapeutic methods of increasing barrier permeability. This has been achieved by introducing substances to the systemic circulation or by direct injection into the CNS parenchyma, CSF, or the vitreous of the eye. The administration of agents by these routes may act by either physical disruption of the junctions, or by causing the barrier to disrupt by different metabolic means, which may be direct or indirect.

Vascular leakage, resulting from breakdown of the blood-retinal or blood-brain barriers, may occur via several different mechanisms (Tso, 1980; Greenwood, 1992b). These include alteration of interendothelial tight junctions, formation of fenestrations, increased pinocytosis, cell lysis, and leucocyte migration.

1.8.1 Hyperosmolar Disruption of the Blood-CNS Barriers

A common method used to cause barrier dysfunction is the raising of the plasma molarity perfusing the retinal and brain vasculature. This causes a reversible disruption of the blood-retinal and blood-brain barriers and has been accomplished by delivering a bolus of hypertonic solution, such as the inert sugars mannitol or arabinose, as a short infusion into the carotid circulation (Greenwood *et al.*, 1988; Cosolo *et al.*, 1989). Disruption of the BBB has also been achieved by superfusing hyperosmolar CSF directly onto exposed pial vessels of the rat *in vivo* (Butt *et al.*, 1990). Experimental evidence suggests that the opening of the barrier occurs through osmotic shrinkage of the endothelium and the pulling apart of the tight junctions in the brain (Brightman *et al.*, 1973; Nagy *et al.*, 1979; Greenwood *et al.*, 1988) and the blood-ocular barriers of the eye (Laties & Rapoport, 1976; Rapoport, 1977).

1.8.2 Experimental Manipulation of the Blood-Brain Barrier

Considerably more experimental work has been performed on the BBB than the BRB, and due to the structural and functional similarities between the two barriers, much of the findings from the BBB have been extrapolated to apply to the BRB.

1.8.2.1 Classic Inflammatory Mediators

A great deal of experimental research has been carried out to examine the effects of classical inflammatory mediators on the cerebral microvasculature and BBB.

Arachidonic Acid and the Eicosanoids

The eicosanoids are potent metabolites formed from the precursor arachidonic acid, an essential polyunsaturated fatty acid which may be ingested or synthesised from linoleic acid by desaturase enzymes. Arachidonic acid is stored in cell membranes and released primarily by the action of phospholipase A_2 and the sequential action of phospholipase C. The eicosanoids are produced by the enzymes cyclooxygenase or lipoxygenase.

The cyclooxygenase products (prostaglandins, prostacyclin (PGI_2) and

thromboxanes) alter smooth muscle tone, vascular permeability, platelet adhesiveness, and lymphocyte function. The lipoxygenase products (which are hydroperoxy fatty acids) include the leukotrienes and long-chain hydroperoxides (HPETEs) and hydroxyacids (HETEs). They increase cell aggregation, chemotaxis, vascular permeability and smooth muscle contractility.

The prostaglandins and leukotreines have been implicated in EC damage and disruption of the BBB. For example, application of prostaglandin G_2 to the brain surface of the cat induced cerebral arteriolar damage (Kontos *et al.*, 1980), and injection of leukotrienes directly into the brain parenchyma of rats caused increased BBB permeability (Black & Hoff, 1985). It is the degradation products of arachidonic acid that are likely to be the mediators responsible for causing barrier dysfunction, as inhibition of their metabolism prevents barrier damage (Black & Hoff, 1985). The precise mechanism by which the eicosanoids cause pathogenesis of the BBB is unclear. Both leukotrienes and prostaglandins (Kontos *et al.*, 1980; Black & Hoff, 1985; Mayhan *et al.*, 1986; Oleson & Crone, 1986), as well as free radicals (Kontos, 1985; Oleson & Crone, 1986; Wei *et al.*, 1986; Olesen, 1987a), have been reported to play a role in BBB breakdown to some degree. However, other investigators have failed to find any increase in BBB permeability with leukotrienes (Mayhan *et al.*, 1986; Wahl *et al.*, 1988) or free radicals (Unterberg *et al.*, 1988). Also, Olesen & Crone (1986) were unable to disrupt the BBB of the frog with either intravascular or extravascular administration of prostaglandins.

Cerebral ECs possess the ability to metabolise arachidonic acid and produce further potentially damaging metabolites. It has been shown that brain microvessels produce the lipoxygenase product 12-hydroxy-eicosatetraenoic acid (12-HETE) when exposed to arachidonic acid, and this may mediate BBB dysfunction (Moore *et al.*, 1989). The topical application of 15-hydroperoxy-eicosatetraenoic acid (15-HPETE) on cerebral arterioles of the cat has been shown to induce arteriolar dilatation and damage to the ECs (Christman *et al.*, 1984).

It has been suggested, however, that arachidonic acid by itself causes breakdown of the BBB, and the pathophysiological effects are not due to its metabolites (Unterberg *et al.*, 1987). An *in vitro* study demonstrated increased permeability of cultured cerebral ECs when directly exposed to arachidonic acid (Kempski *et al.*, 1987). Also, arachidonic acid directly superfused onto the surface of the frog brain was found to reversibly increase

ionic permeability of the cerebral vessels within seconds (Oleson & Crone, 1986). The increase in BBB permeability seen following arachidonic acid administration was thought to be mediated by oxygen radicals (Kontos, 1985; Wei et al., 1986). The generation of free oxygen radicals on to the surface of the frog brain has been shown to cause a decrease in the electrical resistance of blood vessels, indicating an increase in permeability (Olesen, 1987a).

Histamine

Histamine (ß-imidazolyethylamine) is a CNS neurotransmitter and a vasoactive compound that can be released from a variety of cell types, including those of the brain. It is stored pre-formed in the membrane-bound granules of mast cells, basophils and platelets, and its release plays an important role in the acute inflammatory response by causing blood capillary dilatation and increased vessel permeability.

Histamine has been shown to cause perturbations in the permeability of the BBB when applied topically (Martins et al., 1980; Olesen, 1987b), administered intravascularly (Gross et al., 1981; Dux & Joó, 1982; Gross et al., 1982), or superfused directly onto exposed pial vessels (Butt & Jones, 1992). Following the intracarotid administration of histamine, electron microscopy revealed swelling of perivascular astroglial processes and an increase in the number of endothelial pits and vesicles (Dux & Joó, 1982; Gross et al., 1982). Some studies, however, have failed to induce BBB breakdown to tracers following the administration of histamine (Saria et al., 1983; Kilzer et al., 1985; Oleson & Crone, 1986). The reports on the role of histamine in causing BBB breakdown is therefore contradictory, and may be associated with differences in experimental methods.

The route of tracer extravasation by which histamine causes BBB breakdown has been attributed to the induction of vesicular transport (Dux & Joó, 1982). However, Dux & Joó (1982) also reported tight junction abnormalities which may be the predominant route of extravasation. Indeed, it has been shown that histamine causes the opening of pores through the tight junctions (Olesen, 1987b).

Bradykinin

Bradykinin is a powerful excitant of peripheral nociceptors and is relatively selective, having little effect on other sensory receptors. Bradykinin is released, along with

histamine, following tissue injury, and has been shown to play a role in BBB dysfunction. When bradykinin was superfused onto the exposed cerebral surface of the cat, it caused an immediate arterial dilatation (Unterberg *et al.*, 1984). Bradykinin led to a selective opening of the BBB to Na^+-fluorescein when administered this way, and also when infused via the intracarotid artery (Unterberg *et al.*, 1984). The intracarotid infusion of bradykinin has also been shown to cause an extensive breakdown of the BBB to HRP (Raymond *et al.*, 1986). In that study, the increase in permeability was thought to be due to a significant increase in the number of pinocytotic vesicles in the permeable areas, with no change in the structure of the tight junctions. It has been suggested that these effects are mediated by the activation of the arachidonic acid cascade, particularly the prostaglandins. However, pretreatment of animals receiving a superfusate of bradykinin with dexamethasone, an arachidonic acid inhibitor, did not prevent opening of the BBB (Schurer *et al.*, 1989). Contrary to these studies, Saria *et al.* (1983) were unable to demonstrate protein leakage following the intravenous injection of bradykinin.

Serotonin

Serotonin is a bioactive amine also known as 5-hydroxytryptamine (5-HT). It is a CNS neurotransmitter, and also released by platelets at sites of tissue injury.

The intravenous administration of serotonin causes a dose-dependent and rapid increase in brain microvascular permeability (Olesen, 1985; Sharma *et al.*, 1990), but not when applied to the outside of brain vessels (Olesen, 1985). The permeability increasing effect of serotonin was shown to be mediated via $5\text{-}HT_2$ receptors located at the luminal surface of the cerebrovascular endothelium (Olesen, 1985; Sharma *et al.*, 1990). Inhibition of BBB breakdown to serotonin was achieved with indomethacin, indicating a role for prostaglandins (Sharma *et al.*, 1990). It was proposed that following the binding of serotonin to its receptor, prostaglandin synthesis was stimulated from the cerebral vessels. This then caused an increase in vesicular transport across the EC and thus extravasation of tracer.

1.8.2.2 Cytokines

The soluble molecular communicators between the participating and interacting cells of immune or inflammatory responses are collectively known as cytokines. These include the groups previously described as lymphokines, monokines, interleukins and interferons. They are low molecular weight secreted proteins (15-25 kDa) which regulate the amplitude and duration of the immune-inflammatory response. They must therefore be produced in a transient manner tightly regulated by the presence of foreign material. Unlike endocrine hormones, the majority of cytokines normally act locally in a paracrine or autocrine way. They are highly potent, often acting at femtomolar (10^{-15} M) concentrations. They are generally pleiotropic, that is, with multiple effects on growth and differentiation of a variety of cell types. Production of the cytokines IL-1, TNF and IL-6 is not constitutive, but transiently induced in a variety of cells and by various stimuli, for example, viruses, bacteria, LPS and phorbol esters.

Cytokines have been implicated in increasing the permeability of the BBB in experimental models of bacterial meningitis (Saukkonen *et al.*, 1990; Quagliarello *et al.*, 1991). Also experimental data suggests that overexpression of TNF-α in the brain triggers leakage of the BBB. For example, the intracerebral administration of TNF-α into new-born piglets resulted in vasoconstriction of pial microvessels and a dose-dependent increase in BBB permeability (Megyeri *et al.*, 1992). The intracisternal injection of TNF-α caused breakdown of the BBB, along with cerebral oedema and cerebrospinal fluid leucocytosis, in rabbits (Ramilo *et al.*, 1990) and in rats (Kim *et al.*, 1992). The intracerebral injection of IL-2 induced HRP extravasation in the rat (Watts *et al.*, 1989), and IL-1 has been implicated in the development of brain oedema (Gordon *et al.*, 1990; Yamasaki *et al.*, 1992).

1.8.3 Experimental Manipulation of the Blood-Retinal Barriers

Although most studies investigating the effect of agents on the blood-CNS barriers have concentrated on the BBB, there is experimental evidence to illustrate that, following the injection of agents to the vitreous, breakdown of the BRB can occur.

1.8.3.1 Arachidonic Acid and the Eicosanoids

The effect of arachidonic acid metabolites on the BRB have been investigated. The intravitreal injection of the prostaglandins E_1 (PGE$_1$) and E_2 (PGE$_2$) have been shown to increase vascular permeability within the eye (Bhattacherjee & Paterson, 1990; Vinores *et al.*, 1992). However, the leukotrienes B_4 (LTB$_4$) and D_4 (LTD$_4$) administered in the same way appeared to induce ocular inflammation, but not increased permeability, within the eye (Bhattacherjee & Paterson, 1990; Krauss & Woodward, 1993), which has also been observed in skin (Paulissen *et al.*, 1990).

1.8.3.2 Histamine

The reported effects of histamine on the blood-ocular barriers, like that for the BBB, is conflicting. For example, the intravenous administration of high doses of histamine (15µg) resulted in an increased infiltrate of albumin from the vasculature of the eye, but the values were not increased in the brain (Kilzer *et al.*, 1985). However, the local application of histamine to retinal vessels *in vivo* was unable to cause opening of the interendothelial tight junctions or increased BRB permeability to intravenously administered tracers (Ashton & Cunha-Vaz, 1965; Shakib & Cunha-Vaz, 1966).

1.8.3.3 Cytokines

In 1973, Chandler *et al.* published their observations following the intravitreal injection of an unidentified collection of cytokines. They showed that these lymphokines, produced by mixed cultures of allogenic lymphocytes, induced inflammation in the iris, ciliary body and vitreous. Another early study investigating intravitreal cytokines, derived from concanavilin A-activated lymph node cells in culture, reported a large scale MN cell recruitment to the iris, ciliary body and vitreous, which was also accompanied by protein

extravasation in the vitreous of the rabbit eye (Liu *et al.*, 1983). The intravitreal injection of cytokines has also been shown to cause an inflammatory response in the retina. The injection of the cytokine gamma-interferon (IFN-γ), into the vitreous of rats or rabbits, induced a leucocytic influx to the retina (Lee & Pepose, 1990; Hjelmeland *et al.*, 1992). The intravitreal administration of cytokines has also been implicated in increasing the permeability of the BRB (Brosnan *et al.*, 1990; Martiney *et al.*, 1992), and these will be discussed in more detail later.

1.8.3.4 BRB Breakdown During Experimental Diseases

Breakdown of the BRB also occurs in different experimental conditions. A drug which causes acute hypertension, metaraminol bitartrate, injected intravenously, has been shown to disrupt both the BRB and BBB to the small and relatively large molecular weight tracers, sucrose (342 kDa) and microperoxidase (1,900 kDa) (Lightman *et al.*, 1987b). During chronic hypertension, however, only the BRB becomes permeable and then only to low molecular weight tracers (Lightman *et al.*, 1987b). The route of tracer extravasation in hypertensive animals is believed to be via disrupted EC tight junctions (Giacomelli *et al.*, 1972).

Damage to the ECs, as opposed to the opening of interendothelial junctions, has been implicated in retinal ischaemia and the induction of chemically-mediated injury (Cunha-Vaz & Shakib, 1967). An increase in BRB permeability to carbon and thorium dioxide tracers occurred, although the tight junctions were reported to have remained closed.

Increased transendothelial vesicular transport has been implicated in the breakdown of the BRB of outer retinal capillaries in Royal College of Surgeons rats suffering from retinal dystrophy (Essner *et al.*, 1979; Essner *et al.*, 1980). This condition is characterised by a selective and progressive degeneration of the photoreceptors, and is similar to human retinitis pigmentosa. The dystrophy results from the failure of RPE cells to phagocytose portions of the outer segments which are shed by the photoreceptor cells, which results in an accumulation of cell debris in the subretinal (interphotoreceptor) space. These accumulations may then interfere with the flow of nutrients from the choriocapillaris to the RPE and outer layers of the neural retina.

1.9 LEUCOCYTE POPULATIONS

Along with vasodilatation and increased blood vessel permeability, inflammation is characterised by leucocyte margination in the microvascular bed, and the migration of these leucocytes into the extravascular space. There are five types of leucocytes and these are divided into granulocytes or agranulocytes according to the granularity of their cytoplasm and general nuclear characteristics.

1.9.1 Granulocytes

These have prominent cytoplasmic granules and a single multilobed nucleus. The highly variable shape of the nucleus gives them their name of polymorphonuclear (PMN) leucocytes. The granulocytes are named according to the staining characteristics of their specific granules. The specific granules of neutrophils have little affinity for acidic or basic dyes, whereas the granules of eosinophils are stained by the acidic dye eosin, and basophils by basic dyes such as haematoxylin.

Enhanced PMN leucocyte margination characteristically occurs at sites of acute inflammation.

The Neutrophil

Neutrophils are the most common type of leucocyte in the blood of humans (3000-6000 per μl of blood; 40-75% of leucocytes). Using electron microscopy, neutrophils can be seen to exhibit three distinguishing features.

(i) The nucleus has up to five lobes which can look like separate nuclei in some sections.

(ii) The cytoplasm contains numerous membrane-bound granules; the primary granules are large, rounded and electron-dense, and the specific granules are more numerous, smaller and often rod-like, and of variable density.

(iii) All other cytoplasmic organelles are scarce although the cytoplasm is rich in dispersed glycogen.

Neutrophils are the principle cells involved in the acute inflammatory response. They are highly mobile and migrate from small blood vessels to sites of tissue damage where they engulf and destroy cell debris and microorganisms by phagocytosis. Due to

their limited organelles, neutrophils are incapable of continuous function and degenerate after a single burst of activity. Dead neutrophils are the main cellular constituent of pus and are therefore sometimes referred to as pus cells.

Neutrophils have been described in ocular inflammatory conditions such as phacoanaphylactic endophthalmitis, or lens-induced uveitis (Verhoeff & Lemoine, 1922; Marak et al., 1977), which may occur in humans following cataract surgery. Neutrophils, however, are not a feature of the large-scale leucocytic infiltrate that occurs in posterior uveitis (Lightman & Chan, 1990).

The Eosinophil

Eosinophils are far less common than neutrophils (100-400/µl; 1-6% of leucocytes in peripheral blood). They characteristically possess a bilobed nucleus and the cytoplasm is full of large specific granules of uniform size. Each of these granules contains a dense crystalloid in the long axis of the granule, which is composed of major basic protein. Eosinophils are highly phagocytic for antigen-antibody complexes.

Eosinophils have long been associated with allergic diseases. Allergic patients, such as asthmatics, have increased numbers of eosinophils in their circulation and mucosal tissues, and accumulation of these cells occurs after antigenic challenge in the skin, lungs, and nasal airways of these patients. Eosinophils are also an associated aspect of lens-induced uveitis (Marak, 1981).

The Basophil

Basophils are the least common of the leucocytes (25-200/µl; <1% of leucocytes). They possess a bilobed nucleus and large electron dense specific granules.

Basophils, along with eosinophils, appear as part of a more sustained inflammatory reaction (called the late phase response) that occurs following acute allergic reactions in the skin and airways.

1.9.2 Agranulocytes

These are composed of lymphocytes, monocytes and macrophages. No cytoplasmic granules are visible by light microscopy and the nucleus is not lobed but may be deeply indented, which gives them their name of mononuclear (MN) leucocytes. They are

predominately involved in the chronic phase of an inflammatory response.

The CNS used to be considered an immune-privileged site where leucocytes were thought unable to cross the intact BBB or BRB, but recently cells of the monocyte/macrophage lineage and T cells have been reported to be present within, or able to patrol, the CNS under normal conditions (Perry & Gordon, 1988; Hickey *et al.*, 1991). T cells in the activated state are able to enter the CNS in small numbers regardless of antigen specificity. If they are capable of reacting with a CNS antigen they remain in the tissue or they cyclically re-enter to initiate inflammation if they are able to recognise their antigen in the correct MHC context (Hickey *et al.*, 1991).

The Lymphocyte

Lymphocytes are the smallest of the leucocytes and the second most common (1500-$2700/\mu l$; 20-45% of leucocytes). They are characterised by a round, densely stained nucleus and a relatively small amount of pale, non-granular cytoplasm. There are two subsets of lymphocytes, known as T and B lymphocytes (or T and B cells). T cells are responsible for cell-mediated immune responses as they can destroy foreign or virus-infected cells by direct contact. T cells possess receptors on their cell surface that recognise antigens and are the basis for specific immune responses. B cells are responsible for humoral responses of the immune system and secrete antibodies into body fluids. T cells predominate in the leucocytic infiltrate to the retina in posterior uveitis (Lightman & Chan, 1990).

The Monocyte

Monocytes are the largest of the white blood cells and constitute 2-10% of leucocytes in the peripheral blood (100-$700/\mu l$). Monocytes are characterised by a large indented nucleus that is horseshoe shaped or bilobed in the mature cell. The extensive cytoplasm is filled with small lysosomes, well developed Golgi apparatus and the mitochondria are more prevalent than in any other leucocyte. The accumulation of blood monocytes at sites of chronic inflammatory reactions is a common feature in many inflammatory conditions, including human rheumatoid arthritis and in experimental models of arthritis. These cells differentiate into macrophages (which are also known as histiocytes) in the tissues and are believed to contribute to the inflammatory reaction

through their capacity to present antigen and secrete cytokines, growth factors, oxygen radicals, and proteolytic and degradative enzymes.

Cells of haemopoietic origin are present within the normal CNS, and these so-called tissue resident macrophages are thought to form an important component of the non-neural cell population in the CNS and to be a part of the immune-nervous system interface (Hickey & Kimura, 1988; Perry & Gordon, 1988; Graeber *et al.*, 1989; Sedgwick *et al.*, 1991).

1.9.3 Platelets

Platelets, also known as thrombocytes, are small, non-nucleated cells formed in the bone marrow by budding from the cytoplasm of megakaryocytes. They participate in haemostasis (the limiting of bleeding after vessel injury) and they contribute to the process of clot formation. Platelets also release vasoactive agents such as serotonin, histamine, and platelet activating factor (PAF), and they often form aggregates associated with leucocytes at sites of inflammation.

1.10 LEUCOCYTE TRAFFIC

1.10.1 Adhesion Molecules

The extravasation of leucocytes from blood to tissue is a precisely regulated process critical for homeostasis and for effective host response to immunological challenge. There is a three-step process by which cells leave the circulation and enter tissue: arrest, adhesion and migration (reviewed by Springer, 1994) (*Fig. 1.5*).

Lymphocytes continually patrol the body for foreign antigen by recirculating from blood, through tissue, into lymph, and back to blood. Granulocytes and monocytes emigrate from the bloodstream in response to molecular changes on the surface of blood vessels that signal injury or infection, but they cannot recirculate. The nature of the inflammatory stimulus determines whether lymphocytes, monocytes, neutrophils or eosinophils predominate and thus exercises specificity in the molecular signals that control traffic of particular leucocyte classes.

Selectin molecules are responsible for the initial tethering of a flowing leucocyte to the vessel wall and for rolling adhesions. L-selectin is expressed on all circulating

leucocytes, except for a subpopulation of memory lymphocytes. P-selectin is stored preformed in the Weibel-Palade bodies of ECs and in the α granules of platelets. In response to mediators of acute inflammation, such as histamine, P-selectin is rapidly mobilised to the plasma membrane to bind neutrophils and monocytes. E-selectin is induced on vascular ECs by cytokines (eg. IL-1 or TNF) and LPS, and requires *de novo* mRNA and protein synthesis.

Tethering brings leucocytes into close proximity with chemoattractants that are displayed on, or released from, the endothelial lining of the vessel wall. Chemoattractants are important in the activation of integrin adhesiveness and in directing the migration of leucocytes. Chemotaxis occurs, causing cells to move in the direction of an increasing concentration of the chemoattractant. There are two groups of chemoattractive cytokines, termed chemokines. The C-X-C or α chemokines, which include IL-8, tend to act on neutrophils and nonhaematopoietic cells involved in wound healing. C-C or ß chemokines tend to act on monocytes, and sometimes eosinophils and lymphocyte subpopulations, and include MIP-1α (macrophage inflammatory protein-1α), MIP-1ß, and RANTES (Regulated upon Activation, Normal T cell Expressed and Secreted).

The integrin family are α-ß heterodimers sharing a common ß-chain (CD18) and considerable homology in the α-chain (CD11) and consists of 3 major subclasses (Sanchez-Madrid *et al.*, 1986). The ß1 integrins, also called the very late antigens (VLA 1-6), can bind to components of the extracellular matrix, such as fibronectin or laminin. The ß2 integrins comprise lymphocyte function-associated antigen-1 (LFA-1 or CD11a/CD18) which is constitutively expressed on all leucocytes, Mac-1 (or CD11b/CD18) which is expressed on activated neutrophils and monocytes, and p150,95 (or CD11c/CD18) which is expressed on neutrophils, monocytes, macrophages and some T and B cells and has considerable homology to Mac-1. The ß3 subclass includes the vitronectin receptor and the platelet glycoprotein IIb/IIIa.

The integrins bind to immunoglobulin superfamily members on the endothelium such as intercellular adhesion molecule-1 (ICAM-1) and ICAM-2, and vascular cell adhesion molecule-1 (VCAM-1), increasing adhesiveness and resulting in arrest of the rolling leucocyte. Following directional cues from chemoattractants and using integrins for traction, leucocytes then cross the endothelial lining of the blood vessel and enter the tissue.
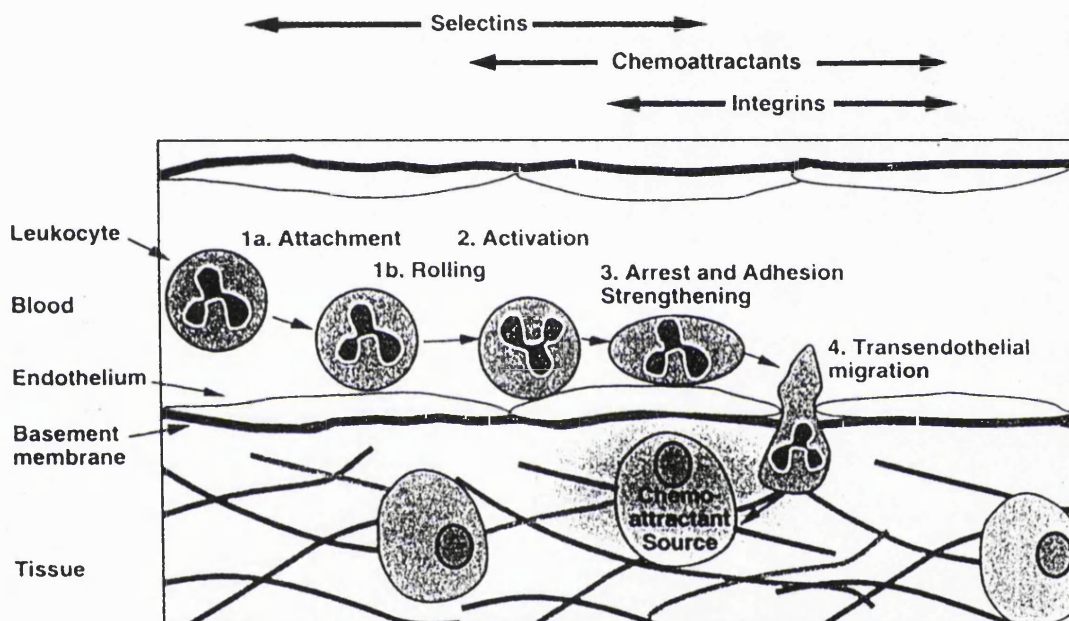
Figure 1.5. *The three step model of leucocyte attachment, adhesion and migration. The selectins, chemoattractants and integrins act in sequence, but some overlap exists.* (From Springer, 1994).

1.10.2 Route of Cellular Migration in the CNS

The path through which leucocytes migrate across the tight vascular barriers of the CNS has been the source of some contention because it is unclear whether the cells migrate through the tight junctions or through the EC itself. Considerable evidence supports the view that lymphocytes are capable of migrating through CNS ECs at a parajunctional site (Lossinsky *et al.*, 1989; Raine *et al.*, 1990; Greenwood *et al.*, 1994). The route which PMN cells extravasate however, is not so clearly defined, although it has been suggested that these cells migrate through the tight junctions (Dorovini-Zis *et al.*, 1992) and transcellularly (Faustmann & Dermietzel, 1985).

1.11 OBJECTIVE OF THIS STUDY

The objective of this study was to define the role of particular inflammatory components which have been implicated in BRB and BBB disruption. Classic inflammatory mediators such as histamine and prostaglandin are well recognised as mediators of blood vessel dilatation and increased vascular permeability, but their exact role within the CNS is not well established. Recently the cytokines have been implicated in the pathology of CNS disorders but again their precise role is uncertain. This study has attempted to elucidate the role of some of these mediators of inflammation by introducing them directly to the vitreous of the Lewis rat and subsequently examining the structure and integrity of the BRB. Other goals of this study included an attempt to define the mechanisms by which the cytokine IL-1ß was causing increased BRB permeability, and to examine the capacity of retinal ECs to produce PGE_2 or histamine in the presence of cytokines.

1.12 INFLAMMATORY AGENTS USED IN THIS STUDY

1.12.1 Cytokines

There is considerable experimental evidence for the concept that cytokines play a major role in the pathogenesis of uveitis (Hoekzema *et al.*, 1990; De Vos *et al.*, 1992).

Interleukin-1β

The proinflammatory cytokine interleukin-1 (IL-1) represents three different proteins: alpha and beta, which possess a wide spectrum of immune and non-immune functions, and the IL-1-receptor antagonist (IL-1ra) which inhibits the activities of IL-1 (reviewed by Dinarello, 1984 & 1989).

IL-1α and β are the product of separate genes. They have different amino acid sequences (there is only 26% homology) but they are structurally related at the three-dimensional level, act through the same cell-surface receptors and share biologic activity. Both are rapidly synthesised by MN cells, primarily monocytic phagocytes, that have been stimulated by microbial products or inflammation. This stimulation activates the cell to transcribe the mRNA for IL-1α and β. Most of the IL-1α remains within the cell or is expressed on the surface of the cell membrane. Extracellular proteases cleave the 31 kDa precursor into the mature form of IL-1α. The IL-1β precursor is cleaved by the IL-1-converting enzyme (ICE), an intracellular protease, to its mature 17.5 kDa form within the cell, after which it is secreted. However, some IL-1β precursor is found outside cells where it is cleaved by other proteases.

IL-1ra provides some protection against the disease-provoking effects of IL-1 (Martin & Near, 1995). It is a specific inhibitor of IL-1 activity that acts by competitively blocking the binding of IL-1 to its cell surface receptors.

IL-1 is able to stimulate the production of the T cell growth factor interleukin-2 (IL-2) which subsequently induces T cell proliferation. This IL-2-inducing property of IL-1 may be one of its most important functions due to the critical role of T cells for both humoral as well as cell-mediated immunity. IL-2 also influences the growth of glial cells, specifically the proliferation and differentiation of oligodendrocytes (Benveniste & Merrill, 1986) and it has a functional significance within the CNS as a potent and selective

modulator of acetylcholine release in the rat brain (Hanisch *et al.*, 1993). Moreover, IL-2 has been shown to be present within the eyes of patients with ocular inflammatory conditions (Hooks *et al.*, 1988; Franks *et al.*, 1992; Mondino *et al.*, 1990).

In studies on non-CNS vasculature, IL-1 has been shown to recruit leucocytes to the site of injection (Cybulsky *et al.*, 1986), to induce neutrophil migration across cultured EC (Furie & McHugh, 1989; Moser *et al.*, 1989), to cause an increase in the permeability of the blood vessels of the skin (Martin *et al.*, 1988; Watson *et al.*, 1989), and to increase the transmonolayer permeability of human umbilical vein EC (HUVEC) monolayers (Burke-Gaffney & Keenan, 1993).

Although IL-1 is synthesised primarily by MN leucocytes, it is also produced by cells of the CNS such as microglia (Hetier *et al.*, 1988) and retinal Müller cells (Roberge *et al.*, 1988). IL-1 has been shown to be present in the vitreous of patients with ocular inflammation (Limb *et al.*, 1991; Franks *et al.*, 1992; Abu El Asrar *et al.*, 1993) and in the brains of rats with EAE (Bauer *et al.*, 1993). Such observations demonstrate that there is a potential for endogenous IL-1 to influence both the blood-brain and blood-retinal barriers *in vivo*.

Recent studies by Brosnan and colleagues have described the effects of IL-1ß on the rabbit BRB following its introduction into the vitreous. In a series of reports IL-1ß was shown to cause perturbations of the BRB including leucocyte recruitment, increased permeability and alterations in EC morphology (Brosnan *et al.*, 1989; Martiney *et al.*, 1990; Martiney *et al.*, 1992; Claudio *et al.*, 1994). These studies, therefore, clearly demonstrate that IL-1 is capable of inducing significant damage to the vasculature of the CNS. The mechanisms by which these changes are brought about, however, remain largely unresolved.

Tumour Necrosis Factor-α

TNF-α is closely related to TNF-ß (also known as lymphotoxin) and they both share similar abilities with respect to inflammation and antitumour activity *in vitro* and *in vivo*. TNF-α is also known as cachectin because of its ability to cause cachexia (progressive wasting) through its inhibition of the enzyme lipoprotein lipase, and it is also an endogenous cytotoxic factor for certain tumour cells. The principal source of TNF-α is from cells of the monocyte/macrophage lineage. TNF-α is proteolytically cleaved from

a 26 kDa precursor to the mature 17 kDa form. Three of these 17 kDa molecules associate noncovalently to form a biologically active trimer (Smith & Baglioni, 1987).

The cellular effects of TNF-α suggest that its actions are both pleiotropic and proinflammatory. The intradermal injection of TNF-α into the rat has been shown to induce a rapid increase in lymphocyte migration into the skin *in vivo* (Issekutz & Stoltz, 1989), and it is chemotactic for neutrophils *in vitro* (Ming *et al.*, 1987). Moreover, the intravitreal injection of TNF in the rabbit has been shown to cause an anterior uveitic response (Rosenbaum *et al.*, 1988).

TNF shares many biological properties with IL-1, such as the ability to act as an endogenous pyrogen and induce sleep (Dinarello, 1987). Other properties of TNF-α include its ability to stimulate the production of IL-1 in monocytes, ECs and fibroblasts (Le & Vilcek, 1987) and it is angiogenic *in vivo*, stimulating neovascularisation in the rabbit cornea (Frater-Schroder *et al.*, 1987). TNF-α is not constitutively produced by CNS astrocytes, but can be produced by these cells when they are stimulated with LPS (Lieberman *et al.*, 1989; Chung & Benveniste, 1990) and it has been implicated as a growth promoting factor of astrocytes *in vitro* (Selmaj *et al.*, 1990).

The intercerebral administration of TNF-α into rats caused a pronounced leucocyte influx to the injection site (Wright & Merchant, 1992). *In vitro*, TNF has been shown to increase the permeability of bovine aortic ECs to small molecular weight solutes (sorbitol, 500 kDa) and macromolecules (albumin, 67,000 kDa), in a concentration-dependent manner (Brett *et al.*, 1989). TNF-α has also been shown to increase the permeability of HUVEC monolayers (Burke-Gaffney & Keenan, 1993).

This cytokine has been shown to be present in the vitreous of patients with ocular inflammation (Limb *et al.*, 1991; Franks *et al.*, 1992) and ocular inflammatory cells have been shown to stain positive for TNF-α in uveitic eyes (Whitcup *et al.*, 1992).

Interleukin-6

Interleukin-6 (IL-6) was first described as a 26 kDa inducible protein derived from fibroblastoid cells stimulated with poly I:C (double stranded RNA), cyclohexamide or virus.

IL-6 is a pleiotropic cytokine that has been shown to be produced by activated monocytes or macrophages, ECs, RPE cells, a variety of tumour cells, astrocytes,

fibroblasts, keratinocytes, bone marrow stroma cells and activated T and B cells. IL-6 acts on a variety of target cell types including T cells, B cells, fibroblasts, myeloid progenitors and hepatocytes. Abnormal production of IL-6 has been suggested to be involved in glomerulonephritis, plasmacytomagenesis and in the pathogenesis of autoimmune diseases (Hirano *et al.*, 1990). Elevated levels of IL-6 have been detected in the synovial fluid of patients suffering from rheumatoid arthritis (Houssiau *et al.*, 1988).

Many of the properties of IL-6 overlap with those of IL-1 and TNF (Hoekzema *et al.*, 1990) such as induction of fever, and T and B cell activation. Raised IL-6 levels in the aqueous humour of patients suffering from Fuch's heterochromic cyclitis and toxoplasma chorioretinitis (Murray *et al.*, 1990) suggest a role for IL-6 during intraocular inflammation. IL-6 has also been detected in vitreous samples from patients with various forms of uveitis as well as proliferative intraocular disorders (Limb *et al.*, 1991; Kauffman *et al.*, 1994; Wakefield *et al.*, 1995), suggesting that IL-6 is a common inflammatory mediator, not related to a specific ocular complaint (de Boer *et al.*, 1992).

1.12.2 Histamine

Along with the reported effects of histamine on the BBB, as discussed above, histamine has also been shown to cause increased vascular permeability of ECs in the skin (Wedmore & Williams, 1981) and increased permeability of HUVEC monolayers *in vitro* (Killackey *et al.*, 1986). Also, the application of histamine to bovine retinal arteries *in vitro* has been shown to induce vessel dilatation (Benedito *et al.*, 1991). The precise role of histamine within the CNS and on the ECs, however, is not clear due to the contradictory evidence that exists, particularly for the BBB, as discussed above.

The enzyme forming histamine is histidine decarboxylase, and the retina contains an active histidine decarboxylase enzyme system. In streptozocin-induced diabetic rats retinal histamine synthesis is greatly increased (Carroll *et al.*, 1988), and it is believed that this retinal metabolic alteration may be one factor responsible for increased retinal vascular permeability in diabetic retinopathy.

Histamine has 3 receptors in the CNS, known as H_1, H_2 and H_3. These receptors can be blocked by specific receptor antagonists, such as diphenhydramine and mepyramine, which block the H_1-receptor, and cimetidine and ranitidine, which block the H_2-receptor. The H_1-histamine receptor has been implicated in mediating increased BRB

permeability in experimental diabetes (Enea *et al.*, 1989), and the H_2-histamine receptors have been shown to be the target for histamine infused via the intracarotid artery, which causes increased brain capillary permeability of hypoxic animals (Dux *et al.*, 1984). Also, the histamine receptor antagonists diphenhydramine and ranitidine have been shown to exert a synergistic effect and reverse BRB permeability in streptozocin-induced diabetic rats (Hollis *et al.*, 1988). The H_3-histamine receptor is the most recently identified and is present on the vasculature of the pig retina and in cerebral neurones of various mammalian species (Schlicker *et al.*, 1994).

1.13 THE EXPERIMENTAL MODEL

In this study the effect of an intravitreal injection of an inflammatory agent on the function of the rat BRB, which is anatomically similar to that of the human, has been investigated. By using a sensitive *in vivo* technique which employs the small radiolabelled tracer [^{14}C]-mannitol, relatively small changes in the permeability of the BRB were able to be detected. Substantial changes in permeability detected by this method were confirmed by using the visual tracer HRP and electron microscopy. In addition, the visual demonstration of BRB leakage also indicated the site of disruption. Leucocyte recruitment and alterations in the structural integrity of the retina were assessed by light and electron microscopy and observations were correlated with changes in the permeability of the BRB. Electron microscopy was also used to examine the interactions between leucocytes and ECs, the route of leucocyte migration out of the circulation and into the tissue parenchyma, and any morphological changes in EC structure. Immunohistochemistry was used to phenotype any cellular infiltrate. Studies were also performed, following the intravitreal injection of IL-1ß, to block the histamine H_2-receptors, inhibit the production of cyclooxygenase metabolites, and matrix metalloproteinase activity, and deplete circulating leucocytes in an attempt to discover the mechanisms by which this cytokine was causing BRB breakdown.

As classic inflammatory mediators appeared to be implicated in IL-1ß-induced BRB breakdown, rat retinal EC were grown *in vitro* and pulsed with IL-1ß, TNF-α and IL-6 to examine their ability to produce PGE_2 and histamine when stimulated with cytokines.

57a

1.14 HYPOTHESIS

The injection of a proinflammatory cytokine to the vitreous of the Lewis rat will induce a leucocytic infiltration to the retina and breakdown of the BRB. Inhibitor studies may then identify the mechanism by which BRB dysfunction is occurring.

CHAPTER TWO

MATERIALS AND METHODS

2.1 THE EXPERIMENTAL ANIMAL

Male Lewis rats (obtained from Harlan Olac UK Ltd, Oxon, UK), weighing 200-250g, were used throughout the study. The animals were fed and watered ad libitum. The histology and permeability studies were performed on animals terminally anaesthetised with sodium pentobarbitone [60mg.kg^{-1}], administered intraperitoneally (IP). All procedures were carried out in accordance with the Animals (Scientific Procedures) Act, 1986.

2.2 AGENTS USED

2.2.1 Cytokines

Interleukin-1β

Murine recombinant interleukin-1ß (IL-1ß; R&D Systems Europe, Oxon, UK) was supplied lyophilised with a specific biologic activity of 1-2 x 10^8 U/mg. This was reconstituted in 5ml sterile-filtered pyrogen-free saline containing 0.1% low endotoxin bovine serum albumin (BSA; Fraction V Powder, Sigma Chemical Co. Dorset, UK) to give a final concentration of 1-2 x 10^5 U/ml. Aliquots of 100μl containing 1-2 x 10^4 U were placed in sterile Eppendorf vials and stored at -70°C until used. Each 10μl injection of IL-1ß therefore consisted of 1-2 x 103 U, or 6.66-13.32ng of protein.

Anti-IL-1β Antibody

To investigate whether IL-1ß neutralised with antibody had the same effect as IL-1ß by itself, the bioactivity of IL-1ß was neutralised with a goat anti-murine IL-1ß neutralising antibody (αIL-1ß Ab; R&D Systems Europe) for 24 hr at 4°C. An antibody concentration of 10mg.ml^{-1} was used to give maximal neutralisation of 1 x 10^4 U (or 66.6ng) of the IL-1ß, as recommended by the manufacturer.

Tumour Necrosis Factor-α

Recombinant murine tumour necrosis factor-α (TNF-α; Genzyme, Kent, UK) was supplied as 1.67×10^7 U in 1ml PBS, with a specific activity of 1.67×10^9 U/mg. To achieve the required concentration of 1×10^4 U per 5μl (5.5ng of protein), or 2×10^4 U per 10μl (11ng of protein), 7.35ml of sterile filtered PBS containing 0.1% BSA was added and 150μl aliquots placed in sterile Eppendorf vials and stored at -70°C.

Interleukin-6

Recombinant murine interleukin-6 (IL-6; Boehringer Mannheim Biochemica, East Sussex, UK) was supplied sterile, at a concentration of 2×10^5 U/ml ($2\mu g.ml^{-1}$) in PBS and $1mg.ml^{-1}$ BSA, with a specific activity of $>1.0 \times 10^8$ U/mg. Aliquots of 100μl were placed in sterile Eppendorf vials and stored at -70°C. Each 5μl injection therefore contained 1×10^3 U of IL-6 (10ng of protein).

2.2.2 Histamine

Histamine dihydrochloride (Sigma) was diluted in saline and sterile filtered. Aliquots of 1×10^{-3} M, 1×10^{-4} M, 1×10^{-5} M were stored in sterile Eppendorf vials at 4°C.

2.2.3 Inhibitors

As IL-1ß was found to cause a substantial inflammatory response accompanied by breakdown of the BRB, studies were performed in an attempt to determine the molecular mechanisms by which IL-1ß was causing BRB dysfunction.

Two inhibitors of classical mediators of inflammation were selected, ranitidine, a histamine H$_2$-receptor antagonist, and indomethacin, a compound which prevents the synthesis of cyclooxygenase products, such as prostaglandins, from arachidonic acid.
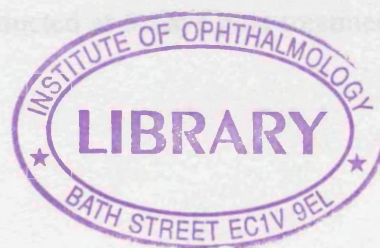
Ranitidine

Ranitidine (Zantac; Glaxo, Herts, UK) was added to the IL-1ß inoculum to give a concentration of 25µg per 10µl intravitreal injection (71µM). Ranitidine (25mg.kg^{-1}; 71mM) was also administered IP at time 0 (when the intravitreal injection was given) to the animals in the 4 hr time point group, and at 0, 8 and 22 hr PI in the 24 hr time point group.

Indomethacin

The effect of indomethacin (Sigma) was examined by mixing with the IL-1ß prior to intravitreal injection (5µg; 13.97µM). Indomethacin (5mg.kg^{-1}; 13.97mM) was also administered subcutaneously at time 0 in the 4 hr time point group, and at 0, 8 and 22 hr PI in the 24 hr time point group.

Galardin™

Matrix metalloproteinases (MMPs) are known to be expressed by leucocytes and to play a critical role in cell migration. As BRB disruption may be caused by the infiltrating leucocytes, an attempt was made to inhibit cellular migration with a MMP inhibitor, the hydroxamic acid derivative Galardin™ (Grobelny *et al.*, 1992) (a generous gift from Glycomed, CA, USA). Galardin™ was prepared by dissolving 4mg in 1ml glacial acetic acid, the pH restored to 7.4 with 1M NaOH, and diluted to 1mM (400µg.ml^{-1}) with Dulbeccos modified Eagles medium. This was then mixed with IL-1ß to give a concentration of 100µM per intravitreal injection.

2.2.4 Leucocyte Depletion

Leucocyte depletion was achieved by the method described by Sedgwick et al., (1987). Animals were administered with 1ml busulfan (20mg.kg^{-1} IP; Sigma), which was dissolved in DMSO and diluted to 10% in olive oil. 24 hr later the rats received 0.5ml chlorambucil resuspended in olive oil (12mg.kg^{-1} IP; Sigma). Peripheral blood leucocyte counts were performed at 5 days post-treatment to ensure that sufficient leucopaenia had occurred. Experimental procedures were then conducted at 5 days post treatment.

2.2.4.1 Blood Leucocyte Counts

Blood from a normal control rat and from each rat depleted of leucocytes was collected in heparinised tubes (Becton Dickinson, Oxford, UK) and diluted to 1:20 in 1% glacial acetic acid (Sigma) containing 5% Geimsa stain (Sigma). This diluent lyses erythrocytes and stains the leucocytes blue. The number of leucocytes per μl was then counted using an Improved Neubauer haemacytometer.

2.3 INTRAVITREAL INJECTION PROCEDURE

Rats were anaesthetised with the inhalation anaesthetic methoxyfluorane (Metofane; C-Vet Ltd, Suffolk, UK) for 3-5 minutes until they were unconscious and resistant to a pinch to the footpad. The rat was then placed on a small mammal operating table with a fibre optic light source positioned directly over the right eye. Using direct visualisation, a sterile 30 gauge needle attached to a Hamilton microlitre syringe was inserted via the pars plana with the needle tip entering the central vitreous. Care was taken not to touch the lens. The agent to be studied was then delivered into the vitreous and the animal allowed to recover.

2.4 ULTRASTRUCTURAL STUDIES

Light and transmission electron microscopy was employed to investigate the structural pathology of the retina following the injection of agents into the vitreous.

2.4.1 Controls

Retina from non-injected eyes ($n = 4$) and from vehicle control (saline containing 0.1% BSA) injected eyes at 4 and 24 hr PI ($n \geq 4$ for each time point; total $n = 12$) were inspected for leucocyte infiltration and retinal damage. Animals also received a sham injection, where a sterile needle was inserted into the vitreous without the delivery of test substance, to assess the effect of the injection procedure itself on the retina at 4 and 24 hr PI ($n = 2$ for each time point; total $n = 4$). (Volume of vehicle injected = $10\mu l$.)

2.4.2 Interleukin-1ß

A dose dependency study was performed to find the optimum dose of IL-1ß that could cause ocular inflammation at 24 hr PI. The doses examined were 25-50 U, 50-100 U, 100-200 U, 200-400 U, and 1-2 x10^3 U (n = 2 for each time point; total n = 10). The 1-2 x10^3 U dose was found to cause the most substantial inflammatory response after 24 hr, so all subsequent IL-1ß experiments were performed with this dose.

A time course study was then performed using IL-1ß (1-2 x10^3 U) at 0, 1, 2, 4, 8, 12, 18 hr, and 1, 1.5, 2, 3, 5, 7 and 14 days PI (n ≥ 2 for each time point; total n = 35). The rats from 0 time point group were perfused at 20 min PI to maintain consistency with the [^{14}C]-mannitol study, where the 20 min infusion began immediately after the intravitreal injection was given.

Eyes receiving intravitreal IL-1ß neutralised with αIL-1ß Ab (10mg.ml^{-1}) were examined at 4 and 24 hr PI (n ≥ 2 for each time point; total n = 6).

2.4.3 Tumour Necrosis Factor-α

A preliminary study injecting TNF-α (4 x10^3 U) into the vitreous yielded no inflammatory response after 24 hr (n = 4). Two larger doses were therefore selected, 1 x10^4 U and 2 x10^4 U. Histology was performed on the smaller dose at 1, 2, 3, 4, 5 and 7 days PI (n = 2 for each time point; total n = 12) and the larger dose at 4 hr, 1, 2, 3, 5 and 7 days PI (n ≥ 2 for each time point; total n = 15).

2.4.4 Interleukin-6

Histology was performed on retina from eyes receiving an intravitreal injection of 1 x10^3 U IL-6 at 1, 2, 4, 8 hr, and 1, 2, and 3 days PI (n ≥ 2 for each time point; total n = 18). Doses of 100 U (n = 4) and 2 x10^3 U IL-6 (n = 2) were also investigated at 24 hr PI.

2.4.5 Ranitidine and Indomethacin

Histology was performed at 24 hr following treatment with IL-1ß and ranitidine (n = 6) or IL-1ß and indomethacin, administered as described above (n = 6).

2.4.6 Galardin™

The retina of animals injected intravitreally with IL-1ß and Galardin™ were examined at 4 and 24 hr PI ($n = 3$ for each time point; total $n = 6$). Animals in the 24 hr time point group also received Galardin™ ($4mg.kg^{-1}$) IP at 6 and 18 hr PI.

2.4.7 Leucocyte Depletion

Following leucocyte depletion, the retina of rats injected intravitreally with IL-1ß were examined after 24 hr ($n = 5$).

2.5 LIGHT AND ELECTRON MICROSCOPY

2.5.1 Fixative

A tannic acid-gluteraldehyde solution (0·5% tannic acid and 2·5% gluteraldehyde in a 0·1M sodium cacodylate buffer, pH 6.9), or Karnovsky's half-strength fixative (1.8% paraformaldehyde; 2% gluteraldehyde; 0.2M sodium cacodylate; 6.5 mM calcium chloride; pH 7.4), were used as fixatives for tissue to be examined by light and electron microscopy.

2.5.2 Fixation Procedure

At each time point described above following intravitreal injection, the animals were deeply anaesthetised with sodium pentobarbitone and the heart exposed. The base of the heart was grasped firmly with toothed forceps and an incision made in the right atrium and at the base of the left ventricle. A cannula attached to a peristaltic pump (Harvard Apparatus Ltd, Kent, UK) was then inserted via the left ventricle into the proximal ascending aorta and the animal perfusion fixed at a rate of $25ml.min^{-1}$ for 5 minutes.

Perfusion fixation allows the preservation of vessel tone, obtains rapid fixation and maintains the structural interactions between the retinal endothelial cells and leucocytes (Raine *et al.*, 1990). The use of immersion fixation results in vessel tone not being sustained and fixes the vasculature in a collapsed state. However, the RPE appears to be better preserved with immersion fixation as this method prevents vacuolation of the

junctional region between the cells seen in perfusion fixed material (Greenwood *et al.*, 1994).

2.5.3 Eye Dissection

After 5 minutes of fixation the eyes were enucleated and placed in fixative overnight at 4°C. The posterior eye cup was dissected from the anterior chamber as follows. An incision was made through the sclera in front of the ciliary body (the limbus) that was then extended 360° with micro-scissors. The cornea, iris and lens were removed en bloc and the posterior eye cups washed in 0.1M cacodylate buffer. The eye cups were then cut into quarters at the level of the optic nerve.

2.5.4 Tissue Processing

The eye quarters were transferred into 7ml glass vials with plastic snap-on lids and washed with distilled water (3 x 10 minutes) followed by post-fixation in 1% osmium tetroxide (OsO_4) for one hour. The specimens were allowed to turn gently on a rotator throughout this and the following processing steps. The tissue was washed in distilled water (3 x 10 minutes), and then dehydrated in increasing concentrations of ethanol (50, 70, 90%) for 10 minutes each, and finally dehydrated in 3 changes of 100% ethanol for 10 minutes each. This was followed by immersion in 100% propylene oxide (2 x 15 minutes) and then a 50/50 mixture of propylene oxide and araldite embedding resin for 3 hours. The Araldite embedding resin was made from a kit (Electron Microscopy Laboratories, Berks, UK) and consisted of 25ml DDSA mixed thoroughly with 20ml CY212 and 0·8ml DMP30 accelerator. The tissue was then immersed in 100%Araldite and left rotating overnight.

The segments of retina were then orientated in fresh resin in labelled plastic moulds and placed at 60°C for 24 hr to polymerise.

2.5.5 Semi-Thin Tissue Sectioning for Light Microscopy

Semi-thin (or thick) sections were cut using a glass knife on an Ultracut E microtome (Leica, Bucks, UK). The semi-thin sections were cut at 0.75μm and transferred from the trough, containing filtered distilled water, to a drop of water on a clean microscope slide with a needle. The slide was then placed on a hotplate and allowed to

dry for at least 5 minutes before flood-staining with 1% toluidine blue/1% aqueous borax solution for 10-15 seconds (ie. until vapour is seen). The slides were then rinsed with distilled water and thoroughly dried on the hotplate before mounting in DPX (Electron Microscopy Laboratories) and viewed by light microscopy.

2.5.5.1 Evaluation of Leucocytic Infiltrate to the Retina

The degree of leucocyte recruitment to the retina following the intravitreal injection of IL-1ß was assessed. The retina was measured with a graticule and the retinal leucocyte infiltrate expressed as the number of migrated cells per mm of inner limiting membrane. This method was used to calculate whether the neutralisation of IL-1ß, leucocyte depletion or the concomitant administration of inhibitors, had any effect on IL-1ß-induced leucocyte recruitment. One section of retina from each experimental animal was selected for leucocyte counting.

2.5.6 Thin Tissue Sectioning for Transmission Electron Microscopy

Thin sections were cut from selected areas using a 1.2mm diamond knife (Leica), "stretched" by waving a chloroform-soaked cotton-tipped stick over the sections, and transferred onto 200 mesh copper grids (Agar Scientific, Essex, UK). After drying at room temperature the sections were double stained with the heavy metals uranyl acetate followed by Reynolds lead citrate. This staining was achieved by placing the grids in a drop of uranyl acetate (10% uranyl acetate in 50% ethanol) for 10 minutes, followed by a wash in 50% ethanol. When the grids were dry they were placed inverted on a drop of lead citrate (2.66% lead nitrate; 3.52% sodium citrate; 16% sodium hydroxide [NaOH]) for 10 minutes. The grids were then thoroughly washed with distilled water and allowed to dry before viewing on a Jeol 1010 transmission electron microscope.

2.5.7 Scanning Electron Microscopy

For scanning electron microscopy (SEM) the tissue was prepared as follows. Following fixation and removal of the eyes as described above, the posterior eye cup was removed. After washing in 0.1M cacodylate buffer the eye cups were embedded in 3% agar just before setting and 100μm sagittal sections cut at the level of the optic nerve on a vibroslice (Campden Instruments Ltd, Loughborough, UK). The sections were processed as before, up to and including the ethanol dehydrating stage. The sections were then

placed in a critical point drier, followed by coating with gold palladium for one minute (to give a layer ~ 9nm) with a K550 sputter coater (Emitech, Kent, UK), and viewed on a Jeol JSM-6100 scanning electron microscope.

2.6 PHOTOGRAPHY

Light micrographs of semi-thin sections were recorded on Ilford FP4+ film (Ilford Ltd, Cheshire, UK) using an Axiophot light microscope with camera (Zeiss, Herts, UK), and the film developed in Ilford Ilfotec HC (diluted 1:31) for 6 minutes at 20°C.

Electron micrographs were recorded on Kodak Electron Microscope Film and developed for 3 minutes at 20°C in Phenisol (diluted 1:4).

Both film types were fixed in Hypam (diluted 1:5) and printed onto Ilford Multigrade photographic paper using an Ilford Multigrade 500H magnifier and Ilford 2150RC processing system.

2.7 IMMUNOHISTOCHEMISTRY

Antibodies for immunohistochemical staining do not generally work on tissue fixed for histology as described above. Immunostaining is therefore often performed on frozen tissue which gives excellent preservation of antigens, but the morphology of the tissue is typically of poor quality, in part due to the thickness of the sections cut. In an attempt to preserve the morphology of the retina, immunohistochemical studies were initially performed on eyes fixed in acetone and embedded in a plastic resin, glycol methacrylate, as previously described (Casey *et al.*, 1988). This technique allows for antigenic preservation combined with superior morphology as thinner sections (2μm) can be cut. However, this technique was found not to produce consistent immunostaining, so frozen material was used for all subsequent immunohistochemistry procedures.

Immunohistochemical analysis on frozen sections was performed to identify the leucocytic infiltrate and to examine MHC Class II expression. For IL-1ß, staining was carried out at 24 hr PI ($n = 4$), and for TNF-α at 1, 2 and 3 days PI 2 x10^4 U ($n \geq 1$ for each time point; total $n = 4$). Animals were killed by asphyxiation in an atmosphere of 100% CO_2. Both eyes (injected and contralateral non-injected) were then rapidly

enucleated, placed in flat bottomed polypropylene capsules in OCT compound (Tissue-Tek; RA Lamb, London, UK) and snap frozen in liquid nitrogen. Samples of spleen were also taken and frozen in the same way as positive controls.

Sections of whole eye were cut at 10μm thickness with a cryostat (600 Cryotome, Anglia Scientific, Cambridge, UK) at -20°C and mounted on 3-amino propyl tri-ethoxy silane (APES; Sigma) coated slides. APES is an adhesive used to bond the sections to the slide and these slides were prepared as follows. Cleaned slides were placed into racks and immersed in a 2% solution of APES in 99% industrial methylated spirit for 10 seconds. This was followed by 5 minute washes in 99% methylated spirit and distilled water respectively after which the slides were left to dry overnight at room temperature. Boxes of APES coated slides were stored at room temperature until required.

To ensure that the sections were correctly orientated, and to see whether an inflammatory cell infiltrate was present or not, 1% toluidine blue-immersed sections were checked by light microscopy. Correctly orientated sections were cut and left to air-dry at room temperature for 1-2 hrs before being stored at -20°C.

2.7.1 Staining Procedure

For immunohistochemical analysis tissue sections were fixed in acetone for 10 minutes at room temperature and then washed for 10 minutes in phosphate buffered saline (PBS, pH 7.4) containing 0.1% BSA. The sections were incubated in 0.3% hydrogen peroxide (H_2O_2; Sigma) in 50% methanol for 10 minutes to suppress endogenous peroxidase activity in red blood cells and leucocytes which can give positive staining by binding to the marking enzyme. The slides then received a 10 minute PBS wash, followed by a 20 minute incubation in non-immune sheep serum (Sigma) for 20 minutes, to prevent non-specific staining. This was followed directly by an incubation with a primary rat anti-mouse monoclonal antibody (*Table 2.1*) for 30 minutes at room temperature. Monoclonal antibodies were used at optimum concentrations as established by titration. After a wash the secondary biotinylated sheep anti-mouse antibody (Sera-Lab, Sussex, UK) was applied to the sections for 30 minutes. Following a further wash the sections were incubated with a preformed avidin and biotinylated HRP macromolecular complex (Vectastain ABC kit; Vector Laboratories, Peterborough, UK) for 60 minutes. The peroxidase reaction was then developed with the chromogenic substrate 3-amino-9-ethylcarbazole (AEC; Sigma) which

Antibody Clone	Specificity	Cluster Designation	Dilution	Source
OX29	anti-rat leucocyte common antigen	CD45	1/20 (ascites)	Serotec, Oxford UK
OX19	anti-rat Pan T-cell	CD5	Neat (supernatant)	Sera-Lab, Sussex UK
W3/25	anti-rat T helper cell	CD4	Neat (supernatant)	*
OX8	anti-rat T cytotoxic cell	CD8	Neat (supernatant)	*
ED1	anti-rat monocytes, macrophages & dendritic cells	-	1/100 (ascites)	Serotec
ED2	anti-rat macrophages	-	1/100 (ascites)	Serotec
MOM/3FI2/F2	anti-rat granulocytes	-	1/2 (supernatant)	Serotec
OX6	anti-rat MHC Class II I-A	-	Neat (supernatant)	*
WT3	anti-rat integrin β_2 subunit	CD18	1/20 (ascites)	Serotec

Table 2.1. Specificity, working dilution and source of primary rat anti-mouse monoclonal antibodies used on frozen sections of retina following intravitreal injection of IL-1β or TNF-α.

* These monoclonal antibodies were prepared from hybridoma cell lines (a generous gift from Dr M. Puklavec, MRC, Oxford, UK). The hybridoma cell lines were cultured for 48 hr in 10% foetal calf serum, RPMI-1640 medium, and the supernatant containing the antibody collected.

forms a red end product upon oxidation. The AEC solution was prepared by adding 1ml of 0.4% AEC in dimethylformamide to 14ml of 0.1M acetate buffer, pH 5.2 (4 parts of 0.1M sodium acetate plus 1 part 0.1M acetic acid). The substrate was filtered and 30% H_2O_2 was added to give a final concentration of 0.03% H_2O_2. Sections were developed in AEC for 5 to 7 minutes, washed in distilled water, counterstained in Mayer's haematoxylin, and blued in running tap water for 5 minutes. Finally, the sections were mounted with a water-based glycerol gelatine medium (DAKO Ltd, Bucks, UK) as the AEC reaction product is alcohol soluble. Sections without primary monoclonal antibody and tissue sections from spleen served as negative and positive controls respectively.

2.8 PERMEABILITY STUDIES WITH HORSERADISH PEROXIDASE

The large molecular weight tracer HRP (Type II; Sigma) was used to demonstrate any permeability histologically following injection of IL-1ß at 24 and 48 hr PI ($n \geq 2$ for each time point; total $n = 6$), and at 5 and 7 day PI TNF-α (2×10^4 U; $n = 2$ for each time point; total $n = 4$). As a positive control, animals received an intravitreal injection of 10µl 1M H_2O_2 ($n = 3$) and HRP infused after 2 hr, to demonstrate that the HRP reaction product can be visualised following barrier disruption.

2.8.1 Experimental Procedure

HRP (50mg dissolved in 200µl of saline) was infused via the cannulated femoral vein. After 15 minutes the animal was perfused with one-half strength Karnovsky's fixative via the proximal ascending aorta as described above. Following removal of the eyes and fixation overnight at 4°C the posterior eye cup was removed as before. After washing in 0.1M cacodylate buffer the eye cups were embedded in agar and 100µm sections cut with the vibroslice as described above. The sections were then incubated with diaminobenzidine (DAB; Sigma; 0.15% DAB in 0.05M tris-HCl and 0.01% H_2O_2; pH 7.4) for 10 minutes to produce the electron-dense HRP reaction product. The reaction was stopped by washing with distilled water. After thorough washing, the sections were osmicated and processed up to araldite for electron microscopy as described. Following the overnight incubation in 100% araldite, the sections were embedded in resin between two aluminium-foil coated glass slides. After the resin had polymerised at 60°C, the slides

were separated and small blocks of retina cut from the flat 100µm sections, and glued onto trimmed resin stubs. Semi-thin sections were cut and viewed under the light microscope. Thin sections were then cut from selected areas and placed on copper grids. The sections were viewed unstained and stained with uranyl acetate/Reynolds lead citrate on a Jeol 1010 transmission electron microscope.

2.9 PERMEABILITY STUDIES WITH [^{14}C]-MANNITOL

The small molecular weight tracer [^{14}C]-mannitol (184 kDa) and the sensitive steady-state technique was used to quantitatively demonstrate any permeability following the intravitreal or intra-arterial injection of an agent.

2.9.1 Controls

Permeability studies were performed on animals that had not received an intravitreal injection ($n = 4$), and on those receiving intravitreal vehicle control at 4 and 24 hr PI ($n \geq 4$ for each time point; total $n = 14$). The effect of a sham injection on the BRB was also assessed at 4 hr and 24 hr PI ($n = 6$ for each time point).

As a positive control [1.8M] arabinose ($n = 8$) was infused via the cannulated internal carotid artery. Hyperosmolar arabinose is known to cause hyperosmotic opening of the BRB and BBB when delivered via the intracarotid artery (Greenwood, 1992b) and was used here to demonstrate that this technique was efficient in measuring increases in blood-CNS barrier permeability.

2.9.2 Cytokines

Interleukin-1β

An extensive time course study was performed to examine the effect of intravitreal IL-1ß (1-2 x10^3 U) on the permeability of the BRB, at 0, 1, 2, 4, 8, 12, 18 hr, and 1, 1.5, 2, 3, 5, and 7 days PI ($n \geq 6$ for each time point; total $n = 118$).

Permeability of the BRB was also assessed following an intravitreal injection of 1-2 x10^3 U IL-1ß incubated with αIL-1Ab (10mg.ml^{-1}) at 4 and 24 hr PI ($n \geq 6$ for each time point; total $n = 13$).

Tumour Necrosis Factor-α

The effect of two doses of TNF-α on the integrity of the BRB was investigated. Following the intravitreal injection of 1 x10⁴ U, the permeability of the BRB was measured at 1, 2, 3, and 4 days PI ($n = 4$ for each time point) and at 4 hr, 1, 2, 3, 5, 7, 9, and 14 days PI of 2 x10⁴ U ($n \geq 6$ for each time point; total $n = 71$).

Interleukin-6

Following intravitreal IL-6 (1 x10³ U), BRB permeability was assessed at 4 hr, 1, 2, and 3 days PI ($n = 4$ for each time point).

2.9.3 Histamine

The effect of histamine on the permeability of the BRB and BBB was investigated by administrating histamine to the vitreous or via a cannulated external carotid artery, and measuring the integrity of the barriers after a short delay (up to 30 minutes PI).

The effect of intravitreal histamine on the permeability of the BRB was examined following the injection of each concentration (1 x 10^{-3} M, 1 x 10^{-4} M, and 1 x 10^{-5} M), at time 0 (by beginning the mannitol infusion immediately after the intravitreal injection was given; $n = 4$ for each dose; total $n = 12$), at 15 minutes PI ($n \geq 3$ for each dose; total $n = 11$), and at 30 minutes PI ($n = 4$ for each dose).

The effect of administering histamine to the luminal aspect of the BRB and BBB via the carotid artery was measured for each of the three concentrations at 0 ($n \geq 4$ for each dose; total $n = 14$), at 15 minutes post-administration ($n \geq 4$ for each dose; total $n = 13$), and at 30 minutes post-administration ($n = 4$ for each dose).

The effect of intravascular administration of histamine was examined because it is well known that this compound acts rapidly, therefore the animal can remain anaesthetised for the whole experiment. Recovery experiments for carotid cannulations are not feasible.

2.9.4 Inhibitor Studies

Ranitidine

BRB integrity was assessed at 4 and 24 hr PI in animals treated with IL-1ß and ranitidine as previously described ($n \geq 5$ for each time point; total $n = 11$).

Indomethacin

BRB permeability was evaluated at 4 and 24 hr PI in animals treated with IL-1ß and indomethacin as previously described ($n \geq 8$ for each time point; total $n = 15$).

Galardin™

Following the injection of IL-1ß with 100μM Galardin™, the permeability of the BRB was measured at 4 and 24 hr PI ($n \geq 5$ for each time point; total $n = 11$). The integrity of the BRB was also assessed at 24 hr following the intravitreal injection of IL-1ß and Galardin™ as before, and accompanied by 4mg.kg⁻¹ Galardin™ administered IP at 6 and 18 hr PI ($n = 4$).

2.9.5 Leucocyte Depletion

Following leucocyte depletion and the intravitreal injection of IL-1ß, the permeability of the BRB was measured at 4 and 24 hr PI ($n \geq 5$ for each time point; total $n = 11$).

2.9.6 Experimental Procedure

The anaesthetised rat was laid on its back on a small operating table, heated and maintained at 37°C, and the hind legs taped down securely. The left femoral artery and vein were exposed and the vessels separated from the connective tissue using fine watchmaker forceps and tied off with surgical thread at the base of the exposed part of each vessel. The upper part of the exposed vessel was then clamped and an incision made just above the lower tie with Van Ness scissors. This opening was then stretched using fine watchmaker forceps to allow insertion of polythene cannulae (Portex, Kent, UK), filled with heparinised isotonic saline, which were tied securely in place. Heparin

(50U/ml; Sigma) was then infused via the artery to prevent blood clotting in the cannula (0.5ml) and to allow withdrawal of blood samples. Blood pressure measurements were made by connecting the arterial cannula to a strain gauge transducer (Lectromed, Herts, UK).

To administer histamine to the luminal side of the vasculature, the external carotid artery was exposed and a cannula inserted retrogradely as previously described (Rapoport, 1977). The common carotid was then clamped and the histamine solution injected into the internal carotid. The clamp was then removed to resume normal blood flow.

The small molecular weight tracer, D-1-$[^{14}C]$-mannitol (Amersham International, Bucks, UK) diluted in sterile isotonic saline to give a concentration of $740kBq.ml^{-1}$, was infused via the femoral cannula for 20 minutes at a rate sufficient to rapidly achieve and maintain constant plasma levels (Deane *et al.*, 1984; Luthert *et al.*, 1986). This is accomplished by a syringe drive delivering a continuous injection of $[^{14}C]$-mannitol, given at a rate which is adjusted by a predetermined program, so as to replace the tracer at the rate at which it leaves the circulation (*Fig. 2.1*). An infusion of $[^{14}C]$-mannitol with steady plasma levels is used to enable simple calculation of the tracer concentration presented to the vascular bed over a given period of time. It also reduces backflux of accumulated tracer that may occur from the retina if plasma levels had fallen, which could happen if a single bolus of tracer was given. Arterial blood samples were taken at 2, 10 and 18 minutes, and measured for pCO_2, pO_2 and pH using a pH blood-gas analyser (Ciba Corning, Essex, UK). Towards the end of the mannitol infusion, the jugular veins were exposed and cut at 20 minutes, and the blood washed out of the vasculature rapidly by a forced intra-arterial injection of isotonic saline. The animal was then killed by decapitation and the eyes enucleated.

2.9.7 Eye Dissection

Under the dissection microscope, an incision was made into the eye with a microscalpel through the sclera behind the ciliary body at the level of the ora serrata. The incision was extended 360° using micro-scissors and the cornea, lens, iris and ciliary body removed en bloc. The vitreous was removed by gently lifting with fine watchmaker forceps and placed in a tared plastic 20ml scintillation vial (National Diagnostics, Humberside, UK). The retina was dissected free from the choroid and sclera and the optic

nerve cut, and the retina placed in another tared vial and weighed. The whole procedure was conducted rapidly (~ 1 minute) to ensure minimal cross-contamination between the vitreous and retinal samples. This rapid dissection protocol has previously been shown to prevent contamination of the retina via leakage into the vitreous from the more permeable blood aqueous barrier (Lightman *et al.*, 1987a). The brain was also removed and samples of left and right cerebrum taken, which were also placed in separate tared vials.

2.9.8 Sample Preparation for Radioactivity Analysis

All the tissue samples were weighed to 5 decimal places (g) using a sensitive electronic balance (Sartorius, Surrey, UK). The blood samples were centrifuged and two $50\mu l$ samples of plasma taken from each using a Gilson micropipette. All the samples were digested at 60°C in 1ml of Soluene-350 (Canberra Packard, Berks, UK). The samples were then prepared for scintillation counting by adding 12ml Hionic-Flour scintillant (Canberra Packard). The ß emissions were then counted using a Tri-Carb liquid scintillation analyser (Canberra Packard).

Retinal permeability was then expressed as the ratio:

$$\frac{\text{Radioactivity.g}^{-1} \text{ tissue (Rt)}}{\text{Mean radioactivity.ml}^{-1} \text{ blood plasma (Rp)}}$$
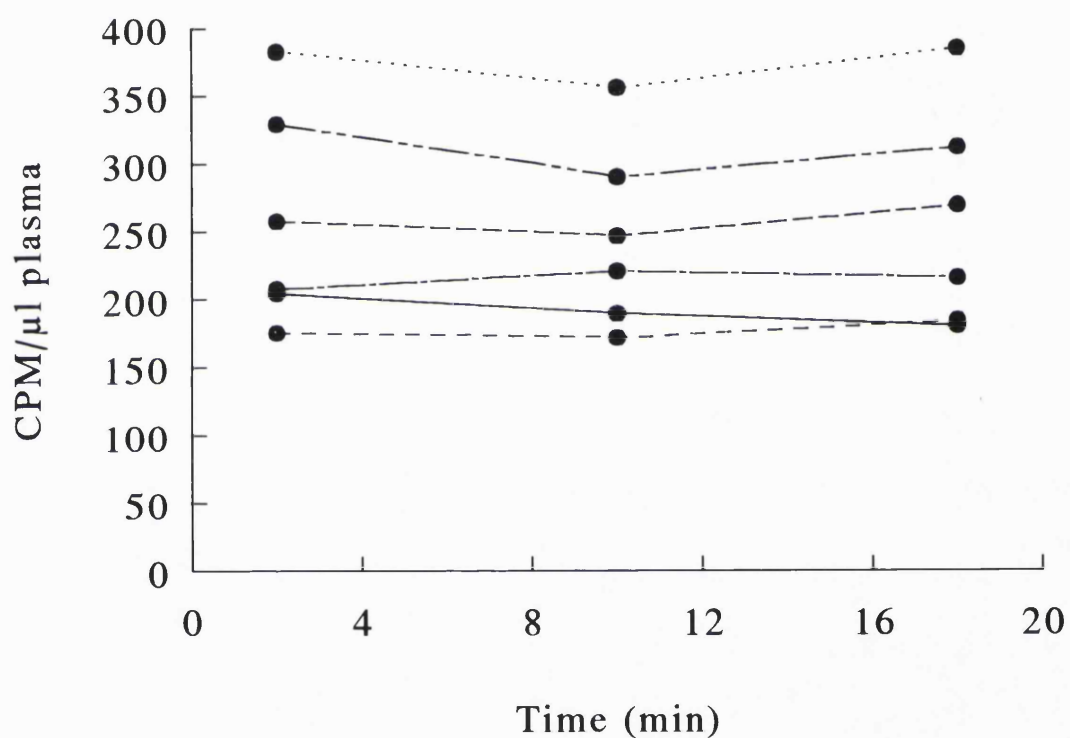
Figure 2.1. *Representative examples of the 3 plasma radioactivity levels, demonstrating the steady level of [^{14}C]-mannitol present in the plasma of each animal, which is maintained throughout the duration of each experiment. CPM = counts per minute.*

2.10 PREPARATION OF RAT RETINAL MICROVESSEL EC

Confluent monolayers of rat retinal EC (REC) were cultured to investigate the ability of cytokines to stimulate REC to produce cyclooxygenase (Cox) metabolites or histamine *in vitro*. Measurement of the eicosanoid PGE_2 was selected as an indicator of Cox metabolism as this is a stable metabolite. The REC cultured using the following method have previously been fully characterised (Greenwood, 1992a).

2.10.1 Buffers

Handling Buffer

The handling buffer was prepared from 100 ml HBSS (Ca^{2+} and Mg^{2+} free) containing 10 mM HEPES and 200 U/ml penicillin/streptomycin and gassed for 10 minutes with oxygen enriched gas (95% O_2 plus 5% CO_2), after which 2.272ml of 22% BSA solution (Advanced Protein Products Ltd (APP), West Midlands, UK) was added. The pH of the buffer was adjusted with 1M NaOH to approximately 7.2 by eye with the indicator phenol red.

Digestion Buffer

The digestion buffer consisted of 5ml collagenase/dispase (Boehringer Mannheim) supplemented with 0.147µg.ml^{-1} of the clostripain inhibitor tosyl-lysine-chloromethylketone (TLCK; Sigma) and 200 U/ml DNAse I (Sigma Type II; Sigma).

Percoll Gradient

Percoll solution (Sigma) was autoclaved before preparing the gradient mixture. 50ml of Percoll was mixed with 45ml of HBSS, and 5ml of 10x concentrated HBSS to restore the osmolarity.

Centrifuge Tubes

High speed centrifuge tubes (Sorvall Instruments, Du Pont, USA) were sterilised with 75% ethanol. After washing, the tube was coated for at least 2 hr with handling

buffer. To establish a gradient, 7ml of the Percoll solution was added to the tube and centrifuged for 1 hr at 25,000g in a high speed centrifuge (Heraeus-Suprafuge 22, Osterode, Germany).

2.10.2 Culture Medium

HAMS F-10 medium supplemented with 17.5% plasma derived serum (PDS; APP), $7.5\mu g.ml^{-1}$ of endothelial cell growth supplement (ECGS; APP), $80\mu g.ml^{-1}$ of heparin (Sigma), 2mM glutamine (Sigma), $0.5\mu g.ml^{-1}$ of vitamin C (L-ascorbic acid; Sigma) and 100 U/ml of penicillin/streptomycin was used for EC cell cultures.

2.10.3 Isolation of Retinal Microvessels

For each preparation 6 Lewis rats were killed by CO_2 asphyxiation. The eyes were removed using sterilised scissors and placed into handling buffer cooled on ice. Under sterile conditions, eyes were dissected using a dissecting microscope. The cornea, lens and vitreous body were carefully removed and the retinas were transferred into handling buffer at 4°C.

The retinas were incubated for 1 hr in 5ml digestion buffer at 37°C. The digested tissue was centrifuged for 15 minutes at 1000g in 22% BSA solution to remove contaminating lipids. The pellet containing microvessels was resuspended and incubated for a further 1 hr in 5ml digestion buffer to separate the pericytes from the microvessels. At the end of the incubation, the digestion buffer was removed after centrifugation and the tissue pellet was resuspended in 1ml of handling buffer.

The suspension was then loaded onto the pre-formed Percoll gradient and centrifuged for 15 minutes at 1000g. The microvessel layer (at about 1/3 from the bottom of the Percoll solution) was aspirated using a sterile pasteur pipette and transferred into handling buffer. Following a wash, the microvessel fragments were resuspended in culture medium.

2.10.4 Cultures

24 well plates (Nunclon; Gibco, Renfrewshire, UK) were used for cell cultures. Prior to use, the plates were coated for at least 2 hr at room temperature with collagen solution (approximately $40\mu g.cm^{-2}$). Excess collagen solution was removed and the plates

were placed in ammonia vapour for 30 minutes to fix the collagen coating. After washing three times with HBSS, the plates were ready for use.

The isolated microvessel fragments resuspended in culture medium were placed onto the culture plates and maintained at 37°C in 5% CO_2 and washed with HBSS and fed with fresh medium every 3 days until confluent EC monolayers had formed.

2.11 PULSING ENDOTHELIAL CELLS WITH CYTOKINES

Supernatants were collected from confluent monolayers of REC either from control (unstimulated), or stimulated with 5, 10 or 20 U/ml IL-1ß for 24 hr (n ≥ 2; total n = 12), or IL-1ß (5 or 10 U/ml) and the cyclooxygenase inhibitor, indomethacin ($5\mu g.ml^{-1}$), or indomethacin ($5\mu g.ml^{-1}$) alone ($n = 2$ for each; total $n = 6$). Endothelial cells were also pulsed with 100, 200 or 300 U/ml TNF-α ($n \geq 3$; total $n = 10$), and 5, 10 or 20 U/ml IL-6 for 24 hr ($n \geq 3$; total $n = 10$). The supernatants were stored in cryovials at -70°C until ready for measurement of PGE_2 production by radioimmunoassay or histamine production by enzyme immunoassay.

2.12 PGE₂ RADIOIMMUNOASSAY

Samples of supernatant (100μl) were placed in labelled vials in duplicate. Polyclonal rabbit anti-PGE_2 antibody (200μl, diluted 1:2000 in phosphate buffer containing 0.1% γ-globulin; Zeneca, Cheshire, UK) was added, followed by 100μl of radiolabelled PGE_2 ($^3H_7$-PGE_2, Amersham International), containing 370Bq of radioactivity, mixed well using a Whirlimixer and left overnight at 4°C. Dextran coated charcoal in phosphate buffer was then added (200μl; 0.5% dextran, 1.0% charcoal; Norit GSX; BDH, Leics, UK) and mixed well (any unbound radiolabelled PGE_2 binds to the charcoal). After 15 minutes the samples were spun down at 3000 rpm for 10 minutes at 4°C. The supernatants were decanted into 4ml of liquiscint scintillant and the radioactivity analysed using a Tri-Carb liquid scintillation analyser (Canberra Packard).

A standard curve was assayed by using a stock solution of PGE_2 in decreasing concentrations in EC growth medium (*Fig. 2.2*). The results of the scintillation counts were expressed in disintegrations per minute (DPM), which were read from the standard

curve to give the PGE$_2$ content in each 100µl sample. This was then divided by 10 to give the concentration in pg.ml^{-1}.

2.13 HISTAMINE ENZYME IMMUNOASSAY

A specific enzyme immunoassay kit (Coulter Electronics, Bedfordshire, UK) was used for detection of histamine from rat REC following stimulation with IL-1ß. Supernatant and standard samples (100µl) were added to acylated Eppendorf vials and incubated at room temperature for 30 minutes. 50µl of each sample was then added to wells of a 96 well microtitre plate, precoated with monoclonal antihistamine antibody. Histamine-acetylcholinesterase conjugate (200µl) was then added to each well and incubated at 4°C for 18 hr. Following 3 rinses with wash solution, 200µl of chromogenic substrate was added and the plate incubated at room temperature in the dark for 20 minutes. The enzymatic reaction was then stopped and the absorbance read at 405 nm against a substrate blank. Histamine concentrations were then extrapolated from the standard curve (*Fig. 2.3*).

2.14 STATISTICS

A superficial view of the distribution of the data indicated that some might be abnormally distributed. Therefore, each group of data was tested for normal distribution using the Shapiro-Wilks and the K-S (Lilliefors) tests for normality. The normality assumption was rejected when the significance level was less than 5% for both tests. If the data was normally distributed, the parametric unpaired two-sample *t* test was used to compare groups of data. However, if the data was abnormally distributed, the non-parametric Mann-Whitney U test was applied. All statistics were calculated using the computer package MINITAB. A *p* value of <0.05 was considered significant.
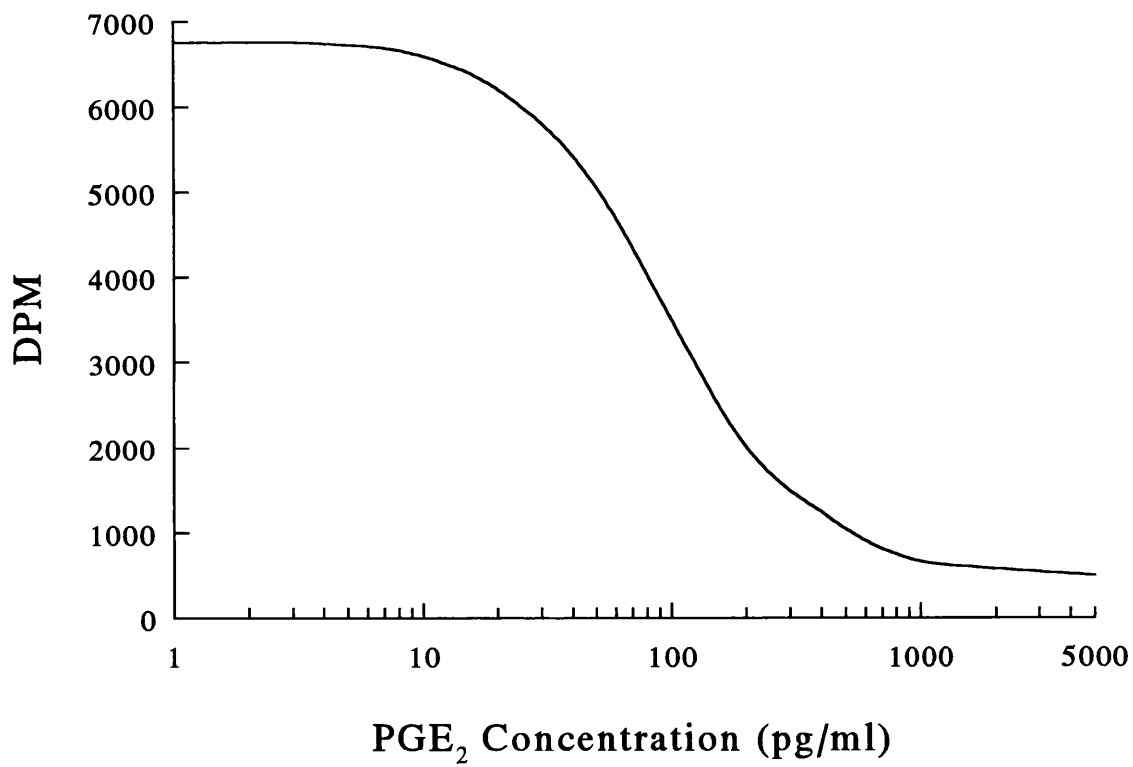
Figure 2.2. Standard curve created by increasing dilutions of PGE$_2$ antibody from which the amount of unknown PGE$_2$ in each sample can be calculated.
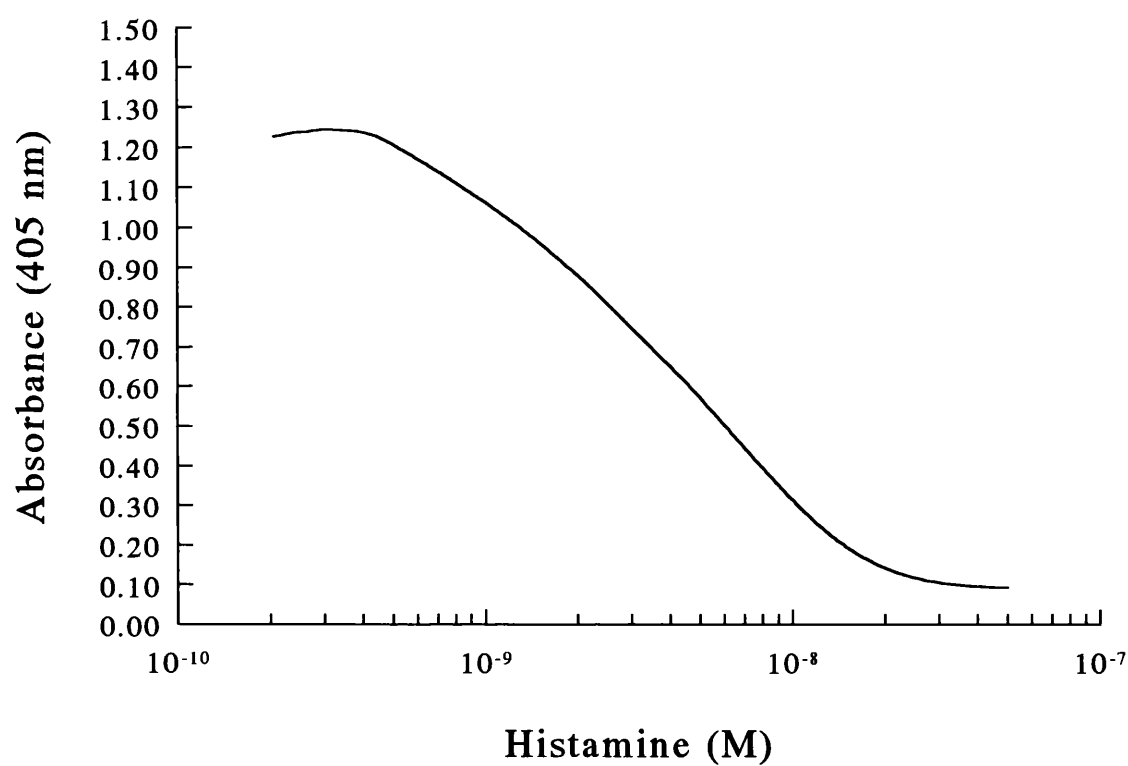
Figure 2.3. Standard curve created by increasing dilutions of histamine antibody from which the amount of unknown histamine in each sample can be calculated.

CHAPTER THREE

RESULTS

CONTROLS

3.1 CONTROLS

3.1.1 Histology

Toluidine blue stained semi-thin resin sections of retina from vehicle- and sham-injected control eyes were examined for leucocyte infiltration and pathology to the retina. At 4 hr post-injection (PI) of vehicle control, very few PMN and MN leucocytes were observed within the lumen of retinal blood vessels. However, no leucocytes were found at either 24 or 48 hr PI, nor was there any evidence of leucocyte recruitment in the ciliary body or vitreous at any time point following vehicle or sham injection. The structure of the retina appeared normal with no obvious tissue injury resulting from the control intravitreal injections. In the choroid, a few leucocytes were observed adhering to the vessel walls but in a similar number to those found in the non-injected eyes.

3.1.2 BRB Permeability to HRP

Following the intravitreal injection of 10μl of 1M H_2O_2, extravasated HRP was detected flooding the basement membrane of blood vessels within the retina (*Fig. 3.1.1*), and also present within the tissue parenchyma. No extravasated HRP was detected in the neuroretina of non-injected control eyes. Extravasated HRP was occasionally observed within the basement membrane of vessels from the choriocapillaris, and of the ciliary vasculature and surrounding the fenestrated vessels of the ciliary body of non-injected eyes.

Figure 3.1.1. *TEM of a retinal vessel, at 2 hr PI of 1M H_2O_2. Extravasated HRP can be observed flooding the basement membrane* (arrows). (Bar = 1μM)

3.1.3 BRB Permeability to [^{14}C]-Mannitol

During the experiments for physiological assessment of the integrity of the BRB, using the small molecular weight tracer [^{14}C]-mannitol, blood pressure and blood-gas and pH measurements were made to ensure that the animals remained normotensive and normoxic throughout the course of each experiment (*Tables 3.1.1 & 3.1.2*). The blood pressure trace (*Fig. 3.1.2*) typically remained constant until after the 10 minute blood sample was withdrawn, when the jugular veins were exposed, where in the majority of animals, the blood pressure dropped but returned to normal levels within 2-3 minutes.

The mean mass of the retina and vitreous samples obtained from the control animals when the eyes were dissected was 6.773 ± 0.233 mg and 6.273 ± 0.474 mg, respectively (mean ± SEM; $n = 36$).

The ratio of tissue to plasma radioactivity (Rt/Rp) found in non-injected animals was 0.02125 ± 0.0192 for the retina and 0.01263 ± 0.00091 for the vitreous (mean ± SEM; $n = 8$). However, following an intravitreal injection of vehicle control there was a significant increase in the Rt/Rp ratio of the retinal and vitreous samples at 4 hr PI, when compared to the non-injected eyes ($p < 0.05$), but there was no significant difference observed at 24 hr PI (*Fig. 3.1.3a*). Following a sham injection at 4 and 24 hr PI there was a significant difference in BRB permeability when compared to the non-injected controls in the vitreous samples only, at both time points studied (*Fig. 3.1.3b*). These increases, however, were not significantly different from the vehicle control injected eyes.

The mean Rt/Rp ratio for the brain samples from the non-injected and vehicle control injected animals was 0.0108 ± 0.0004 (mean ± SEM; $n = 20$) and serves as an internal control to verify the efficacy of the saline washout of radiolabelled blood from the vasculature.

Following the administration of 1.8M arabinose, delivered as a bolus via the carotid artery, a significant increase in BBB ($p < 0.001$) and BRB ($p < 0.05$) permeability was observed (*Fig. 3.1.4*).

n	Systole (mmHg)	Diastole (mmHg)
20	110.95 ± 2.81	89.85 ± 2.27

Table 3.1.1. Mean arterial blood pressure measurements from non-injected and vehicle control injected animals at the beginning of each [^{14}C]-mannitol experiment. Values are means $\pm$ standard error means (SEM).

n	pH	pCO_2 (kPa)	pO_2 (kPa)	% O_2
20	7.38 ± 0.01	6.18 ± 0.22	9.70 ± 0.22	93.3 ± 0.66

Table 3.1.2. Mean pH and blood gas levels (partial pressure of carbon dioxide (pCO$_2$), partial pressure of oxygen (pO$_2$) and % oxygen saturation (% O$_2$)) from non-injected and vehicle control injected animals. Measurements were taken at 2, 10 and 18 minutes throughout the course of the [^{14}C]-mannitol infusion. Values are means $\pm$ SEM.
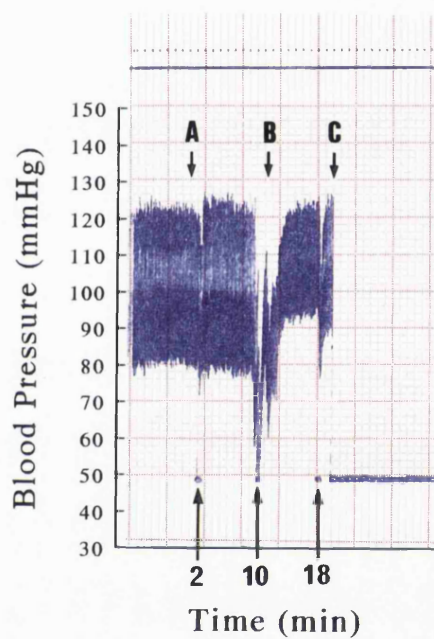
Figure 3.1.2. *Trace of a typical blood pressure measurement made during a 20 minute [^{14}C]-mannitol infusion. The infusion began at point A and the jugular veins were exposed at point B, which was accompanied by a transient decrease in blood pressure. At point C the arterial cannula was transferred to the saline washout device. Blood samples were collected at 2, 10 and 18 minutes* (arrows).

89

a

b
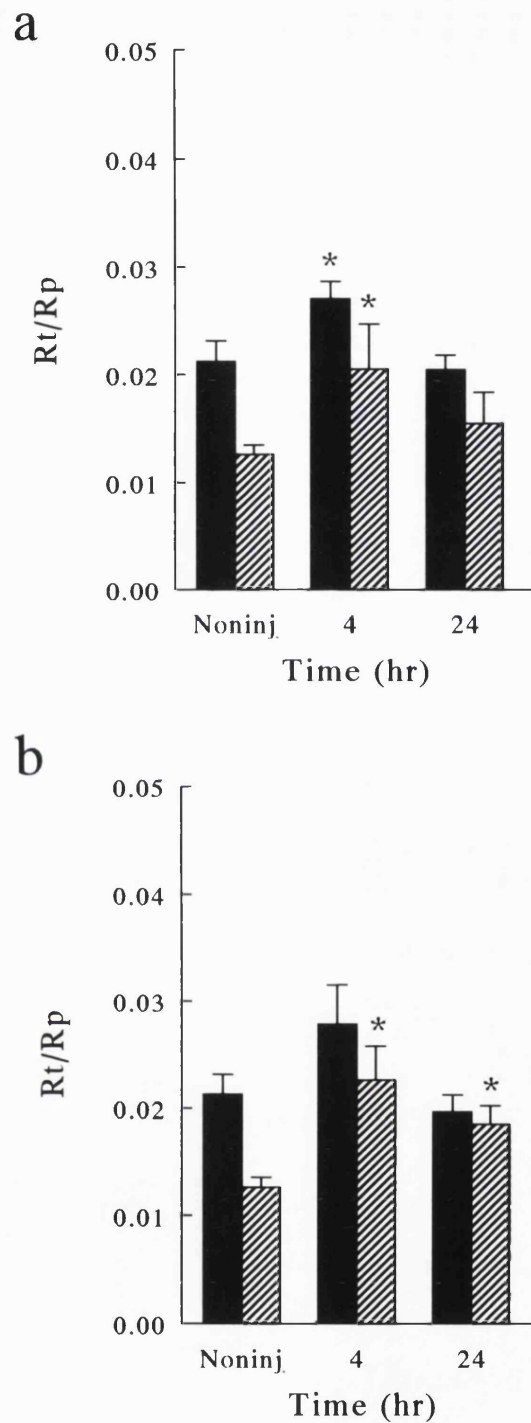
Figure 3.1.3a. Following the intravitreal injection of vehicle control (saline + 0.1% BSA) there was a significant increase in BRB permeability at 4 hr PI, as expressed by an increase in the Rt/Rp ratio for retina (solid bars) and vitreous (hatched bars), when compared to non-injected control values (Noninj.). **3.1.3b.** Following a sham injection, there was a significant increase in the Rt/Rp ratio of the vitreous samples (hatched bars), but not in the retina (solid bars), when compared to non-injected control values. The sham values were not significantly different from the vehicle-injected values. *p <0.05 .
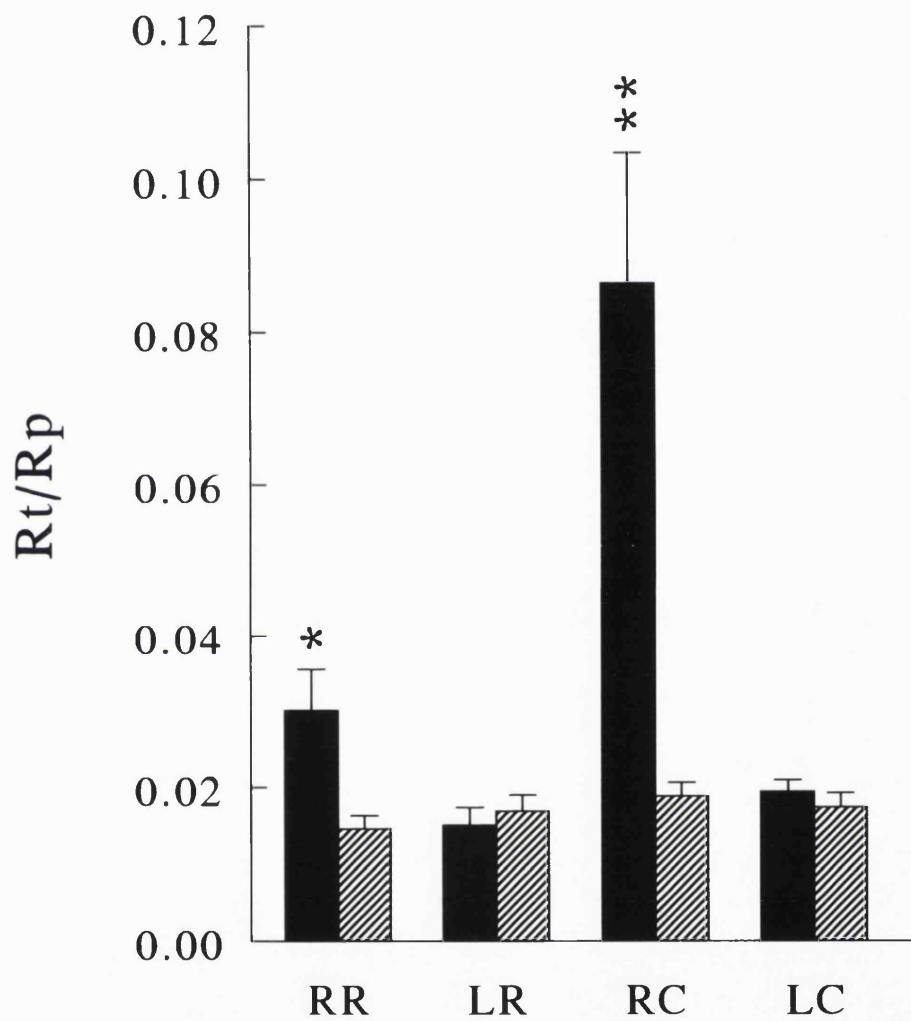
Figure 3.1.4. *Following the administration of 1.8M arabinose via the right carotid artery, a significant increase in BRB and BBB permeability was detected in the right retina and right-hand side of the brain only* (solid bars). *No significant increase in barrier permeability was seen following the infusion of saline administered via the same route* (hatched bars). **p* <0.05; ***p* <0.01. (**RR:** right retina; **LR:** left retina; **RC:** right cerebrum; **LC:** left cerebrum)

INTERLEUKIN-1ß

3.2 INTERLEUKIN-1ß

3.2.1 Histology

3.2.1.1 Light Microscopy

The preliminary dose dependency study revealed only a minor leucocytic infiltrate to the retina at 24 hr PI using doses of 200-400 U and lower. However, the intravitreal injection of 1-2 x10^3 U IL-1ß produced a substantial and reproducible inflammatory cell infiltrate within the retina at 24 hr PI. Toluidine blue stained semi-thin resin sections of retina from intravitreally injected rats were subsequently examined for structural changes and leucocyte infiltration over a 14 day time course using this dose.

Following intravitreal injection of IL-1ß, no leucocytes were observed within the retinal blood vessels or parenchyma at either 15 min or 1 hr PI. At 2 hr PI, MN cells were occasionally seen, but mainly within blood vessels of the retina.

By 4 hr PI, both PMN and MN leucocytes were found in the retina adhering to the endothelium of vessels (*Fig. 3.2.1a*) in numbers that greatly exceeded those seen in the vehicle injected controls. Occasionally, leucocytes were also present in the parenchyma. Over the next 14-24 hr there was a gradual increase in the number of extravasated leucocytes, especially in the perivascular region, and haemorrhagic lesions were observed (*Fig. 3.2.1b* & *Fig. 3.2.2a*). In some animals increased numbers of leucocytes were present in the choroid (*Fig. 3.2.1b*). The leucocytic infiltrate reached a peak at between 24 and 48 hr PI (*Fig. 3.2.2b*). At this time, inflammatory cells were present in large numbers within the retinal vessels and in the tissue parenchyma, where they extended from the inner limiting membrane to the rod outer segments. Many leucocytes were also seen in the vitreous, with more MN present than PMN.

The number of migrated leucocytes within the retinal parenchyma per mm of inner limiting membrane was calculated at 24 hr PI from IL-1ß injected eyes (*n* = 5). There was a mean of 59.49 ± 9.33 migrated cells per mm inner limiting membrane at 24 hr PI.
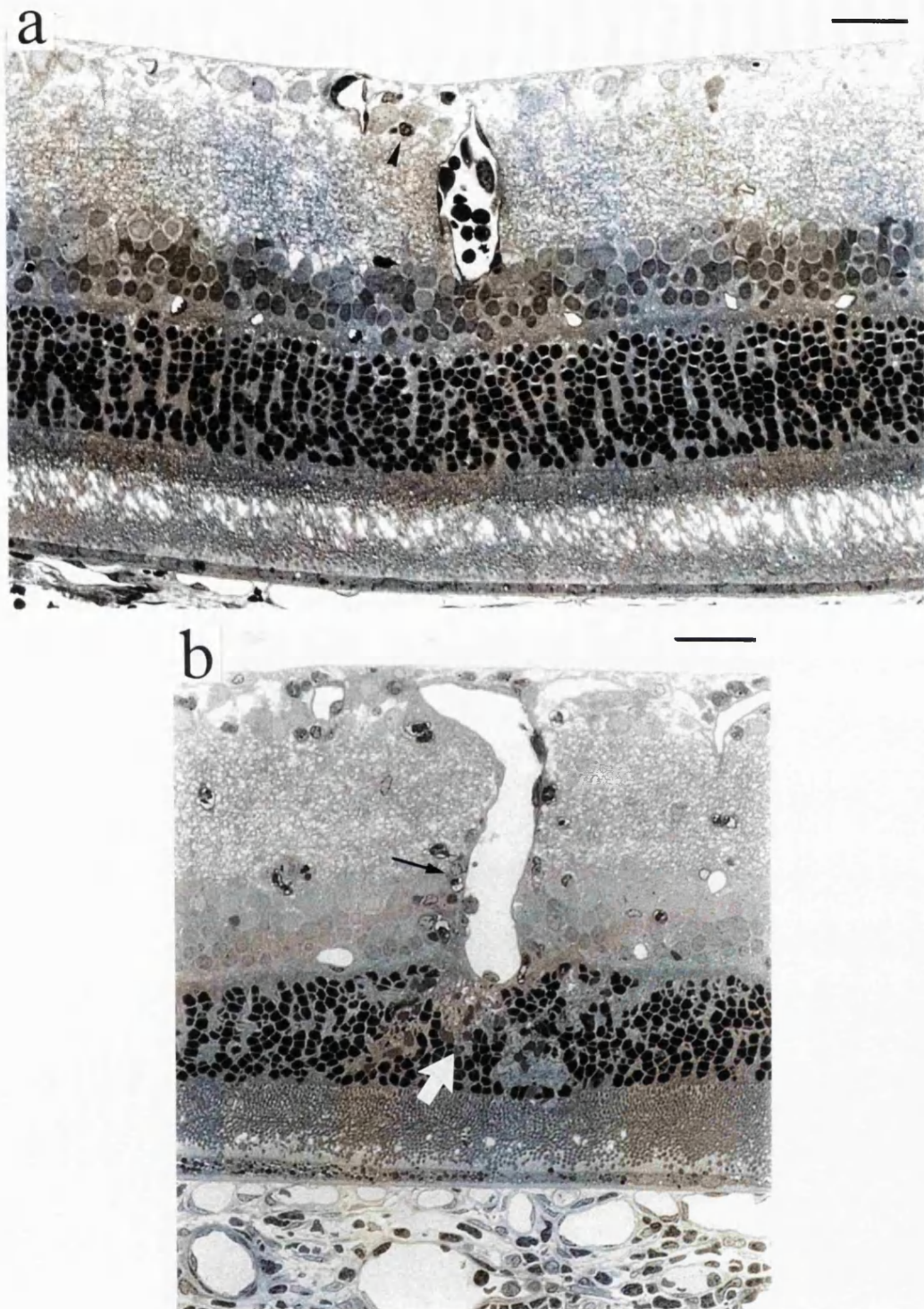
Figure 3.2.1. *Toluidine blue stained resin sections of retina following the intravitreal injection of IL-1ß.* **a.** *4 hr PI. Leucocytes are adhering to the endothelium of a blood vessel and are occasionally seen within the tissue parenchyma* (arrow head) (Bar = 25μM). **b.** *18 hr PI. Adherent cells are present and there is perivascular cuffing of inflammatory cells* (arrow). *Red blood cells are present within the parenchyma and there is a substantial oedematous appearance to the outer nuclear layer* (white arrow). *Note increased presence of leucocytes within choroid* (Bar = 25μM).
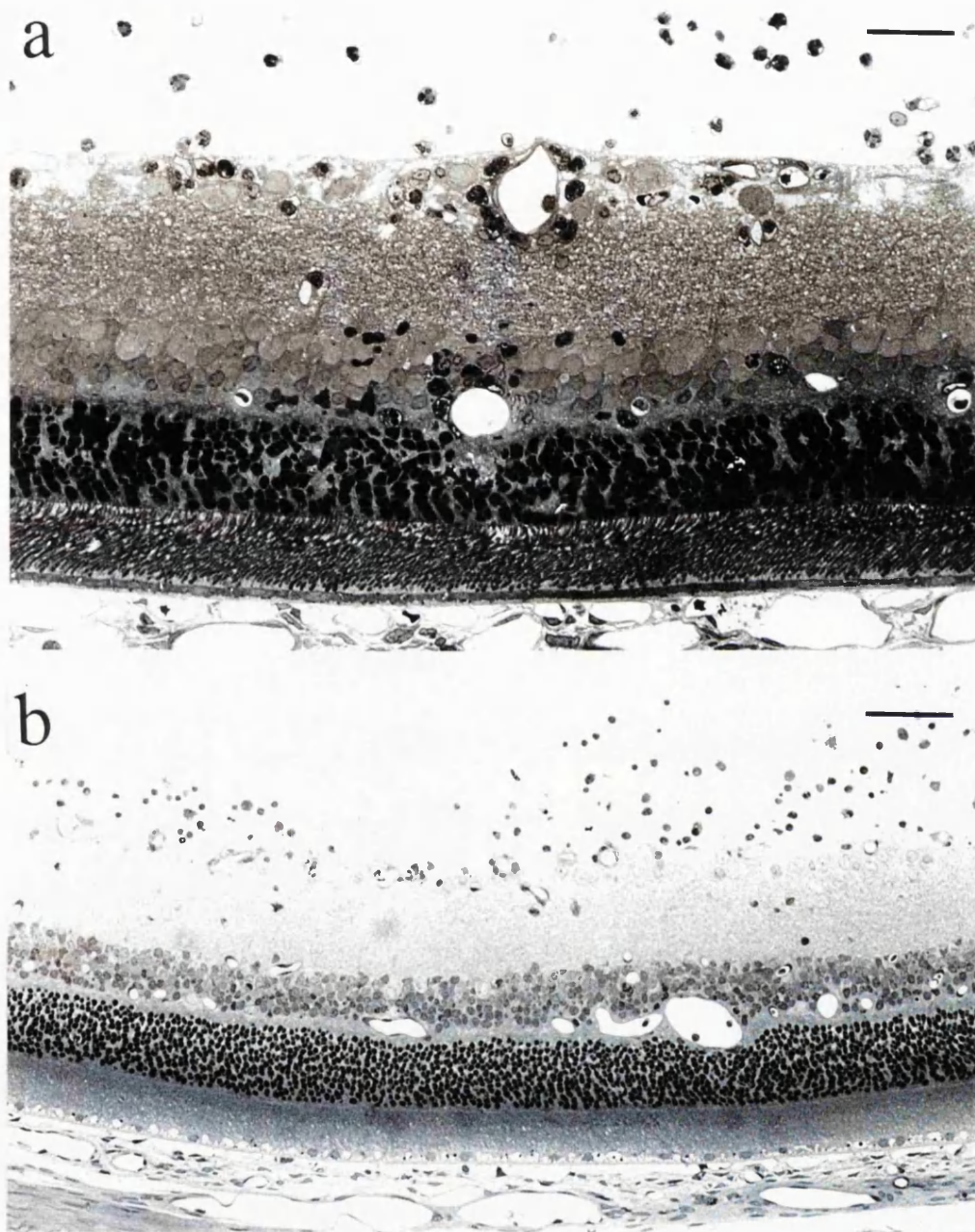
Figure 3.2.2. *Toluidine blue stained resin sections of retina following intravitreal IL-1β.*
a. 18 hr PI. Leucocytes can be seen within the retinal parenchyma, cuffing blood vessels
and in the vitreous (Bar = 25μM). *b. 48 hr PI, during peak of the inflammatory response.*
Numerous leucocytes are present in the vitreous, and throughout the tissue parenchyma
(Bar = 50μM).

96

Leucocytes were occasionally seen in the RPE layer but were almost always adjacent to the ciliary body from where they were believed to have originated (*Fig. 3.2.3a*). Leucocytes in the RPE layer, and within the rod outer segments, can be seen more clearly in a transmission electron microgaph (TEM) (*Fig. 3.2.3b*). There was no evidence of leucocytes migrating across the posterior aspect of the BRB from the choroidal circulation.

At 72 hr PI the large scale cellular infiltrate was still present (*Fig. 3.2.4a & b*), although by 5 days PI only a few MN cells could be detected within the retinal parenchyma, vitreous and ciliary body (*Fig. 3.2.5a*). By 7 days PI, only occasional leucocytes could be found, primarily within the vitreous (*Fig. 3.2.5b*), and no cells could be seen at all by 14 days PI.

IL-1ß neutralised with αIL-1ß Ab and injected intravitreally induced a reduced inflammatory response at 24 hr PI with cells, predominantly PMN and occasionally MN in appearance, present within the retinal parenchyma and vitreous, but rarely within the lumen of blood vessels. The number of migrated cells was counted (26.40 ± 3.92 cells per mm of inner limiting membrane; mean ± SEM; $n = 4$) and found to be significantly decreased from the number of migrated cells seen at 24 hr PI IL-1ß ($p < 0.01$). No cells were seen within the retina at 4 hr PI of neutralised IL-1ß.
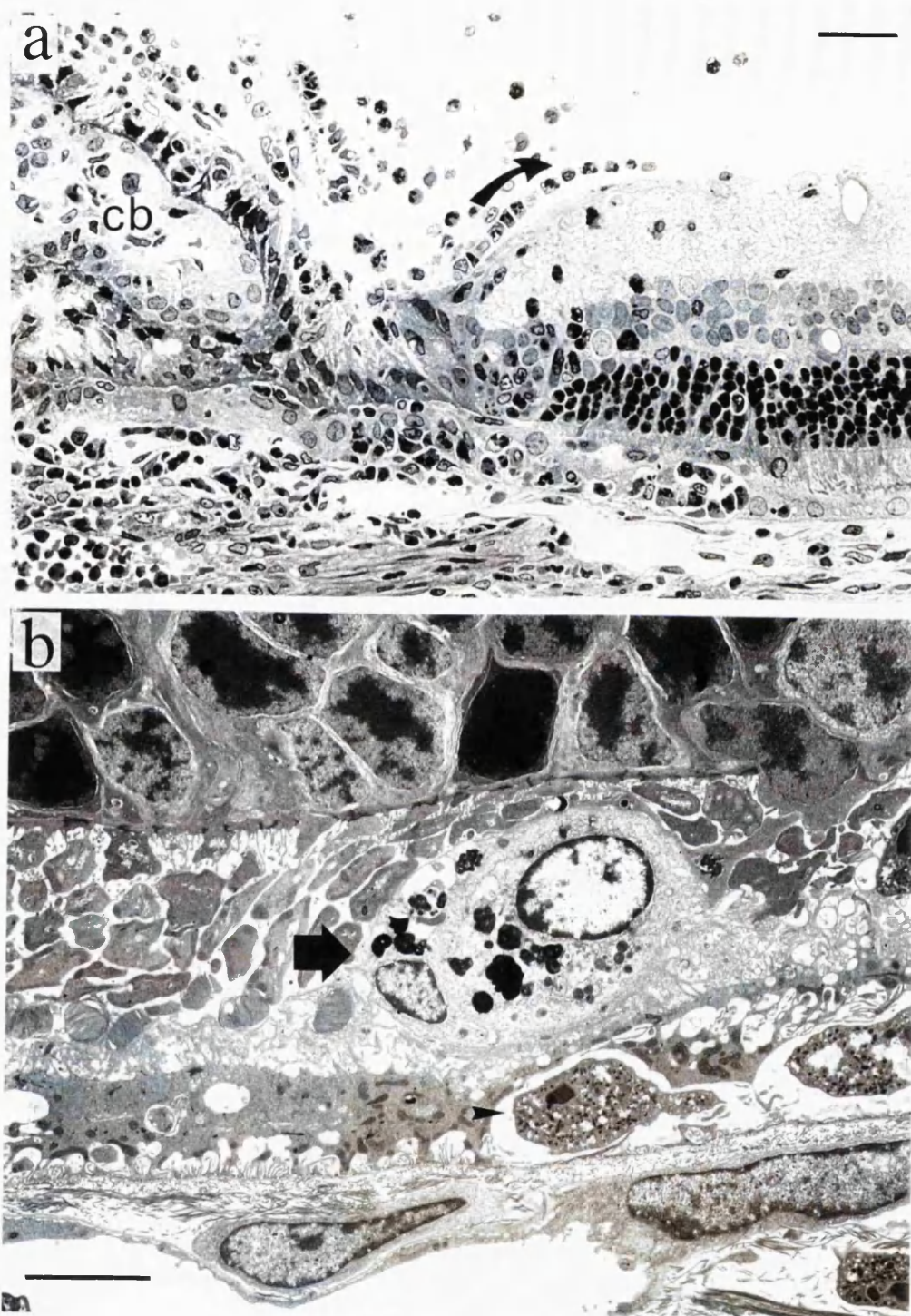
Figure 3.2.3a. *Toluidine blue stained resin section of retina, 48 hr PI IL-1ß. Many leucocytes can be seen within the ciliary body (cb), RPE and vitreous. The leucocytes in the vitreous appear to have originated from the ciliary body and are tracking along the inner limiting membrane of the retina in the direction of the curved arrow.* (Bar = 25µM). **3.2.3b.** *Transmission electron micrograph (TEM) of posterior portion of retina and RPE in close proximity to the ciliary body at 48 hr PI IL-1ß. A MN cell, probably a macrophage, is present within the rod outer segments* (arrow) *and neutrophils are present within the RPE layer* (arrow head). (Bar = 5µM).
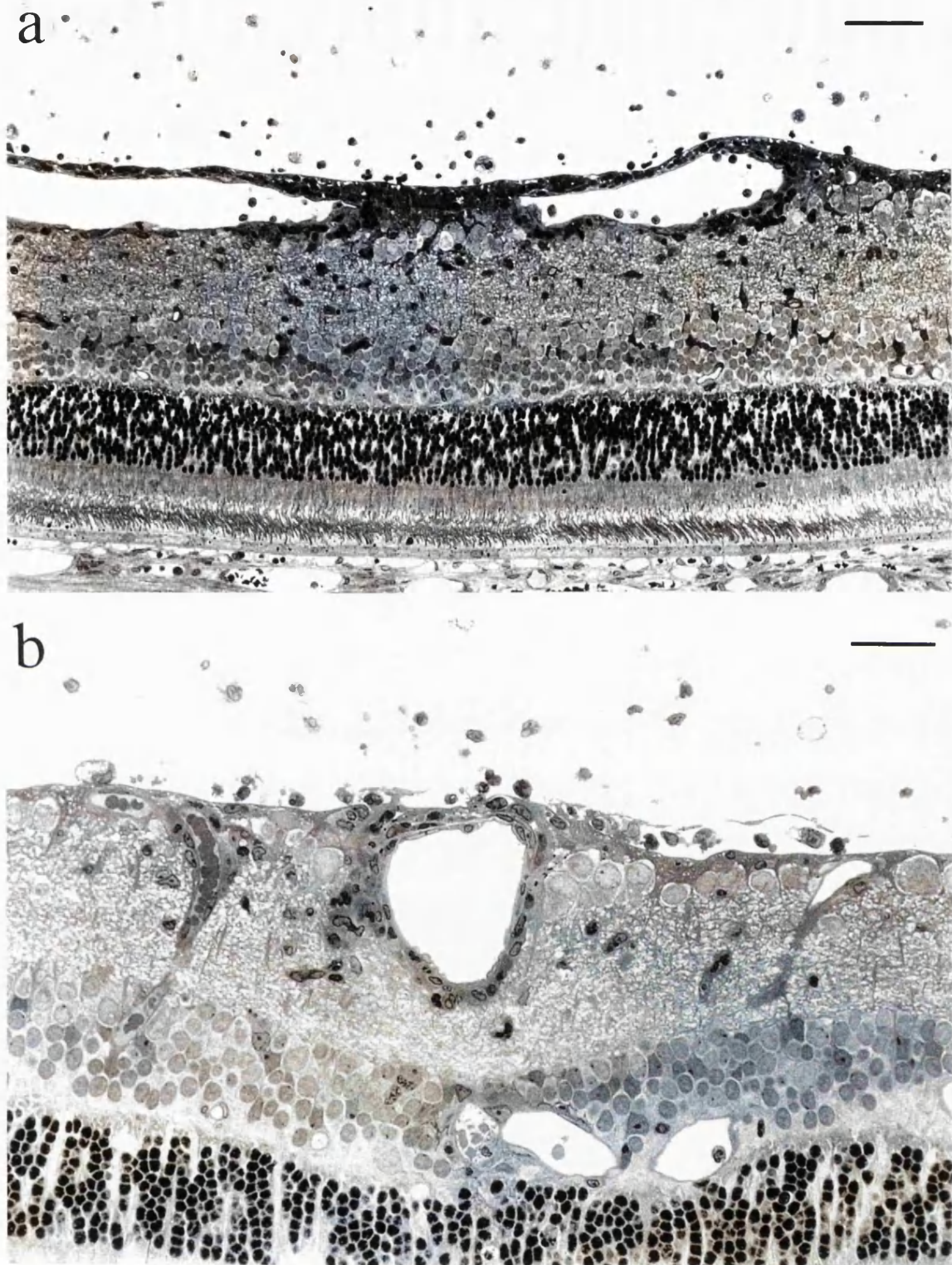
Figure 3.2.4a & b. Toluidine blue stained resin sections of retina at 72 hr PI IL-1ß. A large scale inflammatory cell presence still exists with leucocytes in the vitreous, tissue parenchyma and within retinal vessels. (a, bar = 50µM; b, bar = 25µM)
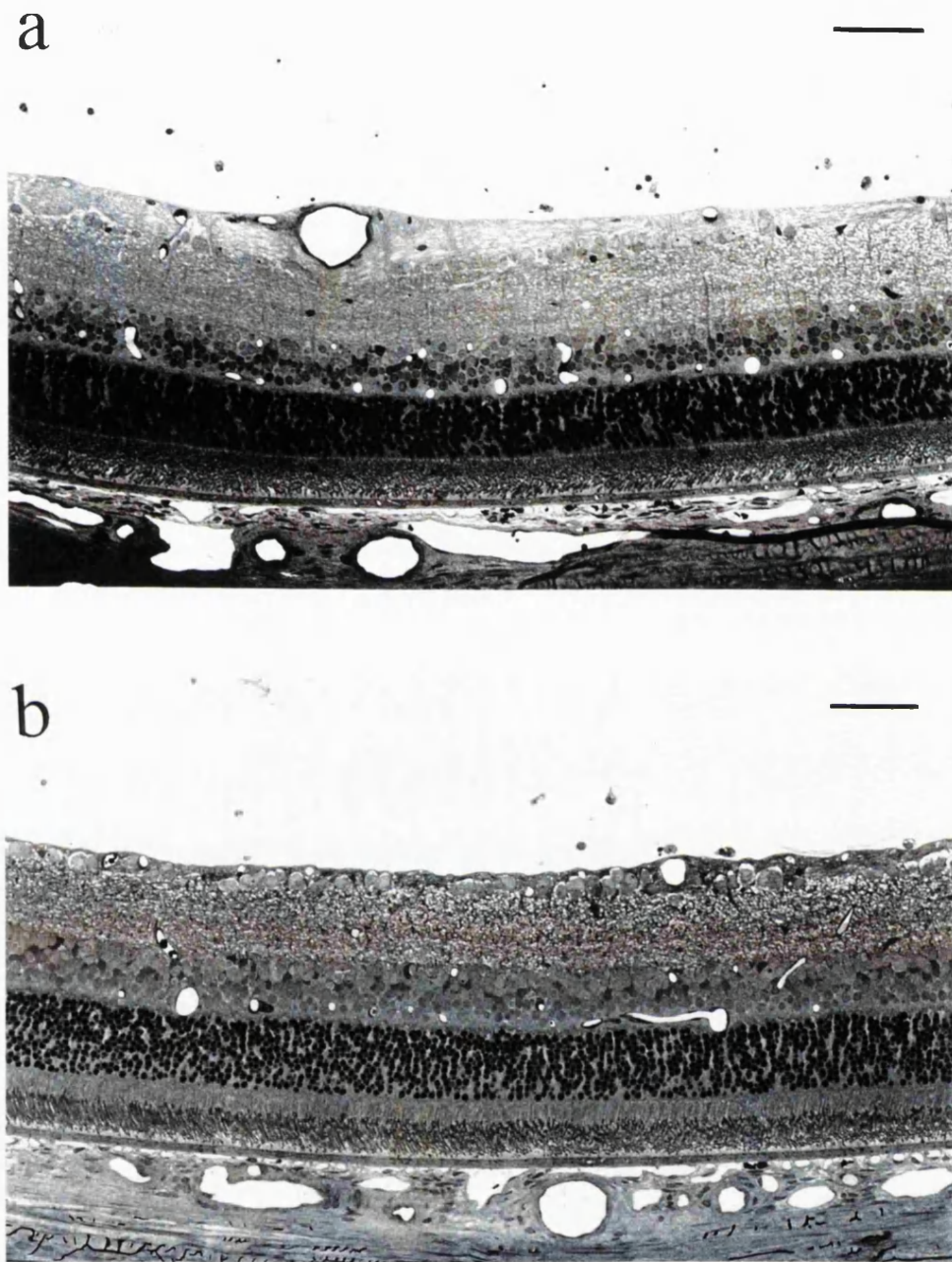
Figure 3.2.5. *Toluidine blue stained resin sections of retina following intravitreal IL-1β.* *a.* *5 day PI. A few inflammatory cells can be seen within the retina and vitreous* (Bar = 50μM). *b.* *7 day PI. The inflammatory response has almost completely subsided with no leucocytes present within the retina, but some remain in the vitreous* (Bar = 50μM).

3.2.1.2 Electron Microscopy

Ultrastructurally, leucocytes were observed adhering to, and probing the wall of retinal vessels (*Figs. 3.2.6 & 3.2.7*) and in the process of diapedesis (*Figs. 3.2.8-3.2.12*).

The most common granulocyte observed throughout the inflammatory response was the neutrophil. Eosinophils were seen infrequently, and identified by their characteristic banded granules (*Fig. 3.2.13a*). Platelets were also observed within retinal blood vessels throughout the course of inflammation, frequently in the company of leucocytes and sometimes present in large numbers (*Fig. 3.2.13b*).

At 4 hr PI an exudate was sometimes observed which typically revealed cross striations with a periodicity consistent with fibrin (Lampert, 1967). This fibrinous exudate was always in close proximity to blood vessels, particularly to those in the outer plexiform layer, and sometimes extending into the outer nuclear layer (*Fig. 3.2.14*). In these vessels leucocytes were frequently present in the lumen and adhering to the EC wall. This exudate became more pronounced throughout the course of the inflammatory response.

In areas of the retina with a large-scale infiltrate (ie. at 18-48 hr PI), the tissue was extremely vacuolated and edematous (*Fig. 3.2.15a*) although this was mostly restricted to the anterior portion of the retina. In two of the animals studied (one at 18 hr and another at 24 hr PI), large areas were observed that were devoid of cells and which contained amorphous material consistent with a proteinaceous exudate, particularly in the outer nuclear layer. These large acellular regions nearly always contained leucocytes (*Fig. 3.2.15b*).

Retinal endothelia remained morphologically normal except where they were in close association with adherent or migrated leucocytes. Endothelia in these regions were thickened and showed signs of increased surface microvilli (*Fig. 3.2.8*). During peak inflammation, and particularly noticeable at 72 hr PI, endothelia in close proximity to infiltrating leucocytes sometimes exhibited elevated numbers of cell organelles such as endoplasmic reticulum and vesicular-like profiles (*Fig.3.2.16a & b*).

Despite these significant structural alterations to the retina found at earlier time-points, by 7 days PI the retina appeared to be relatively normal with resolution of the damage seen beforehand.
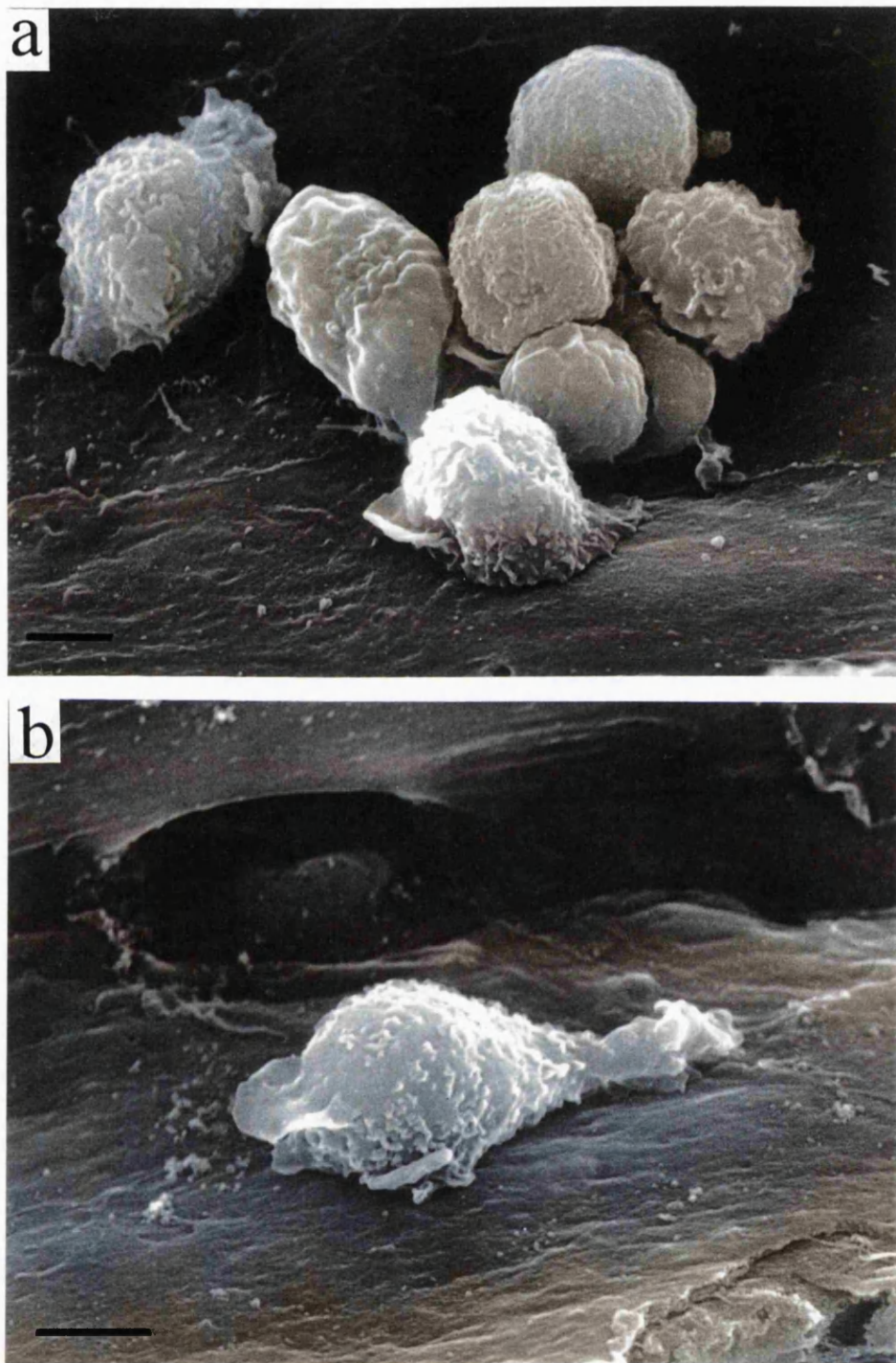
Figure *3.2.6. Scanning electron micrographs at 24 hr PI IL-1β. a. A mixed population of leucocytes adhering to the endothelium of a large blood vessel, which is probably a vein (Bar = 2μM). b. A single leucocyte adhering to the endothelium (Bar = 1μM).*
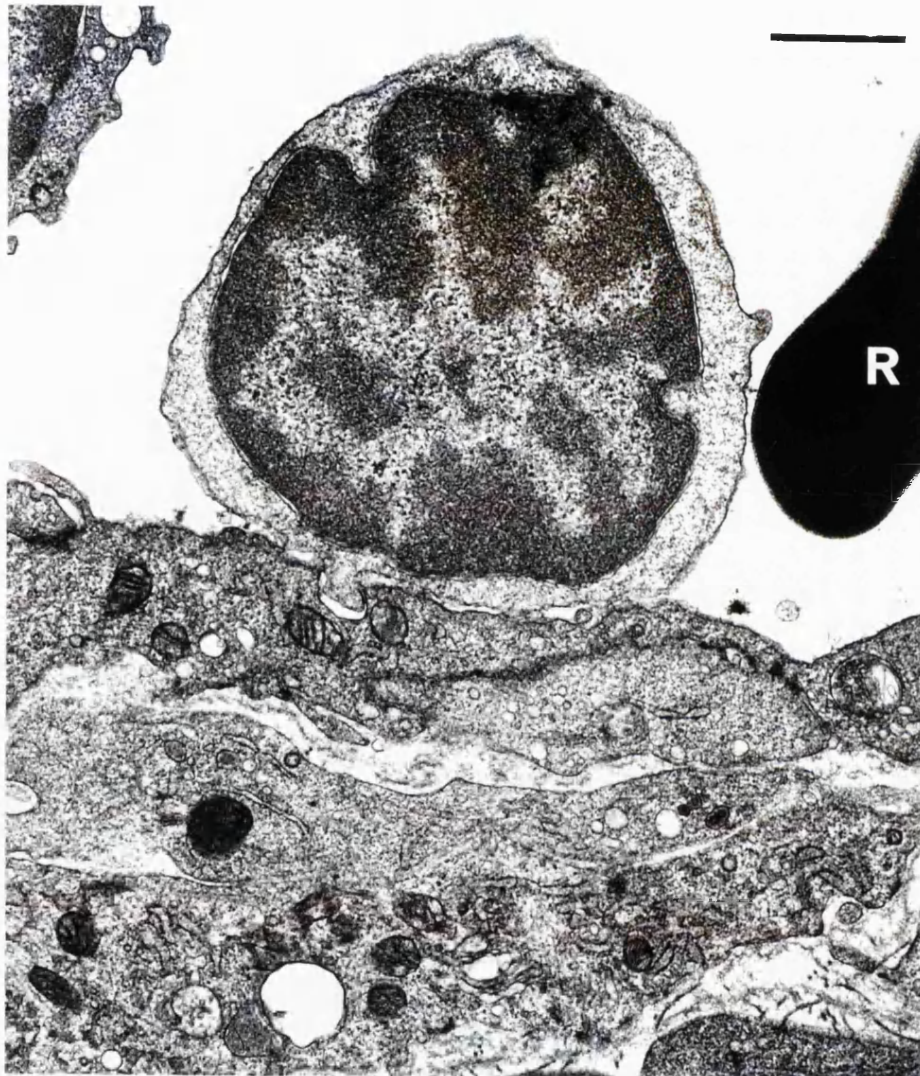
Figure 3.2.7. *TEM, 72 hr PI IL-1β. A MN cell, most probably a T lymphocyte, is adhering to a retinal EC and projecting a small pseudopodia into the endothelium. A red blood cell* (**R**) *is present next to the leucocyte* (Bar = 1μM).
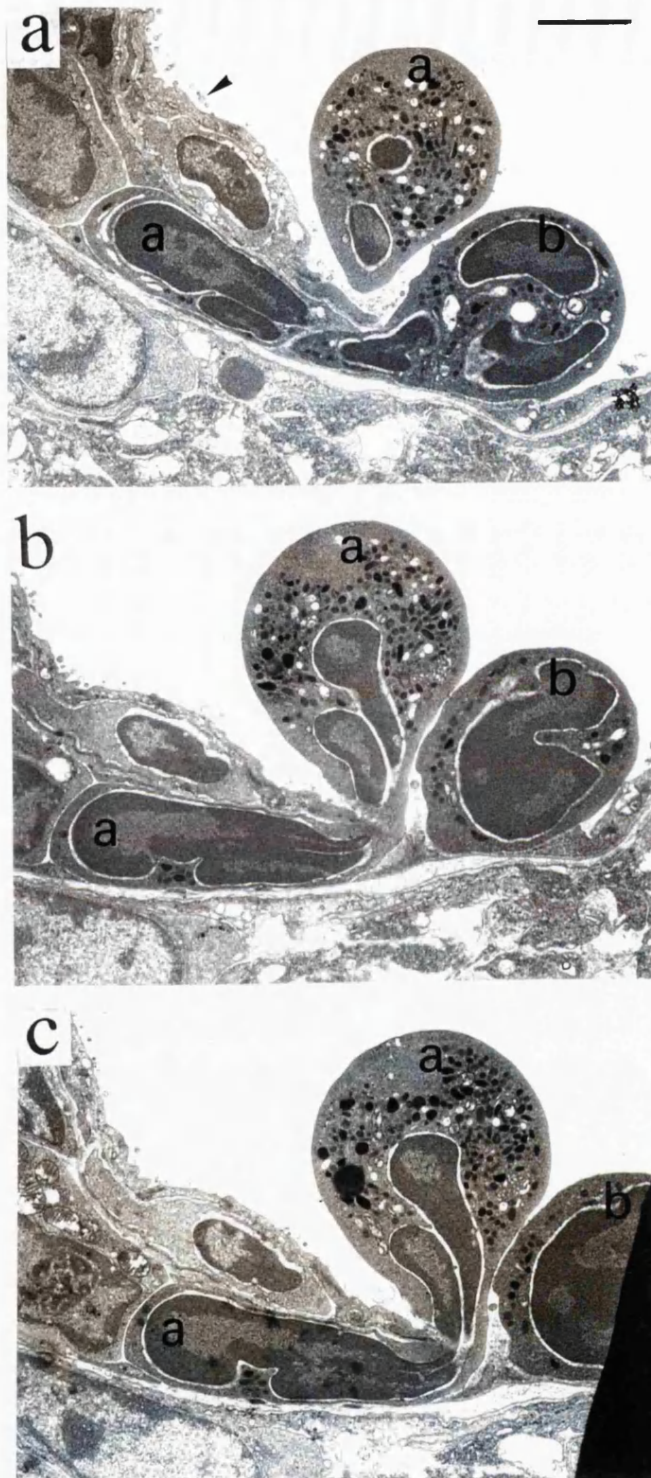
Figure 3.2.8. *TEM, 4 hr PI IL-1β. Serial sections of two neutrophils in the process of migrating at approximately the same location on the endothelium. **a.** The leading process of cell* b *can be seen penetrating the endothelium whilst the process from cell* a *is not in continuity with the cell body. Note the increased presence of microvilli extending from the endothelium (arrow head). **b.** The process from cell* b *is no longer visible. **c** The cell body and process of cell* a *is almost in continuity.* (Same magnifications, bar = 2μM).
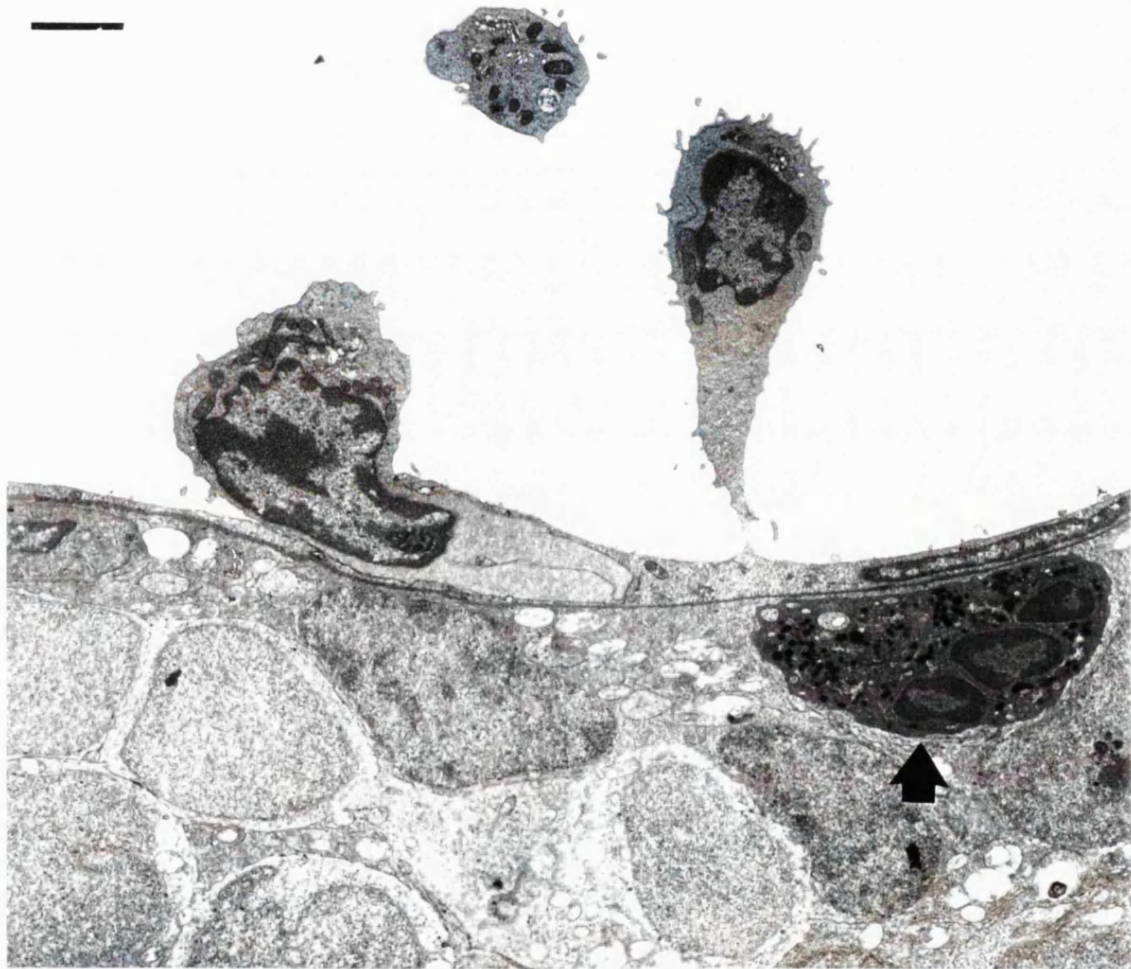
Figure 3.2.9. *TEM, 24 hr PI IL-1β. A MN in the process of diapedesis. Another MN has adhered to the EC by extending a pseudopodia. A previously migrated PMN* (arrow) *lies beneath the EC nucleus.* (Bar = 2μM)

Figure 3.2.10. *TEM, 72 hr PI IL-1β. A neutrophil in the process of migrating into the endothelium, above the EC nucleus* (E). *The endothelium has not yet rejoined to completely engulf the leucocyte* (arrow heads) (Bar = 1μM).

105
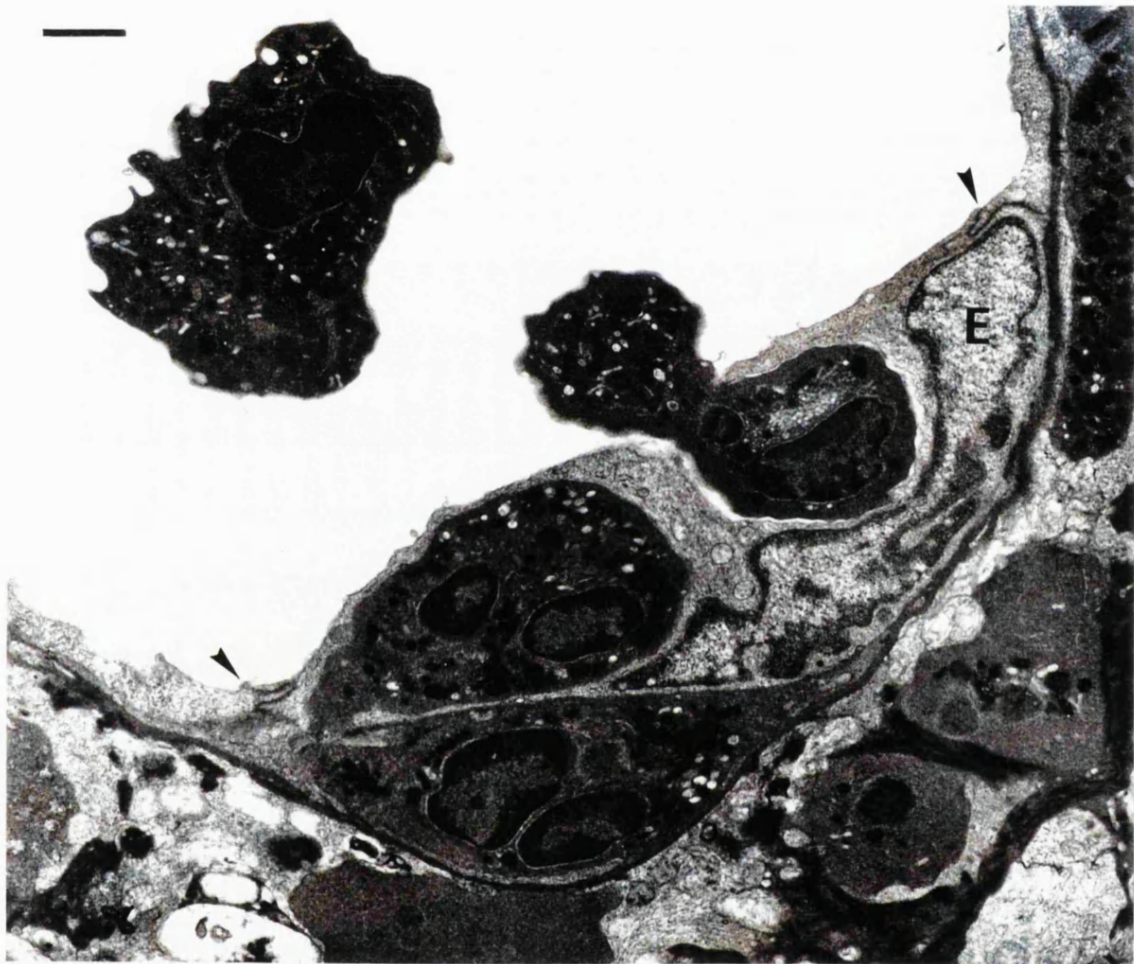
Figure 3.2.11. *TEM, 24 hr PI IL-1ß. A neutrophil in the process of migrating into the EC directly above the cell nucleus* (E) *at a distance from two tight junctions which can clearly be seen* (arrow heads). *What appears to be two other neutrophils, already appear to lie within the EC.* (Bar = 1μM).
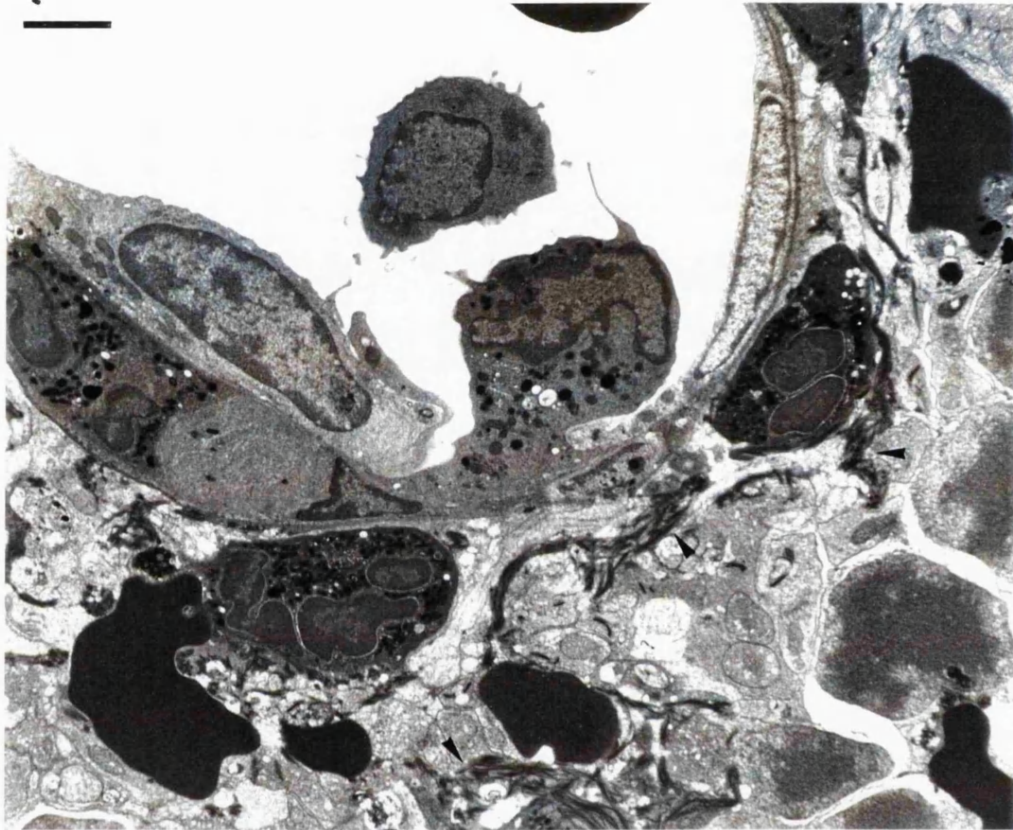
Figure 3.2.12. *TEM, 24 hr PI IL-1ß. A leucocyte in the process of migrating through the endothelium. Fibrin deposits can also be observed* (arrow heads). (Bar = 5µM).
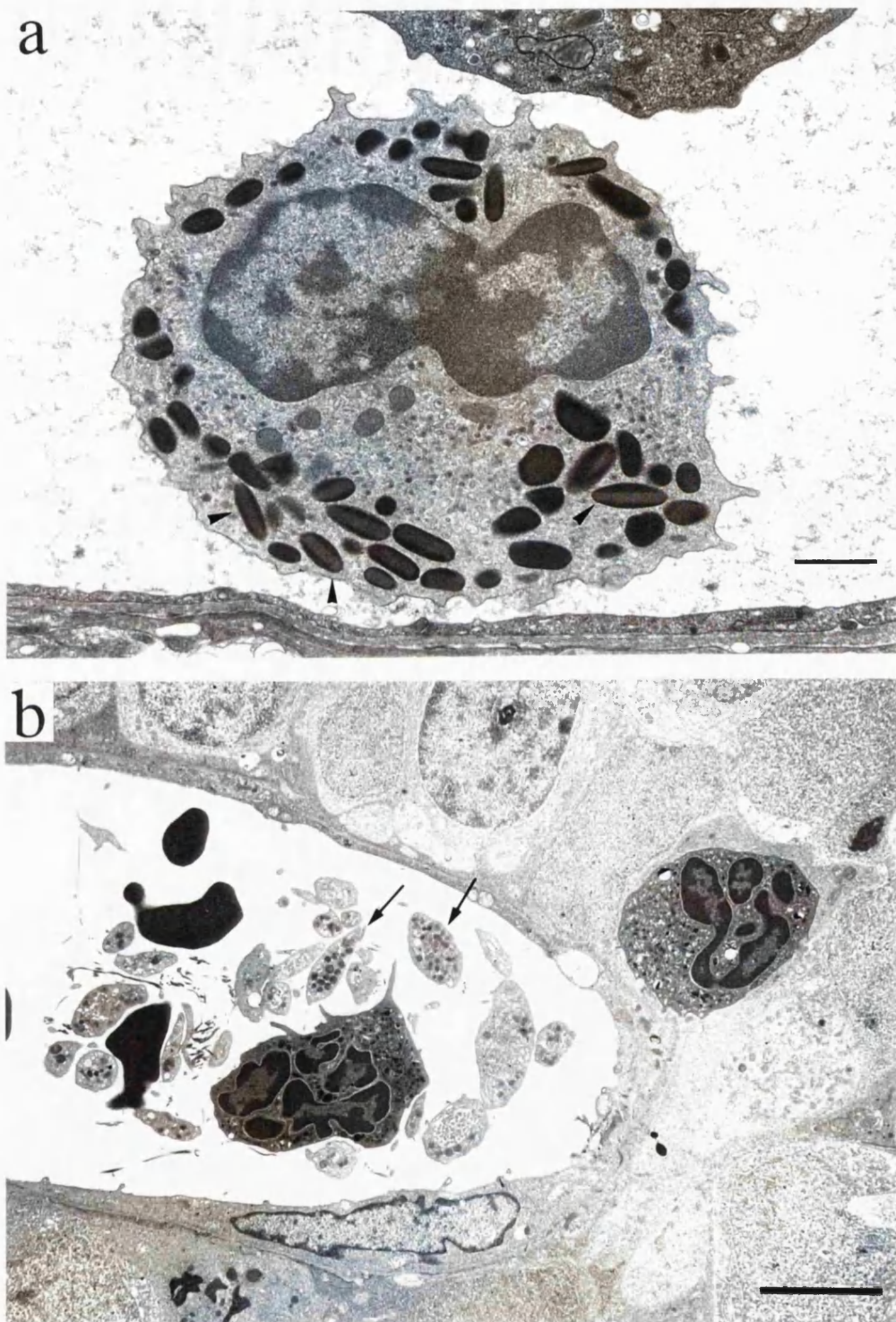
Figure 3.2.13. *TEMs following intravitreal IL-1ß.* **a.** *An eosinophil, which were occasionally observed throughout the course of inflammation, at 12 hr PI. Note the characteristic bands within the granules* (arrow heads) (Bar = 1µM). **b.** *Platelets* (arrows) *can be seen surrounding a neutrophil within a blood vessel situated in the outer plexiform layer at 48 hr PI. A migrated neutrophil is present within the tissue parenchyma beneath the basement membrane* (Bar = 5µM).
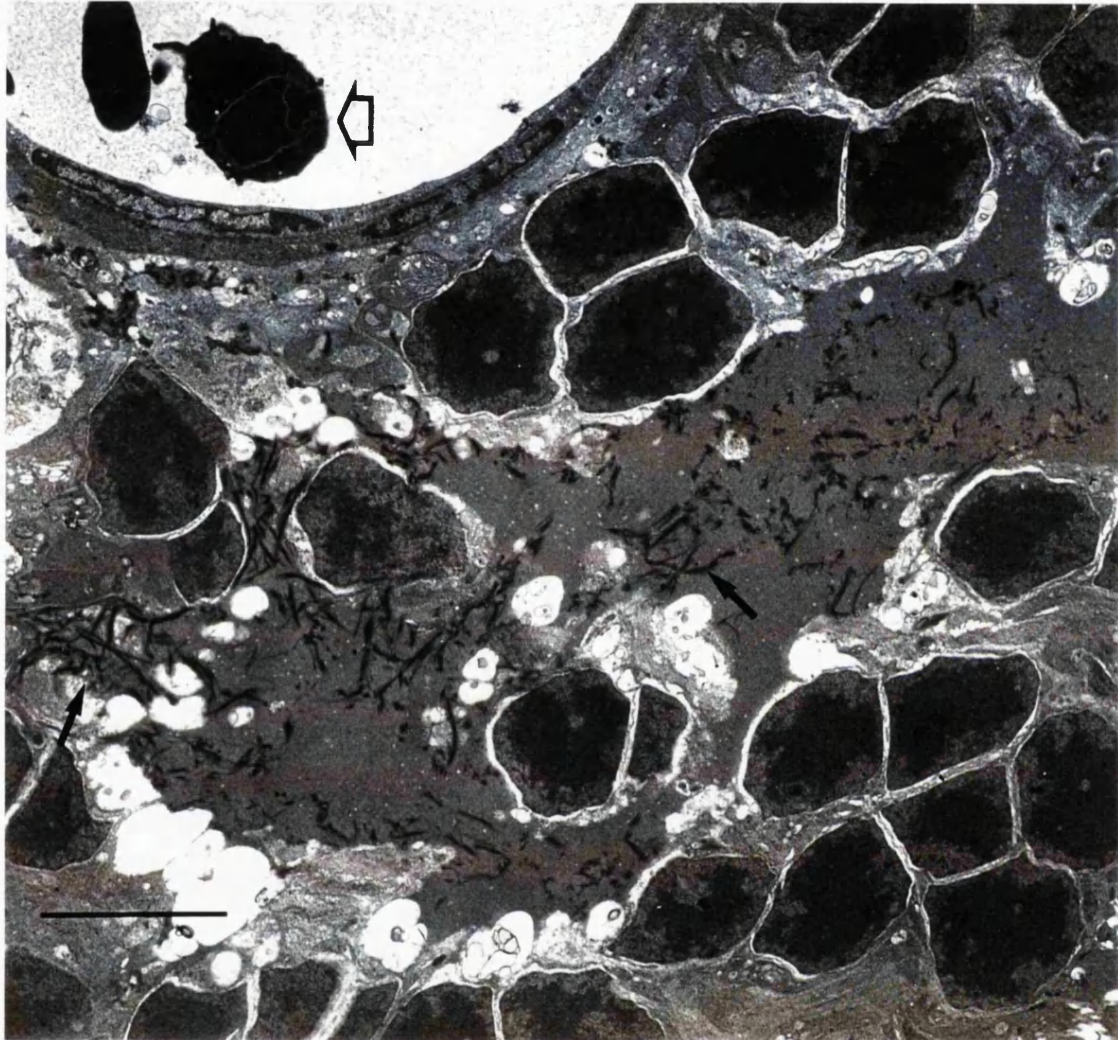
Figure 3.2.14. *TEM, 8 hr PI IL-1β. An exudate, that occasionally reveals a periodicity consistent with fibrin* (arrows), *extending into the outer nuclear layer. A PMN is present in the lumen of a blood vessel* (open arrow) (Bar = 2μM).
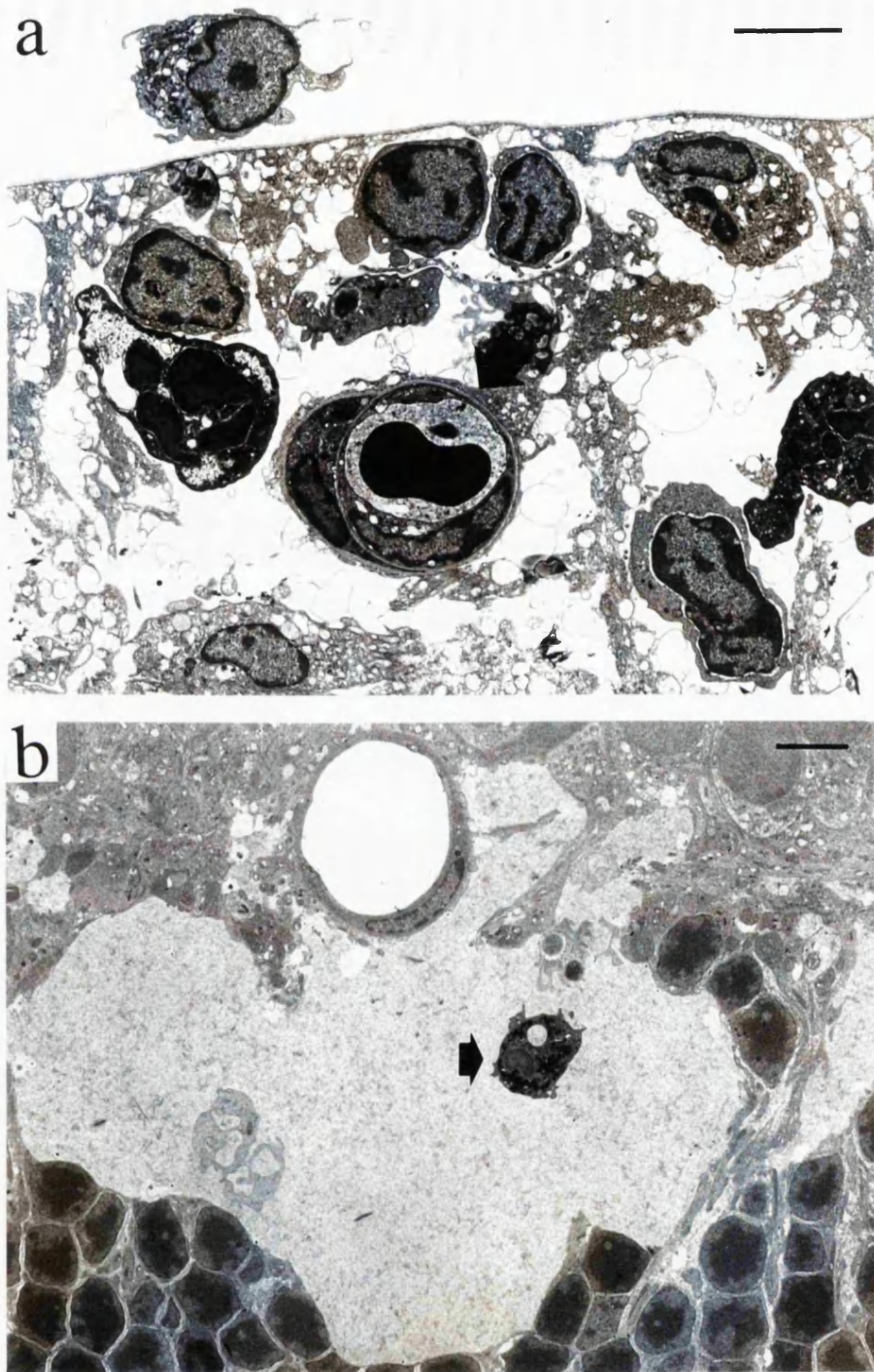
Figure 3.2.15. *TEMs, PI IL-1β. **a.** At 18 hr PI the tissue appears vacuolated and oedematous in the anterior portion of the retina, just below the inner limiting membrane. A MN cell can be seen in the vitreous, and within the parenchyma there are many extravasated cells. A small blood vessel, containing an erythrocyte, (arrow) within the vacuolated region appears structurally normal (Bar = 5μM). **b.** TEM, 24 hr PI IL-1β. Area of extravasated fluid extending into the outer nuclear layer and containing a neutrophil (arrow). The EC of the blood vessel appears to be structurally normal (Bar = 5μM).*
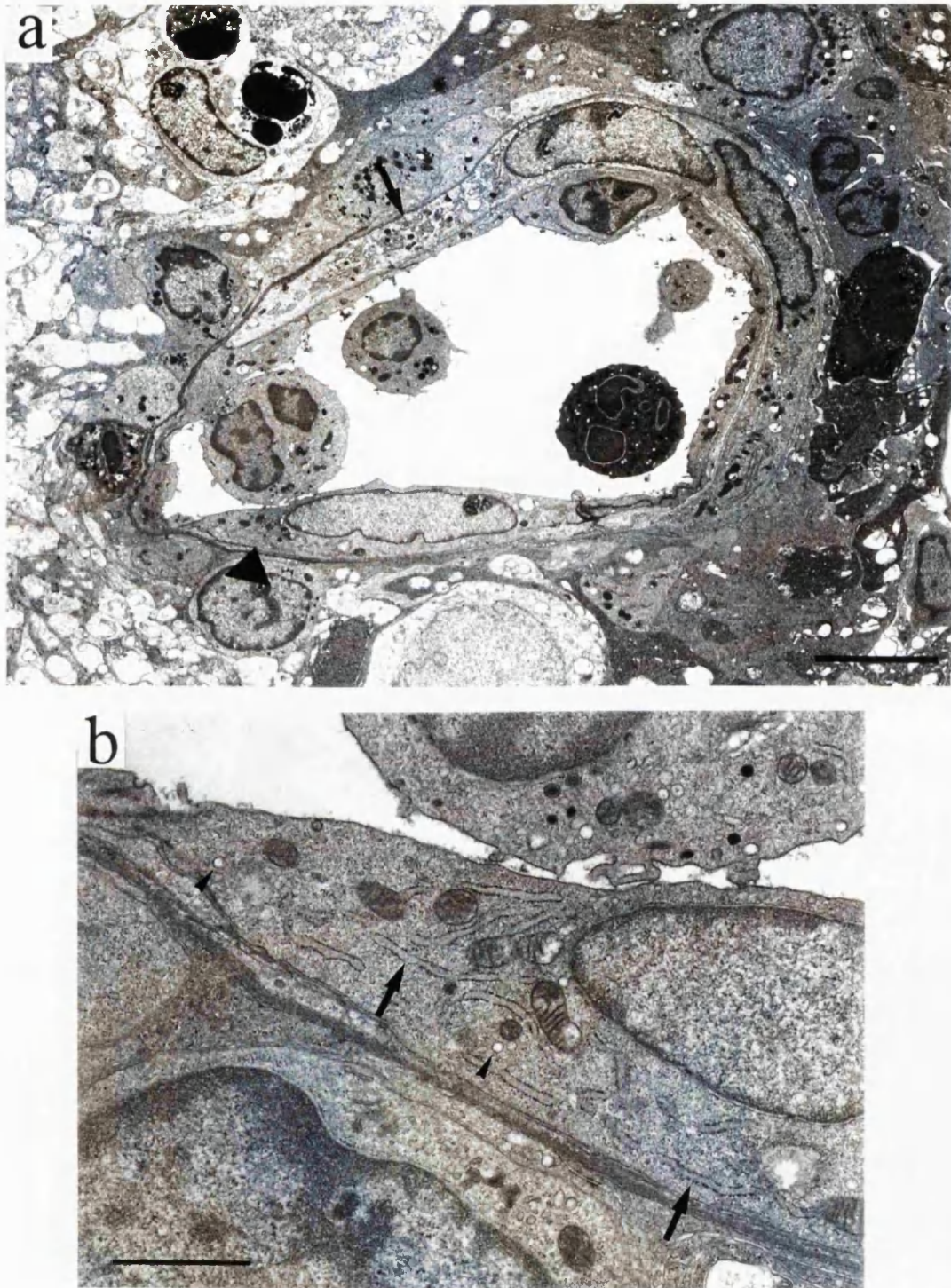
Figure 3.2.16. *TEMs, 72 hr PI IL-1ß.* ***a.*** *Vessel containing adherent PMN and MN and with highly reactive pericyte* (arrow) *and ECs* (arrow head) *showing increased amounts of cytosolic organelles* (Bar = 5μM). ***b.*** *Higher power of EC in* ***a*** *showing increased numbers of endoplasmic reticulum* (arrows) *and vesicular-like profiles* (arrow heads) (Bar = 1μM).

111

3.2.2 Immunohistochemistry

No positive staining was observed in sections of retina incubated without primary monoclonal antibodies. Sections of spleen stained positive for each antibody used.

Immunohistochemical staining for leucocytes on frozen sections of retina at 24 hr PI IL-1ß revealed a large scale positive staining for the ED1 marker, representing monocytes and macrophages (*Fig. 3.2.17a*), and positive staining, but to a lesser degree, was observed for the marker for macrophages, ED2 (*Fig. 3.2.17b*). Positive immunostaining was also observed for the marker for granulocytes, MOM/3F12/F2 (*Fig. 3.2.18a*) and $CD8^+$ cytotoxic T cells, OX8 (*Fig. 3.2.18b*). Positive staining was also seen for OX6 (MHC class II) and WT3 (CD18) within the retina and on infiltrating inflammatory cells. No positive staining was seen in the retina from the non-injected contralateral eyes, but staining was observed in the choroid.

3.2.3 BRB Permeability to HRP

Following HRP infusion at 48 hr post IL-1ß injection, tracer was observed flooding the basement membrane of blood vessels *(Figs. 3.2.19a & b)* and extending into the perivascular region. Extravasation of HRP was found primarily in vessels where there was evidence of leucocytic adhesion or migration (*Fig. 3.2.20a*). Occasionally, HRP could be seen extending along the length of a "tight junction" which was considered to be the major route of extravasation (*Figs. 3.2.20b & c*). No indication of HRP-filled pinocytotic vesicles was observed except at the abluminal side where omega profiles filled with HRP reaction product were seen. Extravasated HRP was sometimes observed surrounding the fenestrated vessels of the ciliary body at 48 hr PI (*Fig. 3.2.21a*) and also within the basement membrane of vessels from the ciliary vasculature (*Fig. 3.2.21b*). Similar observations were also made in the ciliary body of the contralateral non-injected eyes.

HRP was observed within the RPE layer at 48 hr PI IL-1ß where it could be seen between two RPE cells but not penetrating beyond the apically located terminal bar of the tight junction into the photoreceptor layer (*Fig. 3.2.22*)
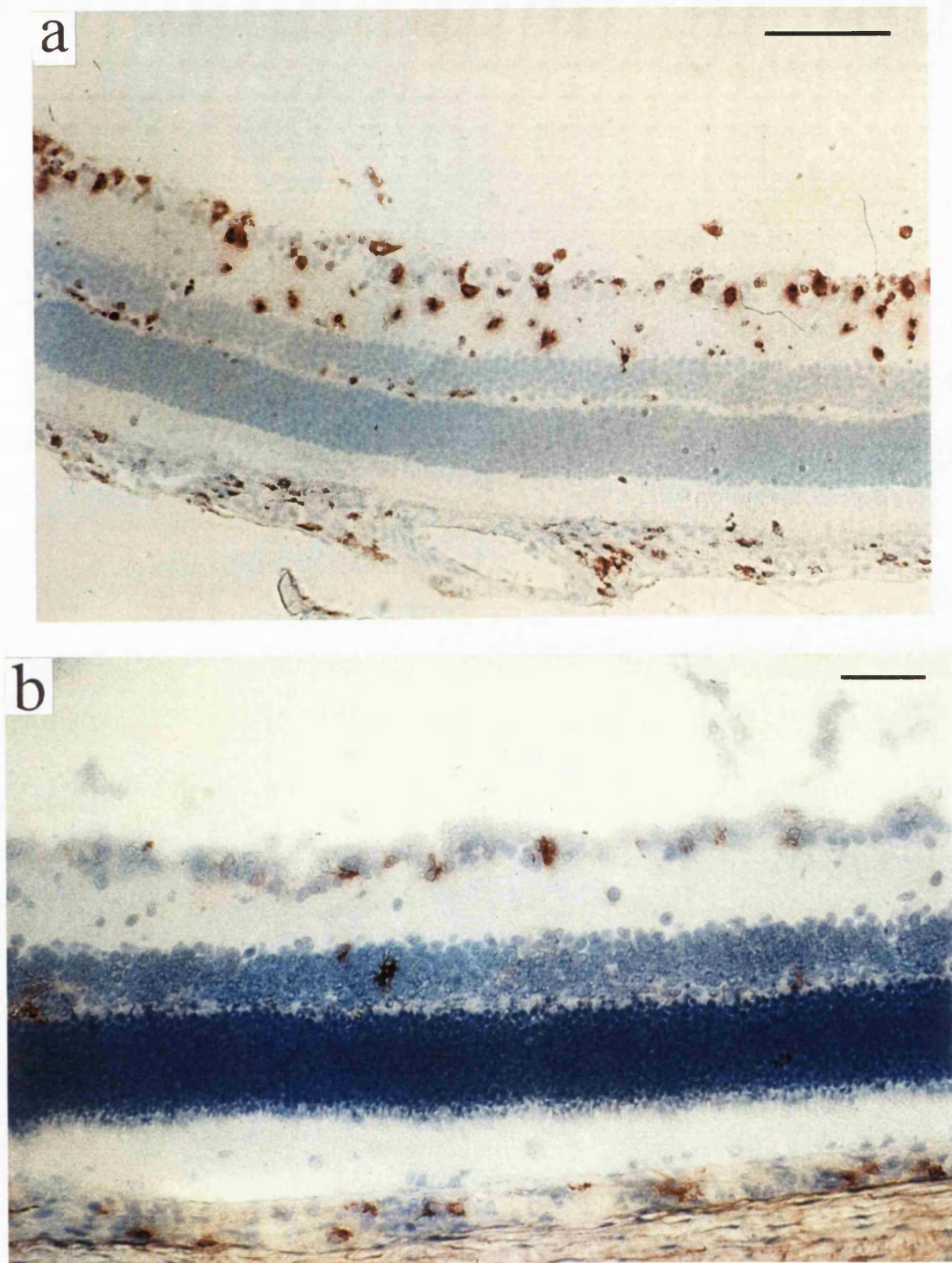
Figure *3.2.17. Immunohistochemistry on frozen sections of retina at 24 hr following intravitreal IL-1β.* **a.** *Positive immunostaining for the monocyte/macrophage marker ED1* (Bar = 100μM). **b.** *Positive staining for ED2, the marker for macrophages* (Bar = 50μM).
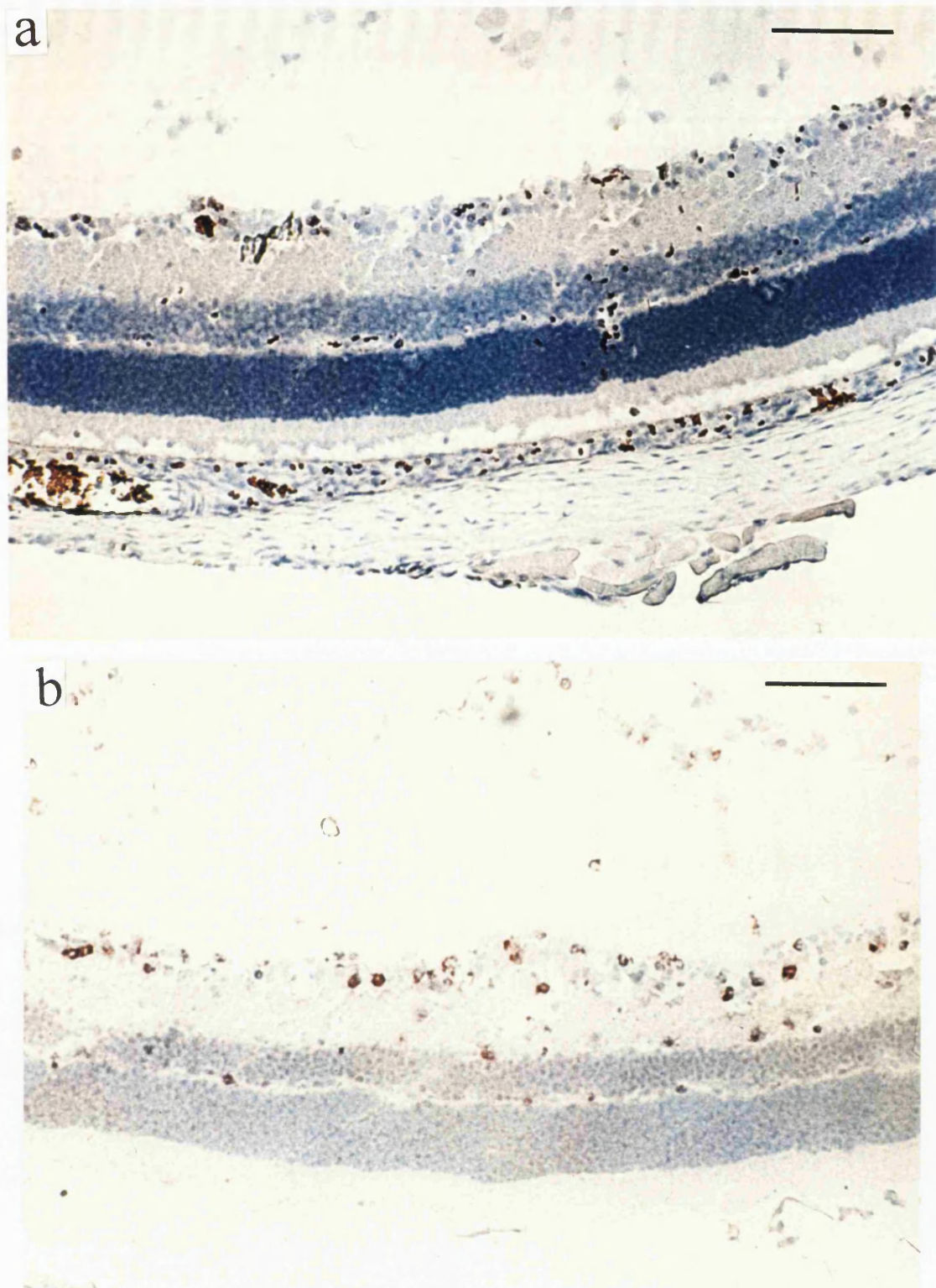
Figure 3.2.18. *Immunohistochemistry on frozen sections of retina at 24 hr following intravitreal IL-1β.* **a.** *Positive immunostaining for the granulocyte marker MOM/3F12/F2* (Bar = 100μM). **b.** *Positive immunostaining for OX8, the marker for cytotoxic T cells* (CD8⁺) (Bar = 100μM).
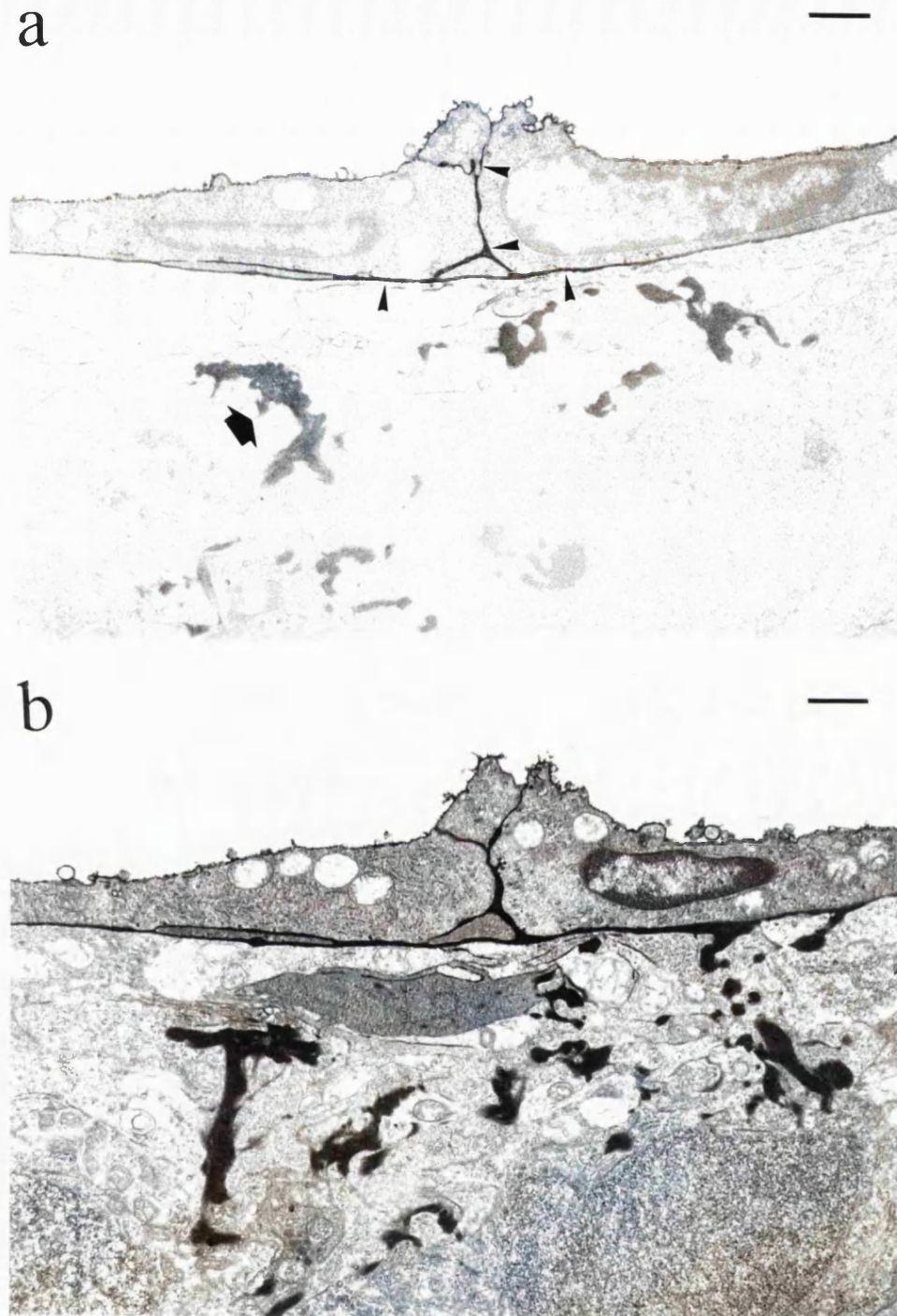
Figure 3.2.19. TEM, 48 hr PI IL-1ß. *a.* Unstained section of endothelium from a large blood vessel. HRP reaction product can be seen permeating the basement membrane and extending the length of the tight junction (arrow heads). Fibrin is present within the parenchyma (arrow) (Bar = 1μM). *b.* Stained serial section of endothelium from *a* (Bar = 1μM).
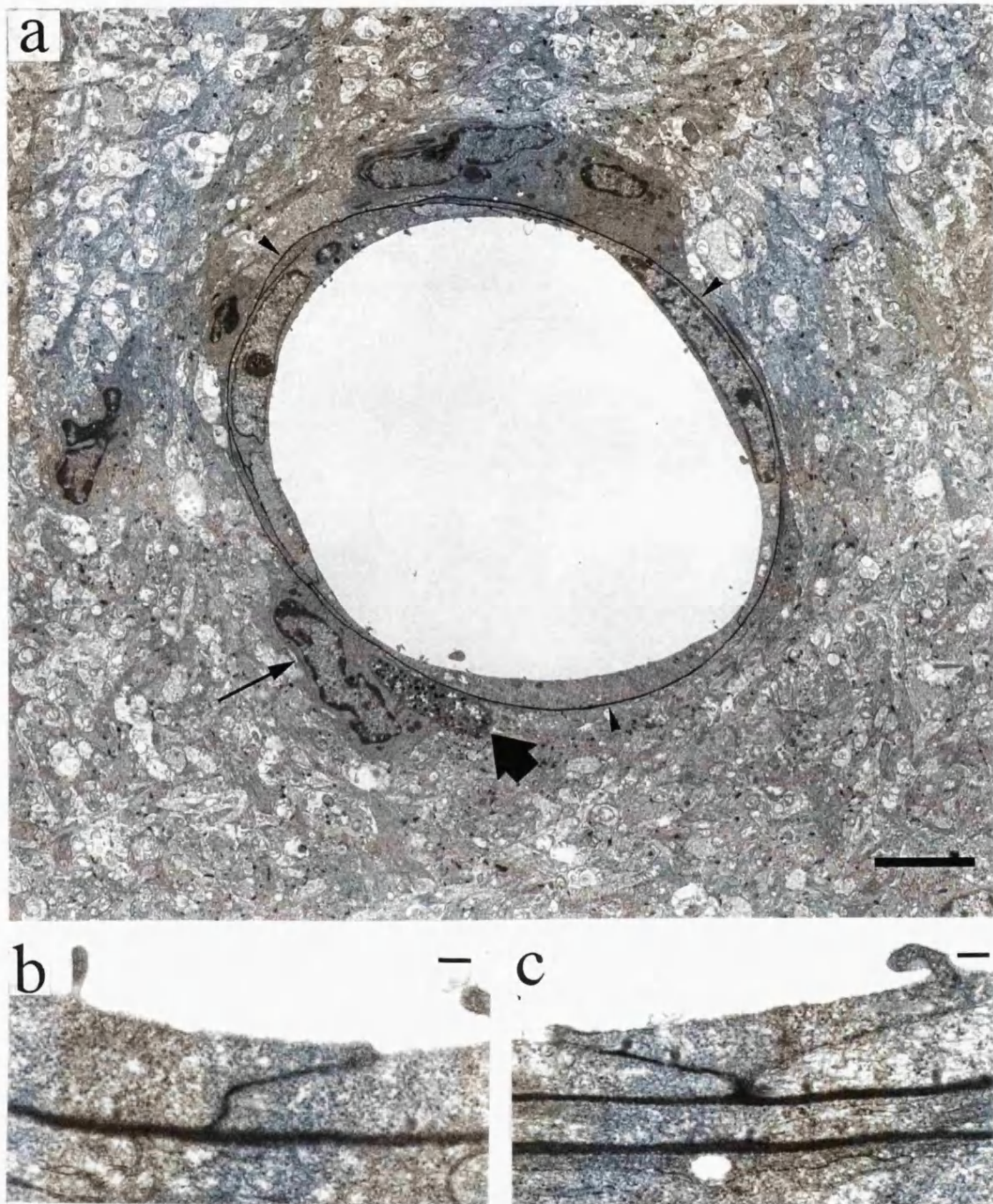
Figure 3.2.20. *TEM, 48 hr PI IL-1β.* ***a.*** *Section of a retinal microvessel. The basement membrane is continuously filled with HRP reaction product* (small arrow heads). *Extravasated cells, PMN* (short arrow) *and MN* (long arrow) *can be seen beneath the basement membrane* (Bar = 5μM). ***b & c.*** *High power micrographs of tight junctions from vessel in* ***a*** *showing HRP reaction product almost completely present along the length of the EC tight junctions* (Magnifications the same, bar = 200nm).
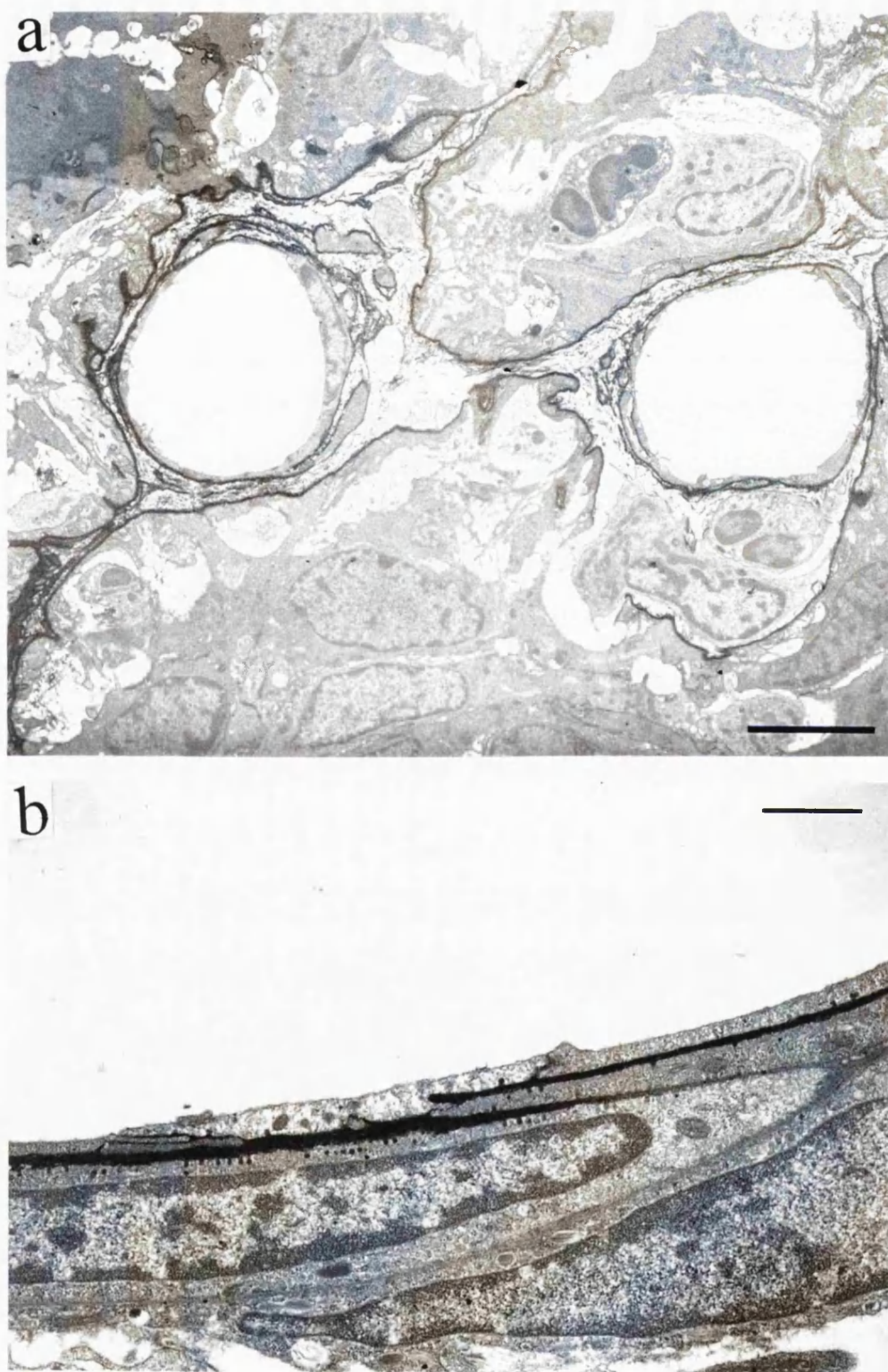
Figure 3.2.21. *TEMs, 48 hr PI IL-1β. a. Unstained section of two fenestrated vessels from the ciliary body are surrounded by HRP reaction product, an occurrence that was also observed in the ciliary bodies of eyes not receiving an intravitreal injection of cytokine (Bar = 5μM). b. A vessel from the ciliary vasculature has HRP reaction product flooding the basement membrane (Bar = 1μM).*
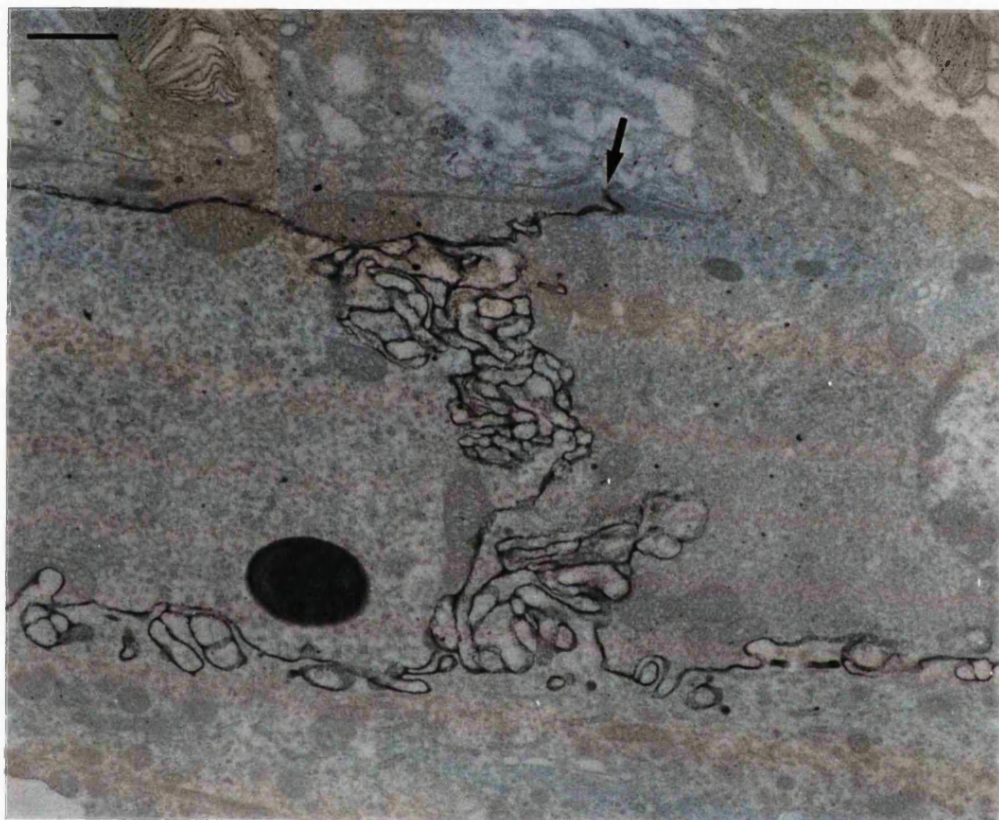
Figure 3.2.22. *TEM 48 hr PI IL-1β. Unstained section of the RPE layer with HRP reaction product extending between two RPE cells. The passage of the HRP is apparently restricted at the terminal bar of the RPE cell junctional complex* (arrow) *and is unable to penetrate into the photoreceptor layer. The structure of the RPE layer in this section appears to be abnormal as the base of the RPE does not abut onto Bruch's membrane* (Bar = 1μM).

3.2.4 BRB Permeability to [^{14}C]-Mannitol

Up to 2 hr following IL-1ß injection, no significant opening of the BRB was detected as indicated by an increase in the retinal Rt/Rp [^{14}C]-mannitol ratio. However, a distinct biphasic pattern of opening of the BRB was subsequently observed (Fig. 3.2.23a). The initial disruption, which coincided with the first cohort of infiltrating leucocytes, occurred at 4 hr PI (p <0.001) and remained elevated up to 8 hr PI (p <0.05). The Rt/Rp ratio for the retina returned to control values by 12 hr PI and remained unaltered over the subsequent 6 hr, although leucocytes continued to infiltrate into the retina during this time period. A more substantial and prolonged increase in BRB permeability then occurred at 24-48 hr PI (p <0.01) which coincided with the peak of leucocyte infiltration. ($n \geq 6$ for each time point; total $n = 118$)

The Rt/Rp ratio of the vitreous samples following IL-1ß injection was significantly increased from control values (p <0.05) at all time points from 4 to 48 hr PI (Fig. 3.2.23b). A small but significant increase in permeability was also recorded at time 0 (p <0.05), immediately after the intravitreal injection was administered.

IL-1ß neutralised with αIL-1ß Ab and injected intravitreally had no significant effect on BRB permeability to [^{14}C]-mannitol at 4 and 24 hr PI when compared to the effect of vehicle control (Fig. 3.2.24). ($n \geq 6$ for each time point; total $n = 13$)

The mean Rt/Rp ratio for the brain samples from the IL-1ß injected animals (mean ± SEM: 0.0116 ± 0.0002; $n = 116$) was not significantly different from the brain samples taken from the non-injected and vehicle control injected animals and demonstrates the efficacy of the saline washout.

The mean blood pressure, blood-gas and pH measurements made during the course of each mannitol experiment (Table 3.2.1 & 3.2.2) were not significantly different from those from the control studies.

The permeability results are expressed as the mean Rt/Rp ratio. This is the ratio calculated from the [^{14}C]-mannitol activity measured in the tissue (Rt) and plasma (Rp) samples harvested at the end of each experiment.
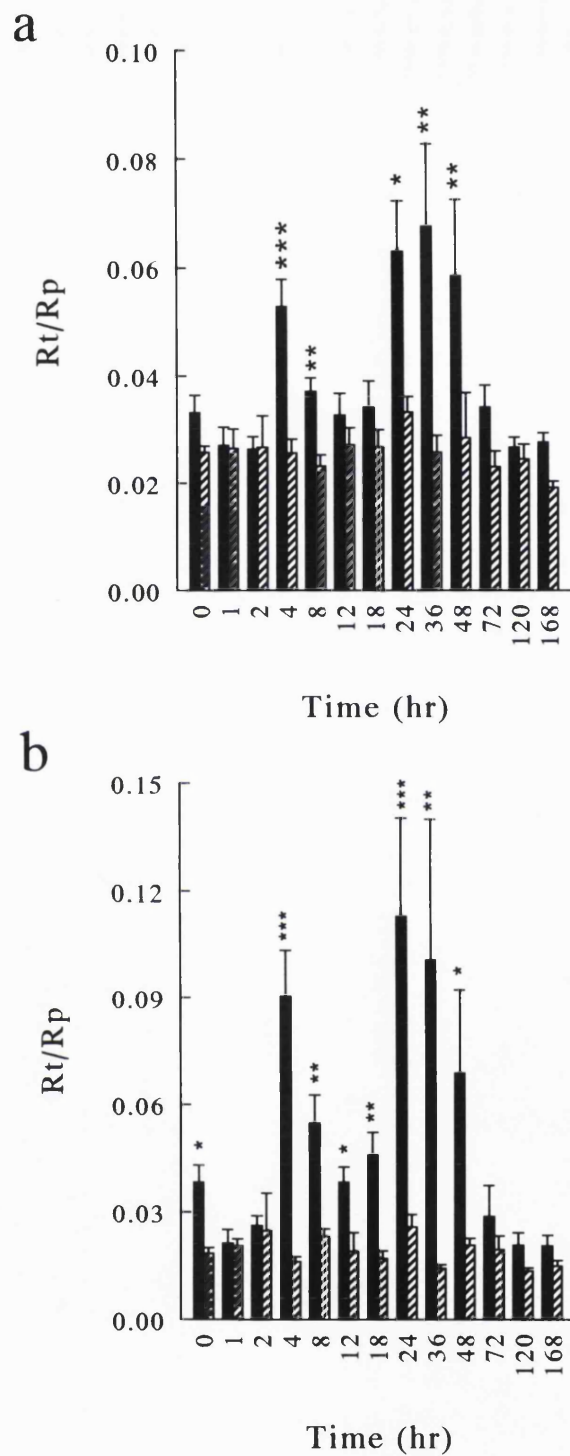
Figure 3.2.23. *Permeability of the BRB as measured by [^{14}C]-mannitol extravasation.* **a.** *A reversible and distinct biphasic increase in the permeability of the retina from the IL-1ß injected eyes* (solid bars) *was observed, when compared to the values obtained from the contralateral eyes* (hatched bars). **b.** *The Rt/Rp values for the vitreous samples from the injected eyes* (solid bars) *are significantly increased at 0 and from 4 to 48 hr PI, when compared to the values obtained from the contralateral eyes* (hatched bars).
*p <0.05; **p <0.01; ***p <0.001 .

120

a

b
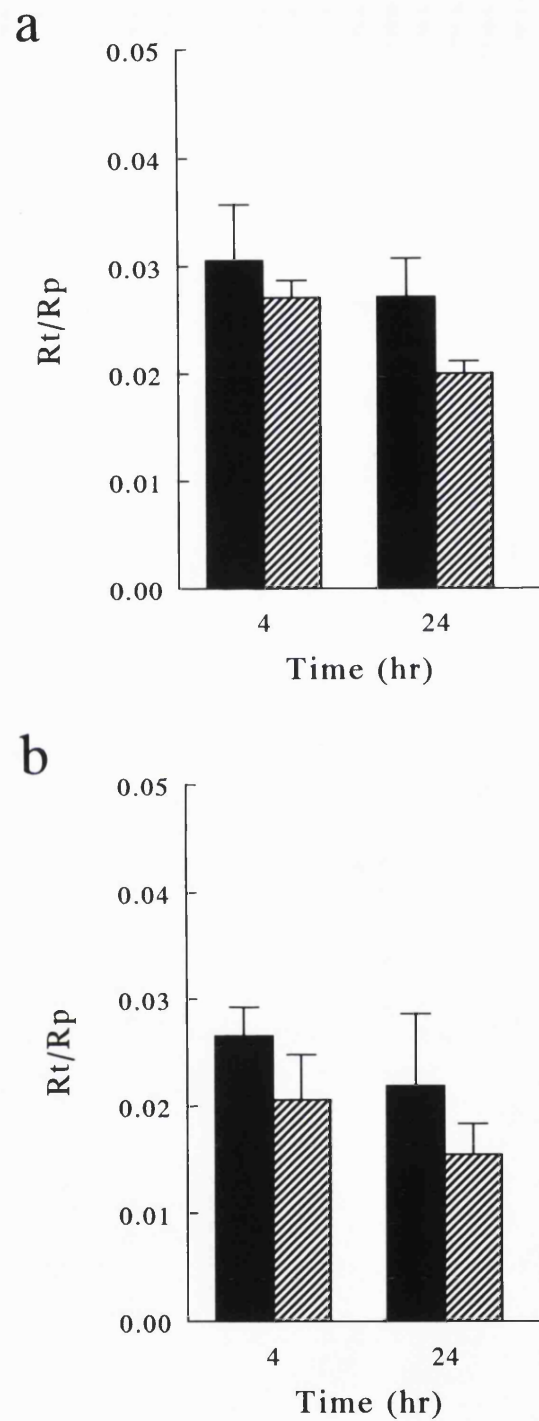
Figure 3.2.24. BRB *permeability following intravitreal administration of IL-1β neutralised with specific antibody.* **a.** *No significant increase in BRB permeability was observed at 4 or 24 hr PI in the retina* (solid bars) *when compared to vehicle control-injected values* (hatched bars). **b.** *No significant increase in the Rt/Rp ratio of the vitreous samples occurred in the IL-1β and antibody injected eyes* (solid bars) *compared to vehicle control-injected values* (hatched bars).

n	Systole (mmHg)	Diastole (mmHg)
80	112.09 ± 1.09	86.48 ± 0.88

Table 3.2.1. Mean arterial blood pressure measurements from IL-1β injected animals at the beginning of each [^{14}C]-mannitol experiment. Values are means ± SEM. There is no significant difference from the values obtained for the non-injected and vehicle control-injected animals (see Table 3.1.1, page 88).

n	pH	pCO$_2$ (kPa)	pO$_2$ (kPa)	% O$_2$
107	7.37 ± 0.004	6.48 ± 0.09	9.43 ± 0.13	92.2 ± 0.43

Table 3.2.2. Mean pH and blood gas levels from IL-1β injected animals. Measurements were taken at 2, 10 and 18 minutes throughout the course of the [^{14}C]-mannitol infusion. Values are means ± SEM. There is no significant difference from the values obtained for the non-injected and vehicle control-injected animals (see Table 3.1.2, page 88).

INHIBITOR STUDIES

3.3 Inhibitor Studies

3.3.1 Ranitidine

The administration of ranitidine (71μM) along with IL-1ß (1-2 x10³ U) intravitreally, accompanied by ranitidine delivered IP (25mg.kg⁻¹) at 0 for the 4 hr time point group, and at 0, 8 and 22 hr PI for the 24 hr time point group, was successful in inhibiting the opening of the BRB at 4 and 24 hr PI as measured in the retina (p <0.01) and vitreous samples (p <0.05), when compared to the effect of IL-1ß alone (*Fig. 3.3.1*). The Rt/Rp ratio for the vitreous at 4 hr PI was significantly higher (p <0.05) than vehicle control injected eyes at that time point, but there was no significant difference from the other values. ($n ≥ 5$ for each time point; total $n = 11$)

Histology at 24 hr PI revealed a significant decrease in the number of migrated leucocytes per mm of inner limiting membrane when compared to the number of migrated cells following IL-1ß injection ($n = 6$; p <0.01) (*Fig. 3.3.2*).

3.3.2 Indomethacin

Indomethacin (13.97μM) injected intravitreally with IL-1ß (1-2 x10³ U) and injected subcutaneously (5mg.kg⁻¹) at 0 for the 4 hr time point group, and at 0, 8 and 22 hr PI for the 24 hr time point group, significantly inhibited the opening of the BRB at 24 hr PI (p <0.05) as measured in the retina and vitreous (*Fig. 3.3.3*) when compared to the effect seen following intravitreal IL-1ß alone. However, indomethacin had no effect on reducing BRB permeability at the 4 hr time point when compared to IL-1ß.

Histology at 24 hr PI revealed a significant decrease in the number of migrated leucocytes per mm of inner limiting membrane when compared to the number of migrated cells following IL-1ß injection ($n = 6$; p <0.01) (*Fig. 3.3.2*).

(For the permeability experiments $n ≥ 8$ for each time point; total $n = 15$)
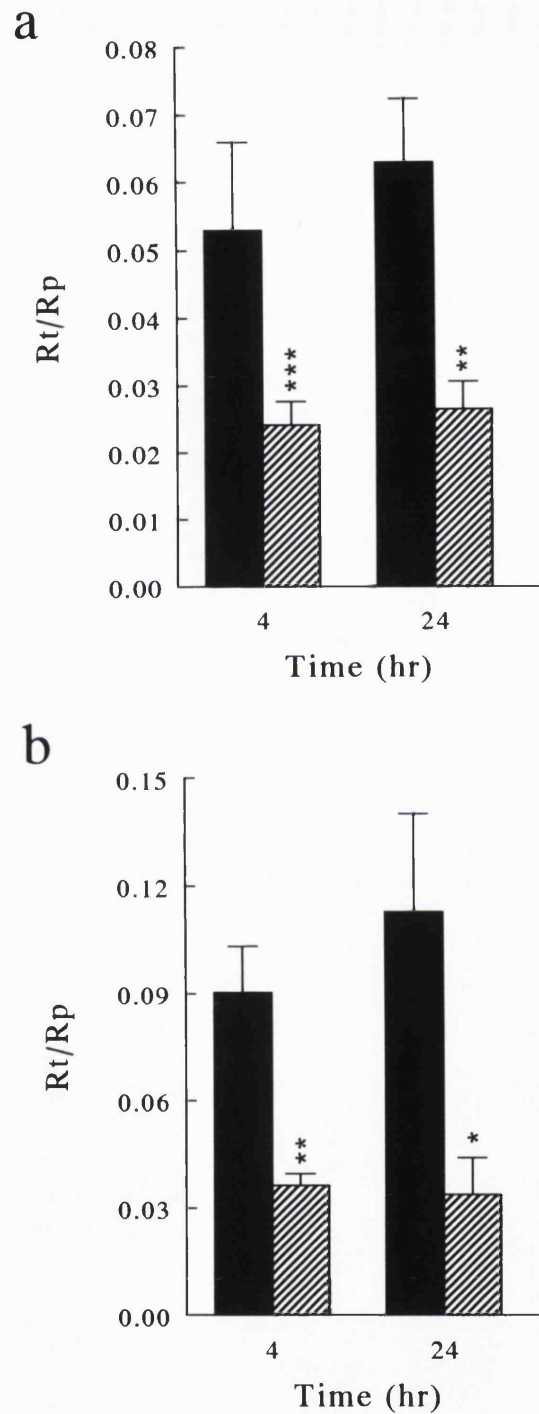
Figure 3.3.1. *Following the intravitreal injection of ranitidine (71μM) mixed with 1-2 x10³ U IL-1β, and accompanied by the administration of ranitidine (25mg.kg⁻¹ IP) (hatched* bars), *there was a significant inhibition in BRB permeability at 4 and 24 hr PI observed in the retina **(a)** and vitreous samples **(b)**, when compared to the effect of intravitreal IL-1β alone* (solid bars). * p <0.05; ** p <0.01; *** p <0.001.
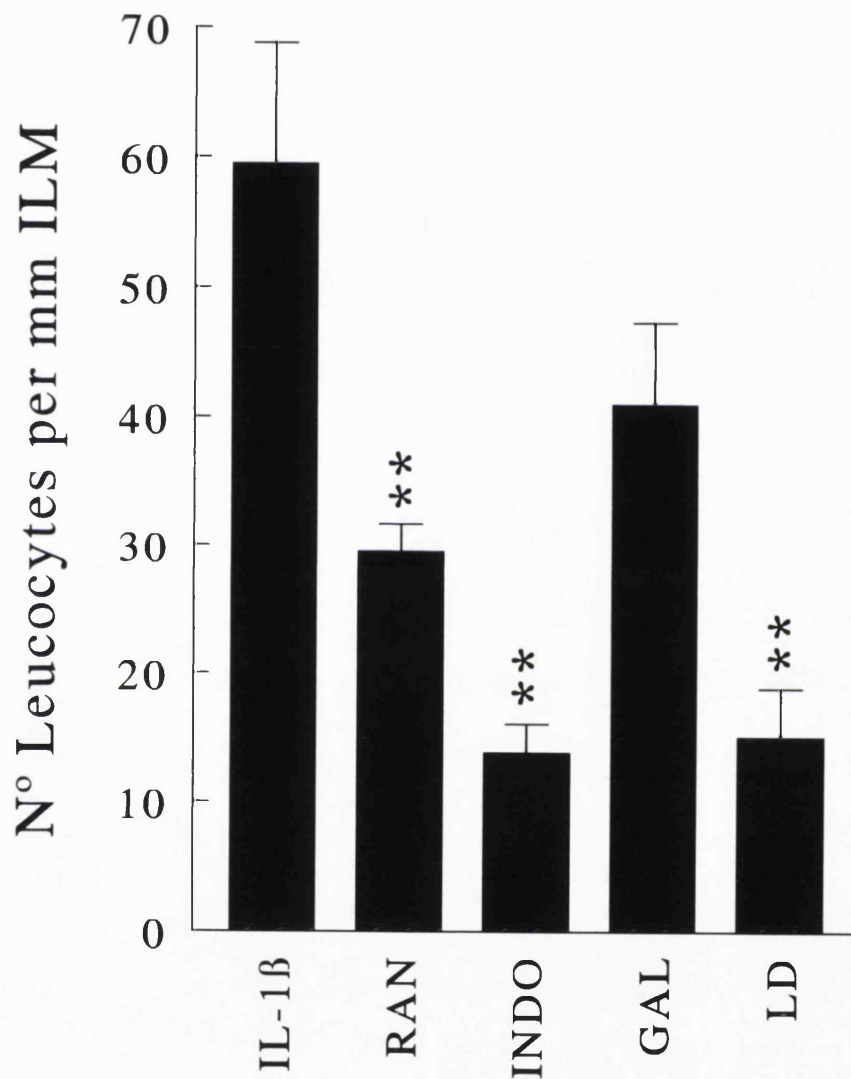
Figure 3.3.2. Significant difference in number of migrated leucocytes per mm of inner limiting membrane (ILM) following intravitreal IL-1ß with ranitidine (RAN; *n* = 6), *indomethacin* (INDO; *n* = 6), *Galardin™* (GAL; *n* = 3) *treatment, or after leucocyte . depletion* (LD; *n* = 5). ** *p* <0.01.

(*n* represents the number of experimental animals. One section of retina was selected from each for leucocyte calculation)
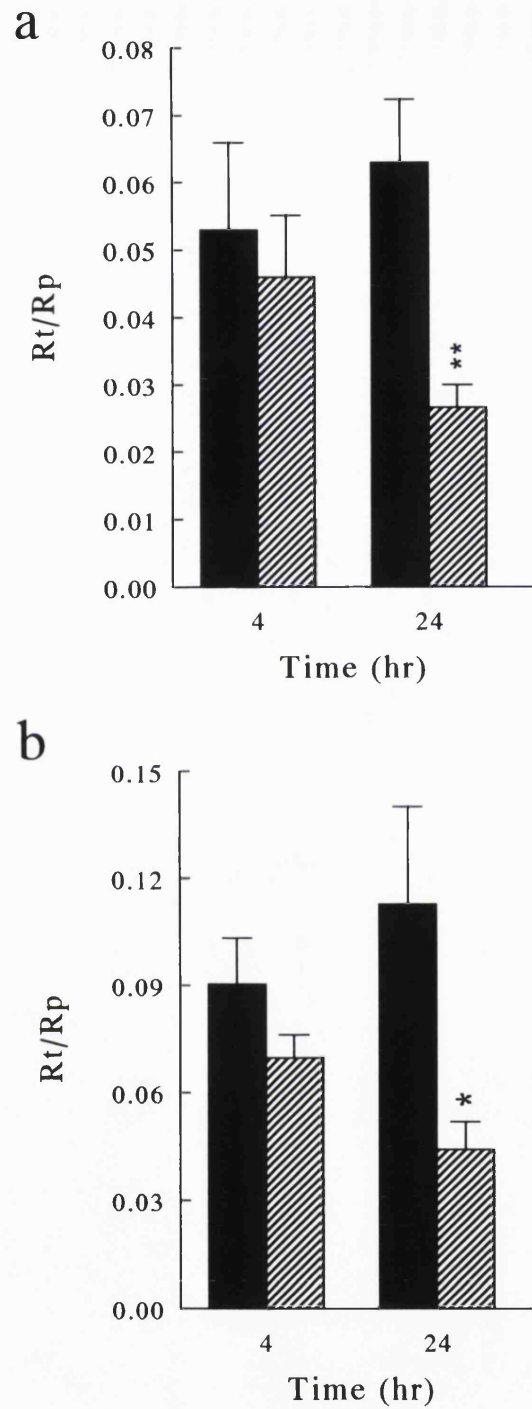
Figure 3.3.3. *Following the intravitreal injection of indomethacin (13.97 μM) mixed with 1-2 x10³ U IL-1β, and accompanied by the administration of indomethacin (5mg.kg⁻¹ subcutaneously)* (hatched bars), *there was a significant inhibition in BRB permeability at 24 hr PI observed in the retina* **(a)** *and vitreous samples* **(b)** *when compared to the effect of intravitreal IL-1β* (solid bars). **p <0.05; ** p <0.01.*

3.3.3 Galardin™

Following the intravitreal injection of Galardin™ with IL-1ß, there was no significant difference in BRB permeability at 4 or 24 hr PI when compared to the degree of opening seen following IL-1ß at these time points (*Fig. 3.3.4*). When Galardin™ was also delivered IP at 6 and 18 hr PI there was no significant difference in the extent of barrier opening after 24 hr (*Fig. 3.3.5*).

The number of leucocytes observed within the retinal vessels at 4 hr PI of IL-1ß and Galardin™ was not significantly different to that seen at the same time point following IL-1ß alone. As the cellular infiltrate seen at 24 hr PI of IL-1ß and Galardin™ appeared to be reduced when compared to IL-1ß alone, the number of migrated leucocytes was counted ($n = 3$). This revealed a non-significant decrease in cellular recruitment in the Galardin™ treated retinas, when compared to the number of cells in the retina following intravitreal IL-1ß (*Fig. 3.3.2*).

3.3.4 Leucocyte Depletion

Blood leucocyte counts revealed a 99% leucopaenia in the rats receiving the cytotoxic drugs, when compared to the number of leucocytes present in control rat blood.

At 24 hr following the intravitreal injection of IL-1ß in leucocyte depleted rats, a significant decrease in the permeability of the BRB was observed at 4 and 24 hr PI in the retina ($p < 0.05$) (*Fig. 3.3.6a*). However, the decrease in permeability observed in the vitreous samples was only significantly different from IL-1ß injected values at 4 hr PI ($p < 0.05$), and not at the 24 hr time point (*Fig. 3.3.6b*).

Histology at 24 hr PI revealed a significant decrease in the number of migrated leucocytes per mm of inner limiting membrane when compared to the number of migrated cells following IL-1ß injection ($n = 5$; $p < 0.01$) (*Fig. 3.3.2*).
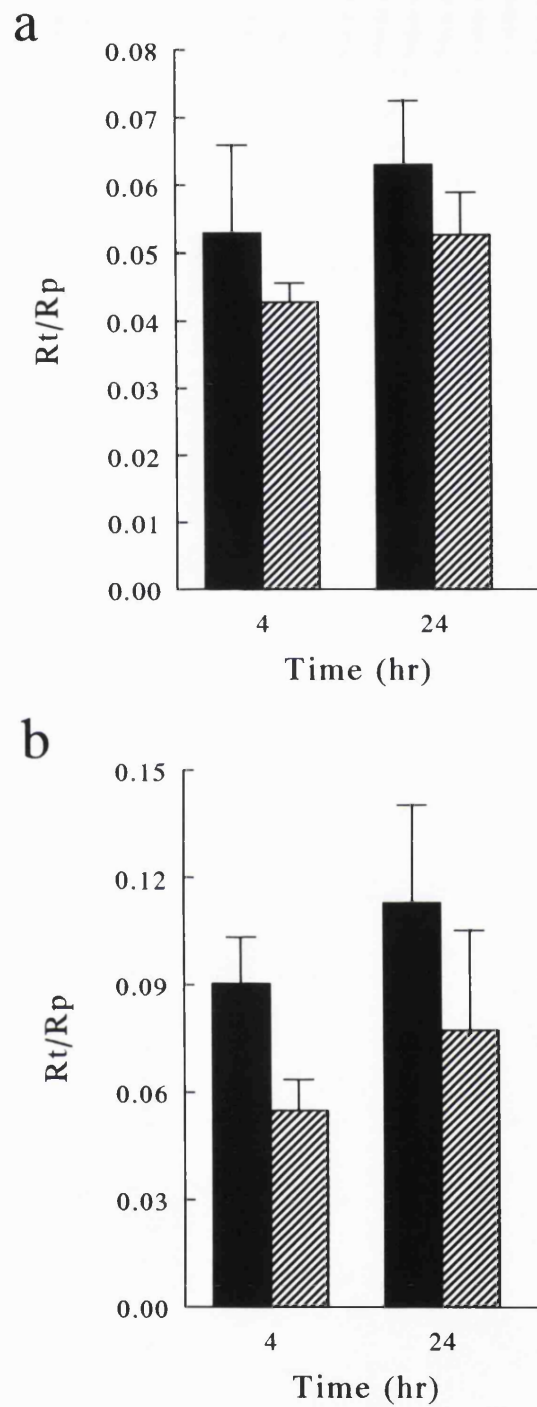
Figure 3.3.4. *Following the intravitreal injection of Galardin™ (100μM) mixed with 1-2 x10³ U IL-1ß* (hatched bars), *there was no significant difference in BRB permeability at 4 and 24 hr PI in the retina (a) and vitreous samples (b), when compared to the effect of intravitreal IL-1ß* (solid bars).
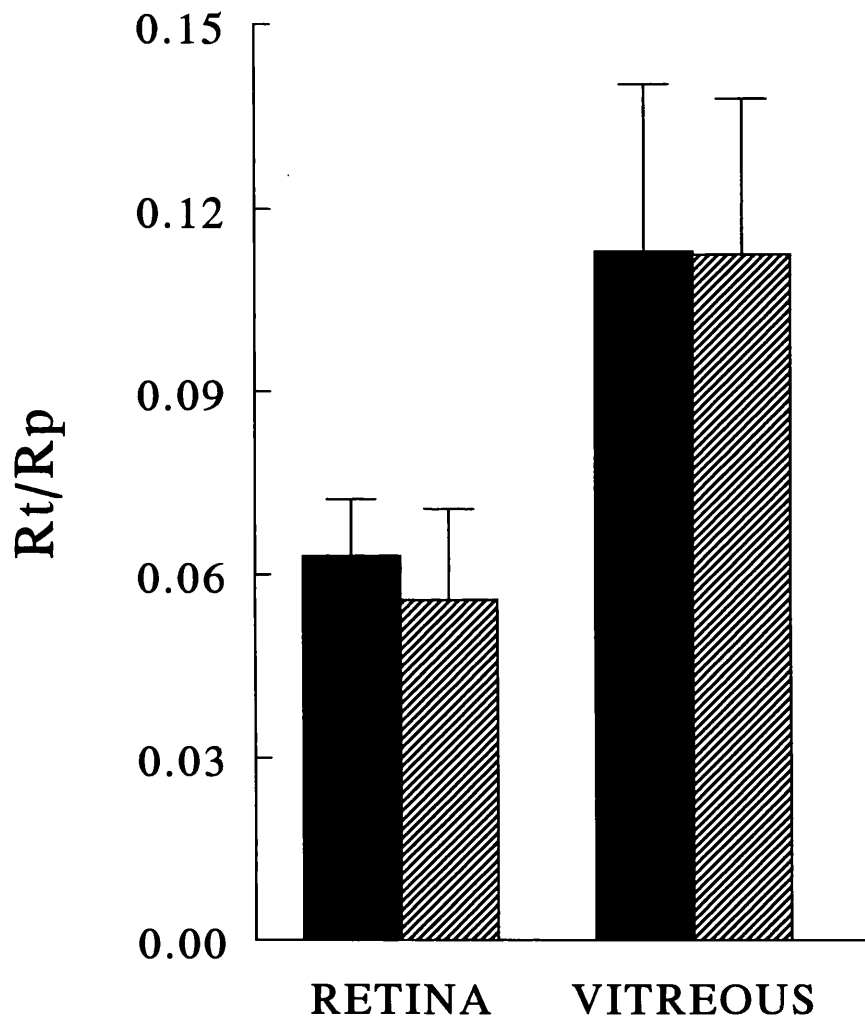
Figure 3.3.5. *When Galardin™ (100μM) was injected intravitreally with 1-2 x10³ U IL-1β, and Galardin™ also administered IP (4mg.kg⁻¹) at 6 and 18 hr PI (hatched bars), no significant difference in BRB permeability was detected when compared to the degree of barrier breakdown seen following intravitreal IL-1β (solid bars).*
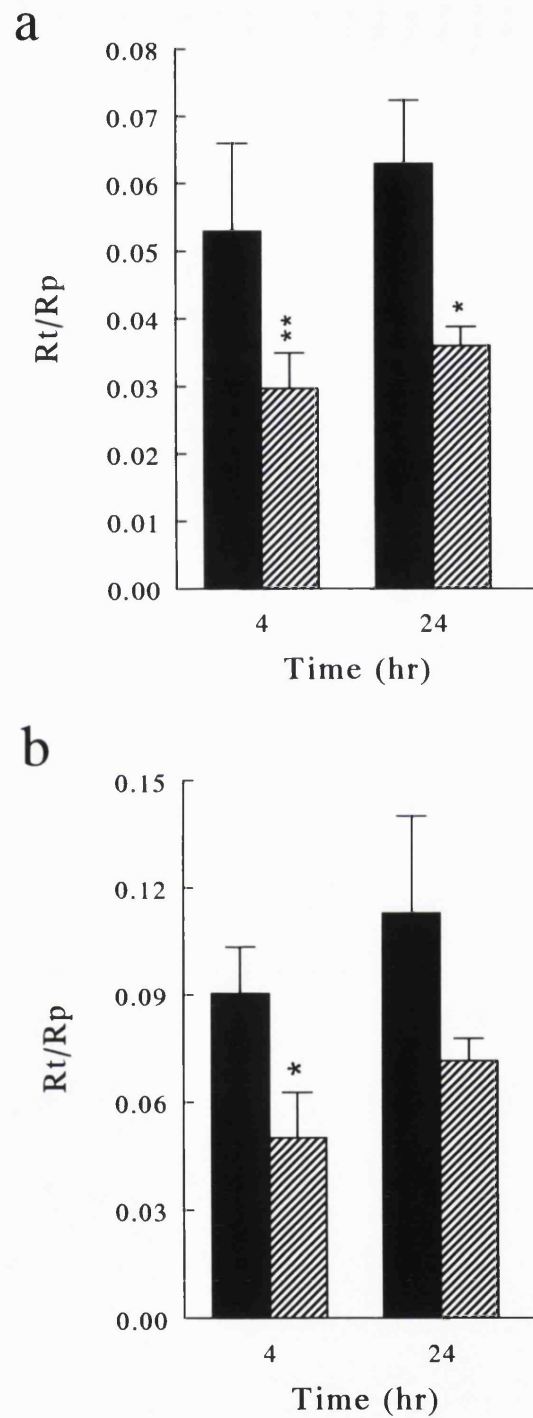
Figure *3.3.6. BRB permeability following the intravitreal injection of 1-2 x10³ U IL-1β in leucocyte depleted rats.* **a** *There was a significant decrease in BRB permeability at 4 and 24 hr PI observed in the retina* (hatched bars), *when compared to the effect of intravitreal IL-1β in normal animals* (solid bars). **b.** *The decrease in permeability observed in the vitreous samples* (hatched bars) *was only significantly different from IL-1β injected values in normal rats at 4 hr PI* (solid bars). *p <0.05; ** p <0.01.*

TUMOUR NECROSIS FACTOR-α

3.4 TUMOUR NECROSIS FACTOR-α

3.4.1 Histology

Following the intravitreal injection of 4 x10³ U TNF-α no inflammatory cells were seen at 24 hr PI (n = 4). However, after the intravitreal injection of either 1 x10⁴ U (n = 2 for each time point; total n = 12) or 2 x10⁴ U TNF-α (n ≥ 2 for each time point; total n = 15), a few leucocytes could be detected within the lumen of blood vessels of the neuroretina and in the vitreous from 4 hr to 5 day PI (*Figs. 3.4.1a & b*). Cells were also observed within the tissue parenchyma. Although there was no apparent difference in leucocyte recruitment between the two doses, more cells were present than would be seen following a sham injection or intravitreal injection of vehicle control. The inflammatory cells seen were all MN in appearance (*Figs. 3.4.2a & b*).

3.4.2 Immunohistochemistry

Increased expression of MHC class II was seen in each retina of the TNF-α (2 x10⁴ U) injected eyes at 1, 2 and 3 days PI (n ≥ 1 for each time point; total n = 4) (*Fig. 3.4.3a*). Positive staining was also observed in the choroid, which is not part of the neuroretina, and these were thought to represent tissue resident bone-marrow derived cells. ED1 positive cells were also seen in the retina and choroid of the injected eyes (*Fig. 3.4.3b*) as was the occasional ED2 positive cell (*Fig. 3.4.4a*). Very rarely an OX8 positive cell was seen in the neuroretina and choroid (*Fig. 3.4.4b*). There was no staining observed for the CD18 marker. In the retina and vitreous of the contralateral non-injected eye, the occasional ED1 or ED2 positive cell was seen, but there was no upregulation in MHC class II expression or staining for CD18.

3.4.3 BRB Permeability to HRP

No HRP leakage was seen in the retina of the TNF-α injected eyes at 5 and 7 day PI (n ≥ 2 for each time point; total n = 6). However, extravasated HRP was observed within the ciliary body of injected and non-injected eyes as expected (not shown).
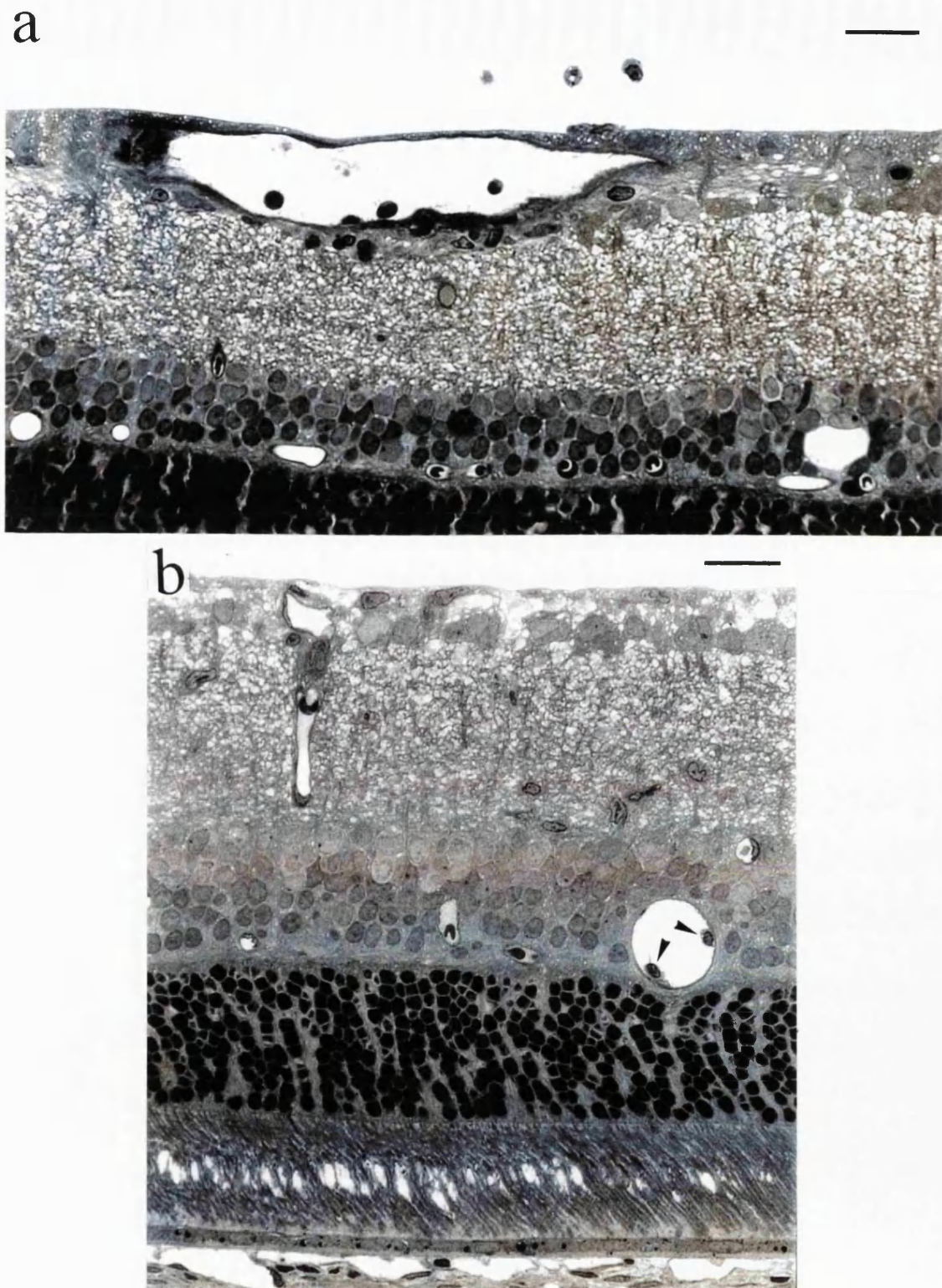
Figure 3.4.1. *Toluidine blue stained resin sections of retina following an intravitreal injection of TNF-α. a. 5 day PI TNF-α (1 x10⁴ U). MN leucocytes are present within the lumen of a blood vessel, in the tissue parenchyma and also in the vitreous* (Bar = 25μM). *b. 24 hr PI TNF-α (2 x10⁴ U). MN leucocytes can be seen adhering to the endothelium of a blood vessel* (arrow heads) (Bar = 25μM).
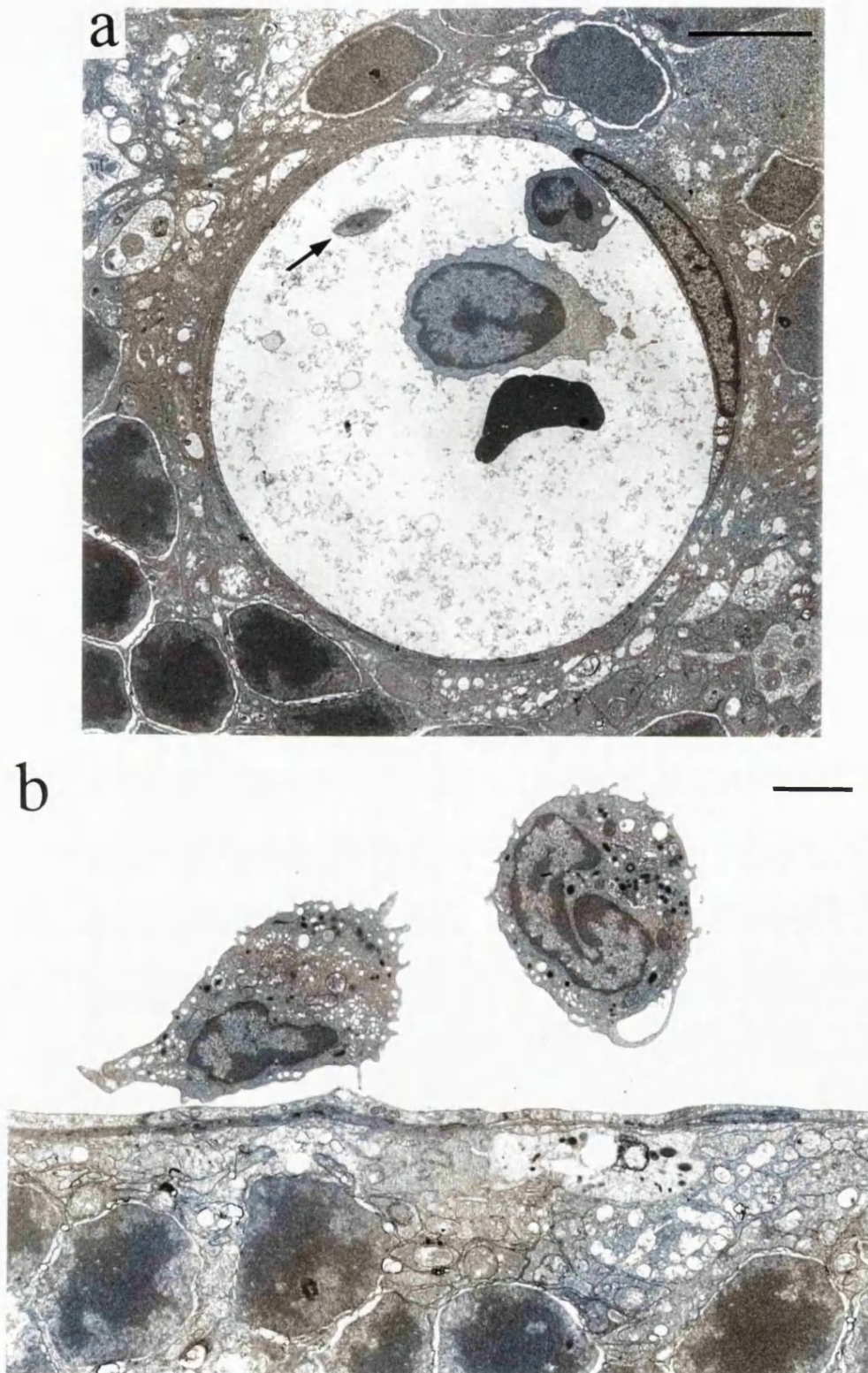
Figure 3.4.2. TEMs following an intravitreal injection of 2×10^4 U TNF-α. **a.** 4 hr PI. Two MN leucocytes and a platelet (arrow) within the lumen of a blood vessel. (Bar = 5μM). **b.** 24 hr PI. Two MN cells adhering to the EC of a retinal blood vessel (Bar = 2μM). No PMN leucocytes were observed.
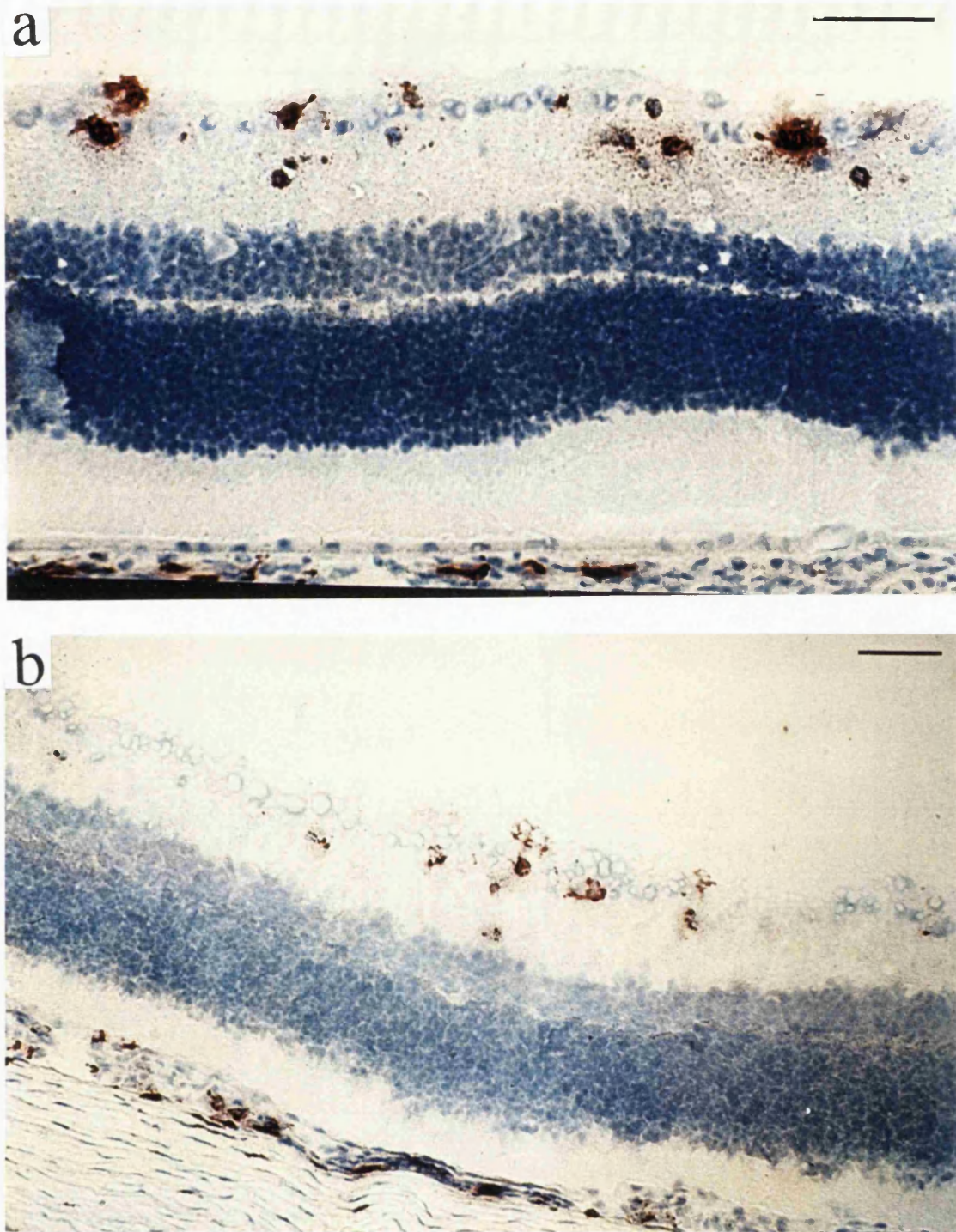
Figure 3.4.3. Immunohistochemistry on frozen sections of retina following intravitreal injection of TNF-α (2 x10⁴ U). a. Expression of MHC class II at 2 days PI (Bar = 50μM). b. Positive staining for ED1 (macrophages and monocytes) at 3 days PI (Bar = 50μM).
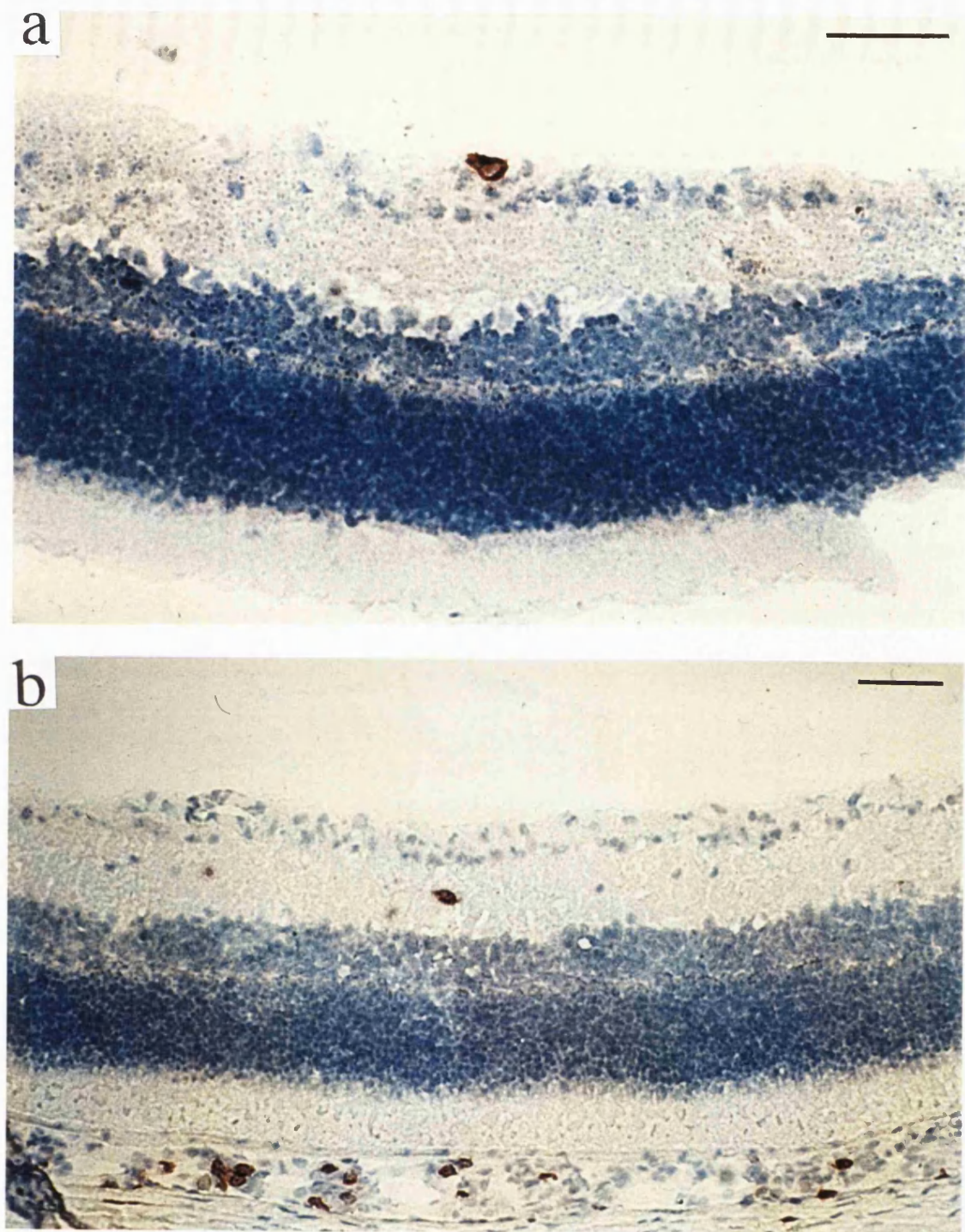
Figure 3.4.4. *Immunohistochemistry on frozen sections of retina following intravitreal injection of TNF-α (2 x10⁴ U). a. The occasional cell staining positive for ED2 (macrophages) was observed* (Bar = 50μM). *b. Very rarely staining for OX8 (CD8⁺ cytotoxic T cell) was also observed* (Bar = 50μM).

137

3.4.4 BRB Permeability to [^{14}C]-Mannitol

Following an intravitreal injection of 1 x10^4 U TNF-α, no significant opening of the BRB was detected over a 4 day period within the retina (*Fig. 3.4.5a*) or vitreous samples (*Fig. 3.4.5b*). Using a dose of 2 x10^4 U TNF-α, however, a significant increase in BRB permeability was detected from 1 to 5 days PI ($p < 0.01$) (*Fig. 3.4.6a*). An increase in [^{14}C]-mannitol extravasation was also determined in the vitreous samples at 4 hr PI and from 1 to 5 days PI ($p < 0.05$) (*Fig. 3.4.6b*).

It was noticed that the contralateral non-injected eyes of those that received the larger dose of TNF-α in this study yielded an unexpected response. The Rt/Rp values were significantly increased in the retina of the non-injected eyes from 1 to 5 days PI of the test eye ($p < 0.05$) (*Fig. 3.4.7a*), indicating an increase in BRB permeability. The vitreous samples also presented an increase in [^{14}C]-mannitol accumulation at 4 hr and from 1 to 9 days PI of the test eye ($p < 0.05$) (*Fig. 3.4.7b*).

The mean Rt/Rp ratio for the brain samples from the 1 x10^4 U TNF-α injected animals (mean ± SEM: $0.0113 ± 0.0005$; $n = 16$) was not significantly different from the non-injected and vehicle control injected animals. However, the mean permeability value from the cerebral samples of the 2 x10^4 U TNF-α injected animals (mean ± SEM: $0.0141 ± 0.0004$; $n = 71$) was very significantly different from the control injected animals ($p < 0.001$).

Mean blood pressure, blood-gas and pH measurements were made during the course of each mannitol experiment for the 1 x10^4 U TNF-α dose (*Table 3.4.1 & 3.4.2*) and the 2 x10^4 U TNF-α dose (*Table 3.4.3 & 3.4.4*). For the 1 x10^4 U dose, there were significant differences in the mean pH ($p < 0.05$), and pCO_2 ($p < 0.01$) measurements. However, as there was no significant increase in BRB permeability using this dose, it is unlikely that such small differences in these measurements would contribute to altered blood-CNS barrier permeabilities.

There was no significant difference in the mean blood-gas and pH measurements in the experiments using the larger dose of TNF-α, but there was a significant increase in the mean arterial systolic blood pressure ($p < 0.01$).

a

b
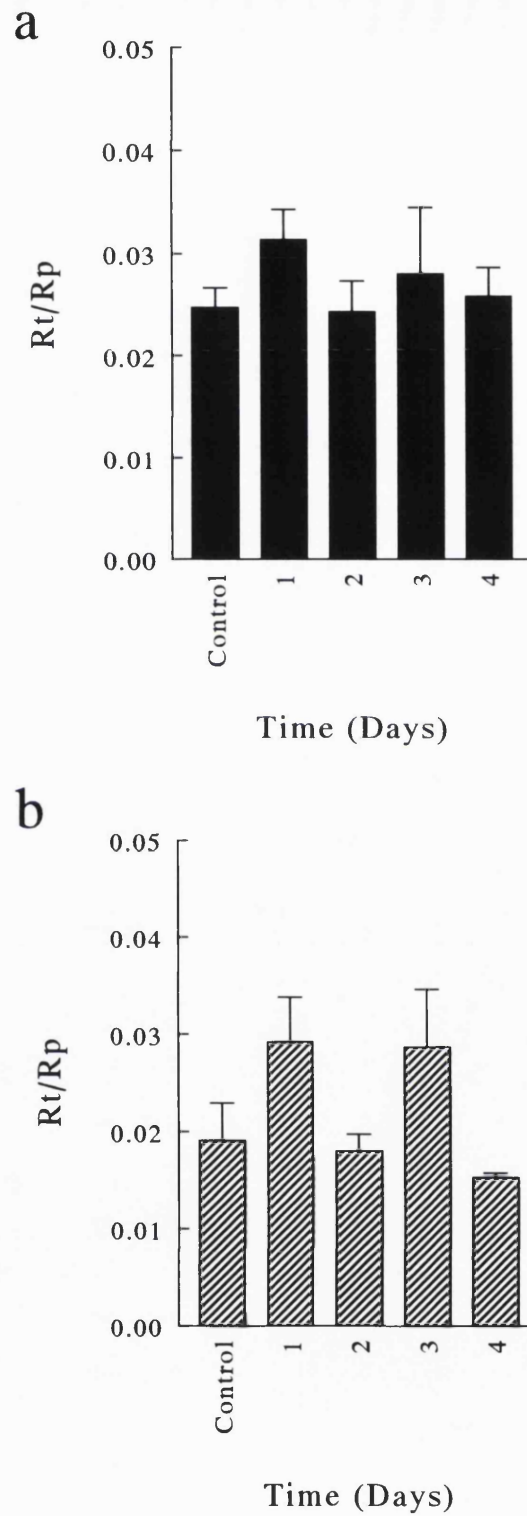
Figure 3.4.5. No significant increase in the Rt/Rp ratio was seen following the intravitreal injection of 1 x10^4 U TNF-α in **(a)** the retina or **(b)** the vitreous samples.

139

a

b
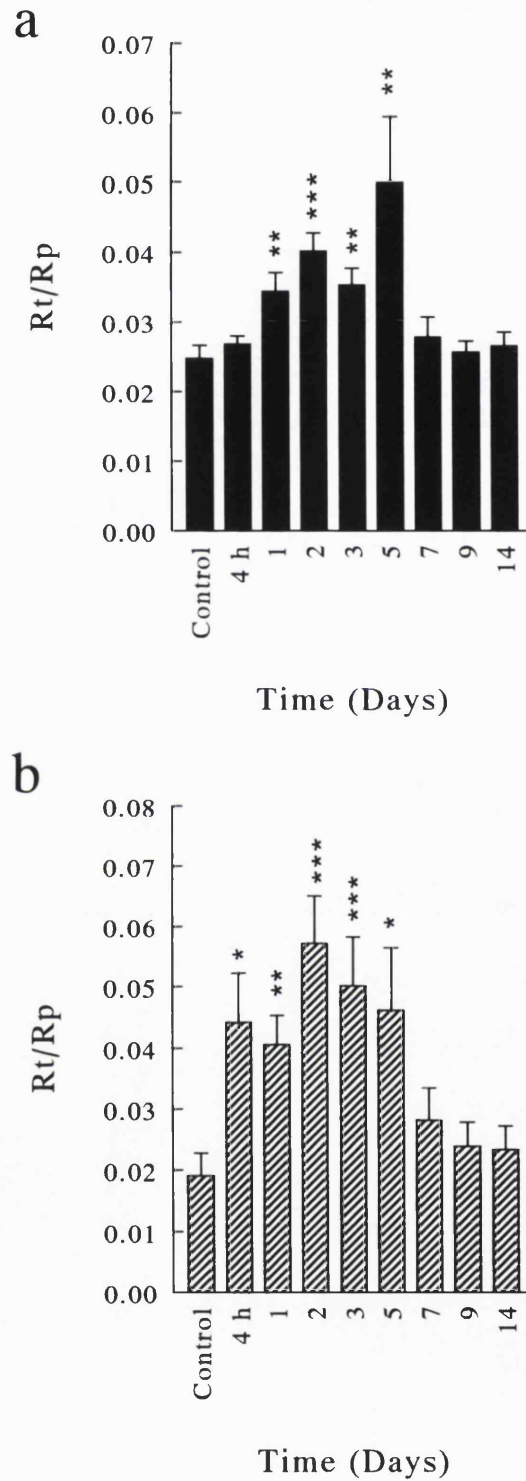
Figure 3.4.6. *Following the intravitreal injection of 2 x10^4 U TNF-α, a monophasic increase in the Rt/Rp ratios was observed in the retina (a) and in the vitreous samples (b) when compared to the effects of vehicle control.* * p <0.05; ** p <0.01; *** p <0.001.

140
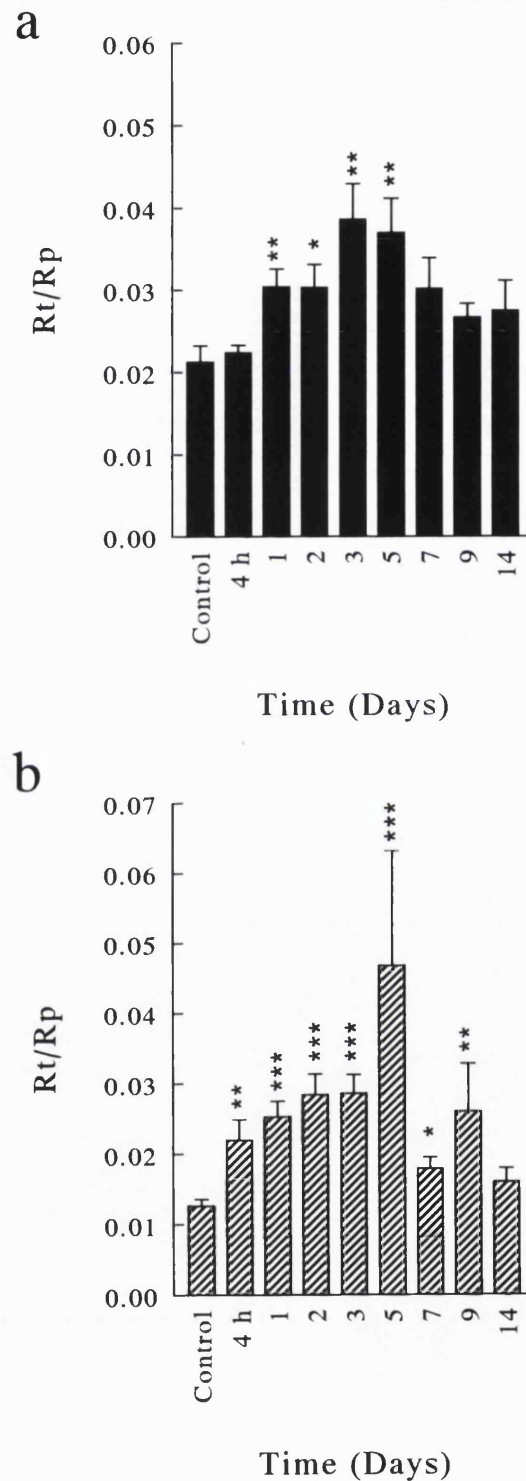
Figure 3.4.7. *A significant increase in BRB permeability was detected in the non-injected contralateral eyes of those receiving 2 x10⁴ U TNF-α, when compared to the Rt/Rp ratios from non-injected animals, in the retina (a) from 1 to 5 days PI, and in the vitreous samples (b) up to 9 days PI. * p <0.05; ** p <0.01; *** p <0.001.*

n	Systole (mmHg)	Diastole (mmHg)
15	106.93 ± 2.60	85.07 ± 2.08

Table 3.4.1. *Mean arterial blood pressure measurements from 1 x10^4 U TNF-α injected animals at the beginning of each [^{14}C]-mannitol experiment. Values are means ± SEM. There is no significant difference from controls (see Table 3.1.1, page 88).*

n	pH	pCO$_2$ (kPa)	pO$_2$ (kPa)	% O$_2$
16	7.34 ± 0.013*	7.41 ± 0.33**	9.91 ± 0.40	91.5 ± 1.81

Table 3.4.2. *Mean pH and blood gas levels from 1 x10^4 U TNF-α injected animals. Measurements were taken at 2, 10 and 18 minutes throughout the course of the [^{14}C]-mannitol infusion. Values are means ± SEM. * p <0.05; ** p <0.01 (Significant difference from non-injected and vehicle control-injected animals, see Table 3.1.2, page 88).*

n	Systole (mmHg)	Diastole (mmHg)
62	120.71 ± 1.42**	93.19 ± 1.13

Table 3.4.3. *Mean arterial blood pressure measurements from 2 x10⁴ U TNF-α injected animals at the beginning of each [¹⁴C]-mannitol experiment. Values are means ± SEM.* ** *Significant difference from non-injected and vehicle control-injected animals, p <0.01; see Table 3.1.1, page 88).*

n	pH	pCO₂ (kPa)	pO₂ (kPa)	% O₂
43	7.37 ± 0.006	6.67 ± 0.18	9.38 ± 0.19	92.2 ± 0.54

Table 3.4.4. *Mean pH and blood gas levels from 2 x10⁴ U TNF-α injected animals. Measurements were taken at 2, 10 and 18 minutes throughout the course of the [¹⁴C]-mannitol infusion. Values are means ± SEM. There is no significant difference from controls (see Table 3.1.2, page 88).*

INTERLEUKIN-6

3.5 INTERLEUKIN-6

3.5.1 Histology

By 4 hr PI of 1 $\times 10^3$ U IL-6, a few MN cells were observed adhering to the endothelium of retinal vessels and frequently accompanied by platelets (*Fig. 3.5.1a*). The inflammatory response did not notably change over the subsequent 3 days, with the occasional leucocyte appearing predominantly in the vitreous. Rarely, mast cells were noticed in the choroid (*Fig. 3.5.1b*). However, using a dose of 2 $\times 10^3$ U IL-6, at 24 hr PI MN cells were observed more regularly, also in the presence of platelets (*Fig. 3.5.2a*), along with PMN leucocytes within the lumen of retinal vessels, in the tissue parenchyma and in the vitreous (*Fig. 3.5.2b*). No cells were seen in the process of migrating through the endothelium. No cells were observed following the intravitreal injection of 100 U IL-6 after 24 hr.

3.5.2 BRB Permeability to [^{14}C]-Mannitol

IL-6 administered intravitreally had no significant effect on increasing BRB permeability (*Fig. 3.5.3*).

The mean Rt/Rp ratio for the brain samples from the IL-6 injected animals was 0.011 ± 0.0003 (mean ± SEM; n=18) and was not significantly different from the non-injected and vehicle control injected eyes.

The mean blood pressure, blood-gas and pH measurements made during the course of each mannitol experiment (*Table 3.5.1 & 3.5.2*) were not significantly different from those from the control studies.
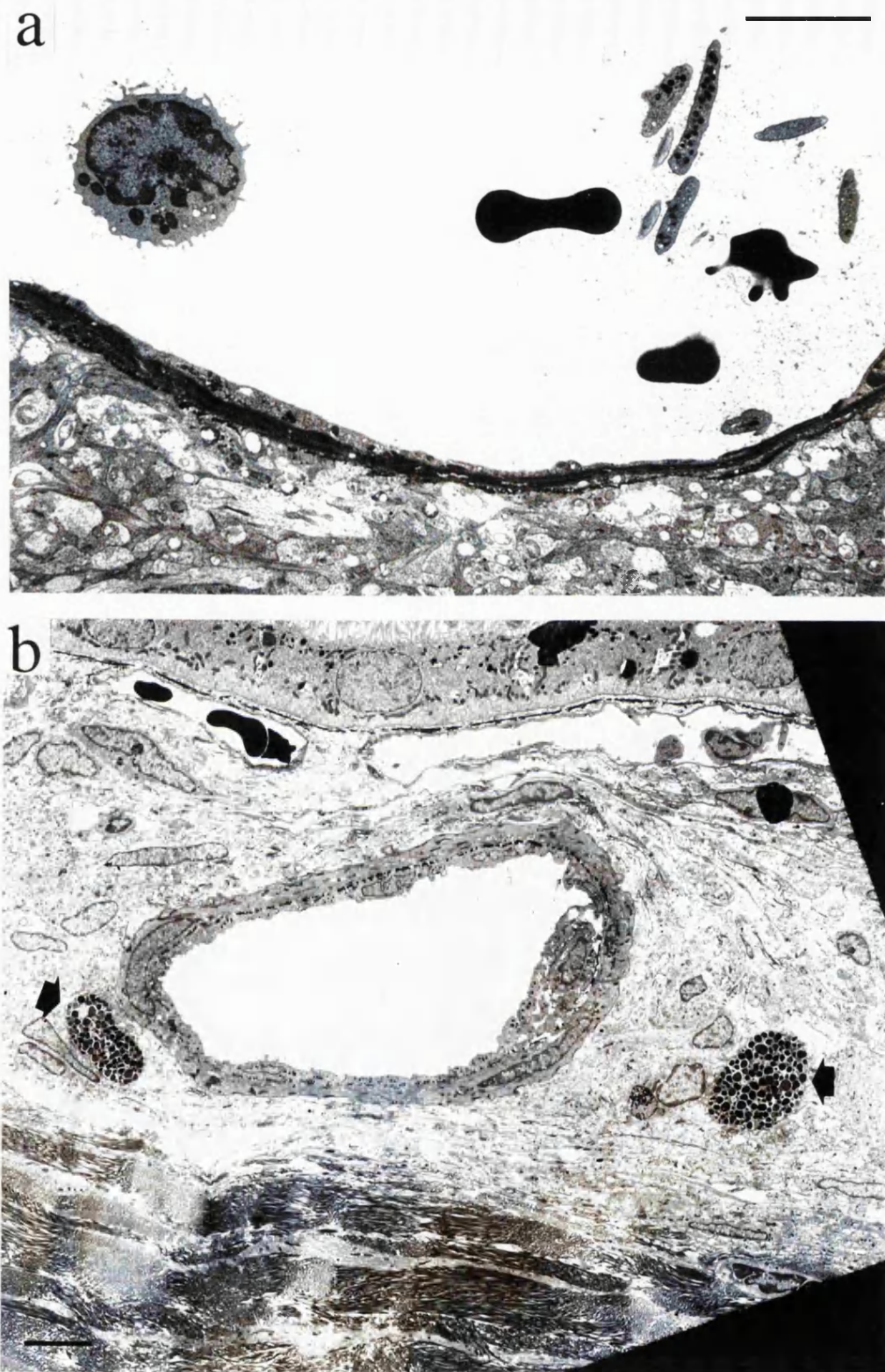
Figure *3.5.1.* *TEMs following intravitreal IL-6 (1 x10³ U).* *a. 4 hr PI. A MN cell is present within the lumen of a retinal blood vessel accompanied by several platelets* (Bar = 5μM). *b. 8 hr PI. Two mast cells can be seen in the choroid* (arrows). (Bar = 10μM).
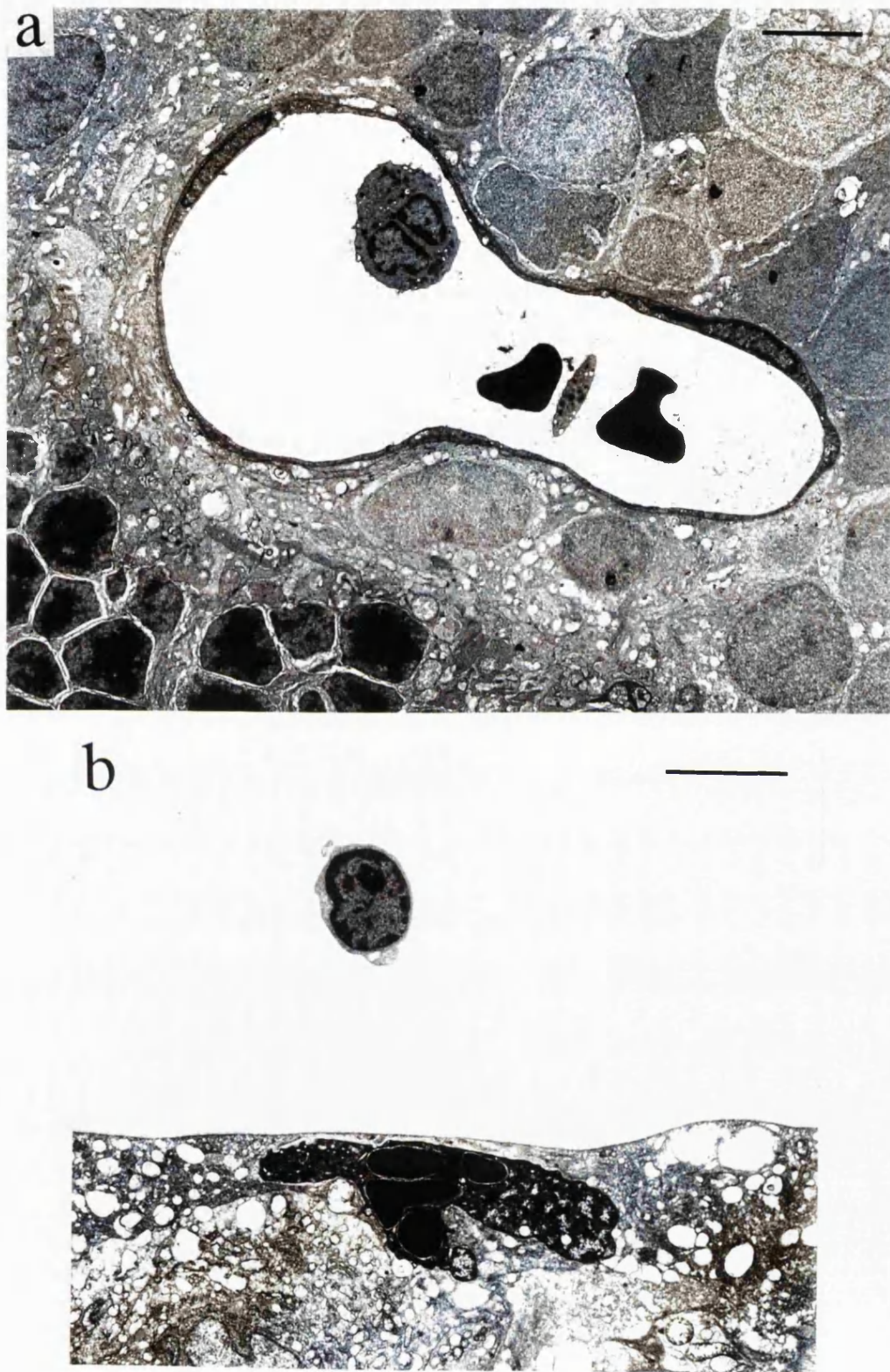
Figure 3.5.2. *TEMs, 24 hr PI 2 x10³ U IL-6. a. A MN cell and a platelet are present within the lumen of a blood vessel* (Bar = 5μM). *b. A PMN is lying beneath the inner limiting membrane of the retina within the parenchyma. A cell that appears to be a small lymphocyte is present in the vitreous* (Bar = 5μM).
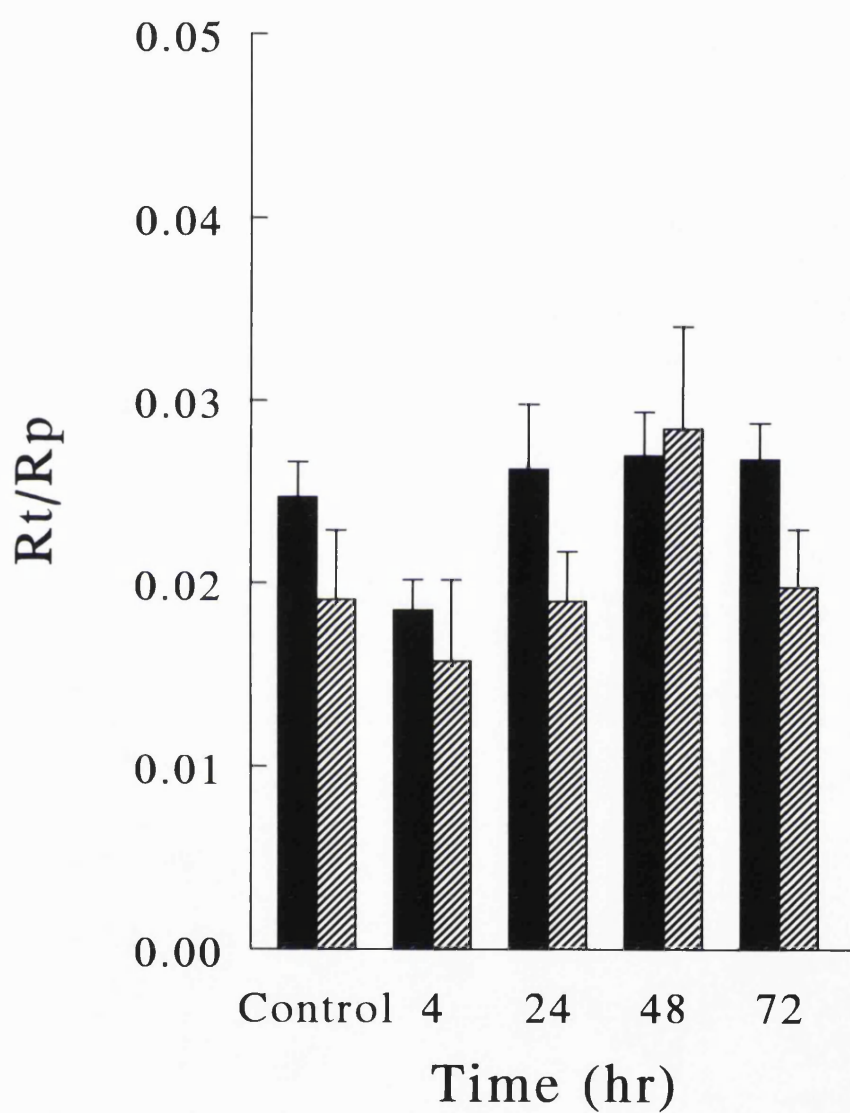
Figure 3.5.3. *Following an injection of 1 x10³ U IL-6 to the right vitreous, no significant increase in BRB permeability was detected in the retina* (solid bars) *or vitreous samples* (hatched bars).

n	Systole (mmHg)	Diastole (mmHg)
17	117.94 ± 2.86	92.71 ± 2.53

Table 3.5.1. Mean arterial blood pressure measurements from IL-6 injected animals at the beginning of each [^{14}C]-mannitol experiment. Values are means ± SEM and are not significantly different from vehicle and non-injected controls (see Table 3.1.1, page 88)..

n	pH	pCO$_2$ (kPa)	pO$_2$ (kPa)	% O$_2$
18	7.40 ± 0.01	6.25 ± 0.13	9.52 ± 0.26	93.3 ± 0.52

Table 3.5.2. Mean pH and blood gas levels from IL-6 injected animals. Measurements were taken at 2, 10 and 18 minutes throughout the course of the [^{14}C]-mannitol infusion. Values are means ± SEM, and are not significantly different from vehicle and non-injected control animals (see Table 3.1.2, page 88).

HISTAMINE

3.6 HISTAMINE

3.6.1 Intravitreal Histamine

Breakdown of the BRB, following the intravitreal injection of histamine, occurred only at the 0 time point in the retinal samples for the 1×10^{-3} M and 1×10^{-4} M concentrations, when compared to the effect of intravitreal saline ($p < 0.05$) (*Fig 3.6.1a*). A significant increase in the Rt/Rp ratio of the vitreous samples of the injected eyes at the 0 time point was also recorded ($p < 0.05$) following intravitreal histamine (1×10^{-4} M) (*Fig. 3.6.1b*). No significant increase in BRB permeability was detected at 15 or 30 min PI for any of the concentrations used.

3.6.2 Intracarotid Histamine

A significant increase in BRB permeability occurred following the intracarotid administration of 1×10^{-4} M histamine at the 0 time point and at 15 minutes post-administration, when compared to the effects of intracarotid-delivered saline ($p < 0.05$) (*Fig. 3.6.2a & b*). A significant increase in the Rt/Rp ratio of the vitreous samples of the animals that received an intracarotid injection of 1×10^{-3} M at the 0 time point was also recorded ($p < 0.05$). The permeability ratio remained at control values by 30 min post-administration, and no significant increase in BBB permeability occurred for any concentration of histamine at any of the time points studied.
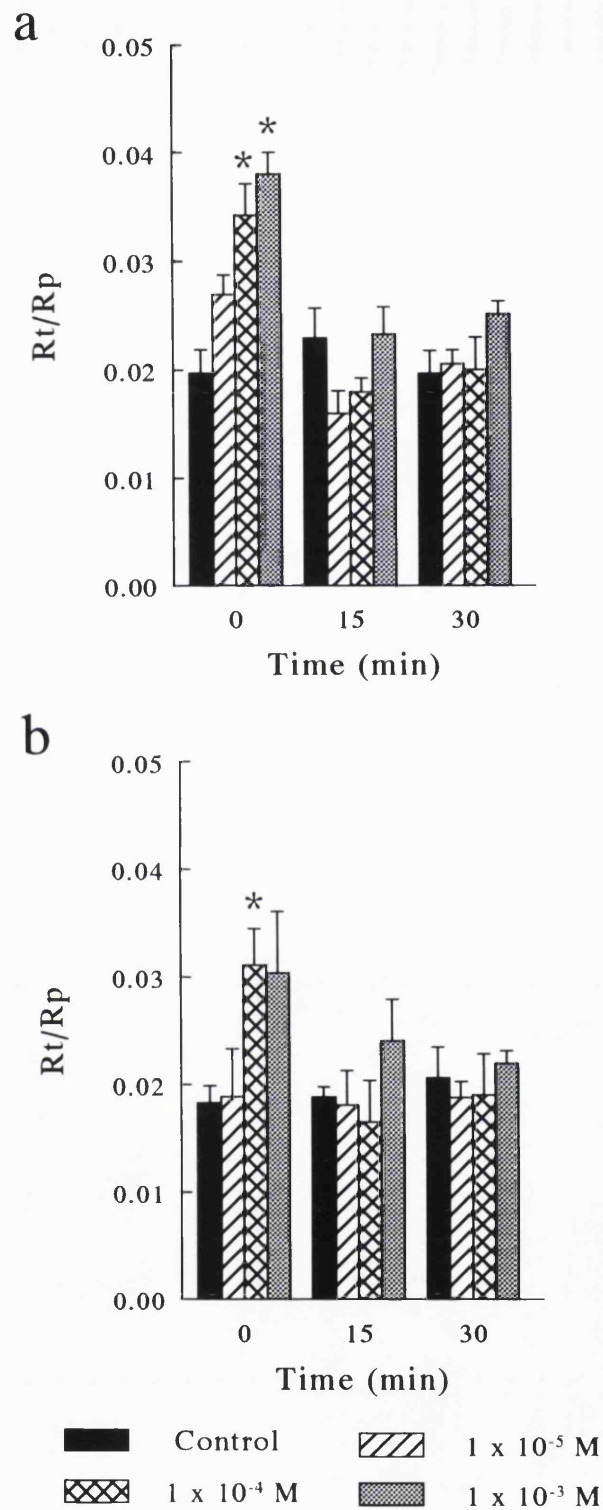
Figure 3.6.1. BRB permeability following the intravitreal injection of various doses of histamine. *a.* A significant increase in the permeability of the retina was detected at the 0 time point using the 1×10^{-3} M and 1×10^{-4} M concentrations. *b.* A significant increase in the Rt/Rp ratio was recorded in the vitreous samples from the 1×10^{-3} M concentration at the 0 time point. * $p < 0.05$.
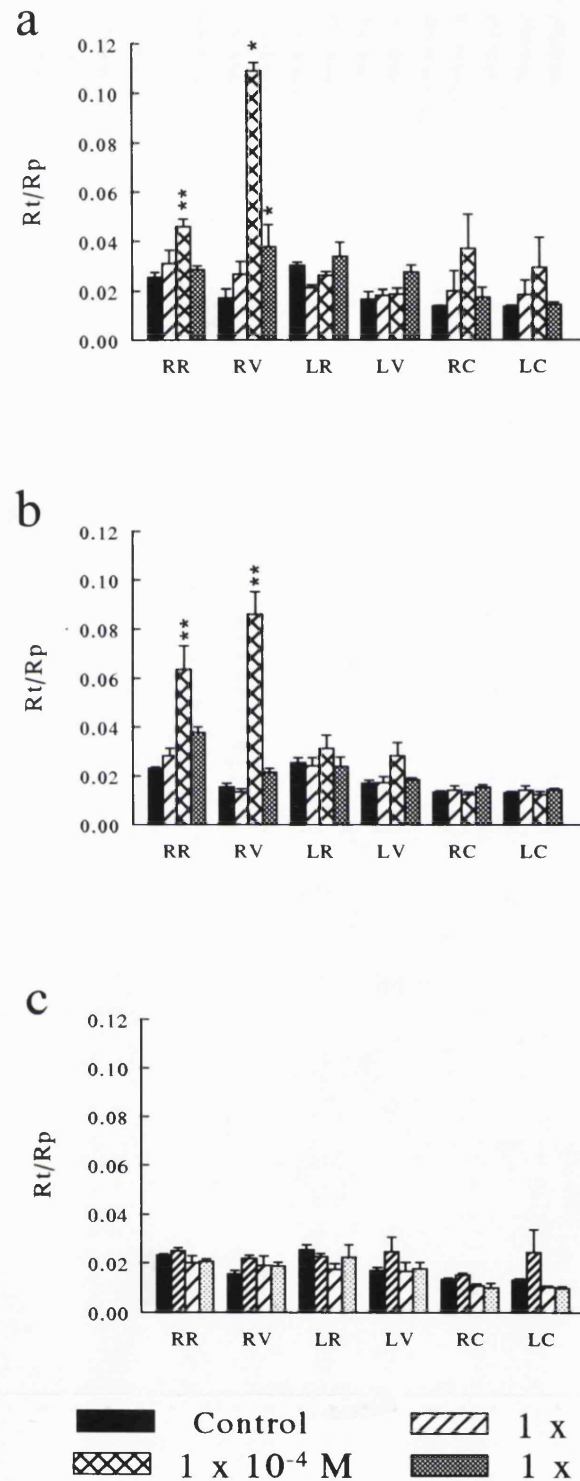
Figure 3.6.2. Following the intracarotid administration of various doses of histamine, a significant increase in BRB permeability was detected at the 0 (a) and 15 minute time point (b) using the 1 x 10⁻⁴ M concentration. A significant increase in the Rt/Rp ratio was also recorded in the vitreous samples from the 1 x 10⁻³ M concentration at the 0 time point (a). No increases in the Rt/Rp ratio were observed at the 30 minute time point (c). * p <0.05; ** p <0.01. (**RR:** right retina; **RV:** right vitreous; **LR:** left retina; **LV:** left vitreous; **RC:** right cerebrum; **LC:** left cerebrum)

154

IMMUNOASSAYS

3.7 IMMUNOASSAYS

3.7.1 Radioimmunoassay

Specific radioimmunoassays were performed to detect PGE_2 production from rat REC (*Fig. 3.7.1*) following stimulation with cytokines for 24 hr.

3.7.1.1 Interleukin-1ß

A significant increase in PGE_2 levels within the supernatants taken from IL-1ß stimulated rat REC was recorded for each dose of cytokine tested (5, 10 and 20 U/ml after 24 h; $p < 0.01$ when compared to supernatant from unstimulated EC) as measured by a specific radioimmunoassay (*Fig. 3.7.2*).

The cyclooxygenase inhibitor, indomethacin (5 µg/ml), added to 5 U/ml IL-1ß blocked the production of PGE_2 from the REC, and produced no significant effect by itself. However, IL-1ß at 10 U/ml with indomethacin produced significantly less PGE_2 levels than the control samples ($p < 0.05$) (*Fig. 3.7.2*).

3.7.1.2 Tumour Necrosis Factor-α

Following stimulation of REC with TNF-α, there was a significant increase in PGE_2 production only with the highest concentration used (300 U/ml after 24 h; $p < 0.01$) and this was noticeably less than the values seen for IL-1ß (*Fig. 3.7.3*).

3.7.1.3 Interleukin-6

A significant increase in PGE_2 levels was measured following stimulation with 10 U/ml IL-6 after 24 hr ($p < 0.05$) (*Fig. 3.7.4*), but this value was less than the significant values obtained for IL-1ß and TNF-α.

3.7.2 Enzyme immunoassay

No detectable levels of histamine were observed in the supernatants of IL-1ß stimulated rat REC by enzyme immunoassay.

Figure 3.7.1. *Freshly isolated fragments of rat retinal microvessels plated onto collagen coated tissue culture wells had formed a confluent monolayer by 2 weeks.* (Bar = 100μM).
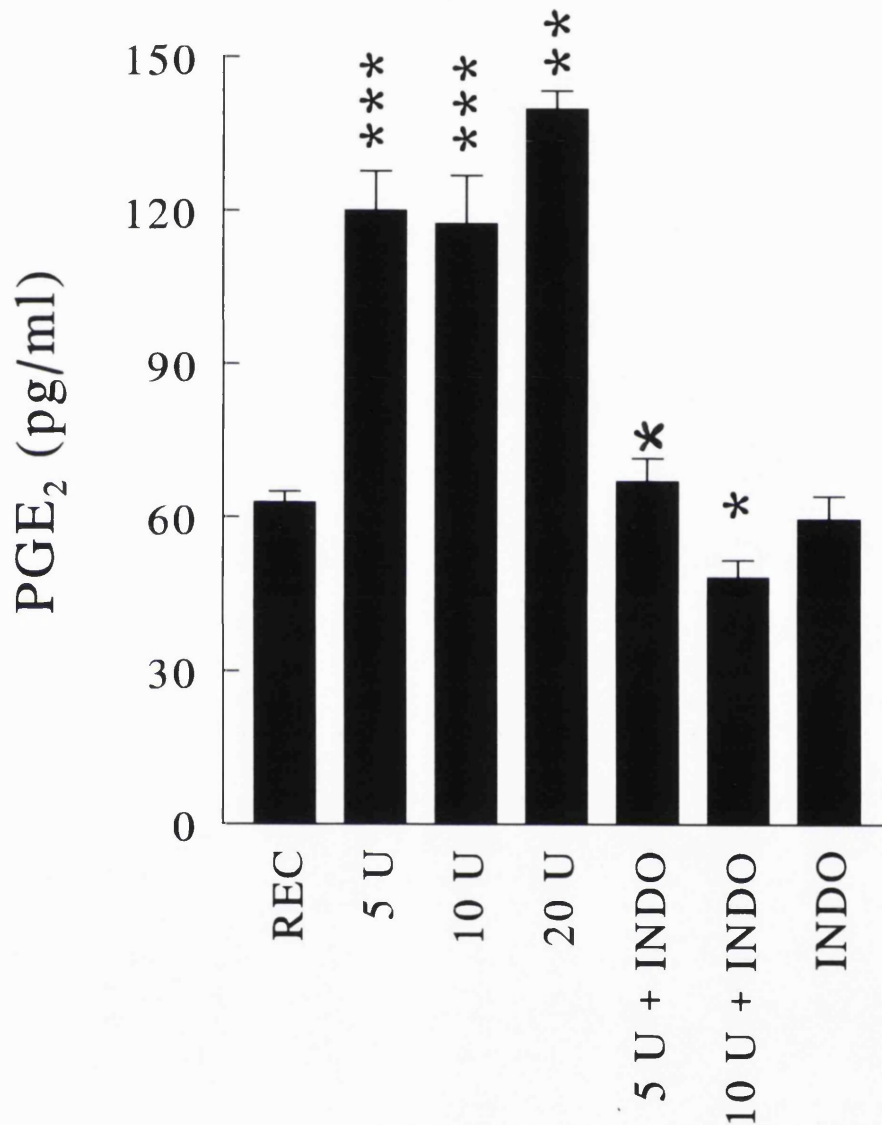
Figure. 3.7.2. *A highly significant increase in* PGE$_2$ *levels was found in the supernatants of rat retinal EC* (REC) *at 24 hr following stimulation with IL-1ß at concentrations of 5 U/ml* (5 U; *n = 4),* 10 U/ml *(10 U; n = 6) and 20 U/ml (20 U; n = 2). Indomethacin* (INDO) *with 5+℅ U/ml IL-1ß successfully inhibited the production of* PGE$_2$.
* p <0.05; ** p <0.01; *** p <0.001.
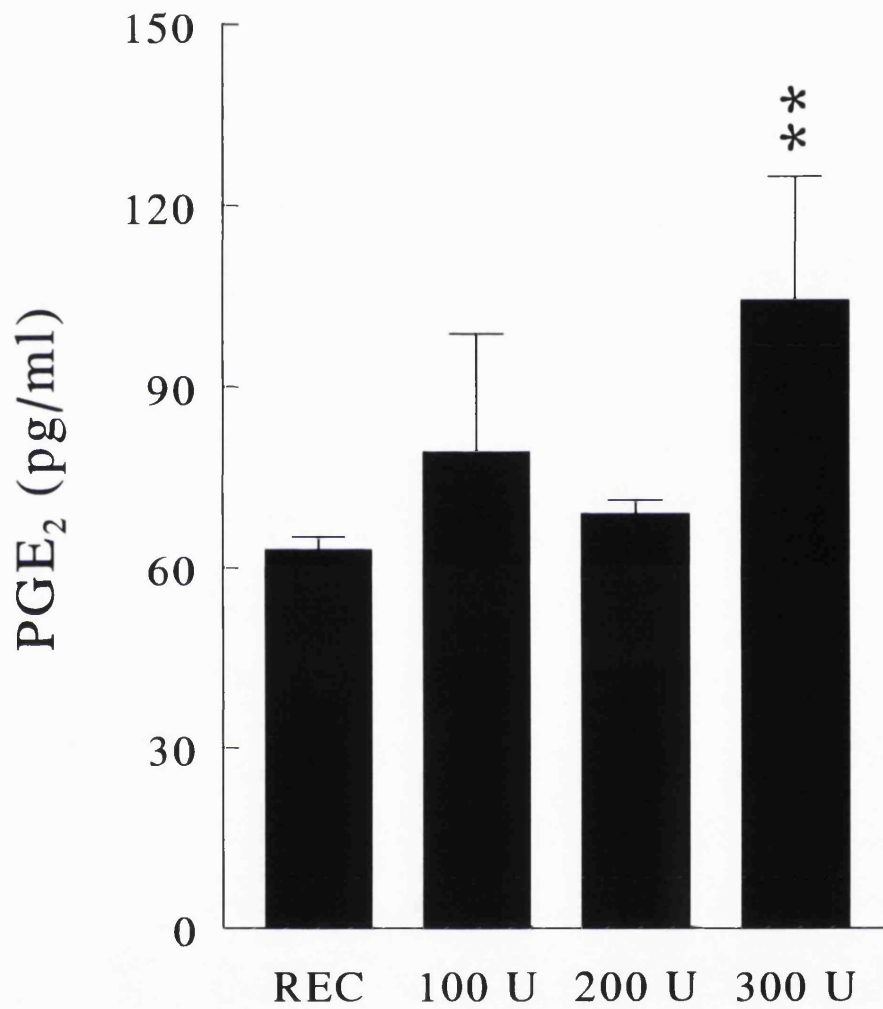
Figure 3.7.3. *A significant increase in PGE$_2$ production from rat REC was observed 24 hr following stimulation with 300 U/ml of TNF-α. ** p <0.01.*
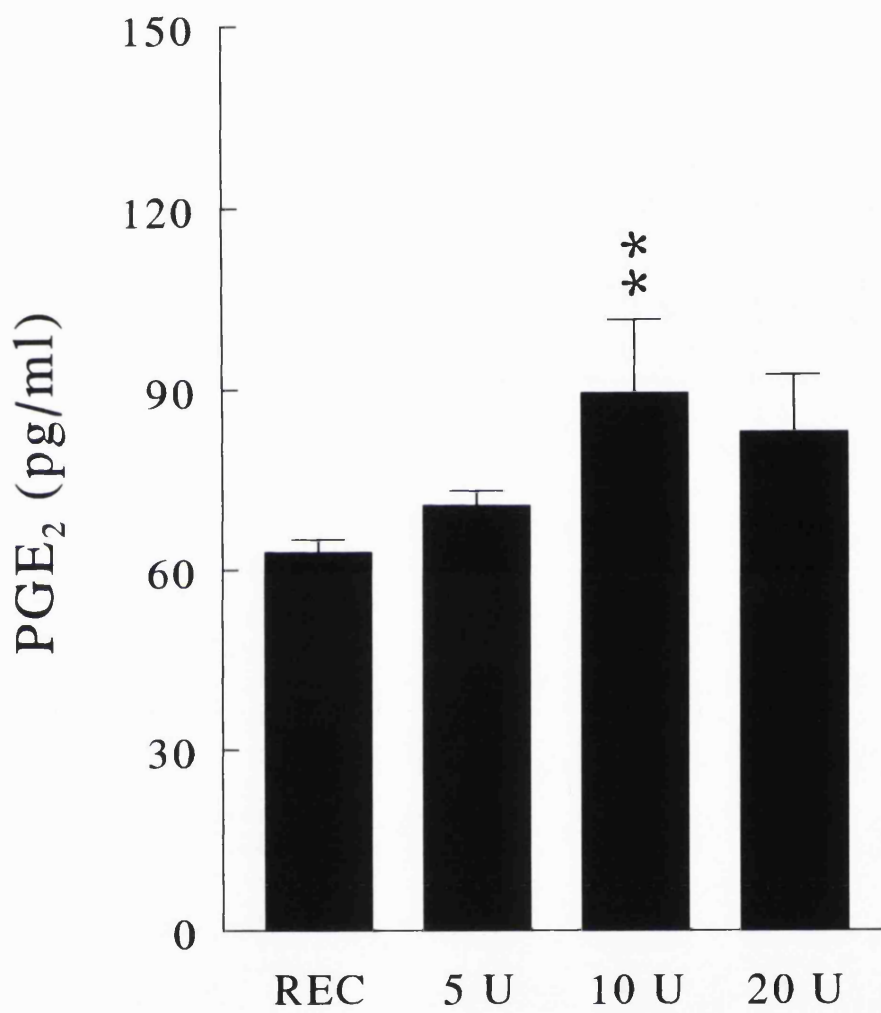
Figure 3.7.4. *Significant increases in* PGE$_2$ *production from REC were seen 24 hr following stimulation with 10 U/ml IL-6.* ** *p* <0.01.

CHAPTER FOUR

DISCUSSION

This study has investigated the effects of various inflammatory agents on the integrity of the BRB of the Lewis rat following an intravitreal injection. The cytokine IL-1ß was found to be the most potent agent examined, causing a large scale inflammatory cell infiltrate to the retina and vitreous, accompanied by a reversible and biphasic breakdown of the BRB. This barrier dysfunction appeared to be dependent on leucocyte recruitment to the retina, as determined by inhibitor and leucocyte depletion studies.

In contrast to IL-1ß, intravitreal TNF-α caused a monophasic and reversible opening of the BRB, and this was accompanied by a persistent small scale MN infiltrate, and the upregulation of MHC class II molecules. It was also demonstrated that there was an opening of the BRB of the non-injected contralateral eye, but with no concomitant MHC class II expression.

The injection of IL-6 to the vitreous caused a minimal inflammatory cell infiltrate, but did not appear to have any effect on the permeability of the BRB at the dose examined.

4.1 THE EXPERIMENTAL MODEL

Many studies investigating the role of intravitreally administered inflammatory agents in the eyes of experimental animals have used the rabbit. Although the vasculature of the rabbit retina has proved to be experimentally accessible and useful for investigating the specialised vasculature of the CNS, the anatomy of the rabbit retina, including the BRB, does not resemble that of the human. Unlike most mammalian species, the rabbit retina is only partially vascularised along the myelinated fibres with the majority of vessels lying on the surface. The anatomical architecture of the rat retina, however, is similar in many respects to that in man, and therefore provides an ideal model for investigating the mechanisms of human retinal inflammatory disease. In particular the retinal vasculature, unlike the pre-retinal vessels of the rabbit retina, are intraretinal (Kuwabara & Cogan, 1960) and are thus more suited for investigating the role of the BRB in retinal disease. In the rabbit the retinal vessels are restricted to the medullary rays, a myelinated nerve fibre layer extending in two broad white bands from the optic nerve head. Also, the rabbit eye is known to be exquisitely sensitive to ocular trauma, which

results in a rapid breakdown of the blood aqueous barrier (Bito, 1984), and therefore may present difficulties in deciphering results obtained following the intravitreal injection of an agent. It is for this reason that the rat was chosen as the animal of investigation.

The injection of agents to the vitreous, which may be described as a fluid compartment of the CNS, is an ideal method of introducing substances directly to the retina, whilst inducing a minimal amount of trauma. It has been shown that when tritiated water is injected into the mid-vitreous, more than 88% is cleared to the choroid across the intact retina, and only 3% leaves the vitreous by way of the anterior chamber (Moseley et al., 1984). It takes approximately 32 minutes for the first molecule of water injected into the vitreous to leave the eye via the choroid, and half of the injected water passes to the choroid every 36 minutes (Foulds, 1987). Hyaluronic acid, a major constituent of the vitreous, however, may impede the movement of molecules larger than water, such as peptides, as well as leucocytes, but it is unlikely that it would prevent small molecular weight proteins such as cytokines from reaching the retina. Indeed, the intravitreal injection of the large molecular weight protein HRP has been shown to penetrate the retina down to the RPE layer (Peyman et al., 1971; Peyman & Apple, 1972).

In previous studies examining the effect of intravitreal cytokines, increased blood-ocular barrier permeability has been confirmed by measuring increased protein concentrations in the aqueous and vitreous humours (Rosenbaum et al., 1987; Rosenbaum et al., 1988; Fleisher et al., 1990; Hoekzema et al., 1991; Hoekzema et al., 1992; Kulkarni & Mancino, 1993). However, this does not precisely indicate which of the blood-ocular barriers has become permeable, that is, it does not dissociate between breakdown of the blood aqueous and the blood-retinal barriers. The steady state technique employed in this study, using the small molecular weight tracer [^{14}C]-mannitol, and the subsequent eye dissection, which has been shown to prevent contamination of the retina with tracer from the vitreous (Lightman et al., 1987a), accurately and specifically measured BRB breakdown. This barrier dysfunction could also be confirmed visually by HRP extravasation into the retinal parenchyma.

Throughout the [^{14}C]-mannitol experiments it was noticed that the BBB Rt/Rp ratio was consistently lower than the BRB Rt/Rp ratio, permeability characteristics of the blood-CNS barriers which have previously been reported (Ennis & Betz, 1986; Stewart & Tuor, 1994). Although the retina and the brain have almost identical capillary surface

area measurements (Gratton *et al.*, 1992), the basal infoldings of the RPE provide a much greater surface area for solute uptake. This therefore provides the retina with a far greater potential area for exchange than the brain, and may account for the greater levels of [^{14}C]-mannitol present in normal retina than in cerebral cortex.

The majority of the experimental work performed in this study was *in vivo*. Although *in vitro* studies allow for more experimental control, with fixed parameters and a lack of interaction with other structures or molecules, no system works in isolation. However, results acquired from *in vitro* studies can be extrapolated to *in vivo* to a degree, and *in vivo* studies can then be applied to check that these extrapolations are correct.

4.2 CONTROLS

The injection of diluent alone into the vitreous produced a small increase in the number of leucocytes seen in the lumen of blood vessels compared with non-injected normal retina at 4 hr PI. This slight inflammatory response was attributed to the manipulation of the eye and the minimal trauma caused during the intravitreal injection procedure as a similar response was seen following a sham injection, where no test substance was delivered. This minor trauma also appeared to be sufficient to cause a slight but significant increase in BRB permeability as measured by [^{14}C]-mannitol extravasation, when compared to the values obtained for non-injected eyes. However, these subtle changes seen following vehicle injection were transient and did not approach the large scale and prolonged breakdown of the BRB seen following the intravitreal injection of IL-1ß. Indeed, the breakdown of the BRB at 4 and 24 hr following IL-1ß administration was considerably greater when compared to the values obtained following vehicle control injection at the same time points (p <0.001).

The presence of occasional inflammatory cells observed within the choroid in control and non-injected eyes was expected as non-CNS endothelia exhibit a greater level of constitutive leucocyte binding and recruitment than endothelia of the CNS (Male *et al.*, 1990; Wang *et al.*, 1993).

Samples of cerebral cortex were taken from each animal following infusion of [^{14}C]-mannitol as an indicator for the efficacy of the saline washout. However, the mean Rt/Rp ratio for the samples of cerebrum taken from the animals injected intravitreally with

2×10^4 U TNF-α were significantly higher than the value obtained from non-injected and vehicle-injected control animals ($p < 0.001$). Although the increase in permeability was very small, and still much lower than the permeability values obtained from normal retina, this does not exclude the possibility that the slight increase in BBB permeability was a real effect caused by the injection of TNF-α to the vitreous, particularly as intravitreal TNF-α was shown to be capable of opening the contralateral BRB at this dose.

An intravitreal injection of 1M H_2O_2 was used to cause a severe increase in the vascular permeability of the retina, to demonstrate that BRB breakdown can be visualised histologically with a large molecular weight tracer such as HRP. H_2O_2 was selected as it was thought to exert its permeability effects through the generation of free oxygen radicals, which have been shown to cause BBB breakdown (Kontos, 1985; Wei et al., 1986; Olesen, 1987a). The intracameral injection (an injection to the anterior chamber) of this agent into the rabbit, sufficient to give a total aqueous concentration of 3.3 mM, has been shown to cause an increase in the permeability of the iris vessels, as detected by fluorescein angiography (Csukas & Green, 1988). Also, the role of H_2O_2, and its reactive by-products, in the pathogenesis of increased vascular permeability of the BBB in EAE was demonstrated by detoxification of H_2O_2 with catalase and glutathione peroxidase. This substantially reduced HRP leakage in experimental optic neuritis (Guy et al., 1989).

The presence of HRP reaction product in the ciliary body of non-injected eyes was expected as the fenestrated vasculature of this structure is permeable to macromolecules. The tight junctions, however, that exist between the apical portions of the non-pigmented epithelial cells lining the ciliary processes, and which form part of the functional BAB, exclude the further passage of HRP (Smith, 1971; Smith & Rudt, 1973; Uusitalo et al., 1973; Raviola, 1974).

The intracarotid infusion of hyperosmolar arabinose significantly increased the permeability of the BRB and BBB as expected (Greenwood, 1992b). This demonstrates that the steady state technique employing $[^{14}C]$-mannitol as a tracer is suitable for detecting relatively small increases in CNS barrier permeability, even when working with the small tissue samples of the retina and vitreous.

The blood pressure and blood gas and pH measurements obtained during these studies closely resemble published values for anaesthetised rats (Bivin et al., 1979; Ringler & Dabich, 1979; Lightman et al., 1990). The measurement of blood gases in these

experiments is important as hypercapnia (above normal blood-CO_2 levels) has been implicated in the breakdown of the BRB (Rapoport *et al.*, 1980) and hypoxia (below normal blood-O_2 levels) caused increased permeability in brain capillaries (Dux *et al.*, 1984). The pH values were measured to ensure that the blood of the animals did not deviate from the normal range and fall into the category of alkylosis or acidosis during the mannitol infusion. The principle physiological effect of acidosis (blood pH ranges from 7.35 to 6.80) is depression of the CNS through inhibition of synaptic transmission. The major physiologic effect of alkylosis (blood pH ranges from 7.45 to 8.00) is over-excitability of the CNS and PNS through facilitation of synaptic transmission. The mean blood pH value from the 1×10^4 U TNF-α injected animals was 7.34 ± 0.013 (mean $\pm$ SEM), and was significantly decreased from control values ($p < 0.05$). This decrease, however, was only marginally below the given normal range and did not result in any perturbation of the BRB in the control eyes.

Blood pressure measurements were used to ensure that hypertension did not occur, which is known to cause BRB and BBB breakdown (Giacomelli *et al.*, 1972; Laties *et al.*, 1979; Lightman *et al.*, 1987b). The mechanism involved in hypertensive barrier breakdown may involve the glycocalyx that coats the luminal surface of the BRB and BBB ECs. The glycocalyx is negatively charged, primarily due to the large number of sialic acid residues, and appears to play an important part in the function of the barrier (Vorbrodt, 1987). In acutely hypertensive animals the negative luminal surface charge is found to be greatly reduced with a concomitant increase in BBB permeability (Mayhan *et al.*, 1989). Mean blood pressure values from the measurements made throughout the course of each mannitol infusion in the 2×10^4 U TNF-α injected animals exhibited an increase over control values ($p < 0.01$). The mean arterial systolic blood pressure value was 120.71 ± 1.42 (mean $\pm$ SEM) mmHg, but this was comparable with a normal rat systolic blood pressure of 116 mmHg (Bivin *et al,.* 1979), and lay within the normal range (Baker *et al,.* 1979). Indeed, work on experimental hypertension has used rats with a mean systolic blood pressure greater than 200 mmHg to achieve BRB breakdown (Giacomelli *et al.*, 1972), and a carotid blood pressure of 160 mmHg to cause breakdown of the BBB (Laties *et al.*, 1979).

4.3 INTERLEUKIN-1ß

An intravitreal injection of IL-1ß into the vitreous of the Lewis rat eye caused an acute and reversible inflammatory response that was characterised by a leucocytic infiltration and a biphasic breakdown of the BRB.

Leucocyte Recruitment

The recruitment of leucocytes from the circulation in response to IL-1ß injection into the rat vitreous correlated closely with the expected induction and upregulation of EC adhesion molecules with time. It has previously been reported that IL-1ß stimulates vascular ECs to express E-selectin (Pober et al., 1986; Luscinskas et al., 1991) which peaks 4-6 hr after stimulation, but is below the level of detection after 24 hr (Leeuwenberg et al., 1992). Because E-selectin is involved in the initial tethering of circulating leucocytes, this may explain the early increase in PMN and MN recruitment. The level of leucocyte traffic escalates as other adhesion molecules, with longer induction times, come into effect. Both ICAM-1 (Luscinskas et al., 1991; Wong & Dorovini-Zis, 1992) and VCAM-1 (Osborn et al., 1989) are upregulated and induced respectively by IL-1ß as early as 4 hr after treatment, peaking at 24-48 hr and persisting for up to 72 hr. L-selectin is also involved in the initial tethering of leucocytes to endothelium, and its ligand is expressed on HUVEC between 2 and 4 hr after EC stimulation with IL-1ß, and persists for at least 24 hr (Spertini et al., 1991). L-selectin supports neutrophil adhesion (Spertini et al., 1991), unlike VCAM-1 (Rice et al., 1990; Bochner et al., 1991).

Consistent with the observed leucocytic recruitment is the finding that the adhesion of PMN and MN to HUVEC is significantly increased by IL-1 (Bevilacqua et al., 1985; Beekhuizen et al., 1991; Bochner et al., 1991; Kuijpers et al., 1991). Moreover, IL-1ß treatment of retinal endothelia in vitro increases lymphocyte adhesion (Wang et al., 1993) and transendothelial migration (Greenwood et al., 1995) which corresponds to an increase in the expression of both ICAM-1 and VCAM-1.

Another adhesion molecule, PECAM-1, which is located at the intercellular junctions of the BRB and BBB ECs, and is also constitutively expressed on leucocytes and platelets, has recently been shown to be required for the recruitment of leucocytes into

inflammatory sites (Muller *et al.*, 1993). Inflammatory cytokines, however, do not upregulate the surface expression of PECAM-1, but they appear to induce a change in the surface distribution of PECAM-1 molecules, with a loss of the typical staining usually seen at intercellular junctions (Romer *et al.*, 1995). It was thought that this redistribution of PECAM-1 caused by cytokines may represent a mechanism for regulating the migration of leucocytes.

The cellular infiltrate seen following intravitreal IL-1ß in this study is similar in time course to previously reported IL-1ß-induced recruitment of leucocytes into the anterior chamber of rabbit or rat eyes (Rosenbaum *et al.*, 1987; Ferrick *et al.*, 1991; Kulkarni & Mancino, 1993). Increased blood-ocular barrier permeability, as measured by extravasated protein, was also recorded in aqueous samples. Several studies investigating intravitreal IL-1 have therefore reported relatively consistent findings in regard to the dose and time course of inflammation and increased blood-ocular barrier permeability. However, one relatively early study described an intravitreal injection of human IL-1 into the rabbit vitreous which portrayed a different pathogenesis. In this study just 5 U of IL-1 induced a leucocytic infiltrate to the anterior chamber which peaked at 4 hr PI (Bhattacherjee & Henderson, 1987). This inflammatory response, however, was not accompanied by a significant increase in aqueous protein levels, indicating that the blood-ocular barriers were not disrupted by the invading leucocytes.

In another study investigating the time course of inflammation induced by intravitreal IL-1ß in the rabbit, the cellular infiltrate peaked much later at 7-14 days PI, and BRB breakdown was demonstrated at 7 days PI, which persisted up to 35 days PI (Martiney *et al.*, 1992). At the 35 day time point the highest degree of EC pathology was observed, whereas, in the current study, the ECs appeared structurally normal by 5 days PI, when the cellular infiltrate had almost completely resolved.

All of these results differ, however, from the inflammatory response to the brain following an injection of 100 U of IL-1ß into the hippocampus of the mouse (Andersson *et al.*, 1992). In this model, no leucocyte extravasation was observed except where it had diffused to the subarachnoid space and choroid plexus where it caused a large-scale extravasation of leucocytes. Whether this is a genuine difference between the two sites in their respective abilities to support leucocyte recruitment, or to the substantial difference in dose used, remains unresolved. Certainly the lower dose used in the mouse study was

sufficient to elicit leucocyte recruitment at other sites. It may also be argued that the leucocyte infiltration seen in the retina is due to migration from non-CNS sites such as the choroid and ciliary body. However, although the ciliary body may contribute to the infiltrate seen in the vitreous and the RPE, it is quite clear from the histology that leucocyte migration is also occurring at the site of the retinal vessels.

Leucocytes entering the retina may be derived from three separate vascular beds; the choriocapillaris, the retinal vessels or the vasculature of the ciliary body. As has already been stated, direct recruitment into the neuroretina by the retinal vascular endothelium undoubtedly occurs as adherent and migrated leucocytes can be seen, as well as perivascular cuffing of leucocytes. The contribution, however, of these other sites to the retinal pool of leucocytes, and whether the profile of cells recruited by these different vascular beds is similar, is unknown. The origin of the population of leucocytes seen in the vitreous during the peak of the inflammatory response was most likely derived from the large cellular infiltrate observed in the ciliary body. No leucocytes were seen migrating across the inner limiting membrane of the retina although it is known that antigen-specific T cells injected into the vitreous are able to enter the retinal parenchyma (Kim *et al.*, 1988). Whether the neuroretinal and vitreal leucocyte pools remain largely separate, however, is not clear. There was also no evidence of leucocytes migrating across the RPE, the posterior aspect of the BRB, from the choroidal circulation, which is a route suggested for the migration of cells into the retina during EAU (Lin *et al.*, 1991). The increased number of extravasated cells usually seen within the choroid in EAU are most likely to have been recruited by the choroidal endothelium in response to cytokines and other inflammatory molecules released from the RPE (Elner *et al.*, 1991; Elner *et al.*, 1992; Whitcup *et al.*, 1992). As with the vitreal pool of leucocytes the extent of mixing between the choroidal and retinal recruited populations is uncertain. The lack of obvious migration across the posterior barrier would suggest that such mixing is limited or occurs mostly in the later stages of the disease. However, it is likely that leucocytes can cross the RPE, at least in some species, as leucocytes appear in the avascular retina of the guinea pig during EAU (Caspi *et al.*, 1986). In the current study, the inflammatory cells seen in the RPE layer were always in close proximity to the ciliary body suggesting that they originated from this site. This may indeed be possible as the RPE is continuous anteriorly with the pigment epithelium of the ciliary body.

The precise route through which leucocytes migrate across the BRB was not clear but most evidence pointed to a transcellular and not a junctional path of migration. Both PMN and MN cells were often observed exhibiting a pattern of migration that was similar to emperiopolesis (Pulvertaft, 1959; Marchesi & Gowans, 1964; Åström et al., 1968), a term originally given to describe the ability of lymphocytes to be engulfed by, and move about within, other cells. In this study leucocytes were frequently seen completely surrounded by, and enclosed within, ECs. However, the interpretation of two dimensional images makes it difficult to ascertain precisely the location where the leucocytes migrate through the EC, although the point of penetration was often over the nucleus which strongly supports the concept that leucocytes can penetrate the endothelial barrier at sites other than the tight junction. This process, in which the EC plasma membrane remains intact, may require active participation by the endothelium although at present this remains conjecture. It has been reported that PMNs appear to be able to migrate by either route, that is, through the BRB tight junctions between ECs, as well as through pores formed through the EC (Smith et al., 1994).

Immunohistochemistry

In this study, using immunohistochemistry, it was demonstrated that there was no expression of ED1, ED2, W3/25, CD8, MOM/3F12/F2, OX6 or WT3 in the normal Lewis rat retina. However, a positive staining for these epitopes in the choroid was noticed in all of the sections of retina that were immunostained, and this constitutive expression of immunohistochemical markers in the choroid is consistent with a previous report (Forrester et al., 1994).

Immunostaining on frozen sections of retina at 24 hr PI of IL-1ß identified the majority of infiltrating leucocytes as monocytes, with a few macrophages and CD8+ T cells also present. Toluidine blue and TEM sections revealed a high number of PMN neutrophils present within the retina and vitreous but these were not detected immunohistochemically. The presence of MHC class II positive staining within the retina was also observed. Whether this staining represents infiltrating macrophages, or tissue resident cells such as pericytes and glial cells, was impossible to determine due to the lack of morphological resolution in frozen sections of retina. Positive staining for CD18, the marker for the ß2 integrins, was widespread throughout the retina, and on leucocytes

within the vitreous, and may be expected as these molecules play a major role in the adhesion and migration of leucocytes from blood to tissue (Springer, 1994). No positive staining for CD18 was observed in the normal Lewis rat retina as has been described in the normal rabbit retina, however. In the rabbit, these cells were reported to appear as a population of ramified cells associated with the epiretinal vessels, which were not pericytes, but were identified as perivascular macrophages (Cuff *et al.*, 1994). Following the intravitreal injection of IL-1ß these tissue resident macrophages lost their ramified appearance, detached from the epiretinal vessels and showed signs of phagocytic activity. Whether any of these cells were present in the Lewis rat retina following IL-1ß injection could not be determined due to the poor morphology.

Retinal Pathology

The structural damage to the retina, such as vacuolation and oedema, brought about by the injection of IL-1ß, is most probably the result of the large numbers of infiltrating leucocytes and the subsequent release of other inflammatory cytotoxic compounds. IL-1ß alone does not appear to cause cytotoxic tissue damage *in vivo* (Dinarello, 1989; Pober & Cotran, 1990). More subtle alterations, such as retinal endothelial thickening and increased surface microvilli, which were observed in close association with adherent or migrated leucocytes, have previously been described in both EAU (Lin *et al.*, 1991; McMenamin *et al.*, 1992; Greenwood *et al.*, 1994) and EAE (Claudio *et al.*, 1989; Raine *et al.*, 1990). These vascular changes are characteristic of "reactive" endothelia and are likely to be a consequence of increased cellular metabolism and protein synthesis.

Following IL-1ß injection, platelets were often observed in the lumen of retinal blood vessels, sometimes in large numbers and accompanied by leucocytes. The release of vasoactive agents from platelets, such as serotonin, histamine, and PAF, may play a significant part in contributing to the increased permeability of the BRB found in this experimental model. Indeed, the intravascular administration of histamine was shown in this study to be capable of rapidly disrupting the BRB. Furthermore, the intravitreal injection of PAF caused breakdown of the BRB in the rabbit (Smith *et al.*, 1994). Increased numbers of circulating platelets have been found in response to IL-1ß administered to humans in clinical trials (Tewari *et al.*, 1990), and following IP administration in mice (Kimura *et al.*, 1990). It has been suggested that activated

neutrophils may increase platelet aggregation due to neutrophil thromboxane release stimulated by IL-1 (Dinarello, 1989). Platelet aggregation may also be stimulated by the release of cathepsin G, a chymotrypsin-like enzyme, from activated neutrophils (Selak *et al.*, 1988). Leucocyte-platelet aggregates have been described in other experimentally induced inflammatory conditions associated with increased permeability, such as following reperfusion of ischaemic tissue (Kuruse *et al.*, 1994a), or following the superfusion of a water extract of *Helicobacter pylori* (Kuruse *et al.*, 1994b).

The intravitreal injection of IL-1ß has also been demonstrated to induce an alteration in the visual evoked potentials of the rabbit as measured by electrophysiologic response to flash stimulation (Martiney *et al.*, 1990). It was suggested that the intravitreal IL-1ß altered nerve conduction in the retinal ganglion cells before they enter into the optic chiasm, and was associated with increased BRB permeability.

The intravitreal injection of IL-1ß or IL-1α into the rabbit caused the release of IL-1ß into the aqueous (Kulkarni & Mancino, 1993). The source of this *de novo* IL-1 was not identified but, *in vitro*, IL-1α induced the synthesis of IL-1ß from monocytes (Dinarello *et al.*, 1987) and IL-1α and IL-1ß induced increases in IL-1ß mRNA levels in human EC (Warner *et al.*, 1987). IL-1 therefore seems to possess the ability to induce the synthesis of biologically active IL-1, that is, a positive feedback mechanism. This implies that IL-1 will amplify the production of itself and this may propagate the inflammatory reaction to extend the duration of the response.

BRB Breakdown to HRP

The exudation of plasma fibrin filaments observed during the course of inflammation has been described in both EAE (Lampert, 1967; Raine *et al.*, 1990) and EAU (de Kozak *et al.*, 1981; Lin *et al.*, 1991). This observation, along with the finding that HRP was able to extravasate into the retinal parenchyma, demonstrated that there was a significant disruption of the vascular BRB. HRP extravasation has previously been described in the rabbit retina 6 hr after intravitreal injection of IL-1ß (Claudio *et al.*, 1994). The tracer was found to be present in perivascular cells and Müller cells, but was not observed in the basement membrane. Although the presence of HRP beyond the barrier would suggest that there was an increase in protein extravasation, no significant increase in protein levels in the vitreous was recorded until 24 hr PI. It was suggested,

therefore, that extravasated protein is initially taken up by perivascular cells until they become saturated, resulting in delayed protein diffusion into the vitreous. However, by using the non-proteinaceous tracer mannitol, increased levels of [^{14}C]-mannitol were detected in the retina and vitreous by 4 hr PI, which suggests that mannitol is not removed by the perivascular cells. Moreover, the small molecular weight of mannitol (184 kDa) will allow it to diffuse more rapidly through the extracelluar space than large molecular weight proteins.

The observation that HRP-filled pinocytotic vesicles were not detected except at the abluminal side, where omega-shaped profiles filled with HRP reaction product were seen, is reported to be a normal phenomenon (Broadwell & Salcman, 1981; Broadwell, 1989; Greenwood et al., 1994). These represent invaginations or pits of the abluminal surface of ECs, known as caveolae, and are not membrane bound vesicles and are therefore not an indication of increased vesicular transport and exocytosis across the blood-CNS barriers (Broadwell, 1989).

The presence of HRP within the RPE at 48 hr PI IL-1ß, extending between two RPE cells up to the apically located terminal bar, has been reported in normal retina (Shiose, 1970). It appears that the posterior aspect of the BRB, formed by the RPE, remained impermeable to HRP during the inflammatory response caused by IL-1ß, and indicates that the breakdown of the BRB may be specifically located to the EC of the vascularised anterior aspect of the BRB.

Extravasated HRP was also observed within the basement membrane of vessels from the ciliary vasculature and surrounding the fenestrated vessels of the ciliary body at 48 hr PI. Similar observations were also seen in the ciliary body of the contralateral non-injected eye which, as already discussed, was expected.

BRB Breakdown to [^{14}C]-Mannitol

Using the small molecular weight tracer [^{14}C]-mannitol and the sensitive steady-state technique to evaluate BRB breakdown, it is shown for the first time that IL-1ß causes a biphasic increase in BRB permeability.

Following IL-1ß injection, the BRB remained intact for up to 2 hr PI which is consistent with a previous study where IL-1ß introduced into the vasculature did not acutely disrupt the BBB (Banks & Kastin, 1992). The initial increase in BRB permeability

was first detected at 4 hr PI, at a time when inflammatory cells were beginning to appear in the retina in relatively large numbers. The second phase of BRB dysfunction occurred at 24-48 hr PI when the peak infiltration of leucocytes was present.

The small but significant increase in permeability recorded at time 0 in the vitreous samples, immediately after the intravitreal IL-1ß injection was administered, can be attributed to the insertion of the needle causing transient physical damage. This may have allowed a small amount of tracer into the vitreous, rather than IL-1ß having an instantaneous effect on the permeability of the BRB.

The higher levels of [^{14}C]-mannitol found in the vitreous may be due to this site providing a much larger sink for mannitol than the extracellular space of the retinal parenchyma, which, if figures for the brain are extrapolated to the retina, only accounts for less than 20% of the tissue volume (Henkind et al,. 1980). Also, because the vitreous body is situated between the BRB and BAB, substances moving from the extracellular space of the retina, and also the posterior chamber, have free access to the vitreous (Cunha-Vaz, 1980). Therefore, movement of solutes into the vitreous provides a good measure of the permeability of the blood-ocular barriers, but does not exclusively measure permeability of the BRB (Ennis & Betz, 1986). The breakdown of the BAB is likely to contribute greatly to the amount of tracer found in the vitreous due to the the ciliary body tight junctions being much leakier than the junctions that form the BRB (Raviola, 1977). However, it has previously been shown that the dissection method employed in this study does not involve significant contamination of the retina from the vitreous sample (Lightman et al., 1987a), and therefore the results from retinal tissue in this study are believed to specifically represent BRB breakdown. However, there is a tendency to underestimate the degree of BRB disruption because of the movement of tracer along the concentration gradient from retina to vitreous.

The biphasic breakdown of the BRB observed in the current study is similar in some respects to the breakdown of the BAB following foot pad injection of LPS in the rat (Bhattacherjee et al., 1983). In this model of anterior uveitis (EIU), PMNs were observed in the anterior segment of the eye 24 hr after LPS injection. However, breakdown of the BAB, as detected by radiolabelled protein extravasation into the aqueous humour, was also found to follow a biphasic pattern, peaking initially at 4-6 hr and then again at 20-24 hr after injection, although the authors did not comment on the presence

of the first peak. The intravitreal administration of LPS has also been shown to result in a biphasic increase in vascular permeability to radiolabelled albumin within the aqueous (Howes *et al.*, 1994).

Also, in a recent study investigating the role of ocular-derived cytokines following footpad administration of LPS, it was reported that both TNF and IL-6 in the aqueous humour followed this biphasic pattern (De Vos *et al.*, 1994). Furthermore, IL-1α, IL-1ß and TNF gene expression in the iris-ciliary body has been investigated and a biphasic response was also observed following footpad injection of LPS, with peaks occurring at 3 and 24 hr PI (Yoshida *et al.*, 1994). This suggests that some of the underlying mechanisms of the response to intravitreal injection of IL-1ß and footpad injection of LPS may be similar. In those studies where LPS was injected directly into the vitreous, however, the spatial distribution of the inflammatory response differed from the IL-1ß-induced inflammation. The effect of LPS was predominantly to the anterior chamber and ciliary body of the eye, with inflammatory cells appearing in the retina at a later time point (6 hr PI) (Forrester *et al.*, 1980) and a substantial BAB dysfunction occurring earlier, at 2 hr PI (Csukas *et al.*, 1990).

The estimated quantity of contaminating LPS in each 10µl injection of IL-1ß used in the current study was 1pg, and this is unlikely to be the cause of the inflammation and BRB breakdown observed. Previous studies have shown that following the intravitreal injection of 2pg LPS in the rat, the response consisted almost entirely of an iridial hyperaemia which peaked at 9-12 hr PI (Forrester *et al.*, 1980), and intravitreal LPS (1-10pg) in the rat resulted in an inflammation that was restricted to the anterior uvea (Hoekzema *et al.*, 1992). Furthermore, 25pg of LPS injected into the vitreous of the rabbit did not cause measurable anterior uveitis (leucocyte recruitment or BAB breakdown) after 24 hr (Fleisher *et al.*, 1990).

The recruitment of inflammatory cells by IL-1ß did not appear to have been completely prevented by incubating with αIL-1ß Ab. The number of leucocytes within the retinal parenchyma was significantly reduced and this has also been remarked upon in another study where intravitreal IL-1ß was neutralised with specific antibody (Martiney *et al.*, 1990). However, the ability of intravitreal IL-1ß to cause a biphasic increase in BRB permeability in this study was lost. The reason that IL-1ß treated with specific antibody was still able to cause a reduced leucocytic infiltration may be due to the IL-1ß

not being completely neutralised by the antibody. The dose of antibody used ($10mg.ml^{-1}$), as recommended by the manufacturer, was sufficient to neutralise 1×10^4 U of cytokine. However, each aliquot of cytokine used in this study had a specific activity of $1-2 \times 10^4$ U, therefore some active IL-1ß may have survived which was capable of inducing a mild inflammatory response, but which was not sufficient to cause an increase in BRB permeability.

4.4 INHIBITOR STUDIES

The intravitreal injection of IL-1ß thus resulted in a large scale leucocyte infiltration to the retina, accompanied by a biphasic breakdown of the BRB. It was unclear, however, whether the initial disruption seen at 4 hr PI was due to the direct effect of IL-1ß on the barrier, or to the induction of other disruptive cytokines or vasoactive mediators. The second larger and more prolonged increase in BRB permeability, which occurred at 24-48 hr, would perhaps be consistent with the induction of *de novo* synthesis within the retina of other inflammatory cytokines following IL-1ß activation, or to the release of classic inflammatory mediators. Alternatively, the elevated number of migrating cells at this point could contribute directly to the increased permeability by secreting vasoactive compounds, or by inducing tissue resident cells (such as EC, RPE or glial cells) to do so. It is also possible that these leucocytes may augment the increased permeability by physically damaging the BRB, by pulling across plasma constituents during diapedesis (Lossinsky *et al.*, 1989; Claudio *et al.*, 1990).

In an attempt to elucidate the mechanisms by which IL-1ß was causing BRB breakdown, inhibitor studies were performed by targeting two classic mediators of vascular permeability, histamine and Cox metabolites of arachidonic acid, such as prostaglandins, and by attenuating leucocyte recruitment. There is good evidence to suggest that both histamine and prostaglandins are involved in blood-CNS barrier dysfunction (for reviews see Greenwood, 1992b; Wahl *et al,*. 1995), and it has been shown that surgical exposure of the brain surface induces the release of histamine and Cox metabolites, which elicit formation of leaky sites in brain venules (Olesen, 1987b).

Role of Histamine

The concomitant administration of the histamine H_2-receptor antagonist ranitidine with intravitreal IL-1ß, successfully inhibited the biphasic breakdown of the BRB and reduced the leucocytic infiltrate at 24 hr PI. As histamine therefore appeared to be implicated in the barrier breakdown, it was decided to examine the direct effect of histamine on the BRB by introducing it to the abluminal side of the vasculature by intravitreal injection, or to the luminal aspect by injection via the carotid artery. These experiments demonstrated that the intravitreal and intracarotid administration of histamine was able to rapidly and transiently open the BRB of the Lewis rat, but, however, did not appear to have any effect on the BBB when delivered via the carotid artery.

As discussed previously, the published work on the effect of histamine on the vasculature of the brain is contradictory, which is also the case for the reported effects of histamine within the eye, on retinal vessels and the BRB. For example, intravenously administered histamine resulted in an increased permeability of the blood-ocular barriers to albumin (Kilzer et al., 1985), but the local application of histamine to retinal vessels in vivo was unable to cause opening of the interendothelial tight junctions or increased BRB permeability to intravenously administered tracers (Ashton & Cunha-Vaz, 1965; Shakib & Cunha-Vaz, 1966). This was thought to represent a genuine difference between retinal and non-CNS EC, and was possibly due to the lack of histamine receptors on the abluminal surface. However, cerebral EC possess H_1- and H_2-receptors at the luminal and abluminal membranes, and the cortical superfusion of histamine was demonstrated to open the BBB through mediation of these receptors (Schilling & Wahl, 1994). It is therefore highly probable that retinal ECs have the same distribution of histamine receptors.

The inhibition of the biphasic breakdown of the BRB by ranitidine implies that IL-1ß-induced BRB disruption is mediated through histamine, via the H_2-receptor, which has previously been implicated in breakdown of the BBB following the intravascular administration of histamine (Gross et al., 1981; Dux & Joó, 1982; Gross et al., 1982). The administration of ranitidine reduces BRB permeability in various disorders, such as in streptozocin-induced diabetic rats (Hollis et al., 1988), and in patients suffering from type I diabetes (Gardner et al., 1995). Ranitidine has also been shown to decrease ischaemia-induced brain oedema formation in the rat (Tósaki et al., 1994). Another histamine H_2-

receptor antagonist, cimetidine, has recently been shown to be effective in abrogating the initial BBB dysfunction in a biphasic permeability response caused by Semliki Forest Virus in mice, an experimental model for MS (Egleton et al,. 1996). Cimetidine was also effective in reducing the increased permeability of rat pial vessels induced by the superfusion of histamine, as measured by transendothelial electrical resistance (Butt & Jones, 1992).

The synthesis of histamine within the retina may have been induced directly by the IL-1ß injected into the vitreous. Indeed, when this cytokine was injected intravenously into mice it induced histidine decarboxylase activity in various organs (Endo, 1989). Also, following the injection of IL-1ß directly into the hypothalamus, a significant amount of histamine was demonstrated between 2 and 3 hr after injection (Niimi et al., 1994), indicating that IL-1ß can induce a rapid increase of histamine release in the CNS.

The actual source of IL-1ß-induced histamine release is unclear but it is possible that intravitreal IL-1ß is stimulating the release of histamine from cells within the retina, such as from EC, RPE or glial cells, or from choroidal mast cells. Whether this histamine release is from the mast cells which are located around the choroidal vessels of the Lewis rat, but which are not found in the retina (Mochizuki et al., 1984), is highly speculative as it would require efflux of IL-1ß across the retina. The pathogenesis of EAU and EAE, and associated barrier breakdown, has previously been attributed to the number of choroidal (Mochizuki et al., 1984) and brain mast cells (Bø et al., 1991), respectively. However, the presence of mast cells does not appear to be necessary for histamine production within the CNS as studies have shown that the brains of mice, which are deficient in brain mast cells, do contain histamine (Yamatodani et al., 1982; Hough et al., 1984).

The normal retina also contains non-mast cell derived histamine (Carroll et al., 1988; Nowak, 1990), with the microvasculature suggested as a source (Nowak et al., 1984). Retinal blood vessels were implicated because, following subcellular fractionation of bovine retina, 90% of histamine was located in the heavy cellular elements. These include nervous tissue components such as myelin and membrane fragments, nuclei, mitochondria, inner and outer rod segments, and blood vessels. The enzyme immunoassay performed in the present study, however, revealed no histamine production from IL-1ß stimulated REC after 24 hr, indicating that these cells were not responsible for histamine

production, at least not when stimulated with IL-1ß.

The depletion of circulating leucocytes resulted in a significant decrease in BRB permeability at 4 hr following IL-1ß injection, when compared to the degree of barrier opening seen in normal rats after intravitreal IL-1ß. This suggests that the first phase of BRB breakdown may be mediated in part by histamine release from infiltrating leucocytes, and possibly with tissue resident cells also contributing. The presence of IL-1ß itself within the retina may be stimulating the release of histamine from the infiltrating leucocytes, as IL-1 has been shown to possess the ability to induce histamine release from neutrophils and eosinophils (Dinarello, 1987), from basophils (Haak-Frendscho *et al.*, 1988), and from macrophages (Okamoto & Nakano, 1990).

Histology following ranitidine treatment revealed a significant reduction in leucocyte recruitment at 24 hr PI. It has been shown *in vivo* that histamine can induce leucocyte rolling, an essential event prior to migration, which can be inhibited by pre-treatment with ranitidine, but not diphenhydramine (Ley, 1994), indicating that this is a histamine H_2-receptor mediated event. The effect of histamine on leucocyte rolling appears to be due to the expression of the adhesion molecule P-selectin, which is stored preformed in the Weibel-Palade bodies of ECs. In contrast to that study, however, are two reports indicating that histamine H_1-receptors, but not H_2-receptors, are involved in histamine-induced leucocyte rolling (Kubes & Kanwar, 1994; Asako *et al.*, 1994), which further illustrates the conflicting literature that exists on the role of histamine in inflammation.

Role of Cyclooxygenase Metabolites

The first phase of IL-1ß-induced BRB breakdown may be primarily attributed to histamine as the administration of the Cox inhibitor, indomethacin, was only effective at the 24 hr time point. The inhibition of increased barrier permeability at 24 hr PI indicates that Cox metabolites of arachidonic acid, such as the prostaglandins and thromboxanes, are involved in the second phase of barrier dysfunction. It may therefore be possible that the histamine production induced by IL-1ß led to the subsequent production of these Cox metabolites. In support of this theory, histamine has been shown to cause the release of prostaglandins and thromboxanes *in vitro* from HUVEC (Resink *et al.*, 1987; Revtyak *et al.*, 1988), and to induce PGE_2 production from cerebral microvessels (Dux *et al.*, 1982) and human dermal microvascular EC (Bull *et al.*, 1991). Also, in the newborn pig, the

histamine induced dilation of pial arterioles was shown to be mediated by prostaglandin production (Mirro *et al.*, 1988). Moreover, IL-1 has been shown to potentiate this histamine-induced release of PGE_2, possibly by regulating the availability of free arachidonic acid (Bull *et al.*, 1991). Cytokines and vasoactive molecules may therefore interact to modulate endothelial responses.

Overexpression of prostaglandins within the eye may have detrimental consequences. The long term exposure of the retina to elevated PGE_2 levels in the vitreous has been implicated in BRB breakdown (Naveh & Weissman, 1990) and retinal detachment (Naveh *et al.*, 1990). Also, the topical application of prostaglandins has been shown to cause an increase in the permeability of ocular vessels. PGE_1 caused the anterior parts of the ciliary processes and their iridial processes to become permeable to lanthanum (Pederson, 1979), and PGE_2 resulted in an increased concentration of plasma proteins in the aqueous humour with HRP penetrating the tight junctions of the non-pigmented layer of the ciliary epithelium (Vegge *et al.*, 1975). In the rabbit, the intracameral injection of PGE_2 caused a sustained rise in intraocular pressure and increased aqueous protein concentration, due to breakdown of the BAB (Beitch & Eakins, 1969; Bhattacherjee & Paterson, 1990). Furthermore, the intravitreal injection of PGE_1 induced the opening of retinal EC tight junctions, resulting in albumin exudation into the extracellular space or fluorescein leakage into the vitreous (Sen & Campochiaro, 1991; Vinores *et al.*, 1992). All these observations suggest that prostaglandins may cause blood-ocular barrier breakdown by opening tight junctions.

Leucocytes, endothelia and epithelia can all produce eicosanoids when correctly stimulated (Parker & Stenson, 1989), and these eicosanoids may play an important role in the regulation of blood flow during CNS injuries. For example, increased levels of prostaglandins have been detected in the ischaemic cat brain (Stevens & Yaksh, 1988) and in guinea pigs suffering from chronic relapsing EAE (Bolton *et al.*, 1986). *In vivo*, the injection of LPS into rats resulted in increased levels of PGE_2 in the microvasculature of the brain (Van Dam *et al.*, 1993). Cytokines have been reported to produce eicosanoids within the anterior chamber of experimental animals following intravitreal injection. For example, IL-1 induced an elevation in PGE_2 in the aqueous humour after 24 hr in the rat (Fleisher *et al.*, 1992) and rabbit (Rubin & Rosenbaum, 1988; Kulkarni & Mancino, 1993), and the intravitreal injection of TNF-α caused increases in PGE_2 and LTB_4 concentrations

in the aqueous of rabbits (Fleisher *et al.*, 1990; Fleisher *et al.*, 1991).

The source of prostaglandins may originate from many cell types but in this study it was demonstrated *in vitro* that the REC are themselves able to produce PGE_2 in response to IL-1ß. Indeed, the potent stimulating effect of IL-1 on producing prostaglandins from non-CNS EC, such as HUVEC, has also been reported (Rossi *et al.*, 1985; Zavoico *et al.*, 1989). In a recent study *in vitro*, the effect of cytokines on increasing the trans-endothelial electrical resistance of cultured cerebral EC was abolished in the presence of indomethacin (de Vries *et al.*, 1996). This indicates that cytokines induce BBB ECs to produce eicosanoids which subsequently act on the ECs and increase transmonolayer permeability. Whether this is the case *in vivo* is uncertain because high doses of prostaglandins have been reported to produce only small changes in vascular permeability in the skin of experimental animals (Williams & Peck, 1977; Wedmore & Williams, 1981), and it was thought unlikely that prostaglandins contribute to oedema by a direct effect on blood vessel permeability (Williams & Higgs, 1988). There is experimental evidence to suggest, however, that prostaglandins promote other inflammatory mediators to produce oedema. For example, PGE_2 causes a dose-dependent increase in blood flow with little or no plasma leakage in rabbit skin, but when PGE_2 is mixed with histamine or bradykinin there is a marked increase in plasma exudation (Johnston *et al.*, 1976). These observations gave rise to a "two mediator" concept of oedema formation (Williams & Peck, 1977; Wedmore & Williams, 1981), where vasoactive substances such as histamine are responsible for increased vascular permeability, and the subsequent plasma leakage is potentiated by increased blood flow induced by vasodilator prostaglandins.

Indomethacin may thus be exerting its effect on reducing BRB permeability by preventing the formation of PGE_2. However, following leucocyte depletion, the intravitreal injection of IL-1ß resulted in a decrease in BRB permeability at 24 hr PI, when compared to the degree of barrier opening seen in normal rats following intravitreal IL-1ß. Also, the histology performed at 24 hr following indomethacin treatment revealed a significant decrease in the number of migrated leucocytes within the retina. This indicates that leucocyte recruitment to the retina is also involved in barrier dysfunction at this time point, and suggests that indomethacin may prevent an increase in IL-1ß-induced BRB permeability by reducing the number of leucocytes to the retina. Although prostaglandins

do not appear to be directly involved in leucocyte recruitment (Jordan *et al.*, 1986; Williams & Higgs, 1988), thromboxanes, which are also Cox derivatives of arachidonic acid, have been implicated in platelet aggregation (and hence histamine release), and adhesion and migration of leucocytes (Granstrom *et al,.* 1983; Doukas *et al.*, 1989). Thromboxane B_2 (TxB$_2$), a stable but less active metabolite of TxA$_2$, originates from platelets in the circulation, and from accumulated PMNs at sites of local inflammation (Higgs *et al.*, 1983). *In vitro* studies have demonstrated that thromboxanes can indeed be produced by PMNs and ECs when stimulated with histamine (Puustinen & Uotila, 1984; Resink *et al.*, 1987). Also, the stimulation of cultured rat brain EC with LPS results in a significant increase in TxB$_2$ production at 5 and 24 hr after treatment (de Vries *et al.*, 1995). Moreover, thromboxane metabolites have been reported to be an early mediator in blood-ocular barrier disruption following induction of EIU (Herbort *et al.*, 1988; Okumura *et al.*, 1990). Therefore, indomethacin would also prevent the formation of these mediators and would explain the decrease in the inflammatory cell recruitment to the retina seen at 24 hr PI.

It therefore appears that the effect of indomethacin on preventing BRB permeability is two-fold. It is acting by suppressing inflammatory dilatation, and, as a consequence, inflammatory oedema, by preventing the production of a vasodilator substance, such as PGE$_2$ via the Cox pathway, as well as reducing leucocyte recruitment by preventing the formation of thromboxanes. In support of this theory, *in vitro* studies performed on cultured bovine aortic EC have demonstrated that not only do these cells produce eicosanoids when exposed to histamine, but these two mediators interact to reduce EC monolayer integrity and facilitate leucocyte migration (Doukas *et al.*, 1989). This effect was also abrogated with indomethacin.

Indomethacin has previously been shown to be effective in preventing cytokine-induced increases in vascular permeability. For example, breakdown of the rabbit BAB, which was induced by the intravitreal injection of TNF-α, was reduced by indomethacin (10mg.kg^{-1} IP) (Fleisher *et al.*, 1991), indicating a role for Cox products. The intravitreal injection of IL-1, along with inducing increased vascular permeability and leucocyte infiltration in the rabbit eye, was also accompanied by an elevation in aqueous humour PGE$_2$ levels (Rubin & Rosenbaum, 1988). The vascular permeability response in this study was attenuated with a Cox inhibitor, flurbiprofen. Also, trauma to the spinal cord causes

oedema formation, but pretreatment with indomethacin 30 minutes before trauma induction significantly reduced the oedema and the increased microvascular permeability (Sharma et al., 1993).

Indomethacin, however, has been shown to be ineffective, particularly in experimental models where there is a rapid increase in permeability. The intradermal injection of a macrophage-derived neutrophil chemotactic factor caused a rapid increase in capillary permeability which was abrogated by ranitidine (Khanna et al., 1994), but not indomethacin. Comparisons may be drawn between this and the current study, particularly as indomethacin was ineffective in reducing BRB permeability at 4 hr PI, when ranitidine was successful.

The cytokines IL-1ß, TNF-α and IL-6, as demonstrated by specific radioimmunoassay, were all able to stimulate the production of PGE_2 from rat REC after 24 hr. Of these IL-1ß was the most potent and caused a highly significant increase in PGE_2 production, which was greater than that seen for TNF-α and IL-6. This more pronounced effect on the release of PGE_2 by IL-1ß has also been remarked upon by de Vries et al. (1995), who studied the effect of LPS and cytokines on eicosanoid production from cerebral microvascular EC. In that study, PGE_2 production was also upregulated by IL-1ß, and IL-6, at 3 hr following stimulation. However, IL-6 did not have a significant effect on PGE_2 production after 24 hr (de Vries et al., 1995), which is in contrast to the results from this study, where 10 U/ml IL-6 caused a significant increase in PGE_2 levels. However, 20 U/ml IL-6 did not cause a significant increase, although this may be due to the small sample number ($n = 3$) preventing the mean from achieving significance. IL-6-induced PGE_2 production from rat REC was significantly, but only slightly, increased over unstimulated EC after 24 hr. Whether the increase in PGE_2 following 10 U/ml IL-6 demonstrates a genuine difference in response between brain and retinal ECs is uncertain as the supernatants were only sampled at 24 hr. As the amount of PGE_2 detected was relatively small at 24 hr, it is possible that this was produced at 3 hr only, and IL-6 may therefore exert only a short-term effect on prostaglandin formation. Alternatively IL-6 may be exerting a reduced biological effect on the EC after 24 hr.

A significant decrease in PGE_2 levels, when compared to supernatant from unstimulated EC in culture, was observed following IL-1ß and indomethacin treatment. This may be due to indomethacin inhibiting the activities of the constitutively expressed Cox. Cox, which is localised primarily in the endoplasmic reticulum, exists in two different forms: Cox-1 and Cox-2. Cox-1 exists as a constitutive form, and Cox-2 is unique because it is highly induced in response to cell activation processes, including

inflammation. IL-1ß has been shown to dramatically upregulate Cox-2 mRNA from freshly explanted rheumatoid synovial tissue, whereas Cox-1 expression was not affected (Crofford *et al.*, 1994). IL-1α also induces a sustained increase in the expression of the Cox-2 mRNA, as well as the functional enzyme, in a human cell line (ECV304) (Ristimaki *et al.*, 1994).

Leucocyte Depletion

Following leucocyte depletion and the intravitreal injection of IL-1ß, there was a decrease in BRB permeability when compared to the effects of IL-1ß-induced BRB permeability in normal rats at 4 and 24 hr PI. BRB permeability, as measured in the retinal samples, was significantly decreased at 4 and 24 hr PI IL-1ß. However, the mean Rt/Rp value for the vitreous samples at 24 hr PI was reduced, but not significantly different from the value seen following intravitreal IL-1ß in normal rats. This may be due to the relatively small sample size ($n = 5$) combined with the data exhibiting a high variance, and thereby not reaching significance. Alternatively, there may indeed be a real similarity between the Rt/Rp ratio of the two vitreous samples. This may be caused by a breakdown of the BAB, perhaps through the action of IL-1ß inducing the release of vasoactive substances from mast cells found in the anterior chamber (Li *et al.*, 1993), and allowing mannitol tracer into the vitreous from the iris and ciliary body.

Most experimental work investigating the effect of leucocyte depletion on vascular permeability appears to have concentrated on the depletion of PMNs. In this study the phenotype of the few remaining cells in the circulation was not determined, but the majority of the few migrated leucocytes in the retina at 24 hr PI IL-1ß were PMN. It appears, therefore, that the presence of migrating leucocytes in the retina is necessary for breakdown of the BRB, and this is consistent with other reports. For example, leucocyte depletion was associated with a reduction in the vascular permeability associated with ischaemia-reperfusion in the dog (Korthius *et al.*, 1988). Also, the presence of migrating PMNs in response to intravitreally injected PAF was associated with increased BRB permeability (Smith *et al.*, 1994), and PMNs have been implicated in controlling vascular permeability of the EC in rabbit skin to plasma proteins (Wedmore & Williams, 1981). These PMNs interact with vascular EC to regulate permeability within a few minutes of the inflammatory stimulus. However, the depletion of PMNs has also been shown not to

affect increased vascular permeability within the eye following intravitreal LPS (Howes *et al.*, 1985).

At 24 hr following leucocyte depletion, histology revealed a significant decrease in the number of migrated inflammatory cells within the retinal parenchyma. The presence of cells within the retina may be explained by the remaining cells (a 99% leucopaenia would still leave around 1 x10^6 leucocytes circulating within the blood of a 250g rat) being recruited by the upregulation of adhesion molecules on the vascular endothelia induced by the intravitreal IL-1ß injection.

Galardin™

In an attempt to inhibit leucocyte recruitment to the retina, and perhaps BRB breakdown, following intravitreal IL-1ß, an inhibitor of MMP activity, Galardin™, was used. This, however, was unsuccessful in preventing increased barrier permeability, but did cause a decreased, although not a significant reduction, in the cellular infiltrate to the retina. The reason that a MMP inhibitor was selected was because leucocytes are known to secrete MMPs, among which are enzymes that can degrade basement membrane and permit the extravasation of inflammatory cells from the circulation through the endothelium (Gordon *et al.*, 1978; Uitto *et al.*, 1980; Opdenakker *et al.*, 1991). Also, proteolytic enzymes are among agents with a potential to permeabilise the BBB and allow cellular migration into the CNS (Rosenberg *et al.*, 1992).

The release and activation of MMPs is stimulated by inflammatory cytokines such as IL-1ß (Ogata *et al.*, 1992) and TNF-α (Dayer *et al.*, 1985). It has been shown in the rabbit that following the intravitreal injection of IL-1ß there is an increase in MMPs within the vitreous after 24 hr (Kosnosky *et al.*, 1994). This increased MMP activity could be produced by the infiltrating leucocytes or by the RPE, which has been shown to secrete MMPs in culture in response to IL-1ß (Hunt *et al.*, 1993). MMP inhibitors might be expected to work by blocking the extravasation of leucocytes in the initial stage of inflammation by preventing degradation of extracellular matrix and basement membrane. Although the administration of Galardin™ had no significant effect on decreasing IL-1ß-induced BRB permeability in this study, the administration of a MMP inhibitor has been shown to reduce the breakdown of the BBB following the intracerebral administration of gelatinase (also known as type IV collagenase), which belongs to the family of MMPs

(Rosenberg *et al.*, 1992). MMP inhibitors have also been shown to suppress or reverse EAE (Gijbels *et al.*, 1994; Hewson *et al.*, 1995).

The dose of inhibitor used for these experiments (4mg.kg^{-1} IP) was selected because it was successful in suppressing BBB permeability during EAE in the mouse, although no significant reduction in inflammation occurred (Gijbels *et al.*, 1994). The inhibitor was initially injected IP at 6 hr PI because levels are not detectable in the CSF of normal animals (Gijbels *et al.*, 1994), indicating that the inhibitor does not cross the intact BBB, and therefore presumably, the BRB.

Combined Role of Histamine, Cox Metabolites, and Leucocytes in IL-1ß-Induced BRB Dysfunction

The IL-1ß-induced biphasic breakdown of the BRB in the Lewis rat therefore appeared to be mediated by histamine, and was dependent on the presence of leucocytes within the retina (*see Fig. 4.1*). The initial breakdown of the BRB observed, following the intravitreal injection of IL-1ß, was prevented by the administration of ranitidine, and this indicated that IL-1ß-induced histamine release within the retina was acting directly on the retinal endothelium to cause increased vascular permeability via histamine H_2-receptors. Histamine may have also contributed to leucocyte accumulation by inducing endothelial P-selectin expression. The intravitreal IL-1ß would have induced the further upregulation of other adhesion molecules, with infiltrating cells providing a further source of histamine through stimulation by IL-1ß. The BRB, which has an impressive capacity to repair (see review by Greenwood, 1992c), is able to regain its integrity prior to the second phase of vasodisruptive insults. The second increase in BRB permeability at 24-48 hr PI appeared to be mediated by the release of Cox products of arachidonic acid metabolism, and this may have been induced through the action of histamine and IL-1ß on the EC, with a possible contribution from the recruited leucocytes. Prostaglandin release may have been responsible for the second larger BRB dysfunction, and this was possibly potentiated by histamine. The production of thromboxanes resulted in the further recruitment of leucocytes to the retina, and these cells appeared to be crucial for increased vascular permeability.
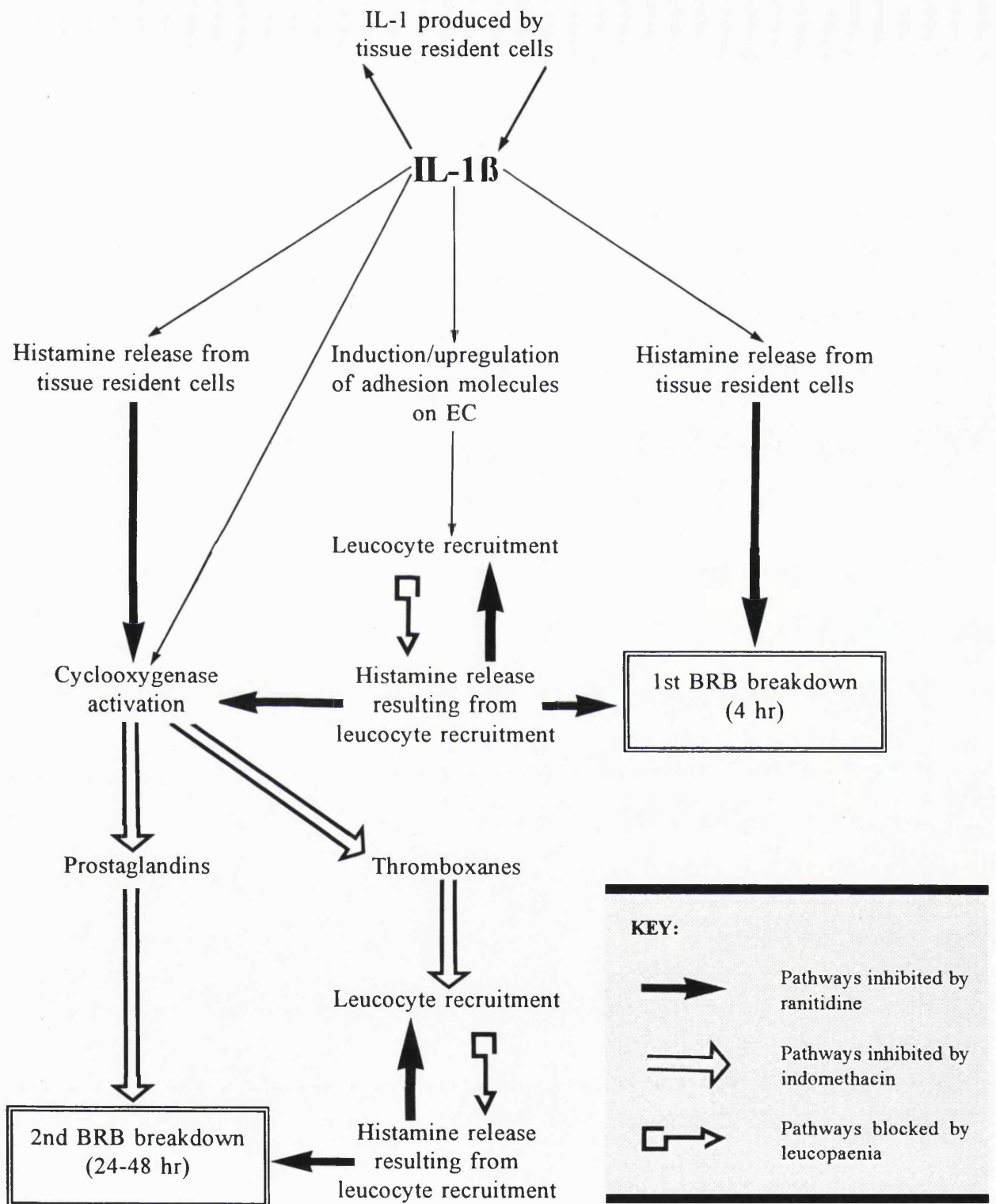
Figure 4.1. *Possible mechanisms involved in the biphasic opening of the BRB induced by IL-1β.*

4.5 TUMOUR NECROSIS FACTOR- α

The intravitreal injection of TNF-α in the Lewis rat caused a monophasic increase in BRB permeability accompanied by a small but persistent infiltration of leucocytes, which was in direct contrast to the effects seen following an intravitreal injection of IL-1ß. Unlike IL-1ß, where MN and PMN leucocytes were seen in large numbers throughout the neuroretina, ciliary body and vitreous, the TNF-α injected eyes only exhibited a small-scale MN infiltrate, albeit greater than with the control injection.

The results observed following the intravitreal injection of TNF-α in the Lewis rat are consistent with previous studies where TNF has been injected into the eye. The inflammatory consequences of intraocular TNF have been described as both mild and inconsistent, even when up to 500,000 U (22µg) was injected (Rosenbaum et al., 1988), particularly when compared to the effects of intraocular administration of either IL-1 (Martiney et al., 1992; Claudio et al., 1994) or LPS (Forrester et al., 1980). In this study very few cells were observed in the retina and this minimal inflammatory response to TNF-α in vivo has also been reported following intracerebral injection into mice (Andersson et al., 1992), and into the skin of rabbits, where an intradermal injection resulted in either a mild PMN infiltrate, even at 1×10^5 U (Wankowicz et al., 1988), or had no effect at all (Watson et al., 1989). Intravitreal TNF has other reported effects upon the rabbit retina, apart from inflammation, such as inducing an increase in visual evoked potentials (Brosnan et al., 1989) and a transient increase in endothelial cell pinocytotic activity in the capillary bed (Brosnan et al., 1990).

However, some reports have shown a substantial ocular inflammatory response to intravitreal TNF, but these studies have employed very high concentrations of cytokine in doses ranging from 1µg (Fleisher et al., 1991) to 10µg (Kulkarni & Srinivasan, 1988) compared to the doses of 5.5 and 11 ng used in this study. Also, a high dose of TNF-α (6×10^4 U) injected into the cerebrum of the rat resulted in a leucocytic infiltrate, composed mainly of macrophages and neutrophils, to the injection site which was maximal after 48 hr (Wright & Merchant, 1992).

In comparison to this study, De Vos et al. (1995) also injected murine recombinant TNF-α intravitreally into rats, but found that 50ng of protein was the minimum dose

required to achieve a uveitis score, which was considerable by 4 hr PI. Blood-ocular barrier breakdown differed from the present study, as protein extravasation into the aqueous humour was significantly increased at 4 hr PI, but not at 24 hr PI, when compared to control injection values. Also, the cellular infiltrate to the anterior segment contained PMNs whereas, in this study, only MN cells were seen in the retina, predominantly in the vessels, but occasionally in the parenchyma and vitreous. MNs have also been reported to be the predominant leucocytes present in the retina following intravitreal TNF (Rosenbaum *et al.*, 1988; Brosnan *et al.*, 1989; Fleisher *et al.*, 1990), with PMNs only rarely detected (Claudio *et al.*, 1994).

Immunohistochemistry

A recent study, as mentioned above, has described the presence of CD18 positive cells in the rabbit retina following IL-1ß injection that were thought to represent perivascular macrophages (Cuff *et al.*, 1994). In an attempt to determine whether tissue resident cells were being activated in the retina in response to intravitreal TNF-α, frozen sections of retina were stained for various markers including MHC class II and the macrophage, monocyte, dendritic cell marker ED1. The results from these investigations demonstrated that there was a significant increase in the expression of both MHC class II and ED1 positive cells, whereas the macrophage marker, ED2, only stained occasional cells. This suggests that a significant proportion of the MHC class II/ED1 positive cells are likely to be activated tissue resident cells, particularly as the leucocytic infiltrate was so minimal. MHC class II positive cells have also been described in the inner retinal layers of Lewis rats at 24 hr following the intravitreal injection of 50ng TNF-α (De Vos *et al.*, 1995), a much larger dose than used in this study. TNF-α has also been shown to upregulate MHC class II expression on astrocytes from organotypic cultures of mouse spinal cord *in vitro* (Cannella & Raine, 1989). However, TNF-α was unable to induce MHC class II upregulation in rat astrocytes (Benveniste *et al.*, 1989), but did synergise with IFN-γ for enhanced MHC class II expression.

An upregulation in MHC class II expression in the CNS is apparent in inflammatory disease states such as posterior uveitis (Lightman & Chan, 1990), EAU (Chan *et al.*, 1986), MS (Traugott *et al.*, 1985) and EAE (Butter *et al.*, 1991). APCs express MHC class II molecules in association with antigenic epitopes and generate the

necessary co-stimulatory signals to lymphocytes during an immunological response. Whether the EC functions as an APC along with CNS resident cells remains uncertain (Calder & Greenwood, 1995, Wang *et al.*, 1995). *In vitro*, retinal and cerebral EC constitutively express MHC class I molecules (Risau *et al.*, 1990; Liversidge *et al.*, 1990; Wang *et al.*, 1995) and are therefore able to interact with CD8$^+$ T cells in an MHC class I-restricted manner, but they do not constitutively express class II molecules. However, when CNS EC are stimulated *in vitro* with the cytokine IFN-γ, the expression of class I molecules is enhanced and class II molecules are induced (Male & Pryce, 1988; Wang *et al.*, 1995).

Following intravitreal TNF-α, the observation that most of the MHC class II positive cells lay in the ganglion cell/inner plexiform layers of the retina, just below the inner limiting membrane, is consistent with this area being an interface with the vitreous through which infectious agents may enter the retina. The presence of high concentrations of MHC class II reactive cells has also been reported in other areas of the CNS where there exists the possibility of entry of infectious agents, such as the subarachnoid space and pial surface (Broadwell *et al,.* 1995). However, due to the lack of morphological preservation in the frozen sections it was impossible to deduce exactly what type of cells were expressing MHC class II or ED1.

BRB Disruption

The mechanism by which TNF-α causes BRB breakdown is not clear. It is possible that TNF-α is acting directly upon the cells that form the BRB by causing disruption of the tight junctions. However, this would seem unlikely as the effect is so prolonged. Alternatively, this cytokine may be acting on immunoresponsive tissue resident cells such as the so-called perivascular cells and microglia (Giulian *et al.*, 1988; Selmaj *et al.*, 1990; Andersson *et al.*, 1992). These cells, once activated, may release other vasoactive compounds which might subsequently play a role in disrupting the BRB. For example, TNF has been shown to interact with EC in culture and induce the synthesis and release of IL-1 (Nawroth *et al.*, 1986; Libby *et al.*, 1986). TNF-α also stimulates cultured mouse astrocytes to produce IL-6 (Sawada *et al.*, 1992), although the intravitreal injection of IL-6 in the present study did not induce any perturbations in the integrity of the BRB.

A further possible cause of BRB disruption is the induction of a MN cell infiltrate

which followed a similar time-course to the duration of barrier opening. However, as the number of infiltrating cells was very small, and as a similar number of leucocytes were observed following the injection of the lower dose of TNF-α, where no BRB disruption was detected, it is unlikely that this is the cause of barrier dysfunction.

Of particular interest was the observation that following an intravitreal injection of 2×10^4 U of TNF-α there was a significant and prolonged disruption of the BRB in the contralateral non-injected eye. This leakage of the contralateral BRB, which did not occur with intraocular vehicle control, or following IL-1ß administration, nor with the lower dose of TNF-α investigated, followed a similar time-course to that of the injected eye. Disruption of the contralateral blood-ocular barriers and cellular infiltration has also been reported following the intravitreal injection of IL-6 (Hoekzema et al., 1991) and LPS (Forrester et al., 1980). In these studies, however, the left eye served as an injected control and was therefore subject to a degree of trauma which may have resulted in the observed increase in protein leakage into the aqueous humour. In a further study, where IL-1 or IL-8 was injected into the rat eye, the contralateral non-injected eye yielded a cellular inflammatory response (Ferrick et al., 1991) although there was no indication of whether barrier disruption also occurred.

Possible Mechanisms of TNF-α-Induced Disruption of the Contralateral BRB

The mechanism responsible for the opening of the contralateral BRB is not clear but may be due a variety of possible factors. It is most unlikely, however, that this is due to leakage of TNF-α from the vitreous into the systemic circulation as dilution in the blood would reduce the concentration delivered to the contralateral vasculature by several orders of magnitude. An alternative explanation may result from the observation that TNF-α injected into the vitreous of the mouse can induce morphological changes in the optic nerve (Butt & Jenkins, 1994) and cause both an increase in axonal transport of protein and demyelination of optic nerve fibres (Jenkins & Ikeda, 1992). Whether this optic nerve damage can lead to perturbations of the contralateral retina, however, remains highly speculative. Indeed, no structural damage or inflammatory reaction, as determined by increased expression of MHC class II or CD18 by immunohistochemistry in the non-injected eye, was detected.

A further possible explanation is that TNF-α may be acting centrally, involving

the brain stem nuclei which may provoke dilatation of the contralateral ocular vasculature. It is well recognised that vasodilatation is associated with increased vascular leakage which may explain the observed disruption of the BRB. The involvement of a reflex arc mechanism has previously been discussed as a likely mechanism for contralateral effects (Perkins, 1957; Butler *et al.*, 1979; Forrester *et al.*, 1980).

Early research into contralateral ocular effects during inflammation was conducted by Davson and colleagues (Davson & Quilliam, 1947; Davson & Matchett, 1951). When nitrogen mustard (N-mustard) was administered into the conjunctival sac an acute inflammatory oedema and breakdown of the BAB to Evans Blue occurred. This response, however, was not confined to the treated eye as the dose required to produce a lesion in one eye was smaller when the other eye was treated simultaneously. The administration of N-mustard to the eye was found to induce a rise in intraocular pressure (IOP) due to blood vessel dilatation and a rapid plasma exudation into the eye. This overloaded the outflow mechanism resulting in increased IOP, but also induced an increase in the contralateral IOP in 48% of the animals tested. It was hypothesised that this contralateral effect may be either caused by a reflex rise in pressure in response to the increased IOP in the treated eye, or alternatively it may be due to the presence of N-mustard circulating in the blood. The latter hypothesis was rejected due to the small amount injected (0.6mg) and confirmed by control experiments where subcutaneous injections of larger amounts of N-mustard were unable to elicit a rise in IOP. A purely vascular interpretation of the results of sympathetic stimulation was therefore unlikely.

A consistent increase in the IOP of the contralateral eyes of rabbits receiving an intracameral injection of prostaglandins, which produced a sustained ocular hypertension and breakdown of the BAB, has also been observed (Beitch & Eakins, 1969; Chiang & Thomas, 1972a). This was attributed to the transfer of prostaglandin from the injected eye to the contralateral eye via the systemic blood circulation, and not due to a reflex mechanism via the trigeminal nerve (Chiang & Thomas, 1972b). However, it is unlikely that prostaglandin from the test eye could reach the contralateral eye in sufficient quantities to induce BAB breakdown particularly as prostaglandins are rapidly inactivated by the liver and pulmonary circulation of the lungs (Ferreira & Vane, 1967; Piper *et al.*, 1970). It was thought possible that the observed effect was due to a neuronal response in the contralateral eye causing a local release of prostaglandin from the ocular tissues

(Kottow & Seligman, 1978). There is evidence, however, that prostaglandins are not involved in this contralateral response at all. Formaldehyde administered onto the eye caused a pupil constriction, an increase in IOP and raised protein content of the aqueous (Butler *et al.*, 1979). However this response could not be blocked with indomethacin, suggesting that prostaglandins were not involved. Moreover, mechanical stimulation of the intra-cranial portion of the trigeminal nerve caused increased IOP and BAB breakdown (Perkins, 1957) but no prostaglandin was detected in the aqueous following stimulation of this nerve (Cole & Unger, 1973).

The exact mechanism responsible for the contralateral effect observed in this study following intravitreal TNF-α remains unresolved.

Permeability to HRP

Although 2×10^4 U of TNF-α induced a significant and prolonged extravasation of mannitol, the large molecular weight tracer HRP was excluded from entering the neuroretina   at 5 days PI. This would suggest that the size of the pores formed through the BRB by the action of TNF-α were small enough to allow the passage of mannitol but not HRP. An alternative explanation may be that only isolated areas of the BRB were disrupted and that these were missed during sampling for electron microscopy. This explanation, however, is unlikely as no HRP reaction product was observed anywhere macroscopically in the retina during processing or in the semi-thin sections used for light microscopy.

TNF-α certainly appears to possess the ability to induce an acute uveitis in animals when injected to the vitreous in very high doses. In this study however, a dose which was sufficient to induce only a minimal leucocytic response, was able to cause a prolonged increase in BRB permeability. A long term blood-ocular barrier disruption has also been described in the rabbit following the intravitreal injection of 1μg TNF-α (Fleisher *et al.*, 1990). This dose induced maximal protein extravasation at 48 hr PI and a cellular infiltrate to the aqueous consisting mainly of MNs. A small but significant increase in vitreous humour protein was also measured from 24 hr and up to 7 days PI.

4.6 INTERLEUKIN-6

Following the intravitreal injection of IL-6 no significant retinal inflammation or breakdown of the BRB was observed up to 3 days PI. A small scale leucocytic infiltrate did occur within the retina, following a dose of 1 x10^3 U, from 4 hr PI, but did not noticeably increase over the 3 day period examined. All the leucocytes observed at this dose were MN in appearance, located in the lumen of retinal blood vessels, and were frequently accompanied by platelets. As previously mentioned, leucocyte-platelet aggregates are a feature of certain inflammatory responses, but in this case, however, they were not associated with an increase in vascular permeability. IL-6, when administered IP to the mouse, is able to induce an increase in the production of platelets through its effect on megakaryocytes (Ishibashi *et al.*, 1989), but it is unlikely that the intravitreal injection of IL-6 would produce this effect. The platelet aggregating effect is more likely due to the cytokine activating the retinal EC, which allows for leucocyte adhesion and which subsequently induces platelet aggregation.

The effect of increasing the dose of intravitreal IL-6 to 2 x10^3 U resulted in a slightly increased cellular infiltrate to the retina, which was comprised of PMNs within the parenchyma, as well as MN cells. The effect of 2 x10^3 U IL-6 on the permeability of the BRB was not investigated, but at the ultrastructural level there was no evidence of increased vascular permeability, such as fibrin and oedema.

The minimal response to intravitreal IL-6 seen in this study is in direct contrast to previous studies, which have been successful in inducing a cellular infiltrate into the Lewis rat retina, accompanied by breakdown of the blood-ocular barriers (Hoekzema *et al.*, 1991; Hoekzema *et al.*, 1992). The main difference in experimental design between the studies of Hoekzema *et al.* and this study is the source of IL-6. This study employed murine recombinant IL-6 whereas Hoekzema *et al.* used human recombinant IL-6. It is possible that the differences in response between these two studies could therefore be attributed to the source of cytokine used. Between human and murine IL-6 there is a 65% homology at the DNA level, and only a 42% homology at the amino acid level (van Snick *et al.*, 1988). It appears, therefore, that the human cytokine is more potent in the rat eye, which may be relatively insensitive to certain murine cytokines. However, human

recombinant IL-6 has been shown to be active in the rat *in vivo* when injected IP (Marinkovic *et al.*, 1989). The active uveitis demonstrated by Hoekzema and colleagues occurred at 24 hr following the intravitreal injection of 1 x10^3 U IL-6 (Hoekzema *et al.*, 1991). The greatest amount of extravasated protein in the anterior chamber, however, occurred following 100 U IL-6, which also induced an acute uveitis, and increasing amounts of IL-6 resulted in decreasing levels of extravasated protein, an occurrence known as a prozone effect. To ensure that a prozone effect was not occurring in the current study, a dose of 100 U IL-6 was injected intravitreally and the retina examined histologically after 24 hr. This demonstrated that no leucocytic response had occurred and the possibility of a prozone effect rejected. Immunohistochemistry performed on Lewis rat retinas after the intravitreal injection of 1 x10^3 U IL-6 (Hoekzema *et al.*, 1992), demonstrated that PMNs were beginning to accumulate in the iris as early as 2 hr PI, and in the retina by 4 hr PI. This cellular infiltrate appears to be similar to that seen in this study following intravitreal IL-1ß with the exception that ED2 positive cells were not present in the retina following IL-6.

The intracameral injection of IL-6 into rabbits has also been reported to induce an inflammatory cell infiltrate to the aqueous humour (Malecaze *et al.*, 1991). This response was maximal at 4 hr PI using a dose of just 10pg of IL-6, which demonstrates the sensitivity of the rabbit anterior chamber to this cytokine. Increased BAB permeability was not assessed by protein extravasation, however, because the vehicle in which the IL-6 was delivered possessed a high quantity of protein (Ringer's solution with 5% FCS). The intravitreal injection of IL-6 (doses ranging from 100 pg to 100 ng) also caused an anterior uveitis in the rabbit accompanied by increased aqueous protein levels after 24 hr (Hoekzema *et al.*, 1990).

It has been suggested that the production of IL-6 in uveitis is the end product of a cytokine cascade and that the presence of IL-6 itself is not required for the induction of uveitis (Murray *et al.*, 1990). This may explain why, in this study, an intravitreal injection of IL-6 by itself was not able to induce a significant leucocytic infiltrate to the retina, or to alter the permeability properties of the BRB.

In vitro studies measuring the permeability inducing effects of IL-6 have been conflicting. In one study, IL-6 was unable to increase the permeability of HUVEC monolayers as measured by electrical resistance (Burke-Gaffney & Keenan, 1993).

However, other studies have shown IL-6 to increase the permeability of bovine vascular ECs to FITC-labelled albumin (Maruo *et al.*, 1992) and 100ng.ml^{-1} IL-6 was able to induce a decrease in transendothelial electrical resistance of cultured rat cerebral EC (de Vries *et al.*, 1996).

Very rarely, mast cells were observed in the choroid of IL-6 injected eyes. However, the normal Lewis rat choroid has been reported to contain around 50 mast cells per mm^2 of choroid (Mochizuki *et al.*, 1984). It is therefore possible that the mast cells observed in the IL-6 injected eyes were part of the normal choroid and not recruited by IL-6. Indeed, mast cells are a relatively fixed resident of the tissue in which they are found. Also, as only a small portion of the posterior eye cup is sectioned for histological analysis, this may explain why mast cells were not seen regularly in any of the sections of retina examined.

CONCLUSIONS

CONCLUSIONS

In this study the cytokines IL-1ß, TNF-α and IL-6, which are key mediators of acute inflammation, were examined to investigate their effects on the BRB of the Lewis rat. Although *in vitro* these cytokines express similar and overlapping activities, this was certainly not apparent *in vivo*. It appears that these cytokines are each only part of a complex network of interacting cytokines and other inflammatory mediators, such as histamine and the eicosanoids, and each may play a certain role in the different stages of an acute inflammatory reaction, which includes vascular permeability, leucocyte adhesion and migration.

This study demonstrates for the first time that a single injection of IL-1ß to the vitreous of the Lewis rat produces an acute and reversible retinal inflammation that is accompanied by a biphasic breakdown of the BRB. This breakdown, however, can be prevented by the administration of ranitidine, and partly by indomethacin, and appears to be associated with leucocyte recruitment.

The intravitreal injection of IL-1ß possibly induces histamine release, either from tissue resident cells or from recruited leucocytes, which cause the first breakdown of the BRB and is mediated via histamine H_2-receptors. The permeability then returns to control values, perhaps because histamine is only effective in a transient manner, but an inflammatory response/mediator cascade continued to recruit leucocytes to the retina. Part of this cascade apparently involved the production of prostaglandins and thromboxanes within the retina (probably from the ECs and infiltrating leucocytes) and it is this that caused the second breakdown of the barrier. Prostaglandins were most likely acting directly through vasodilatation, and thromboxanes by contributing to leucocyte recruitment. Histamine, via H_2-receptors, must have also been an integral component responsible for setting up the second breakdown of the BRB, perhaps through leucocyte recruitment or inducing Cox metabolite release from ECs, as ranitidine was also successful in preventing the second phase of BRB dysfunction.

In contrast to IL-1ß, the intravitreal administration of TNF-α caused a monophasic and prolonged opening of the BRB in both the injected eye and the contralateral control eye which may be due to the involvement of a neuronal reflex arc mechanism. This

197

disruption, however, was not associated with a large-scale leucocyte infiltration.

The injection of the cytokine IL-6 into the vitreous had no detectable effect on the integrity of the BRB, despite inducing a mild cellular infiltration.

From this study it can be concluded that the pro-inflammatory cytokines examined act very differently in their abilities to induce a uveitic response or breakdown of the BRB in the Lewis rat. It is also apparent that these cytokines do not act directly to cause pathology, but are part of a complex cascade of interacting inflammatory mediators.

REFERENCES

REFERENCES

Abbott, N.J. (1992) Comparative physiology of the blood-brain barrier. In: M.W.B. Bradbury (Ed.) *Physiology and pharmacology of the blood-brain barrier.* Springer-Verlag, Berlin. Pp. 371-396.

Abu El Asrar, A.M., Maimone, D., Morse, P.H., Gregory, S. & Reder, A.T. (1993) Cytokines in the vitreous of patients with proliferative diabetic retinopathy. *Am J Ophthalmol,* **114:** 731-736.

Albelda, S.M., Muller, W.A., Buck, C.A. & Newman, P.J. (1991) Molecular and cellular properties of PECAM-1 (EndoCAM/CD31) - a novel vascular cell-cell adhesion molecule. *J Cell Biol,* **114:** 1059-1068.

Andersson, P.B., Perry, V.H. & Gordon, S. (1992) Intracerebral injection of proinflammatory cytokines or leucocyte chemotaxins induces minimal myelomonocytic cell recruitment to the parenchyma of the central nervous system. *J Exp Med,* **176:** 255-259.

Asako, H., Kurose, I., Wolf, R., DeFrees, S., Zheng, Z., Phillips, M.L., Paulson, J.C. & Granger, D.N. (1994) Role of H1 receptors and P-selectin in histamine-induced leukocyte rolling and adhesion in postcapillary venules. *J Clin Invest,* **93:** 1508-1515.

Ashton, N. (1965) The blood-retinal barrier and vaso-glial relationships in retinal disease. *Trans Ophthalmol Soc UK,* **85:** 199-229.

Ashton, N. & Cunha-Vaz, J.G. (1965) Effect of histamine on the permeability of the ocular vessels. *Arch Ophthalmol,* **73:** 211-223.

Åström, K.E., Webster, H.F. & Arnason, B.G. (1968) The initial lesion in experimental allergic neuritis. A phase and electron microscopic study. *J Exp Med,* **128:** 469-495.

Baker, H.J., Lindsey, J.R. & Weisbroth, S.H. (1979) Selected normative data. In: H.J. Baker, J.R. Lindsey, & S.H. Weisbroth (Eds.) *The laboratory rat.* Academic Press, New York. Pp. 411-412.

Banks, W.A. & Kastin, A.J. (1992) The interleukins-1α, -1β and -2 do not acutely disrupt the murine blood-brain barrier. *Int J Immunopharmacol,* **14:** 629-636.

Bauer, J., Berkenbosch, F., Van Dam, A. & Dijkstra, C.D. (1993) Demonstration of interleukin-1β in Lewis rat brain during experimental allergic encephalomyelitis by immunocytochemistry at the light and ultrastructural level. *J Neuroimmunol,* **48:** 13-22.

Beekhuizen, H., Corsel-Van Tilburg, A.J., Blokland, I. & van Furth, R. (1991) Characterization of the adherence of human monocytes to cytokine-stimulated human macrovascular endothelial cells. *Immunology,* **74:** 661-669.

Beitch, B.R. & Eakins, K.E. (1969) The effects of prostaglandins on the intraocular pressure of the rabbit. *Br J Pharmacol*, **37:** 158-167.

Benedito, S., Prieto, D., Nielsen, P.J. & Berg Nyborg, N.C. (1991) Histamine induces endothelium-dependent relaxation of bovine retinal arteries. *Invest Ophthalmol Vis Sci*, **32:** 32-38.

Benveniste, E.N. & Merrill, J.E. (1986) Stimulation of oligodendroglial proliferation and maturation by interleukin-2. *Nature*, **321:** 610-613.

Benveniste, E.N., Sparacio, S.M. & Bethea, J.R. (1989) Tumor necrosis factor-α enhances interferon-γ-mediated class II antigen expression on astrocytes. *J Neuroimmunol*, **25:** 209-219.

Bernstein, M.H. & Hollenberg, M.J. (1965) Movement of electron-opaque markers through the capillaries of the retina. In: J.W. Rohen (Ed.) *Eye Structure, II. Symposium.* Schattauer-Verlag, Stuttgart. Pp. 129-138.

Betz, A.L., Firth, J.A. & Goldstein, G.W. (1980) Polarity of the blood-brain barrier: distribution of enzymes between the luminal and antiluminal membranes of brain capillary endothelial cells. *Brain Res*, **192:** 17-28.

Bevilacqua, M.P., Pober, J.S., Wheeler, M.E., Cotran, R.S. & Gimbrone, M.A. (1985) Interleukin 1 acts on cultured human vascular endothelium to increase the adhesion of polymorphonuclear leucocytes, monocytes, and related leucocyte cell lines. *J Clin Invest*, **76:** 2003-2011.

Bhattacherjee, P., Williams, R.N. & Eakins, K.E. (1983) An evaluation of ocular inflammation following the injection of bacterial endotoxin into the rat foot pad. *Invest Ophthalmol Vis Sci*, **24:** 196-202.

Bhattacherjee, P. & Henderson, B. (1987) Inflammatory responses to intraocularly injected interleukin 1. *Curr Eye Res*, **6:** 929-934.

Bhattacherjee, P. & Paterson, C.A. (1990) Further investigation into the ocular effects of prostaglandin E_2, leukotriene B_4 and formyl-methionyl-leucyl phenylalanine. *Exp Eye Res*, **51:** 93-96.

Bill, A. (1975) Blood circulation and fluid dynamics in the eye. *Physiol Rev*, **55:** 383-417.

Bito, L.Z. (1984) Species differences in the responses of the eye to irritation and trauma: a hypothesis of divergence in ocular defense mechanisms, and the choice of experimental animals for eye research. *Exp Eye Res*, **39:** 807-829.

Bivin, W.S., Crawford, M.P. & Brewer, N.R. (1979) Morphophysiology. In: H.J. Baker, J.R. Lindsey, & S.H. Weisbroth (Eds.) *The laboratory rat.* Academic Press, New York. Pp. 74-103.

Black, K.L. & Hoff, J.T. (1985) Leukotrienes increase blood-brain barrier permeability following intraparenchymal injections in rats. *Ann Neurol*, **18**: 349-351.

Bø, L., Olsson, T., Nyland, H., Krüger, P.G., Taule, A. & Mørk, S. (1991) Mast cells in brains during experimental allergic encephalitomyelitis in Lewis rats. *J Neurol Sci*, **105**: 135-142.

Bochner, B.S., Luscinskas, F.W., Gimbrone, M.A., Newman, W., Sterbinsky, S.A., Derse-Anthony, C.P., Klunk, D. & Schleimer, R.P. (1991) Adhesion of human basophils, eosinophils, and neutrophils to interleukin 1-activated human vascular endothelial cells: contributions of endothelial cell adhesion molecules. *J Exp Med*, **173**: 1553-1556.

Bolton, C., Parker, D., McLeod, J. & Turk, J.L. (1986) A study of the prostaglandin and thromboxane content of the central nervous tissues with the development of chronic relapsing allergic encephalomyelitis. *J Neuroimmunol*, **10**: 201-208.

Bora, N.S., Kim, M.C., Kabeer, N.H., Simpson, S.C., Tandhasetti, M.T., Cirrito, T.P., Kaplan, A.D. & Kaplan, H.J. (1995) Experimental autoimmune anterior uveitis. Induction with melanin-associated antigen from the iris-ciliary body. *Invest Ophthalmol Vis Sci*, **36**: 1056-1066.

Bradbury, M.W.B. & Lightman, S.L. (1990) The blood-brain interface. *Eye*, **4**: 249-254.

Brett, J., Gerlach, H., Nawroth, P., Steinberg, S., Godman, G. & Stern, D. (1989) Tumour necrosis factor/cachectin increases permeability of endothelial cell monolayers by a mechanism involving regulatory G proteins. *J Exp Med*, **169**: 1977-1991.

Brightman, M.W., Hori, M., Rapoport, S.I., Reese, T.S. & Westergaard, E. (1973) Osmotic opening of tight junctions in cerebral endothelium. *J Comp Neurol*, **152**: 317-326.

Broadwell, R.D. & Salcman, M. (1981) Expanding the definition of the blood-brain barrier to protein. *Proc Natl Acad Sci USA*, **78**: 7820-7824.

Broadwell, R.D. (1989) Transcytosis of macromolecules through the blood-brain barrier: a cell biological perspective and critical appraisal. *Acta Neuropathol*, **79**: 117-128.

Broadwell, R.D., Baker, B.J. & Hickey, W.F. (1995) CNS transplants and the host immune response: the blood-brain barrier and immunological privilege within the mammalian brain. In: J. Greenwood, D. Begley, & M. Segal (Eds.) *New concepts of a blood-brain barrier.* Plenum Press, London. Pp. 299-309.

Brosnan, C.F., Litwak, M.S., Schroeder, C.E., Selmaj, K., Raine, C.S. & Arezzo, J.C. (1989) Preliminary studies of cytokine-induced functional effects on the visual pathways in the rabbit. *J Neuroimmunol*, **25**: 227-239.

Brosnan, C.F., Claudio, L., Tansey, F.A. & Martiney, J. (1990) Mechanisms of autoimmune neuropathies. *Ann Neurol*, **27**: S75-S79.

Bull, H.A., Cohen, J. & Dowd, P.M. (1991) Responses of human dermal microvascular endothelial cells to histamine and their modulation by interleukin 1 and substance P. *J Invest Dermatol*, **97**: 787-792.

Burke-Gaffney, A. & Keenan, A.K. (1993) Modulation of human endothelial cell permeability by combinations of the cytokines interleukin-1 α/β, tumor necrosis factor-α and interferon-γ. *Immunopharmacology*, **25**: 1-9.

Butler, J.M., Unger, W.G. & Hammond, B.R. (1979) Sensory mediation of the ocular response to neutral formaldehyde. *Exp Eye Res*, **28**: 577-589.

Butt, A.M., Jones, H.C. & Abbott, N.J. (1990) Electrical resistance across the blood-brain barrier in anaesthetized rats: a developmental study. *J Physiol*, **429**: 47-62.

Butt, A.M. & Jones, H.C. (1992) Effect of histamine and antagonists on electrical resistance across the blood-brain barrier in rat brain-surface microvessels. *Brain Res*, **569**: 100-105.

Butt, A.M. & Jenkins, H.G. (1994) Morphological changes in oligodendrocytes in the intact mouse optic nerve following intravitreal injection of tumour necrosis factor. *J Neuroimmunol*, **51**: 27-33.

Butter, C., O'Neill, J.K., Baker, D., Gschmeissner, S.E. & Turk, J.L. (1991) An immunoelectron microscopical study of the expression of class II major histocompatibility complex during chronic relapsing experimental allergic encephalomyelitis in Biozzi AB/H mice. *J Neuroimmunol*, **33**: 37-42.

Calder, V.L. & Lightman, S.L. (1992) Experimental autoimmune uveoretinitis (EAU) versus experimental allergic encephalomyelitis (EAE): a comparison of T cell mediated mechanisms. *Clin Exp Immunol*, **89**: 165-169.

Calder, V. & Greenwood, J. (1995) Role of vascular endothelium in immunologically mediated neurological disease. In: C.O.S. Savage & J.D. Pearson (Eds.) *Immunological aspects of the vascular endothelium*. Cambridge University Press, Cambridge. Pp. 96-123.

Caldwell, R.B. & Slapnick, S.M. (1992) Freeze-fracture and lanthanum studies of the retinal microvasculature in diabetic rats. *Invest Ophthalmol Vis Sci*, **33**: 1610-1619.

Cannella, B. & Raine, C.S. (1989) Cytokines up-regulate Ia expression in organotypic cultures of central nervous system tissue. *J Neuroimmunol*, **24**: 239-248.

Carroll, W.J., Hollis, T.M. & Gardner, T.W. (1988) Retinal histamine synthesis is increased in experimental diabetes. *Invest Ophthalmol Vis Sci*, **29**: 1201-1204.

Casey, T.T., Cousar, J.B. & Collins, R.D. (1988) A simplified plastic embedding and immunohistologic technique for immunophenotypic analysis of human hematopoietic and lymphoid tissues. *Am J Path*, **131**: 183-189.

Caspi, R.R., Roberge, F.G., McAllister, C.G., El-Saied, M., Kuwabara, T., Gery, I., Hanna, E. & Nussenblatt, R.B. (1986) T cell lines mediating experimental autoimmune uveoretinitis (EAU) in the rat. *J Immunol*, **136:** 928-933.

Chan, C., Hooks, J.J., Nussenblatt, R.B. & Detrick, B. (1986) Expression of Ia antigen on retinal pigment epithelium in experimental autoimmune uveoretinitis. *Curr Eye Res*, **5:** 325-330.

Chandler, J.W., Heise, E.R. & Weiser, R.S. (1973) Induction of delayed-type sensitivity-like reactions in the eye by the injection of lymphokines. *Invest Ophthalmol*, **12:** 400-409.

Chiang, T.S. & Thomas, R.P. (1972a) Consensual ocular hypertensive response to prostaglandin. *Invest Ophthalmol*, **11:** 169-176.

Chiang, T.S. & Thomas, R.P. (1972b) Consensual ocular hypertensive response to prostaglandin E_2. *Invest Ophthalmol*, **11:** 845-849.

Christman, C.W., Wei, E.P. & Kontos, H.A. (1984) Effects of 15-hydroperoxy-eicosatetraenoic acid (15-HPETE) on cerbral arteries of cats. *Am J Physiol*, **16:** H631-H637.

Chung, I.Y. & Benveniste, E.N. (1990) Tumor necrosis factor-α production by astrocytes. Induction by lipopolysaccharide, IFN-γ, and IL-1β. *J Immunol*, **144:** 2999-3007.

Citi, S., Sabanay, H., Jakes, R., Geiger, B. & Kendrick-Jones, J. (1988) Cingulin, a new peripheral component of tight junctions. *Nature*, **333:** 272-276.

Citi, S. (1993) The molecular organization of tight junctions. *J Cell Biol*, **121:** 485-489.

Claudio, L., Kress, Y., Norton, W.T. & Brosnan, C.F. (1989) Increased vesicular transport and decreased mitochondrial content in blood-brain barrier endothelial cells during experimental autoimmune encephalomyelitis. *Am J Path*, **135:** 1157-1168.

Claudio, L., Kress, Y., Factor, J. & Brosnan, C.F. (1990) Mechanisms of edema formation in experimental autoimmune encephalomyelitis. *Am J Path*, **137:** 1033-1045.

Claudio, L., Martiney, J.A. & Brosnan, C.F. (1994) Ultrastructural studies of the blood-retina barrier after exposure to interleukin-1β or tumor necrosis factor-α. *Lab Invest*, **70:** 850-861.

Cole, D.F. & Unger, W.G. (1973) Prostaglandins as mediators for the responses of the eye to trauma. *Exp Eye Res*, **17:** 357-368.

Cosolo, W.C., Martinello, P., Louis, W.S. & Christophidis, N. (1989) Blood-brain barrier disruption using mannitol: time course and electron microscopy studies. *Am J Physiol*, **256:** R443-R447.

Cousins, S.W., Guss, R.B., Howes, E.L. & Rosenbaum, J.T. (1984) Endotoxin-induced uveitis in the rat: Observations on altered vascular permeability, clinical findings, and histology. *Exp Eye Res*, **39**: 665-676.

Crofford, L.J., Wilder, R.L., Ristimaki, A.P., Sano, H., Remmers, E.F., Epps, H.R. & Hla, T. (1994) Cyclooxygenase-1 and -2 expression in rheumatoid synovial tissues. Effects of interleukin-1β, phorbol ester, and corticosteroids. *J Clin Invest*, **93**: 1095-1101.

Csukas, S.C. & Green, K. (1988) Effects of intracameral hydrogen peroxide in the rabbit anterior chamber. *Invest Ophthalmol Vis Sci*, **29**: 335-339.

Csukas, S., Paterson, C.A., Brown, K. & Bhattacherjee, P. (1990) Time course of rabbit ocular inflammatory response and mediator release after intravitreal endotoxin. *Invest Ophthalmol Vis Sci*, **31**: 382-387.

Cuff, C., Berman, J.W. & Brosnan, C.F. (1994) Perivascular cells of the rabbit retina are disrupted by IL-1-induced inflammation. *J Neuroimmunol*, **54**: 154 (Abstract).

Cunha-Vaz, J.G., Shakib, M. & Ashton, N. (1966) Studies on the permeability of the blood-retinal barrier. I. On the existence, development, and site of a blood-retinal barrier. *Br J Ophthalmol*, **50**: 441-453.

Cunha-Vaz, J.G. & Shakib, M. (1967) Ultrastructural mechanisms of breakdown of the blood-retina barrier. *J Pathol Bacteriol*, **93**: 645-652.

Cunha-Vaz, J., Faria de Abreu, J.R., Campos, A.J. & Figo, G.M. (1975) Early breakdown of the blood-retinal barrier in diabetes. *Br J Ophthalmol*, **59**: 649-655.

Cunha-Vaz, J.G. (1980) Sites and functions of the blood-retinal barriers. In: J.G. Cunha-Vaz (Ed.) *The blood-retinal barriers*. Plenum Press, New York. Pp. 101-118.

Cybulsky, M.I., Colditz, I.G. & Movat, H.Z. (1986) The role of interleukin-1 in neutrophil leukocyte emigration induced by endotoxin. *Am J Path*, **124**: 367-372.

Davson, H. & Quilliam, J.P. (1947) The effects of nitrogen mustard on the permeability of the blood-aqueous humour barrier to Evans blue. *Br J Ophthalmol*, **31**: 717-721.

Davson, H. & Matchett, P.A. (1951) The control of the intra-ocular pressure in the rabbit. *J Physiol*, **113**: 387-397.

Davson, H. & Spaziani, E. (1959) The blood-brain barrier and the extracellular space of the brain. *J Physiol*, **149**: 135-143.

Davson, H., Welch, K. & Segal, M.B. (1987) *The physiology and pathophysiology of the cerebrospinal fluid*. Churchill Livingstone: Edinburgh.

Dayer, J.M., Beutler, B. & Cerami, A. (1985) Cachectin/tumor necrosis factor stimulates collagenase and prostaglandin E_2 production by human synovial cells and dermal fibroblasts. *J Exp Med*, **162**: 2163-2168.

de Boer, J.H., van Haren, M.A.C., de Vries-Knoppert, W.A.E.J., Baarsma, G.S., de Jong, P.V.T.M., Postema, F.J., Rademakers, A.J.J.M. & Kijlstra, A. (1992) Analysis of IL-6 levels in human vitreous fluid obtained from uveitis patients, patients with proliferative intraocular disorders and eye bank eyes. *Curr Eye Res*, **11**: 181-186.

de Kozak, Y., Thillaye, B., Renard, G. & Faure, J. (1978) Hyperacute form of experimental autoimmune uveo-retinitis in Lewis rats; electron microscopic study. *Graefe's Arch Clin Exp Ophthalmol*, **208**: 135-142.

de Kozak, Y., Sakai, J., Thillaye, B. & Faure, J.P. (1981) S antigen-induced experimental autoimmune uveo-retinitis in rats. *Curr Eye Res*, **1**: 327-337.

De La Motte, D.J. (1978) Removal of horseradish peroxidase and flourescein-labelled dextran from CSF spaces of rabbit optic nerve. A light and electron microscopic study. *Exp Eye Res*, **27**: 585-594.

De Vos, A.F., Hoekzema, R. & Kijlstra, A. (1992) Cytokines and uveitis; a review. *Curr Eye Res*, **11**: 581-597.

De Vos, A.F., van Haren, A.C., Verhagen, C., Hoekzema, R. & Kijlstra, A. (1994) Kinetics of intraocular tumor necrosis factor and interleukin-6 in endotoxin-induced uveitis in the rat. *Invest Ophthalmol Vis Sci*, **35**: 1100-1106.

De Vos, A.F., van Haren, M.A.C., Verhagen, C., Hoekzema, R. & Kijlstra, A. (1995) Tumour necrosis factor-induced uveitis in the Lewis rat is associated with intraocular interleukin 6 production. *Exp Eye Res*, **60**: 199-207.

de Vries, H.E., Hoogendoorn, K.H., van Dijk, J., Zijlstra, F.J., van Dam, A., Breimer, D.D., van Berkel, T.J.C., de Boer, A.G. & Kuiper, J. (1995) Eicosanoid production by rat cerebral endothelial cells: stimulation by lipopolysaccharide, interleukin-1 and interleukin-6. *J Neuroimmunol*, **59**: 1-8.

de Vries, H.E., Blom-Roosemalen, M.C.M., van Oosten, M., de Boer, A.G., van Berkel, T.J.C., Breimer, D.D. & Kuiper, J. (1996) The influence of cytokines on the integrity of the blood-brain barrier in vitro. *J Neuroimmunol*, **64**: 37-43.

Deane, B.R., Greenwood, J., Lantos, P.L. & Pratt, O.E. (1984) The vasculature of experimental brain tumours. Part 4. The quantification of vascular permeability. *J Neurol Sci*, **65**: 59-68.

DeBault, L.E. & Cancilla, P.A. (1980) γ-glutamyl transpeptidase in isolated brain endothelial cells: induction by glial cells in vitro. *Science*, **207**: 653-655.

Deem, C.W., Futterman, & Kalina, R.E. (1974) Induction of endothelial cell proliferation in rat retinal vessels by chemical and physical trauma. *Invest Ophthalmol*, **13:** 580-585.

Dermietzel, R. & Krause, D. (1991) Molecular anatomy of the blood-brain barrier as defined by immunocytochemistry. *Int Rev Cytol*, **127:** 57-109.

Dinarello, C.A. (1984) Interleukin-1. *Rev Inf Dis*, **6:** 51-95.

Dinarello, C.A. (1987) The biology of interleukin 1 and comparison to tumor necrosis factor. *Immunol Lett*, **16:** 227-232.

Dinarello, C.A., Ikejima, T., Warner, S.J.C., Orencole, S.F., Lonnemann, G., Cannon, J.G. & Libby, P. (1987) Interleukin 1 induces interleukin 1. I. Induction of circulating interleukin 1 in rabbits in vivo and in human mononuclear cells in vitro. *J Immunol*, **139:** 1902-1910.

Dinarello, C.A. (1989) Interleukin-1 and its biologically related cytokines. *Adv Immunol*, **44:** 153-205.

Dorovini-Zis, K., Bowman, P.D. & Prameya, R. (1992) Adhesion and migration of human polymorphonuclear leucocytes across cultured bovine brain microvessel endothelial cells. *J Neuropathol Exp Neurol*, **51:** 194-205.

Doukas, J., Hechtman, H.B. & Shepro, D. (1989) Vasoactive amines and eicosanoids interactively regulate both polymorphonuclear leukocyte diapedesis and albumin permeability in vitro. *Microvasc Res*, **37:** 125-137.

Dua, H.S., Lee, R.H., Lolley, R.N., Barrett, J.A., Abrams, M., Forrester, J.V. & Donoso, L.A. (1992) Induction of experimental autoimmune uveitis by the retinal photoreceptor cell protein, phosducin. *Curr Eye Res*, **11:** 107-111.

Dux, E. & Joó, F. (1982) Effects of histamine on brain capilaries. Fine structural and immunohistochemical studies after intracarotid infusion. *Exp Brain Res*, **47:** 252-258.

Dux, E., Joó, F., Gecse, A., Mezei, Z., Dux, L., Hideg, J. & Telegdy, G. (1982) Histamine-stimulated prostaglandin synthesis in rat brain microvessels. *Agents Actions*, **12:** 146-148.

Dux, E., Temesvári, P., Joó, F., Ádám, G., Clementi, F., Dux, L., Hideg, J. & Hossman, K.A. (1984) The blood-brain barrier in hypoxia: ultrastructural aspects and adenylate cyclase activity of brain capillaries. *Neuroscience*, **12:** 951-958.

Egleton, R.D., Butt, A.M., Amor, S. & Segal, M.B. (1996) Blood-brain barrier permeability changes during Semliki Forest Virus induced encephalomyelitis in the Balb/c mouse: a role for histamine? In: P.O. Couraud & D. Scherman (Eds.) *Biology and physiology of the blood-brain barrier: transport, cellular interactions, and brain pathologies.* Plenum Press, New York. (In Press)

Elner, S.G., Strieter, R.M., Elner, V.M., Rollins, B.J., Del Monte, M.A. & Kunkel, S.L. (1991) Monocyte chemotactic protein gene expression by cytokine-treated human retinal pigment epithelial cells. *Lab Invest*, **64**: 819-825.

Elner, V.M., Scales, W., Elner, S.G., Danforth, J., Kunkel, S.L. & Strieter, R.M. (1992) Interleukin-6 (IL-6) gene expression and secretion by cytokine-stimulated human retinal pigment epithelial cells. *Exp Eye Res*, **54**: 361-368.

Endo, Y. (1989) Induction of histidine and ornithine decarboxylase activities in mouse tissues by recombinant interleukin-1 and tumor necrosis factor. *Biochem Pharmacol*, **38**: 1287-1292.

Enea, N.A., Hollis, T.M., Kern, J.A. & Gardner, T.W. (1989) Histamine H1 receptors mediate increased blood-retinal barrier permeability in experimental diabetes. *Arch Ophthalmol*, **107**: 270-274.

Ennis, S.R. & Betz, A.L. (1986) Sucrose permeability of the blood-retinal and blood-brain barriers. *Invest Ophthalmol Vis Sci*, **27**: 1095-1102.

Essner, E., Pino, R.M. & Griewski, R.A. (1979) Permeability of retinal capillaries in rats with inherited retinal degeneration. *Invest Ophthalmol Vis Sci*, **18**: 859-863.

Essner, E., Pino, R.M. & Griewski, R.A. (1980) Breakdown of blood retinal barrier in RCS rats with inherited retinal degeneration. *Lab Invest*, **43**: 418-426.

Farquhar, M.G. & Palade, G.E. (1963) Junctional complexes in various epithelia. *J Cell Biol*, **17**: 375-412.

Faustmann, P.M. & Dermietzel, R. (1985) Extravasation of polymorphonuclear leukocytes from the cerebral microvasculature. Inflammatory response induced by alpha-bungarotoxin. *Cell Tissue Res*, **242**: 399-407.

Ferreira, S.H. & Vane, J.R. (1967) Prostaglandins: their disappearance from and release into the circulation. *Nature*, **216**: 868-873.

Ferrick, M.R., Thurau, S.R., Oppenheim, M.H., Herbort, C.P., Ni, M., Zachariae, C.O., Matsushima, K. & Chan, C. (1991) Ocular inflammation stimulated by intravitreal interleukin-8 and interleukin-1. *Invest Ophthalmol Vis Sci*, **32**: 1534-1539.

Fleisher, L.N., Ferrell, J.B. & McGahan, M.C. (1990) Ocular inflammatory effects of intravitreally injected tumour necrosis factor-alpha and endotoxin. *Inflammation*, **14**: 325-335.

Fleisher, L.N., Ferrell, J.B., Smith, M.G. & McGahan, M.C. (1991) Lipid mediators of tumour necrosis factor-α-induced uveitis. *Invest Ophthalmol Vis Sci*, **32**: 2393-2399.

Fleisher, L.N., Ferrell, J.B. & McGahan, M.C. (1992) Synergistic uveitic effects of tumour necrosis factor-α and interleukin-1β. *Invest Ophthalmol Vis Sci*, **33**: 2120-2127.

Foos, R.Y. (1972) Vitreoretinal juncture; topographical variations. *Invest Ophthalmol*, 11: 801-808.

Forrester, J.V., Liversidge, J., Dua, H.S., Towler, H. & McMenamin, P.G. (1990) Comparison of clinical and experimental uveitis. *Curr Eye Res*, 9: 75-84.

Forrester, J.V., McMenamin, P.G., Holthouse, I., Lumsden, L. & Liversidge, J. (1994) Localization and characterization of major histocompatibility complex class II-positive cells in the posterior segment of the eye: Implications for induction of autoimmune uveoretinitis. *Invest Ophthalmol Vis Sci*, 35: 64-77.

Forrester, J.V., Worgul, B.V. & Merriam, G.R. (1980) Endotoxin-induced uveitis in the rat. *Albrecht von Graefes Arch Clin Ophthalmol*, 213: 221-233.

Foulds, W.S. (1987) Is your vitreous really necessary? The role of the vitreous in the eye with particular reference to retinal attachment, detachment and the mode of action of vitreous substitutes. *Eye*, 1: 641-664.

Franks, W.A., Limb, G.A., Stanford, M.R., Ogilvie, J., Wolstencroft, R.A., Chignell, A.H. & Dumonde, D.C. (1992) Cytokines in human intraocular inflammation. *Curr Eye Res*, 11: 187-191.

Frater-Schroder, M., Risau, W., Hallman, R., Gautschi, P. & Bohlen, P. (1987) Tumor necrosis factor type α, a potent inhibitor of endothelial cell growth in vitro, is angiogenic in vivo. *Proc Natl Acad Sci USA*, 84: 5277-5281.

Furie, M.B. & McHugh, D.D. (1989) Migration of neutrophils across endothelial monolayers is stimulated by treatment of the monolayers with interleukin-1 or tumour necrosis factor-α. *J Immunol*, 143: 3309-3317.

Furuse, M., Hirase, T., Itoh, M., Nagafuchi, A., Yonemura, S. & Tsukita, S. (1993) Occludin - a novel intergral membrane-protein localizing at tight junctions. *J Cell Biol*, 123: 1777-1788.

Gardner, T.W., Eller, A.W., Friberg, T.R., D'Antonio, J.A. & Hollis, T.M. (1995) Antihistamines reduce blood-retinal barrier permeability in type I (insulin-dependent) diabetic patients with nonproliferative retinopathy. A pilot study. *Retina*, 15: 134-140.

Giacomelli, F., Juechter, K.B. & Wiener, J. (1972) The cellular pathology of experimental hypertension. VI. Alterations in retinal vasculature. *Am J Path*, 68: 81-96.

Gijbels, K., Galardy, R.E. & Steinman, L. (1994) Reversal of experimental autoimmune encephalomyelitis with a hydroxamate inhibitor of matrix metalloproteinases. *J Clin Invest*, 94: 2177-2182.

Giulian, D., Woodward, J., Young, D.G., Krebs, J.F. & Lachman, L.B. (1988) Interleukin-1 injected into mammalian brain stimulates astrogliosis and neovascularization. *J Neurosci*, 8: 2485-2490.

Gordon, C.R., Merchant, R.S., Marmarou, A., Rice, C.D., Marsh, J.T. & Young, H.F. (1990) Effect of murine recombinant interleukin-1 on brain oedema in the rat. *Acta Neurochir (Wien)*, **51**: 268-270.

Gordon, S., Newman, W. & Bloom, B. (1978) Macrophage proteases and rheumatic diseases: regulation of plasminogen activator by thymus-derived lymphocytes. *Agents Actions*, **8**: 19-26.

Graeber, M.B., Streit, W.J. & Kreutzberg, G.W. (1989) Identity of ED2-positive perivascular cells in rat brain. *J Neurosci Res*, **22**: 103-106.

Granstrom, E., Diczfalusy, U. & Hamberg, M. (1983) The thromboxanes. In: C. Pace-Asciak & E. Granstrom (Eds.) *Prostaglandins and related substances*. Elsevier, Amsterdam. Pp. 45-94.

Gratton, J., Greenwood, J., Luthert, P. & Lightman, S. (1992) A quantitative comparison of blood-retinal and blood-brain barrier capillary distribution and density in the rat using image analysis. *J Physiol*, **446**: 508P (Abstract).

Greenwood, J., Luthert, P.J., Pratt, O.E. & Lantos, P.L. (1988) Hyperosmolar opening of the blood-brain barrier in the energy-depleted rat brain. I. Permeability studies. *J Cereb Blood Flow Metab*, **8**: 9-15.

Greenwood, J. (1992a) Characterization of a rat retinal endothelial cell culture and the expression of P-glycoprotein in brain and retinal endothelium in vitro. *J Neuroimmunol*, **39**: 123-132.

Greenwood, J. (1992b) Experimental manipulation of the blood-brain and blood-retinal barriers. In: M.W.B. Bradbury (Ed.) *Physiology and pharmacology of the blood-brain barrier*. Springer-Verlag, Berlin. Pp. 460-486.

Greenwood, J. (1992c) The blood-retinal barrier in experimental autoimmune uveoretinitis (EAU): a review. *Curr Eye Res*, **11 (Suppl)**: 25-32.

Greenwood, J., Howes, R. & Lightman, S. (1994) The blood-retinal barrier in experimental autoimmune uveoretinitis: leukocyte interactions and functional damage. *Lab Invest*, **70**: 39-52.

Greenwood, J. Wang, Y. & Calder, V.L. (1995) Lymphocyte adhesion and transendothelial migration in the CNS: the role of LFA-1, ICAM-1, VLA-4 and VCAM-1. *Immunology*, **86**: 408-415.

Grobelny, D., Poncz, L. & Galardy, R.E. (1992) Inhibition of human skin fibroblast collagenase, thermolysin, and *Pseudomonas aeruginosa* elastase by peptide hydroxamic acids. *Biochemistry*, **31**: 7152-7154.

Gross, P.M., Teasdale, G.M., Angerson, W.J. & Harper, A.M. (1981) H_2-receptors mediate increase in permeability of the blood-brain barrier during arterial histamine infusion. *Brain Res*, **210:** 396-400.

Gross, P.M., Teasdale, G.M., Graham, D.I., Angerson, W.J. & Harper, A.M. (1982) Intra-arterial histamine increases blood-brain transport in rats. *Am J Physiol*, **12:** H307-H317.

Gumbiner, B. & Simons, K. (1986) A functional assay for proteins involved in establishing an epithelial occluding barrier: identification of a uvoromulin-like peptide. *J Cell Biol*, **102:** 457-468.

Gumbiner, B., Lowenkopf, T. & Apatira, D. (1991) Identification of a 160-kDa polypeptide that binds to the tight junction protein ZO-1. *Proc Natl Acad Sci USA*, **88:** 3460-3464.

Guy, J., Ellis, A., Hope, G.M. & Rao, N.A. (1989) Antioxidant enzymes reduce loss of blood-brain barrier integrity in experimental optic neuritis. *Arch Ophthalmol*, **107:** 1359-1368.

Haak-Frendscho, M., Dinarello, C. & Kaplan, A.P. (1988) Recombinant human interleukin-1β causes histamine release from human basophils. *J Allergy Clin Immunol*, **82:** 218-223.

Hanisch, U.K., Seto, D. & Quirion, R. (1993) Modulation of hippocampal acetylcholine release: a potent central action of interleukin-2. *J Neurosci*, **13:** 3368-3374.

Harper, F.H., Liversidge, J., Thomson, A.W. & Forrester, J.V. (1992) Interphotoreceptor retinoid binding protein induced experimental autoimmune uveitis: an immunophenotypic analysis using alkaline phosphatase anti-alkaline phosphatase staining, dual immunofluorescence and confocal microscopy. *Curr Eye Res*, **11:** 129-134.

Head, J.R. & Griffin, W.S.T. (1985) Functional capacity of solid tissue transplants in the brain: Evidence for immunological privilege. *Proc Roy Soc B*, **224:** 375-387.

Henkind, P., Bellhorn, R.W. & Schall, B. (1980) Retinal edema: postulated mechanism(s). In: J.G. Cunha-Vaz (Ed.) *The blood-retinal barriers*. Plenum Press, New York. Pp. 251-268.

Herbort, C.P., Okumura, A. & Mochizuki, M. (1988) Endotoxin-induced uveitis in the rat. *Albrecht von Graefes Arch Clin Ophthalmol*, **226:** 553-558.

Hetier, E., Denefle, A.P., Bousseau, A., Rouget, P., Mallat, M. & Prochiantz, A. (1988) Brain macrophages synthesize interleukin-1 and interleukin-1 mRNAs in vitro. *J Neurosci Res*, **21:** 391-397.

Hewson, A.K., Smith, T., Leonard, J.P. & Cuzner, M.L. (1995) Suppression of experimental allergic encephalomyelitis in the Lewis rat by the matrix metalloproteinase inhibitor Ro31-9790. *Inflamm Res*, **44:** 345-349.

Hickey, W.F. & Kimura, H. (1988) Perivascular microglial cells of the CNS are bone marrow-derived and present antigen in vivo. *Science*, **239:** 290-292.

Hickey, W.F., Hsu, B.L. & Kimura, H. (1991) T-lymphocyte entry into the central nervous system. *J Neurosci Res*, **28:** 254-260.

Higgs, G.A., Moncada, S., Salmon, J.A. & Seager, K. (1983) The source of thromboxane and prostaglandins in experimental inflammation. *Br J Pharmacol*, **79:** 863-868.

Hirano, T., Akira, S., Taga, T. & Kishimoto, T. (1990) Biological and clinical aspects of interleukin 6. *Immunol Today*, **11:** 443-449.

Hjelmeland, L.M., Li, J.W., Toth, C.A. & Landers, M.B. (1992) Antifibrotic and uveitogenic properties of gamma interferon in the rabbit eye. *Graefe's Arch Clin Exp Ophthalmol*, **230:** 84-90.

Hoekzema, R., Murray, P.I. & Kijlstra, A. (1990) Cytokines and intraocular inflammation. *Curr Eye Res*, **9:** 207-211.

Hoekzema, R., Murray, P.I., van Haren, M.A.C., Helle, M. & Kijlstra, A. (1991) Analysis of interleukin-6 in endotoxin-induced uveitis. *Invest Ophthalmol Vis Sci*, **32:** 88-95.

Hoekzema, R., Verhagen, C., van Haren, M. & Kijlstra, A. (1992) Endotoxin-induced uveitis in the rat. The significance of intraocular interleukin-6. *Invest Ophthalmol Vis Sci*, **33:** 532-539.

Holash, J.A. & Stewart, P.A. (1993) The relationship of astrocyte-like cells to the vessels that contribute to the blood-ocular barriers. *Brain Res*, **629:** 218-224.

Hollis, T.M., Gardner, T.W., Vergis, G.J., Kirbo, B.J., Butler, C., Campos, M.J. & Enea, N.A. (1988) Antihistamines reverse blood-ocular barrier breakdown in experimental diabetes. *J Diabetic Comp*, **2:** 47-49.

Hooks, J.J., Chan, C.C. & Detrick, B. (1988) Identification of the lymphokines, interferon-gamma and interleukin-2, in inflammatory eye disease. *Invest Ophthalmol Vis Sci*, **29:** 1444-1451.

Hough, L.B., Khandelwal, J.K., Goldschmidt, R.C., Diomande, M. & Glick, S.D. (1984) Normal levels of histamine and tele-methylhistamine in mast cell-deficient mouse brain. *Brain Res*, **292:** 133-138.

Houssiau, F.A., Devogelaer, J.P., van Damme, J., Nagant de Deuxchaisnes, C. & van Snick, J. (1988) Interleukin-6 in synovial fluid and serum of patients with rheumatoid arthritis and other inflammatory arthritides. *Arthritis Rheum*, **31:** 784-788.

Howes, E.L., Wong, K.L., Hartiala, K.T., Webster, R.O. & Rosenbaum, J.T. (1985) Complement and polymorphonuclear leukocytes do not determine the vascular permeability induced by intraocular LPS. *Am J Path*, **118:** 35-42.

Howes, E.L., Cole, P.W., Adair, T.M., Cruse, V.K. & Pollycove, M. (1994) Cellular and vascular responses in acute experimental ocular inflammation. *Invest Ophthalmol Vis Sci*, **35:** 4031-4038.

Hudspeth, A.J. & Yee, A.G. (1973) The intercellular junctional complexes of retinal pigment epithelia. *Invest Ophthalmol*, **12:** 354-365.

Hunt, R.C., Fox, A., Al Pakalnis, V., Sigel, M.M., Kosnosky, W., Choudhury, P. & Black, E.P. (1993) Cytokines cause cultured retinal pigment epithelial cells to secrete metalloproteinases and to contract collagen gels. *Invest Ophthalmol Vis Sci*, **34:** 3179-3186.

Ishibashi, T., Kimura, H., Shikama, Y., Uchida, T., Kariyone, S., Hirano, T., Kishimoto, T., Takatsuki, F. & Akiyama, Y. (1989) Interleukin-6 is a potent thrombopoietic factor in vivo in mice. *Blood*, **74:** 1241-1244.

Issekutz, T.B. & Stoltz, J.M. (1989) Stimulation of lymphocyte migration by endotoxin, tumour necrosis factor, and interferon. *Cell Immunol*, **120:** 165-173.

Itoh, M., Yonemura, S., Nagafuchi, A. & Tsukita, S. (1991) A 220-kD undercoat-constitutive protein: its specific localization at cadherin-based cell-cell adhesion sites. *J Cell Biol*, **115:** 1449-1462.

Janzer, R.C. & Raff, M.C. (1987) Astrocytes induce blood-brain barrier properties in endothelial cells. *Nature*, **325:** 253-257.

Jenkins, H.G. & Ikeda, H. (1992) Tumour necrosis factor causes an increase in axonal transport of protein and demyelination in the mouse optic nerve. *J Neurol Sci*, **108:** 99-104.

Johnston, M.G., Hay, J.B. & Movat, H.Z. (1976) The modulation of enhanced vascular permeability by prostaglandins through alteration in blood flow (hyperemia). *Agents Actions*, **6:** 705-711.

Jordan, M.L., Hoffman, R.A., Debe, E.F. & Simmons, R.L. (1986) In vitro locomotion of allosensitized T lymphocyte clones in response to metabolites of arachidonic acid is subset specific. *J Immunol*, **137:** 661-668.

Karnovsky, M.J. (1967) The ultrastructural basis of capillary permeability studied with peroxidase as a tracer. *J Cell Biol*, **35:** 213-236.

Kauffman, D.J.H., van Meurs, J.C., Mertens, D.A.E., Peperkamp, E., Master, C. & Gerritsen, M.E. (1994) Cytokines in vitreous humor: interleukin-6 is elevated in proliferative vitreoretinopathy. *Invest Ophthalmol Vis Sci*, **35:** 900-906.

Kempski, O., Villacara, A., Spatz, M., Dodson, R.F., Cora, C., Merkel, N. & Bembry, J. (1987) Cerebromicrovascular endothelial permeability. In-vitro studies. *Acta Neuropathol*, **74:** 329-334.

Khanna, N., Mathur, A. & Chaturvedi, U.C. (1994) Regulation of vascular permeability by macrophage-derived chemotactic factor produced in Japanese encephalitis. *Immunol Cell Biol*, **72:** 200-204.

Kida, S., Pantazis, A. & Weller, R.O. (1993) CSF drains directly from the subarachnoid space into nasal lymphatics in the rat. Anatomy, histology and immunological significance. *Neuropath Appl Neurobiol*, **19:** 480-488.

Killackey, J.J.F., Johnston, M.G. & Movat, H.Z. (1986) Increased permeability of microcarrier-cultured endothelial monolayers in response to histamine and thrombin. *Am J Path*, **122:** 50-61.

Kilzer, P., Chang, K., Marvel, J., Kilo, C. & Williamson, J.R. (1985) Tissue differences in vascular permeability changes induced by histamine. *Microvasc Res*, **30:** 270-285.

Kim, K.S., Wass, C.A., Cross, A.S. & Opal, S.M. (1992) Modulation of blood-brain brrier permeability by tumor necrosis factor and antibody to tumor necrosis factor in the rat. *Lymphokine Cytokine Res*, **11:** 293-298.

Kim, M.K., Caspi, R.R., Nussenblatt, R.B., Kuwabara, T. & Palestine, A.G. (1988) Intraocular trafficking of lymphocytes in locally induced experimental autoimmune uveoretinitis (EAU). *Cell Immunol*, **112:** 430-436.

Kimura, H., Ishibashi, T., Shikama, Y., Okano, A., Akiyama, Y., Uchida, T. & Maruyama, Y. (1990) Interleukin-1β (IL-1β) induces thrombocytosis in mice: possible implication of IL-6. *Blood*, **76:** 2493-2500.

Konari, K., Sawada, N., Zhong, Y., Isomura, H., Nakagawa, T. & Mori, M. (1995) Development of the blood-retinal barrier in vitro: formation of tight junctions as revealed by occludin and ZO-1 correlates with the barrier function of chick retinal pigment epithelial cells. *Exp Eye Res*, **61:** 99-108.

Kontos, H.A., Wei, E.P., Povlishock, J.T., Dietrich, W.D., Magiera, C.J. & Ellis, E.F. (1980) Cerebral arteriolar damage by arachidonic acid and prostaglandin G_2. *Science*, **209:** 1242-1245.

Kontos, H.A. (1985) Oxygen radicals in cerebral vascular injury. *Circ Res*, **57:** 508-516.

Korthius, R.J., Grisham, M.B. & Granger, D.N. (1988) Leukocyte depletion attenuates vascular injury in postischemic skeletal muscle. *Am J Physiol*, **254:** H823-H827.

Kosnosky, W., Li, T.H., Pakalnis, V.A., Fox, A. & Hunt, R.C. (1994) Interleukin-1-β changes the expression of metalloproteinases in the vitreous humor and induces membrane formation in eyes containing preexisting retinal holes. *Invest Ophthalmol Vis Sci*, **35:** 4260-4267.

Kottow, M.H. & Seligman, L.J. (1978) Consensual reactions to anterior chamber paracentesis in the rabbit. *Am J Ophthalmol*, **85:** 392-399.

Krauss, A.H.P. & Woodward, D.F. (1993) Polymorphonuclear leukocyte infiltration into the subretinal choroid and optic nerve in response to leukotrienes. *Invest Ophthalmol Vis Sci*, **34:** 3679-3686.

Kubes, P. & Kanwar, S. (1994) Histamine induces leukocyte rolling in post-capillary venules. A P-selectin-mediated event. *J Immunol*, **152:** 3570-3577.

Kuijpers, T.W., Hakkert, B.C., Hoogerwerf, M., Leeuwenberg, J.F.M. & Roos, D. (1991) Role of endothelial leukocyte adhesion molecule-1 and platelet-activating factor in neutrophil adherence to IL-1-prestimulated endothelial cells. *J Immunol*, **147:** 1369-1376.

Kulkarni, P.S. & Srinivasan, B.D. (1988) Cachectin: a novel polypeptide induces uveitis in the rabbit eye. *Exp Eye Res*, **46:** 631-633.

Kulkarni, P.S. & Mancino, M. (1993) Studies on intraocular inflammation produced by intravitreal human interleukins in rabbits. *Exp Eye Res*, **56:** 275-279.

Kuruse, I., Anderson, D.C., Miyasaka, M., Tamatani, T., Paulson, J.C., Todd, R.F., Rusche, J.R. & Granger, D.N. (1994a) Molecular determinants of reperfusion-induced leucocyte adhesion and vascular protein leakage. *Circ Res*, **74:** 336-343.

Kuruse, I., Granger, D.N., Evans, D.J., Evans, D.G., Graham, D.Y., Miyasaka, M., Anderson, D.C., Wolf, R.E., Cepinskas, G. & Kvietys, P.R. (1994b) *Helicobacter pylori*-induced microvascular protein leakage in rats: role of neutrophils, mast cells, and platelets. *Gastroenterology*, **107:** 70-79.

Kuwabara, T. & Cogan, D.G. (1960) Studies of retinal vascular patterns. *Arch Ophthalmol*, **64:** 904-911.

Lampert, P. (1967) Electron microscopic studies on ordinary and hyperacute experimental allergic encephalomyelitis. *Acta Neuropathol*, **9:** 99-126.

Laties, A.M. & Rapoport, S. (1976) The blood-ocular barriers under osmotic stress. *Arch Ophthalmol*, **94:** 1086-1091.

Laties, A.M., Rapoport, S.I. & McGlinn, A. (1979) Hypertensive breakdown of cerebral but not retinal blood vessels in rhesus monkey. *Arch Ophthalmol*, **97:** 1511-1514.

Laurent, U.B.G., Laurent, T.C. & Howe, A.F. (1962) Chromatography of soluble proteins from the bovine vitreous body on DEAE-cellulose. *Exp Eye Res*, **1:** 276-285.

Le, J. & Vilcek, J. (1987) Tumour necrosis factor and interleukin 1: Cytokines with multiple overlapping biological activities. *Lab Invest*, **56** (3): 234-248.

Lee, S.L. & Pepose, J.S. (1990) Cellular immune response to Ia induction by intraocular gamma-interferon. *Ophthalmic Res*, **22**: 310-317.

Leeuwenberg, J.F.M., Smeets, E.F., Neefjes, J.J., Shaffer, M.A., Cinek, T., Jeunhomme, T.M.A.A., Ahern, T.J. & Buurman, W.A. (1992) E-selectin and intercellular adhesion molecule-1 are released by activated human endothelial cells in vitro. *Immunology*, **77**: 543-549.

Ley, K. (1994) Histamine can induce leukocyte rolling in rat mesenteric venules. *Am J Physiol*, **267**: H1017-H1023.

Li, Q., Whitcup, S.M., Fujino, Y., Nussenblatt, R.B. & Chan, C. (1993) The role of mast cells in endotoxin-induced uveitis. *Invest Ophthalmol Vis Sci*, **34**: 256-259.

Libby, P., Ordovas, J.M., Auger, K.R., Robbins, A.H., Birinyi, L.K. & Dinarello, C.A. (1986) Endotoxin and tumour necrosis factor induce interleukin-1 gene expression in adult human vascular endothelial cells. *Am J Path*, **124**: 179-185.

Lieberman, A.P., Pitha, P.M., Shin, H.S. & Shin, M.L. (1989) Production of tumor necrosis factor and other cytokines by astrocytes stimulated with lipopolysaccharide or a neurotropic virus. *Proc Natl Acad Sci USA*, **86**: 6348-6352.

Lightman, S., Palestine, A.G., Rapoport, S.I. & Rechthand, E. (1987a) Quantitative assessment of the permeability of the rat blood-retinal barrier to small water-soluble non-electrolytes. *J Physiol*, **389**: 483-490.

Lightman, S., Rechthand, E., Latker, C., Palestine, A. & Rapoport, S. (1987b) Assessment of the permeability of the blood-retinal barrier in hypertensive rats. *Hypertension*, **10**: 390-395.

Lightman, S. & Chan, C. (1990) Immune mechanisms in choroido-retinal inflammation in man. *Eye*, **4**: 345-353.

Lightman, S., Pinter, G., Yuen, L. & Bradbury, M. (1990) Permeability changes at blood-retinal barrier in diabetes and effect of aldose reductase inhibition. *Am J Physiol*, **259**: R601-R605.

Lightman, S. & Greenwood, J. (1992) Effect of lymphocytic infiltration on the blood-retinal barrier in experimental autoimmune uveoretinitis. *Clin Exp Immunol*, **88**: 473-477.

Lightman, S. & Towler, H. (1992) Immunopathology and altered immunity in posterior uveitis in man: a review. *Curr Eye Res*, **11**: 11-15.

Limb, G.A., Little, B.C., Meager, A., Ogilvie, J.A., Wolstencroft, R.A., Franks, W.A., Chignell, A.H. & Dumonde, D.C. (1991) Cytokines in proliferative vitreoretinopathy. *Eye*, **5**: 686-693.

Lin, W. & Essner, E. (1987) Luminal vesicles and endocytosis in the retinal endothelial cells. *Invest Ophthalmol Vis Sci*, **28**: 260 (Abstract).

Lin, W., Essner, E. & Shichi, H. (1991) Breakdown of the blood-retinal barrier in S-antigen-induced uveoretinitis in rats. *Graefe's Arch Clin Exp Ophthalmol*, **229**: 457-463.

Liu, S.H., Prendergast, R.A. & Silverstein, A.M. (1983) The role of lymphokines in immunogenic uveitis. *Invest Ophthalmol Vis Sci*, **24**: 361-367.

Liversidge, J., Sewell, H.F. & Forrester, J.V. (1990) Interactions between lymphocytes and cells of the blood-retina barrier: mechanism of T lymphocyte adhesion to human retinal capillary endothelial cells and retinal pigment epithelial cells *in vitro*. *Immunology*, **70**: 390-396.

Lossinsky, A.S., Badmajew, V., Robson, J.A., Moretz, R.C. & Wisniewski, H.M. (1989) Sites of egress of inflammatory cells and horseradish peroxidase transport across the blood-brain barrier in a murine model of chronic relapsing experimental allergic encephalomyelitis. *Acta Neuropathol*, **78**: 359-371.

Luscinskas, F.W., Cybulsky, M.I., Kiely, J., Peckins, C.S., Davis, V.M. & Gimbrone, M.A. (1991) Cytokine-activated human endothelial monolayers support enhanced neutrophil transmigration via a mechanism involving both endothelial-leukocyte adhesion molecule-1 and intercellular adhesion molecule-1. *J Immunol*, **146**: 1617-1625.

Luthert, P.J., Greenwood, J., Lantos, P.L. & Pratt, O.E. (1986) The effect of dexamethasone on vascular permeability of experimental brain tumours. *Acta Neuropathol*, **69**: 288-294.

Luthert, P. (1992) Opening of the barrier in cerebral pathology. In: M.W.B. Bradbury (Ed.) *Physiology and pharmacology of the blood-brain barrier*. Springer-Verlag, Berlin. Pp. 439-458.

Maddocks, S. & Setchell, B.P. (1990) Recent evidence for immune privilege in the testis. *J Reprod Immunol*, **18**: 9-18.

Male, D.K. & Pryce, G. (1988) Kinetics of MHC gene expression and mRNA synthesis in brain endothelium. *Immunology*, **63**: 37-42.

Male, D., Pryce, G., Hughes, C. & Lantos, P. (1990) Lymphocyte migration into brain modelled in vitro: Control by lymphocyte activation, cytokines, and antigen. *Cell Immunol*, **127**: 1-11.

Malecaze, F., Chollet, P., Cavrois, E., Vita, N., Arne, J.L. & Ferrara, P. (1991) Role of interleukin 6 in the inflammatory response after cataract surgery. An experimental and clinical study. *Arch Ophthalmol*, **109**: 1681-1683.

Marak, G.E., Font, R.L. & Alepa, F.P. (1977) Arthus-type panophthalmitis in rats sensitized to heterologous lens protein. *Ophthalmic Res*, **9**: 162-170.

Marak, G.E. (1981) Abrogation of tolerance to lens protein. In: M.L. Sears (Ed.) *New directions in ophthalmic research*. Yale University Press, New Haven. Pp. 47-61.

Marchesi, V.T. & Gowans, J.L. (1964) The migration of lymphocytes through the endothelium of venules in lymph nodes: an electron microscope study. *Proc Roy Soc B*, **159**: 283-290.

Marinkovic, S., Jahreis, G.P., Wong, G.G. & Baumann, H. (1989) IL-6 modulates the synthesis of a specific set of acute phase plasma proteins in vivo. *J Immunol*, **142**: 808-812.

Martin, D. & Near, S.L. (1995) Protective effect of the interleukin-1 receptor antagonist (IL-1ra) on experimental allergic encephalomyelitis in rats. *J Neuroimmunol*, **61**: 241-245.

Martin, S., Maruta, K., Burkat, V., Gillis, S. & Kolb, H. (1988) IL-1 and IFN-γ increase vascular permeability. *Immunology*, **64**: 301-305.

Martiney, J.A., Litwak, M., Berman, J.W., Arezzo, J.C. & Brosnan, C.F. (1990) Pathophysiologic effect of interleukin-1β in the rabbit retina. *Am J Path*, **137**: 1411-1423.

Martiney, J.A., Berman, J.W. & Brosnan, C.F. (1992) Chronic inflammatory effects of interleukin-1 on the blood-retina barrier. *J Neuroimmunol*, **41**: 167-176.

Martins, A.N., Doyle, T.F., Wright, S.J. & Bass, B.G. (1980) Response of cerebral circulation to topical histamine. *Stroke*, **11**: 469-476.

Maruo, N., Morita, I., Shirao, M. & Murota, S. (1992) Il-6 increases endothelial permeability in vitro. *Endocrinology*, **131**: 710-714.

Mayhan, W.G., Sahagun, G., Spector, R. & Heistad, D.D. (1986) Effects of leukotriene C_4 on the cerebral microvasculature. *Am J Physiol*, **251**: H471-H474.

Mayhan, W.G., Faraci, F.M., Siems, J.L. & Heistad, D.D. (1989) Role of molecular charge in disruption of the blood-brain barrier during acute hypertension. *Circ Res*, **64**: 658-664.

McMenamin, P.G., Forrester, J.V., Steptoe, R.J. & Dua, H.S. (1992) Ultrastructural pathology of experimental autoimmune uveitis. Quantitative evidence of activation and possible high endothelial venule-like changes in retinal vascular endothelium. *Lab Invest*, **67**: 42-55.

McMenamin, P.G. & Crewe, J. (1995) Endotoxin-induced uveitis. Kinetics and phenotype of the inflammatory cell infiltrate and the response of resident tissue macrophages and dendritic cells in the iris and ciliary body. *Invest Ophthalmol Vis Sci*, **36:** 1949-1959.

Megyeri, P., Ábrahám, C.S., Temesvári, P., Kovács, J., Vas, T. & Speer, C.P. (1992) Recombinant human tumour necrosis factor-α constricts pial arteries and increases blood-brain barrier permeability in newborn piglets. *Neurosci Lett*, **148:** 137-140.

Ming, W.J., Bersani, L. & Mantovani, A. (1987) Tumor necrosis factor is chemotactic for monocytes and polymorphonuclear leukocytes. *J Immunol*, **138:** 1469-1474.

Mirro, R., Busija, D.W., Armstead, W.M. & Leffler, C.W. (1988) Histamine dilates pial arterioles of newborn pigs through prostanoid production. *Am J Physiol*, **254:** H1023-H1026.

Mochizuki, M., Kuwabara, T., Chan, C., Nussenblatt, R.B., Metcalfe, D.D. & Gery, I. (1984) An association between susceptibility to experimental autoimmune uveitis and choroidal mast cell numbers. *J Immunol*, **133:** 1699-1701.

Mochizuki, M., Kuwabara, T., McAllister, C., Nussenblatt, R.B. & Gery, I. (1985) Adoptive transfer of experimental autoimmune uveoretinitis in rats. *Invest Ophthalmol Vis Sci*, **26:** 1-9.

Mondino, B.J., Sidikaro, Y., Mayer, F.J. & Sumner, H.L. (1990) Inflammatory mediators in the vitreous humor of AIDS patients with retinitis. *Invest Ophthalmol Vis Sci*, **31:** 798-804.

Moore, S.A., Figard, P.H., Spector, A.A. & Hart, M.N. (1989) Brain microvessels produce 12-hydroxyeicosatetraenoic acid. *J Neurochem*, **53:** 376-382.

Moseley, H., Foulds, W.S., Allan, D. & Kyle, P.M. (1984) Routes of clearance of radioactive water from the rabbit vitreous. *Br J Ophthalmol*, **68:** 145-151.

Moser, R., Schleiffenbaum, B., Groscurth, P. & Fehr, J. (1989) Interleukin 1 and tumour necrosis factor stimulate human vascular endothelial cells to promote transendothelial neutrophil passage. *J Clin Invest*, **83:** 444-455.

Muller, W.A., Weigl, S.A., Deng, X. & Phillips, D.M. (1993) PECAM-1 is required for transendothelial migration of leukocytes. *J Exp Med*, **178:** 449-460.

Murray, P.I., Hoekzema, R., van Haren, M.A.C., de Hon, F.D. & Kijlstra, A. (1990) Aqueous humor interleukin-6 levels in uveitis. *Invest Ophthalmol Vis Sci*, **31:** 917-920.

Nagy, Z., Pappius, H.M., Mathieson, G. & Huttner, I. (1979) Opening of tight junctions in cerebral endothelium. I. Effect of hyperosmolar mannitol infused through the internal carotid artery. *J Comp Neurol*, **185:** 569-578.

Naveh, N., Belkin, M., Ben-Chaim, O., Weissman, C. & Treister, G. (1990) Prostanoids in the vitreous of diabetic and nondiabetic human eyes with retinal detachment. *Ophthalmic Res*, 22: 3-11.

Naveh, N. & Weissman, C. (1990) The correlation between excessive vitreal protein levels, prostaglandin E₂ levels, and the blood-retinal barrier. *Prostaglandins*, 39: 147-156.

Nawroth, P.P., Bank, I., Handley, D., Cassimeris, J., Chess, L. & Stern, D. (1986) Tumor necrosis factor/cachectin interacts with endothelial cell receptors to induce release of interleukin 1. *J Exp Med*, 163: 1363-1375.

Niimi, M., Mochizuki, T., Yamamoto, Y. & Yamatodani, A. (1994) Interleukin-1β induces histamine release in the rat hypothalamus in vivo. *Neurosci Lett*, 181: 87-90.

Nowak, J.Z., Nawrock, J. & Maslinski, C. (1984) Distribution and localization of histamine in bovine and rabbit eye. *Agents Actions*, 14: 335-340.

Nowak, J.Z. (1990) Histamine in the retina: recent progress and perspectives. *Agents Actions*, 30: 202-205.

Ogata, Y., Pratta, M.A., Nagase, H. & Arner, E.C. (1992) Matrix metalloproteinase 9 (92 kDa gelatinase/type IV collagenase) is induced in rabbit articular chondrocytes by cotreatment with interleukin 1β and a protein kinase C activator. *Exp Cell Res*, 201: 245-249.

Okamoto, H. & Nakano, K. (1990) Regulation of interleukin-1 synthesis by histamine produced by mouse peritoneal macrophages *per se*. *Immunology*, 69: 162-165.

Okumura, A., Mochizuki, M., Nishi, M. & Herbort, C.P. (1990) Endotoxin-induced uveitis (EIU) in the rat: A study of inflammatory and immunological mechanisms. *Int Ophthalmol*, 14: 31-36.

Olesen, S.P. (1985) A calcium-dependent reversible permeability increase in microvessels in frog brain, induced by serotonin. *J Physiol*, 361: 103-113.

Oleson, S.P. & Crone, C. (1986) Substances that rapidly augment ionic conductance of endothelium in cerebral venules. *Acta Physiol Scand*, 127: 233-241.

Olesen, S.P. (1987a) Free oxygen radicals decrease electrical resistance of microvascular endothelium in brain. *Acta Physiol Scand*, 129: 181-187.

Olesen, S.P. (1987b) Leakiness of rat brain microvessels to fluorescent probes following craniotomy. *Acta Physiol Scand*, 130: 63-68.

Opdenakker, G., Masure, S., Grillet, B. & van Damme, J. (1991) Cytokine-mediated regulation of human leukocyte gelatinases and role in arthritis. *Lymphokine Cytokine Res*, 10: 317-324.

Osborn, L., Hession, C., Tizard, R., Vassallo, C., Luhowskyj, S., Chi-Rosso, G. & Lobb, R. (1989) Direct expression cloning of vascular cell adhesion molecule 1, a cytokine-induced endothelial protein that binds to lymphocytes. *Cell*, **59**: 1203-1211.

Palm, E. (1947) On the occurrence in the retina of conditions corresponding to the blood-brain barrier. *Acta Ophthalmologica*, **25**: 29-35.

Parker, C.W. & Stenson, W.F. (1989) Prostaglandins and leukotrienes. *Curr Opin Immunol*, **2**: 28-32.

Paulissen, M., Copius Peereboom-Stegeman, J.H.J. & van de Kerkhof, P.C.M. (1990) An ultrastructural study of transcutaneous migration of polymorphonuclear leucocytes following application of leukotriene B_4. *Skin Pharmacol*, **3**: 236-247.

Pederson, O.O. (1979) An electron microscopic study of the permeability of intraocular blood vessels using lanthanum as a tracer in vivo. *Exp Eye Res*, **29**: 61-69.

Perkins, E.S. (1957) Influence of the fifth cranial nerve on the intra-ocular pressure of the rabbit eye. *Br J Ophthalmol*, **41**: 257-300.

Perry, V.H. & Gordon, S. (1988) Macrophages and microglia in the nervous system. *Trends in Neurosci*, **11**: 273-277.

Peyman, G.A., Spitznas, M. & Straatsma, B.R. (1971) Peroxidase diffusion in the normal and photocoagulated retina. *Invest Ophthalmol*, **10**: 181-189.

Peyman, G.A. & Apple, D. (1972) Peroxidase diffusion processes in the optic nerve. *Arch Ophthalmol*, **88**: 650-654.

Piper, P., Vane, J.R. & Wyllie, J.H. (1970) Inactivation of prostaglandins by the lungs. *Nature*, **225**: 600-604.

Planck, S.R., Huang, X., Robertson, J.E. & Rosenbaum, J.T. (1994) Cytokine mRNA levels in rat ocular tissues after systemic endotoxin treatment. *Invest Ophthalmol Vis Sci*, **35**: 924-930.

Pober, J.S., Gimbrone, M.A., Lapierre, L.A., Mendrick, D.L., Fiers, W., Rothlein, R. & Springer, T.A. (1986) Overlapping patterns of activation of human endothelial cells by interleukin 1, tumor necrosis factor, and immune interferon. *J Immunol*, **137**: 1893-1896.

Pober, J.S. & Cotran, R.S. (1990) Cytokines and endothelial cell biology. *Physiol Rev*, **70**: 427-451.

Pratt, O.E. (1992) The movement of vitamins into the brain. In: M.W.B. Bradbury (Ed.) *Physiology and pharmacology of the blood-brain barrier.* Springer-Verlag, Berlin. Pp. 205-220

Pulvertaft, R.J.V. (1959) Cellular associations in normal and abnormal lymphocytes. *Proc Roy Soc Med*, **52:** 315-322.

Puustinen, T. & Uotila, P. (1984) Thromboxane formation in human polymorphonuclear leukocytes is inhibited by prednisolone and stimulated by leukotrienes B_4, C_4, D_4 and histamine. *Prostaglandins Leukotrienes Med*, **14:** 161-167.

Quagliarello, V.J., Wispelwey, B., Long, W.J. & Scheld, W.M. (1991) Recombinant human interleukin-1 induces meningitis and blood-brain barrier injury in the rat. *J Clin Invest*, **87:** 1360-1366.

Rahi, A.H.S., Misra, R.N. & Morgan, G. (1977) Immunopathology of the lens. III. Humoral and cellular immune responses to autologous lens antigens and their roles in ocular inflammation. *Br J Ophthalmol*, **61:** 371-379.

Raine, C.S. (1984) Analysis of autoimmune demyelination: Its impact upon multiple sclerosis. *Lab Invest*, **50:** 608-635.

Raine, C.S., Cannella, B., Duijvestijn, A.M. & Cross, A.H. (1990) Homing to central nervous system vasculature by antigen-specific lymphocytes. II. Lymphocyte/endothelial cell adhesion during the initial stages of autoimmune demyelination. *Lab Invest*, **63:** 476-489.

Ramilo, O., Saez-Llorens, X., Mertsola, J., Jafari, H., Olsen, K.D., Hansen, E.J., Yoshinaga, M., Ohkawara, S., Nariuchi, H. & McCracken, G.H. (1990) Tumor necrosis factor α/cachectin and interleukin 1β initiate meningeal inflammation. *J Exp Med*, **172:** 497-507.

Rapoport, S.I. (1977) Osmotic opening of blood-brain and blood-ocular barriers. *Exp Eye Res*, **25:** 499-509.

Rapoport, S.I., Fredericks, W.R. & Laties, A.M. (1980) Reversible opening of the retinal pigment epithelium by hypercapnia. *Exp Eye Res*, **30:** 129-141.

Raviola, G. (1974) Effects of paracentesis on the blood-aqueous barrier: an electron microscope study on *Macaca mulatta* using horseradish peroxidase as a tracer. *Invest Ophthalmol*, **13:** 828-858.

Raviola, G. (1977) The structural basis of the blood-ocular barriers. *Exp Eye Res*, **25:** 27-63.

Raymond, J.J., Robertson, D.M. & Dinsdale, H.B. (1986) Pharmacological modification of bradykinin induced breakdown of the blood-brain barrier. *Can J Neurol Sci*, **13:** 214-220.

Reese, T.S. & Karnovsky, M.J. (1967) Fine structure localization of a blood-brain barrier to exogenous peroxidase. *J Cell Biol*, **34:** 207-217.

Resink, T.J., Grigorian, G.Y., Moldabaeva, A.K., Danilov, S.M. & Buhler, F.R. (1987) Histamine-induced phosphoinositidide metabolism in cultured human umbilical vein endothelial cells. Association with thromboxane and prostacyclin release. *Biochem Biophys Res Commun*, **144**: 438-446.

Revtyak, G.E., Hughes, M.J., Johnson, A.R. & Campbell, W.B. (1988) Histamine stimulation of prostaglandin and HETE synthesis in human endothelial cells. *Am J Physiol*, **255**: C214-C225.

Rice, G.E., Munro, J.M. & Bevilacqua, M.P. (1990) Inducible cell adhesion molecule 110 (INCAM-110) is an endothelial receptor for lymphocytes. *J Exp Med*, **171**: 1369-1374.

Ringler, D.H. & Dabich, L. (1979) Hematology and clinical biochemistry. In: H.J. Baker, J.R. Lindsey, & S.H. Weisbroth (Eds.) *The laboratory rat*. Academic Press, New York. Pp. 105-121.

Risau, W., Engelhardt, B. & Wekerle, H. (1990) Immune function of the blood-brain barrier: incomplete presentation of protein (auto-) antigens by rat brain microvascular endothelium in vitro. *J Cell Biol*, **110**: 1757-1766.

Ristimaki, A., Garfinkel, S., Wessendorf, J., Maciag, T. & Hla, T. (1994) Induction of cyclooxygenase-2 by interleukin-1α. Evidence for post-transcriptional regulation. *J Biol Chem*, **269**: 11769-11775.

Roberge, F.G., Caspi, R.R. & Nussenblatt, R.B. (1988) Glial retinal Müller cells produce IL-1 activity and have a dual effect on autoimmune T helper lymphocytes. *J Immunol*, **140**: 2193-2196.

Romer, L.H., McLean, N.V., Yan, H.C., Daise, M., Sun, J. & DeLisser, H.M. (1995) IFN-γ and TNF-α induce redistribution of PECAM-1 (CD31) on human endothelial cells. *J Immunol*, **154**: 6582-6592.

Rosenbaum, J.T., McDevitt, H.O., Guss, R.B. & Egbert, P.R. (1980) Endotoxin-induced uveitis in rats as a model for human disease. *Nature*, **286**: 611-613.

Rosenbaum, J.T., Samples, J.R., Hefeneider, S.H. & Howes, E.L. (1987) Ocular inflammatory effects of intravitreal interleukin 1. *Arch Ophthalmol*, **105**: 1117-1120.

Rosenbaum, J.T., Howes, E.L., Rubin, R.M. & Samples, J.R. (1988) Ocular inflammatory effects of intravitreally-injected tumour necrosis factor. *Am J Path*, **133**: 47-53.

Rosenberg, G.A., Kornfeld, M., Estrada, E., Kelley, R.O., Liotta, L.A. & Stetler-Stevenson, W.G. (1992) TIMP-2 reduces proteolytic opening of the blood-brain barrier by type IV collagenase. *Brain Res*, **576**: 203-207.

Rossi, V., Breviario, F., Ghezzi, P., Dejana, E. & Mantovani, A. (1985) Prostacyclin synthesis induced in vascular cells by interleukin-1. *Science*, **229**: 174-176.

Rubin, L.L., Hall, D.E., Porter, S., Barbu, K., Cannon, C., Horner, H.C., Janatpour, M., Liaw, C.W., Manning, K., Morales, J., Tanner, L.I., Tomaselli, K.J. & Bard, F. (1991) A cell-culture model of the blood-brain barrier. *J Cell Biol*, **115:** 1725-1735.

Rubin, R.M. & Rosenbaum, J.T. (1988) A platelet-activating factor antagonist inhibits interleukin 1-induced inflammation. *Biochem Biophys Res Commun*, **154:** 429-436.

Sanchez-Madrid, F., Nagy, J.A., Robbins, E., Simon, P., Thompson, S. & Springer, T.A. (1986) A human leukocyte differentiation antigen family with distinct alpha-subunits and a common beta-subunit: The lymphocyte function-associated antigen (LFA-1), the C3bi complement receptor (OKM1/Mac-1), and the p150,95 molecule. *J Exp Med*, **158:** 1785-1803.

Saria, A., Lundberg, J.M., Skofitsch, G. & Lembeck, F. (1983) Vascular protein leakage in various tissues induced by substance P, capsaicin, bradykinin, serotonin, histamine and by antigen challenge. *Naunyn-Schmiedeberg's Arch Pharmacol*, **324:** 212-218.

Saukkonen, K., Sande, S., Cioffe, C., Wolpe, S., Sherry, B., Cerami, A. & Tuomanen, E. (1990) The role of cytokines in the generation of inflammation and tissue damage in experimental gram-positive meningitis. *J Exp Med*, **171:** 439-448.

Sawada, M., Suzumura, A. & Marunouchi, T. (1992) TNFα induces IL-6 production by astrocytes but not by microglia. *Brain Res*, **583:** 296-299.

Schalken, J.J., Winkens, H.J., Van Vugt, A.H.M., Bovee-Guerts, P.H.M., De Grip, W.J. & Broekhuyse, R.M. (1988) Rhodopsin-induced experimental autoimmune uveoretinitis: dose-dependent clinicopathological features. *Exp Eye Res*, **47:** 135-145.

Schilling, L. & Wahl, M. (1994) Opening of the blood-brain barrier during cortical superfusion with histamine. *Brain Res*, **653:** 289-296.

Schinkel, A.H., Smit, J.J.M., van Tellingham, O., Beijen, J.H., Wagenaar, E., van Deemter, L., Mol, C.A.A.M., van der Valk, M.A., Robanus-Maandag, E.C., te Riele, H.P.J., Berns, A.J.M. & Borst, P. (1994) Disruption of the mouse *mdr1a* P-glycoprotein gene leads to a deficiency in the blood-brain barrier and to increased sensitivity to drugs. *Cell*, **77:** 491-502.

Schlicker, E., Malinowska, B., Kathmann, M. & Gothert, M. (1994) Modulation of neurotransmitter release via histamine H_3 heteroreceptors. *Fundamental Clin Pharmacol*, **8:** 128-137.

Schurer, L., Temesvári, P., Wahl, M., Unterberg, A. & Baethmann, A. (1989) Blood-brain barrier permeability and vascular reactivity to bradykinin after pretreatment with dexamethasone. *Acta Neuropathol*, **77:** 576-581.

Sedgwick, J., Brostoff, S. & Mason, D. (1987) Experimental allergic encephalomyelitis in the absence of a classical delayed-type hypersensitivity reaction. *J Exp Med*, **165:** 1058-1075.

Sedgwick, J.D., Schwender, S., Imrich, H., Dorries, R., Butcher, G.W. & Meulen, V. (1991) Isolation and direct characterization of resident microglial cells from the normal and inflamed central nervous system. *Proc Natl Acad Sci USA*, **88:** 7438-7442.

Selak, M.A., Chignard, M. & Smith, J.B. (1988) Cathepsin G is a strong platelet agonist released by neutrophils. *Biochem J*, **251:** 293-299.

Selmaj, K.W., Farooq, M., Norton, W.T., Raine, C.S. & Brosnan, C.F. (1990) Proliferation of astrocytes in vitro in response to cytokines. *J Immunol*, **144:** 129-135.

Sen, H.A. & Campochiaro, P.A. (1991) Stimulation of cyclic adenosine monophosphate accumulation causes breakdown of the blood-retinal barrier. *Invest Ophthalmol Vis Sci*, **32:** 2006-2010.

Shakib, M. & Cunha-Vaz, J.G. (1966) Studies on the permeability of the blood-retinal barrier. IV. Junctional complexes of the retinal vessels and their role in the permeability of the blood-retinal barrier. *Exp Eye Res*, **5:** 229-234.

Sharma, H.S., Olsson, Y. & Dey, P.K. (1990) Changes in blood-brain barrier and cerebral flow following elevation of circulating serotonin levels in anaesthetized rats. *Brain Res*, **517:** 215-223.

Sharma, H.S., Olsson, Y., Nyberg, F. & Dey, P.K. (1993) Prostaglandins modulate alterations of microvascular permeability, blood flow, edema and serotonin levels following spinal cord injury: an experimental study in the rat. *Neuroscience*, **57:** 443-449.

Shiose, Y. (1970) Electron microscopic studies of blood-retinal and blood-aqueous barriers. *Jpn J Ophthalmol*, **14:** 73-87.

Smith, D., Lee, E.K., Saloupis, P., Davis, J.K. & Hatchell, D.L. (1994) Role of neutrophils in breakdown of the blood-retinal barrier following intravitreal injection of platelet-activating factor. *Exp Eye Res*, **59:** 425-432.

Smith, R.A. & Baglioni, C. (1987) The active form of tumor necrosis factor is a trimer. *J Biol Chem*, **262:** 6951-6954.

Smith, R.S. (1971) Ultrastructural studies of the blood-aqueous barrier. I: Transport of an electron-dense tracer in the iris and ciliary body of the mouse. *Am J Ophthalmol*, **71:** 1066-1077.

Smith, R.S. & Rudt, L.A. (1973) Ultrastructural studies of the blood-aqueous barrier. 2. The barrier to horseradish peroxidase in primates. *Am J Ophthalmol*, **76:** 937-947.

Smith, R.S. & Rudt, L.A. (1975) Ocular vascular and epithelial barriers to microperoxidase. *Invest Ophthalmol*, **14:** 556-560.

Snowden, J.M. & Swann, D.A. (1980) Vitreous structure. V. *Invest Ophthalmol Vis Sci*, **19:** 610-618.

Spertini, O., Luscinskas, F.W., Kansas, G.S., Munro, J.M., Griffin, J.D., Gimbrone, M.A. & Tedder, T.F. (1991) Leukocyte adhesion molecule-1 (LAM-1, L-selectin) interacts with an inducible endothelial cell ligand to support leukocyte adhesion. *J Immunol*, **147**: 2565-2573.

Springer, T.A. (1994) Traffic signals for lymphocyte recirculation and leukocyte emigration: the multistep paradigm. *Cell*, **76**: 301-314.

Stevens, M.K. & Yaksh, T.L. (1988) Time course of release in vivo of PGE_2, $PGF_{2\alpha}$, 6-keto-$PGF_{1\alpha}$, TxB_2 into the brain extracellular space after 15 min of complete global ischemia in the presence and absence of cyclooxygenase inhibition. *J Cereb Blood Flow Metab*, **8**: 790-798.

Stevenson, B.R., Siliciano, J.D., Mooseker, M.S. & Goodenough, D.A. (1986) Identification of ZO-1: a high molecular weight polypeptide associated with the tight junction (zonula occludens) in a variety of epithelia. *J Cell Biol*, **103**: 755-766.

Stewart, P.A. & Wiley, M.J. (1981) Developing nervous tissue induces formation of blood-brain barrier characteristics in invading endothelial cells: a study using quail-chick transplantation chimeras. *Dev Biol*, **84**: 183-192.

Stewart, P.A. & Tuor, U.I. (1994) Blood-eye barriers in the rat: correlation of ultrastructure with function. *J Comp Neurol*, **340**: 566-576.

Streilein, J.W., Wilbanks, G.A., Taylor, A. & Cousins, S. (1992) Eye-derived cytokines and the immunosuppressive intraocular microenvironment: a review. *Curr Eye Res*, **11**: 41-47.

Takata, K., Kasahara, T., Kasahara, M., Ezaki, O. & Hirano, H. (1992) Ultracytochemical localization of the erythrocyte/HepG2-type glucose transporter (GLUT 1) in cells of the blood-retinal barrier in the rat. *Invest Ophthalmol Vis Sci*, **33**: 377-383.

Takeichi, M. (1991) Cadherin cell adhesion receptors as morphology regulators. *Science*, **251**: 1451-1455.

Tewari, A., Buhles, W.C. & Starnes, H.F. (1990) Preliminary report: effects of interleukin-1 on platelet counts. *The Lancet*, **336**: 712-714.

Till, G.O., Lee, S., Mulligan, M.S., Wolter, J.R., Smith, C.W., Ward, P.A. & Marak, G.E. (1992) Adhesion molecules in experimental phacoanaphylactic endophthalmitis. *Invest Ophthalmol Vis Sci*, **33**: 3417-3423.

Tompsett, E., Abi-Hanna, D. & Wakefield, D. (1990) Immunological privilege in the eye: a review. *Curr Eye Res*, **9**: 1141-1145.

Tósaki, A., Szerdahelyi, P. & Joó, F. (1994) Treatment with ranitidine of ischemic brain edema. *Eur J Pharmacol*, **264**: 455-458.

Towler, H.M.A., Greenwood, J. & Butt, A.M. (1994) Electrical resistance across the inner blood-retinal barrier in the intact retina of the anaesthetized Lewis rat. *J Physiol*, **480**: 12P (Abstract).

Traugott, U., Scheinberg, L.C. & Raine, C.S. (1985) On the presence of Ia-positive endothelial cells and astrocytes in multiple sclerosis lesions and its relevance to antigen presentation. *J Neuroimmunol*, **8**: 1-14.

Tso, M.O.M. (1980) Pathology of the blood retinal barriers. In: J.G. Cunha-Vaz (Ed.) *The blood-retinal barriers*. Plenum Press, New York. Pp. 235-250.

Uitto, V.J., Schwartz, D. & Veis, A. (1980) Degradation of basement membrane collagen by neutral proteases from human leukocytes. *Eur J Biochem*, **105**: 409-417.

Unterberg, A., Wahl, M. & Baethmann, A. (1984) Effects of bradykinin on permeability and diameter of pial vessels in vivo. *J Cereb Blood Flow Metab*, **4**: 574-585.

Unterberg, A., Wahl, M., Hammersen, F. & Baethmann, A. (1987) Permeability and vasomotor response of cerebral vessels during exposure to arachidonic acid. *Acta Neuropathol*, **73**: 209-219.

Unterberg, A., Wahl, M. & Baethmann, A. (1988) Effects of free radicals on permeability and vasomotor response of cerebral vessels. *Acta Neuropathol*, **76**: 238-244.

Uusitalo, R., Palkama, A. & Stjernschantz, J. (1973) An electron microscopical study of the blood-aqueous barrier in the ciliary body and iris of the rabbit. *Exp Eye Res*, **17**: 49-63.

Van Dam, A., Brouns, M., Man-A-Hing, W. & Berkenbosch, F. (1993) Immunocytochemical detection of prostaglandin E_2 in the microvasculature and in neurons of rat brain after administration of bacterial endotoxin. *Brain Res*, **613**: 331-336.

van Snick, J., Cayphas, S., Szikora, J.P., Renauld, J.C., van Roost, E., Boon, T. & Simpson, R.J. (1988) cDNA cloning of murine interleukin-HP1: homology with human interleukin 6. *Eur J Immunol*, **18**: 193-197.

Vegge, T., Neufield, A.H. & Sears, M.L. (1975) Morphology of the breakdown of the blood-aqueous barrier in the ciliary processes of the rabbit eye after prostaglandin E_2. *Invest Ophthalmol*, **14**: 33-36.

Verhoeff, F.H. & Lemoine, A.N. (1922) Endophthalmitis phacoanaphylactica. *Am J Ophthalmol*, **5**: 737-745.

Vinores, S.A., Sen, H. & Campochiaro, P.A. (1992) An adenosine agonist and prostaglandin E_1 cause breakdown of the blood-retinal barrier by opening tight junctions between vascular endothelial cells. *Invest Ophthalmol Vis Sci*, **33**: 1870-1878.

Vinores, S.A. (1995) Assessment of blood-retinal barrier integrity. *Histol Histopath*, **10:** 141-154.

Vorbrodt, A.W. (1987) Demonstration of anionic sites on the luminal and abluminal fronts of endothelial cells with poly-L-lysine gold complex. *J Histochem Cytochem*, **35:** 1261-1266.

Wacker, W.B. & Lipton, M.M. (1968) Experimental allergic uveitis. I. Production in the guinea pig and rabbit by immunisation with retina in adjuvant. *J Immunol*, **101:** 151-156.

Wadhwani, K.C. & Rapoport, S.I. (1994) Transport properties of vertebrate blood-nerve barrier: comparison with the blood-brain barrier. *Prog Neurobiol*, **43:** 235-279.

Wahl, M., Unterberg, A., Baethmann, A. & Schilling, L. (1988) Mediators of blood-brain barrier dysfunction and formation of vasogenic brain edema. *J Cereb Blood Flow Metab*, **8:** 621-634.

Wahl, M., Schilling, L., Unterberg, A. & Baethmann, A. (1995) Autacoids as mediators of vasogenic brain oedema. In: J. Greenwood, D. Begley, & M. Segal (Eds.) *New concepts of a blood-brain barrier*. Plenum Press, New York. Pp. 147-157.

Wakai, S. & Hirokawa, N. (1978) Development of the blood-brain barrier to horseradish peroxidase in the chick embryo. *Cell Tissue Res*, **195:** 195-203.

Wakefield, D., McCluskey, P., Roche, N. & Rossio, J.L. (1995) Aqueous humor cytokine profile in patients with chronic uveitis. *Ocular Immunol Inflamm*, **3:** 203-208.

Wang, Y.F., Calder, V.L., Greenwood, J. & Lightman, S.L. (1993) Lymphocyte adhesion to cultured endothelial cells of the blood-retinal barrier. *J Neuroimmunol*, **48:** 161-168.

Wang, Y., Calder, V.L., Lightman, S.L. & Greenwood, J. (1995) Antigen presentation by rat brain and retinal endothelial cells. *J Neuroimmunol*, **61:** 231-239.

Wankowicz, Z., Megyeri, P. & Issekutz, A. (1988) Synergy between tumour necrosis factorα and interleukin-1 in the induction of polymorphonuclear leucocyte migration during inflammation. *J Leuk Biol*, **43:** 349-356.

Warner, S.J.C., Auger, K.R. & Libby, P. (1987) Interleukin 1 induces interleukin 1. II. Recombinant human interleukin 1 induces interleukin 1 production by adult human vascular endothelial cells. *J Immunol*, **139:** 1911-1917.

Watson, M.L., Lewis, G.P. & Westwick, J. (1989) Increased vascular permeability and polymorphonuclear leucocyte accumulation in vivo in response to recombinant cytokines and supernatant from cultures of human synovial cells treated with interleukin 1. *Br J Exp Path*, **70:** 93-101.

Watson, P.M., Anderson, J.M., VanItallie, C.M. & Doctrow, S.R. (1991) The tight-junction-specific protein ZO-1 is a component of the human and rat blood-brain barriers. *Neurosci Lett*, **129:** 6-10.

Watts, R.G., Wright, J.L., Atkinson, L.L. & Merchant, R.E. (1989) Histopathological and blood-brain barrier changes in rats induced by an intracerebral injection of human recombinant interleukin 2. *Neurosurgery*, **25:** 202-208.

Wedmore, C.V. & Williams, T.J. (1981) Control of vascular permeability by polymorphonuclear leukocytes in inflammation. *Nature*, **289:** 646-650.

Wei, E.P., Ellison, M.D., Kontos, H.A. & Povlishock, J.T. (1986) O_2 radicals in arachidonate-induced increased blood-brain barrier permeability to proteins. *Am J Physiol*, **251:** H693-H699.

Wheater, P.R., Burkitt, H.G. & Daniels, V.G. (1987) *Functional histology: a text and colour atlas*. Churchill Livingstone, Edinburgh.

Whitcup, S.M., Chan, C., Li, Q. & Nussemblatt, R.B. (1992) Expression of cell adhesion molecules in posterior uveitis. *Arch Ophthalmol*, **110:** 662-666.

Williams, K.I. & Higgs, G.A. (1988) Eicosanoids and inflammation. *J Pathol*, **156:** 101-110.

Williams, T.J. & Peck, M.J. (1977) Role of prostaglandin-mediated vasodilatation in inflammation. *Nature*, **270:** 530-532.

Wimalaratna, H.S.K. & Capildeo, R. (1989) Management of stroke- the place of steroids. In: R. Capildeo (Ed.) *Steroids in diseases of the central nervous system*. John Wiley & Sons, Chichester. Pp. 275-290.

Wong, D. & Dorovini-Zis, K. (1992) Upregulation of intercellular adhesion molecule-1 (ICAM-1) expression in primary cultures of human brain microvessel endothelial cells by cytokines and lipopolysaccharide. *J Neuroimmunol*, **39:** 11-22.

Wright, J.L. & Merchant, R.E. (1992) Histopathological effects of intracerebral injections of human recombinant tumour necrosis factor-α in the rat. *Acta Neuropathol*, **85:** 93-100.

Yamasaki, Y., Suzuki, T., Yamaya, H., Matsuura, N., Onodera, H. & Kogure, K. (1992) Possible involvement of interleukin-1 in ischaemic brain edema formation. *Neurosci Lett*, **142:** 45-47.

Yamatodani, A., Maeyama, K., Watanabe, T., Wada, H. & Kitamura, Y. (1982) Tissue distribution of histamine in a mutant mouse deficient in mast cells: clear evidence for the presence of non-mast cell histamine. *Biochem Pharmacol*, **31:** 305-309.

Yoshida, M., Yoshimura, N., Hangai, M., Tanihara, H. & Honda, Y. (1994) Interleukin-1α, interleukin-1β, and tumor necrosis factor gene expression in endotoxin-induced uveitis. *Invest Ophthalmol Vis Sci*, **35:** 1107-1113.

Zavoico, G.B., Ewenstein, B.M., Schafer, A.I. & Pober, J.S. (1989) IL-1 and related cytokines enhance thrombin-stimulated PGI_2 production in cultured endothelial cells without affecting thrombin-stimulated von Willebrand factor secretion or platelet-activating factor biosynthesis. *J Immunol*, **142:** 3993-3999.

Zinn, K.M. & Benjamin-Henkind, J.V. (1979) Anatomy of the human retinal pigment epithelium. In: K.M. Zinn & M.F. Marmor (Eds.) *The retinal pigment epithelium*. Harvard University Press, Cambridge, Massachusetts, London. Pp. 3-31.

PUBLICATIONS ARISING FROM THIS WORK

Towler, H.M.A., Bamforth, S.D., Greenwood, J. & Lightman, S. (1993) The effect of intravitreal leukotrienes and prostaglandins on the blood-retinal barrier of the Lewis rat. *Invest Ophthalmol Vis Sci*, **34:** 1426 (Abstract).

Bamforth, S.D., Greenwood, J. & Lightman, S.L. (1994) The effect of interleukin-1β on blood-retinal barrier permeability in the anaesthetized rat. *J Physiol*, **480:** 19 (Abstract).

Bamforth, S.D., Greenwood, J. & Lightman, S. (1994) The effect of TNF-α on blood-retinal barrier permeability. *Immunology*, **83 (Suppl 1):** 54 (Abstract).

Greenwood, J., Bamforth, S.D., Wang, Y. & Devine, L. (1995) The blood-retinal barrier in immune-mediated diseases of the retina. In: J. Greenwood, D. Begley, & M. Segal (Eds.) *New concepts of a blood-brain barrier.* Plenum Press, London. Pp. 315-326.

Greenwood, J., Bamforth, S.D., Joó, F. & Luthert, P.J. (1996) Intraocular glutamic acid injections lead to increased permeability of the blood-retinal barrier. *Invest Ophthalmol Vis Sci*, **37:** S584 (Abstract).

Bamforth, S.D., Lightman, S.L. & Greenwood, J. (1996) The effect of TNF-α and IL-6 on the permeability of the rat blood-retinal barrier in vivo. *Acta Neuropathol*, (In press).

Bamforth, S.D., Towler, H.M.A., Lightman, S.L. & Greenwood, J. (1996) The effect of inflammatory agents upon the blood-retinal barrier. In: P.O. Couraud & D. Scherman (Eds.) *Biology and Physiology of the Blood-Brain Barrier: Transport, Cellular Interactions, and Brain Pathologies.* Plenum Press, New York. (In press).

Bamforth, S.D., Lightman, S.L. & Greenwood, J. (1996) Interleukin-1β induced disruption of the vascular barrier of the central nervous system is mediated through histamine. *J Exp Med*, (Submitted).

Bamforth, S.D., Lightman, S.L. & Greenwood, J. (1996) The effect of intravitreal interleukin-1β on retinal morphology, leucocyte recruitment and blood-retinal barrier permeability in the Lewis rat. An ultrastructural study. (In preparation).

S. D. Bamforth · S. Lightman · J. Greenwood

The effect of TNF-α and IL-6 on the permeability
of the rat blood-retinal barrier in vivo

Abstract The blood-retinal barrier (BRB), which is formed by the retinal vascular endothelium and the retinal pigment epithelium, is responsible for controlling the passage of cells and molecules into the neuroretina. During ocular inflammatory diseases, however, this selective control is altered due to changes in BRB function such as increased permeability and leucocyte recruitment. The causative factors leading to barrier breakdown are not entirely understood although cytokines have recently been implicated. We have investigated the effect of the cytokines tumour necrosis factor-α (TNF-α) and interleukin-6 (IL-6) upon the integrity of the rat BRB. Lewis rats received a dose of each cytokine by intravitreal injection and the permeability of the BRB was assessed using the small molecular weight vascular tracer ^{14}C mannitol. A significant opening of the barrier to mannitol was detected following an intravitreal injection of 2×10^4 U of TNF-α which persisted from day 1 to day 5 post-injection (PI). The permeability of the BRB returned to normal values by day 7 PI. Only occasional mononuclear inflammatory cells were seen in the retina and vitreous of the TNF-α-treated eyes although they remained in evidence up to day 5 PI. In the TNF-α-injected eye there was immunohistological evidence of activation of tissue-resident cells' particularly in the inner plexiform layer. Of particular interest was the observation that the BRB of the non-injected contralateral eye also exhibited increased permeability over a similar time-course but without any evidence of cellular infiltration or activation of tissue-resident cells. Unlike TNF-α, the administration of 1×10^3 U of IL-6 into the vitreous caused no measurable increase in BRB permeability despite inducing a small infiltration of inflammatory cells.

Introduction

The vascular blood-retinal barrier (BRB) of the eye functions in an identical manner to that of the blood-brain barrier, being responsible for controlling the passage of molecules and cells between the blood and the anterior portion of the neuroretina. Transfer of cells and molecules into the posterior aspect of the retina is regulated by the presence of a tight epithelial cell monolayer, the retinal pigment epithelium, that separates the permeable vasculature of the choriocapillaris from the photoreceptors. The maintenance of controlled homeostasis within the CNS environment is especially important as small fluctuations in extracellular fluid composition may, among other deleterious actions, seriously effect the sensitivity of synaptic signalling [1].

During inflammatory disorders of the eye, such as posterior uveitis, the integrity of the BRB may become altered leading to an increase in permeability, vasogenic oedema and loss of vision [26]. The sequence of events that result in this breakdown in barrier integrity have not been fully elucidated but are thought to involve the release of inflammatory products [19]. Amongst the list of candidate molecules, cytokines released from both tissue-resident and infiltrated inflammatory cells have been implicated in this process. The evidence for a role of cytokines on vascular permeability has come from both in vitro [3, 7, 31] and in vivo [2, 10, 30] studies.

The proinflammatory cytokines tumour necrosis factor-α (TNF-α) and interleukin-6 (IL-6) have been reported to be involved in the pathogenesis of various forms of uveitis [12, 18, 23, 37] and their presence in ocular tissue in experimental models of uveitis [13, 38]. In a number of previous studies the effect of these cytokines on the retina, and their action on the blood-ocular barriers (comprising both the BRB and the blood-aqueous barrier) have been investigated. Intravitreal injections of TNF-α [34]

S. D. Bamforth · S. Lightman · J. Greenwood (✉)
Department of Clinical Ophthalmology,
Institute of Ophthalmology, University College London,
Bath Street, London EC1V 9EL, UK
Tel.: 0171 608 6858; Fax: 0171 608 6810;
e-mail: j.greenwood@ucl.ac.uk

and IL-6 [22] have been reported to induce an ocular inflammatory response which is often accompanied by breakdown of the blood-ocular barriers as detected by increased protein concentrations within either the aqueous or vitreous humours [15, 21, 34]. However, it remains unclear which of the blood-ocular barriers is disrupted and the spatial and temporal effects of these cytokines on the retina and BRB have not been resolved.

By using a sensitive in vivo technique to assess BRB permeability we have investigated the temporal changes in barrier integrity following the intravitreal injection of TNF-α and IL-6. Alterations in morphology and the infiltration of leucocytes into the neuroretina were determined by both light and electron microscopy.

Materials and methods

Animals and cytokines

Male Lewis rats (200–300 g, Harlan Olac UK) were anaesthetized with the inhalation anaesthetic methoxyfluorane. Test animals were then injected using a 30-gauge needle into the right vitreous with either 10 μl of murine recombinant TNF-α (4×10^3, 1×10^4 U or 2×10^4 U; Genzyme, Kent, UK) in sterile-filtered saline containing 0.1% bovine serum albumin (BSA, fraction V; Sigma, Dorset, UK) or 10 μl of 2×10^3 U murine recombinant IL-6 (Boehringer Mannheim, East Sussex, UK) in an identical diluent. After the intravitreal injection animals were allowed to recover. Control animals received a 10-μl intravitreal injection of vehicle alone. The left eye served as a contralateral non-injected control in each case.

Histology

Light and electron microscope studies were carried out for ultrastructural assessment of the rat retina. Tissue was fixed by perfusion fixation via the left ventricle into the proximal ascending aorta with 2% gluteraldehyde and 0.5% tannic acid in 0.1 M sodium cacodylate buffer (pH 7.0) at a rate of 25 ml·min⁻¹ for 5 min. The eyes were enucleated and placed in fixative and stored overnight at 4°C. The posterior eye cup was then dissected from the cornea, iris and lens, and processed conventionally into araldite. Semi-thin (0.75 μm) sections were cut using a Reichart-Jung Ultracut E microtome (Leica, Bucks, UK) and stained with toluidine blue. Ultrathin sections were then taken from selected areas, counterstained with uranyl acetate and lead citrate, and viewed under a transmission electron microscope (Jeol 1010).

Ultrastructural analysis was carried out on a series of animals at various time points post-injection (PI). Animals injected intravitreally with 4×10^3 U TNF-α were perfusion fixed at 24 h PI ($n = 4$). Those injected with 1×10^4 U TNF-α perfused at 1, 2, 3, 4, 5 and 7 days PI ($n = 12$) and animals injected with 2×10^4 U TNF-α were investigated at 4 h, 1, 2, 3, 5 and 7 days PI ($n = 17$). Animals injected with 1×10^3 U IL-6 were perfusion fixed at 1, 2, 4 and 8 h and at 1, 2 and 3 days PI ($n = 18$) and following 2×10^3 U IL-6 at 1 day PI ($n = 2$). The vehicle-injected controls were fixed at 4 and 24 h PI ($n = 12$).

Immunohistochemistry

Immunohistochemistry was performed on TNF-α (2×10^4 U) injected eyes. Animals were killed by carbon dioxide asphyxiation at 1, 2 and 3 days PI ($n = 4$) and the eyes enucleated and embedded in OCT (Tissue-Tek, Lamb, London, UK) and snap frozen in liquid nitrogen. Cryostat sections (10 μm) were cut and mounted on 3-aminopropyl-triethoxy-silane-coated slides. The sections were

then stained for the presence of leucocytes, MHC class II and CD18 using a standard avidin-biotin-peroxidase method (Vectastain ABC kit, Vector Laboratories, Peterborough, UK) and developed with the substrate 3-amino-9-ethylcarbazole in dimethyl formamide and hydrogen peroxide in 0.1 M acetate buffer. The sections were counterstained in haematoxylin and the slides mounted in Glycergel mounting medium (Dako, Bucks, UK).

Sections were stained with anti-rat monoclonal antibodies specific for granulocytes (MOM/3F12/F2), macrophages, monocytes and dendritic cells (ED1), macrophages (ED2), CD18 (WT3), the pan-T-cell marker OX-19 (all from Serotec, Oxon, UK), CD4 (W3/25), CD8 (OX-8) and MHC class II (OX-6) (supernatants from cultured hybridoma cell lines generously provided by Dr. M. Puklavec, MRC, Oxford).

Sections of spleen were used for positive controls. Negative controls were sections incubated without the primary antibody.

Detection of BRB disruption

The permeability of the BRB was assessed with the small-molecular-weight tracer ¹⁴C mannitol. Animals were anaesthetized with sodium pentobarbitone (60 mg · kg⁻¹ IP) and the femoral artery and vein exposed. Heparinized polythene cannulae were then inserted into the exposed artery and vein and the arterial cannula connected to a strain gauge transducer (Lectromed, Herts, UK) for the measurement of blood pressure. ¹⁴C mannitol (Amersham International, Bucks, UK; 740 kBq · ml⁻¹) was infused via the venous cannula at a rate sufficient to maintain constant plasma levels [29] for 20 min. Arterial blood samples were taken at 2, 10 and 18 min to confirm steady circulating plasma levels of ¹⁴C mannitol and to measure PCO_2, PO_2 and pH using a pH blood-gas analyser (Ciba Corning, Essex, UK). The jugular veins were cut at 20 min and the vasculature washed out with saline, and the animal killed by decapitation. The eyes were enucleated and the retina and vitreous removed as previously described [28], weighed, and solubilized in Soluene-350 (Canberra Packard, Berks, UK). The blood samples were centrifuged and two 50-μl samples of plasma taken from each and solubilized. Hionic-Fluor scintillant (Canberra Packard) was added to the dissolved tissue and the β-emissions counted using a Tri-Carb liquid scintillation analyser (Canberra Packard).

Retinal permeability was then expressed as the ratio:

$$\frac{\text{Radioactivity/g tissue } (R_t)}{\text{Meanradioactivity/ml blood plasma } (R_p)}$$

All statistics were calculated using the Mann-Whitney U-test. A P value of < 0.05 was considered significant.

BRB permeability studies were carried out on animals following intravitreal injections of 1×10^4 U TNF-α at 1, 2, 3 and 4 days PI ($n = 16$) and 2×10^4 U TNF-α at 4 h and 1, 2, 3, 5, 7, 9 and 14 days PI ($n = 71$). BRB integrity was also determined following intravitreal injection of 1×10^3 U IL-6 at 4 h and at 1, 2 and 3 days PI ($n = 16$). In addition the permeability of vehicle-injected control eyes was determined at 4 h and at 1 and 2 days PI ($n = 14$). As a positive control, to demonstrate the sensitivity of this technique within the retina, hyperosmolar arabinose (1.8 M) or a similar volume of saline was infused into the internal carotid artery over 20 s via a cannula inserted retrogradely into the external carotid ($n = 8$). The 20-min mannitol infusion was started immediately after the hyperosmolar injection followed by the removal of both the retina and cerebral cortex.

The large-molecular-weight tracer horseradish peroxidase (HRP, type II, Sigma) was used as a visual tracer to detect the path of BRB breakdown at 5 and 7 days PI following intraocular injection of 2×10^4 U TNF-α ($n = 4$). Animals were anaesthetized with sodium pentobarbitone (60 mg · kg⁻¹ IP) and HRP (50 mg in 200 μl saline) was infused via a cannulated femoral vein. After 15 min the animals were perfused with half-strength Karnovsky's fixative (pH 7.4) as described above. The eyes were enucleated and placed in fixative at 4°C overnight and processed for light and electron microscopy as previously described [20].
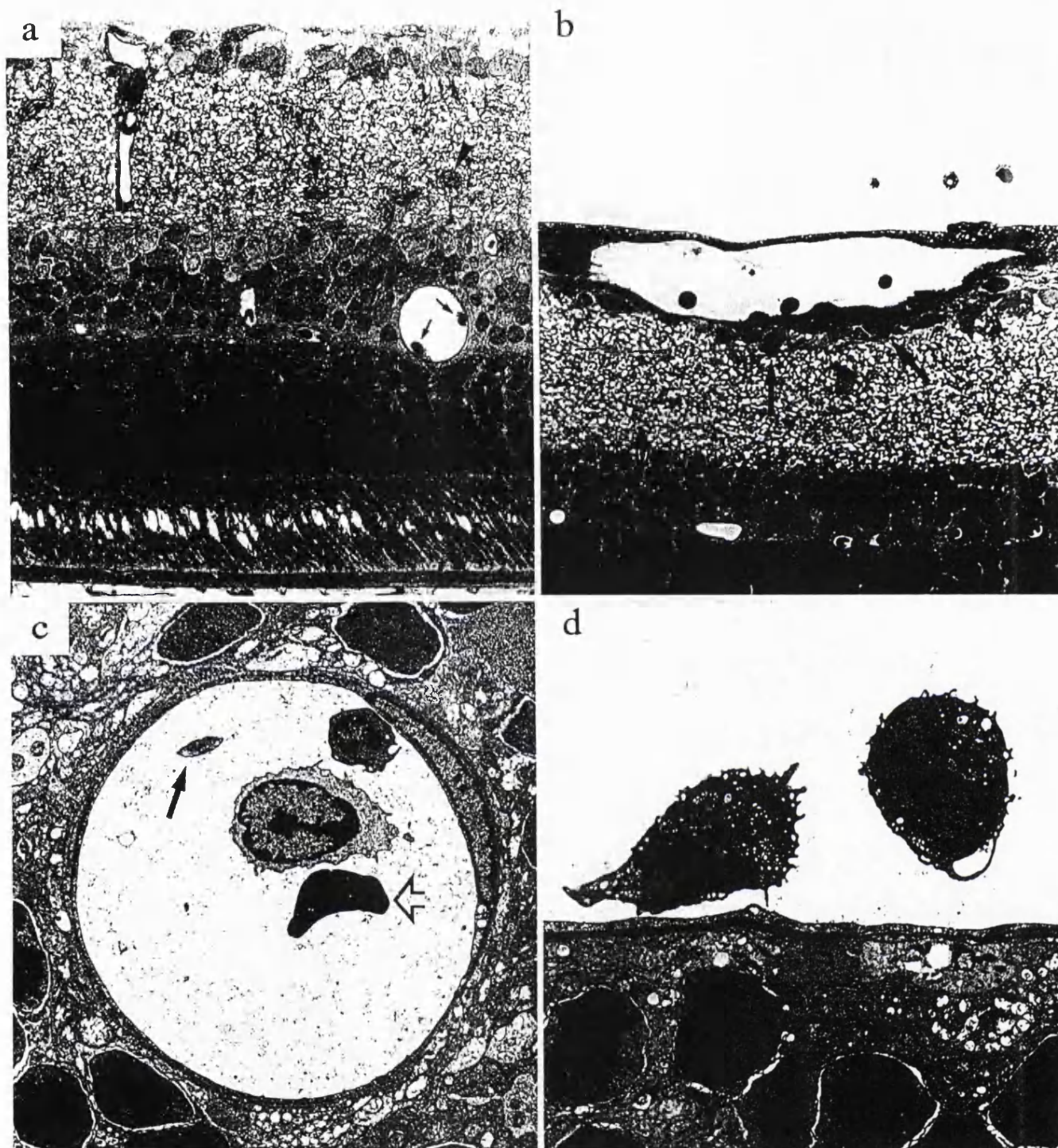
Fig. 1a–d Light and electron micrographs of retina from tumour necrosis factor-α (TNF-α)-injected eyes. **a** Toluidine blue-stained resin section of retina at 24 h post-injection (PI) from a TNF-α (2 × 10⁴ U) injected animal showing two mononuclear (MN) leucocytes (*arrows*) adhering to the luminal wall of a blood vessel in the outer plexiform/inner nuclear layer. Note dark cells present in inner plexiform layer (*arrowheads*). × 430. **b** Toluidine blue-stained resin section of retina at day 5 PI from TNF-α (1 × 10⁴ U) injected animal with MN leucocytes present within the lumen and adhering to the wall of a large blood vessel in the inner plexiform layer, in the neuroretinal parenchyma (*arrows*), and also in the vitreous (*open arrow*). × 460. **c** Transmission electron micrograph of retina from TNF-α (2 × 10⁴ U) injected eye at 4 h PI. Blood vessel from the outer plexiform/inner nuclear layer with two MN leucocytes and a platelet (*arrow*) within the lumen. A red blood cell is also present (*open arrow*). × 3,000. **d** Transmission electron micrograph of retina from TNF-α (2 × 10⁴ U) injected eye at 24 h PI. Two MN leucocytes are seen adhering or in close proximity to the endothelial cell wall of a large blood vessel in the outer plexiform layer. × 4800

Results

Histology

At 4 h after the intravitreal injection of vehicle alone a few mononuclear (MN) leucocytes were seen within the lumen of retinal blood vessels but in numbers no greater than seen following a sham injection at this time point. No inflammatory cells were observed in the retina or vitreous by 24 h PI.
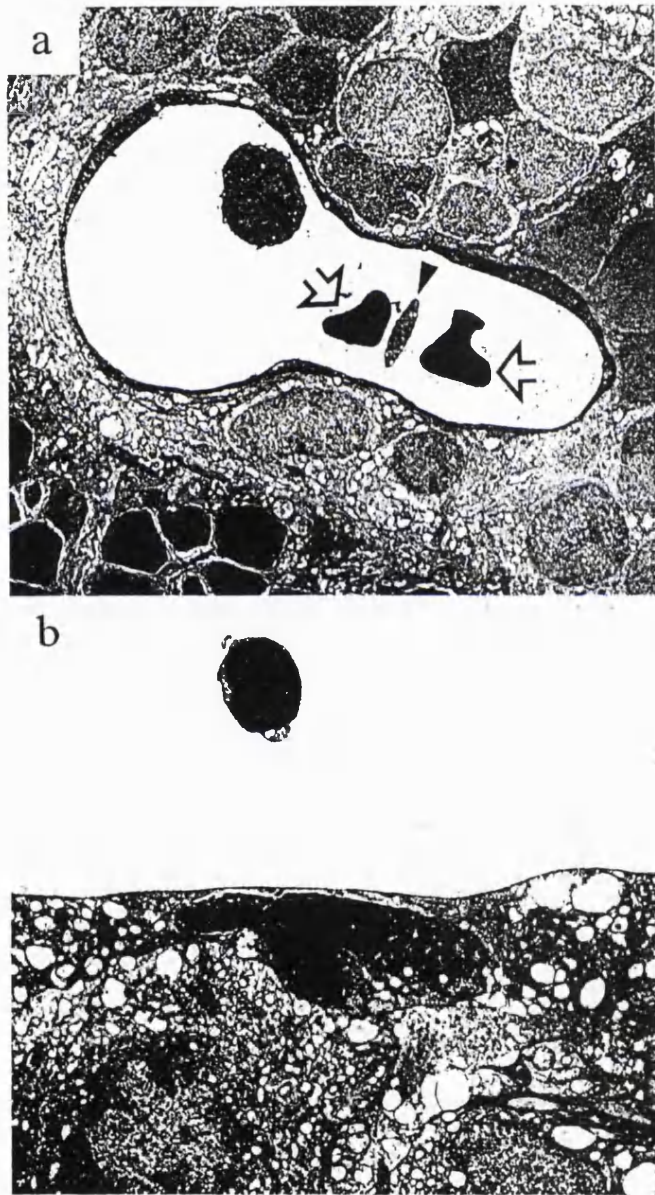

Fig. 2a,b Transmission electron micrographs of retina from interleukin-6 (IL-6; 2×10^3 U) injected eyes. a Retinal vessel from an IL-6-injected eye 4 h PI. MN leucocyte and a platelet (*arrowhead*), between two red blood cells (*open arrows*) within the lumen of a blood vessel from the inner nuclear layer. × 2,000. b Interface between the retina and vitreous 4 h PI with PMN cell in the neuroretinal parenchyma lying beneath the inner limiting membrane. A MN cell, which is possibly a small lymphocyte, can be seen in the vitreous. × 2,750

Following the intravitreal injection of 4×10^3 U of TNF-α no inflammatory cells were seen at 24 h PI. However, after the intravitreal injection of either 1×10^4 U or 2×10^4 U TNF-α, a few inflammatory cells could be detected within the lumen of blood vessels of the neuroretina and in the vitreous from 4 h to 5 days PI which disappeared by day 7 PI (Fig. 1a–d). Inflammatory cells were also occasionally observed within the tissue parenchyma with no apparent difference between the two doses. In all cases the observed inflammatory cells were of MN appearance. The retinal endothelial cells and tissue morphology remained largely normal except for occasional darkened cells appearing in the inner plexiform layer that at electron microscopic level did not appear to be leucocytic. A mild MN infiltrate of similar proportions was also found in the ciliary body in the injected eyes.

In IL-6-treated animals (1×10^3 U intravitreally) a few MN cells could be seen adhering to the endothelium of retinal vessels by 4 h PI. The cellular inflammatory response did not change over the subsequent 3 days, with only the occasional leucocyte appearing predominantly in the vitreous. However, following a dose of 2×10^3 U IL-6 a larger quantity of MN as well as polymorphonuclear (PMN) leucocytes were observed at 24 h PI within the lumen of retinal vessels, the parenchyma and vitreous (Fig. 2a,b). No cells were observed in the process of migrating through the retinal vessel wall.

Immunohistochemistry

An increased expression of MHC class II was seen in each retina of the TNF-α (2×10^4 U) injected eyes (Fig. 3a) particularly just beneath the inner limiting membrane in the ganglion cell and inner plexiform layers. Positive staining was also observed in the choroid, which lies outside the neuroretina, and was thought to represent tissue resident cells. ED1-positive cells (macrophages, monocytes and dendritic cells) were also seen in the retina and choroid of the injected eyes in the same number and location as the MHC class II-positive cells (Fig. 3b). The staining for ED2-positive cells (macrophages) revealed only occasional cells throughout the retina. Very rarely a CD8 (OX-8)-positive cell was seen in the neuroretina and choroid but no positive staining for CD4 (W3/25) cells, CD18 (WT3) or granulocytes (MOM/3F12/F2) was observed. In the retina and vitreous of the contralateral noninjected eye, the occasional ED1- or ED2-positive cell was seen, but there was no induction of MHC class II expression or staining for CD18. The choroid of the contralateral eye, however, did stain positively for class II and ED1.

BRB permeability

In all animals studied the blood gas and pH values remained within the normal range. No significant increase in BRB permeability, as determined by an increased R_t/R_p,
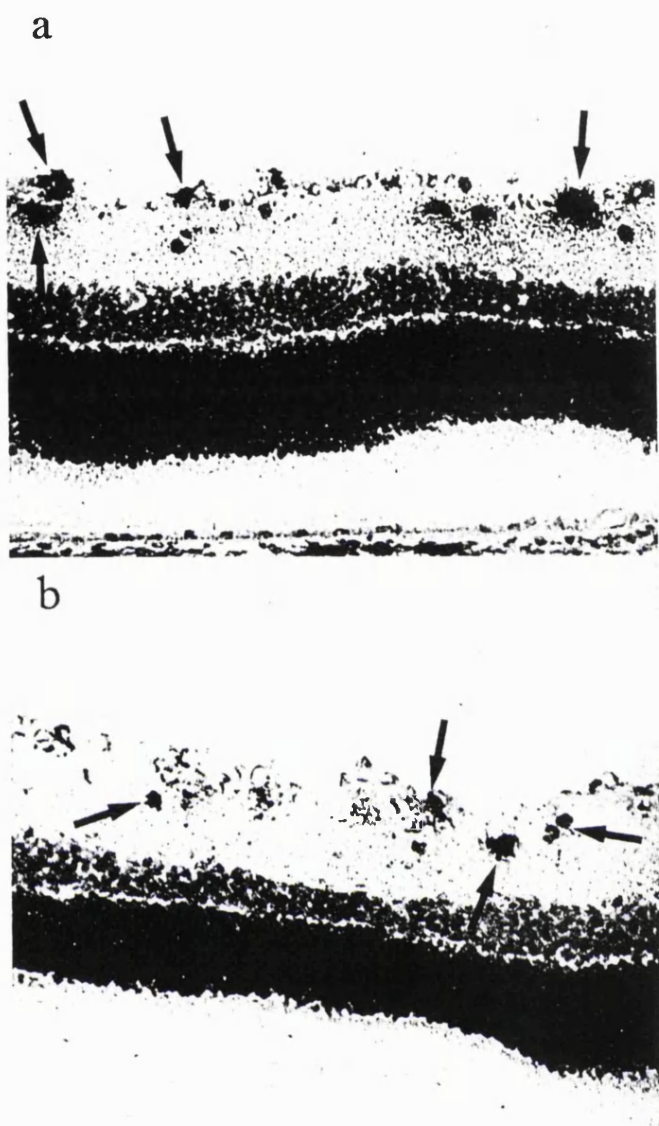
a

b

Fig. 3a,b Immunohistochemistry on frozen sections of retina at 2 days post-intravitreal TNF-α (2 × 10⁴ U). **a** Positive staining (*arrows*) for MHC class II within anterior portion of retina predominantly within the ganglion cell/inner plexiform layer and in the choroid. × 210. **b** Positive staining (*arrows*) for ED1 (macrophages, monocytes and dendritic cells) predominantly within the ganglion cell/inner plexiform layer. × 120
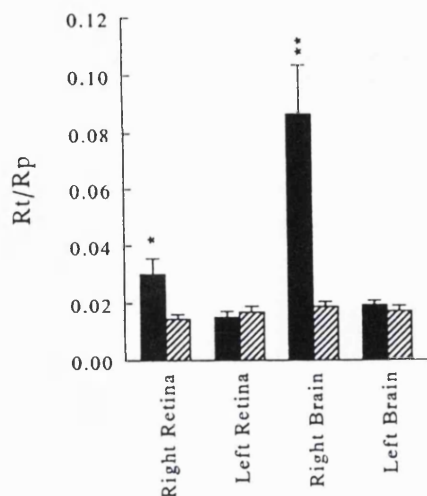

Fig. 4 Permeability of the blood-retinal barrier (BRB) and blood-brain barrier (BBB) to mannitol following the infusion of 1.8 M arabinose via the right carotid artery. A significant increase in BRB and BBB permeability, as expressed by an increased R_t/R_p ratio, was detected in the right, but not left, retina and cerebral cortex (*solid bars*). No significant increase in barrier permeability was seen following the infusion of saline administered via the same route (*hatched bars*). *$P < 0.05$, **$P < 0.001$
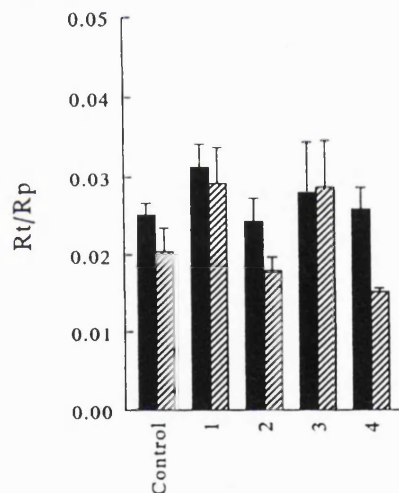

Fig. 5 Permeability of the BRB to mannitol following intravitreal injection of 1 × 10⁴ U of TNF-α. No significant increase in permeability of the barrier as expressed by an increase in the R_t/R_p ratio was seen in the retina (*solid bars*) or vitreous (*hatched bars*)

ratio, was detected following a control intravitreal injection of vehicle alone. Immediately after an intra-carotid infusion of 1.8 M arabinose there was a significant increase in the permeability of the BRB ($P < 0.05$) and the blood-brain barrier ($P < 0.001$) compared to control infusions of saline via the same route (Fig. 4).

Following the intravitreal injection of 1 × 10⁴ U TNF-α, no significant opening of the BRB was detected over a 4-day period (Fig. 5). However, by increasing the dose to 2 × 10⁴ U a significant increase in BRB permeability was detected from 1 to 5 days PI ($P < 0.01$; Fig. 6a). Furthermore, there was also an increase in ¹⁴C mannitol extrava-

sation into the vitreous from 4 h to 5 days PI ($P < 0.05$; Fig. 6b). By day 7 PI the values for both the retina and the vitreous had returned to control values and remained unaltered up to day 14 PI. Although there was a significant increase in BRB permeability to mannitol following an injection of 2 × 10⁴ U of TNF-α, no leakage of HRP was detected in the retina of the injected eyes 5 or 7 days PI although HRP reaction product was observed in the ciliary body.

When comparing the permeability of the BRB of the injected eyes with those of the contralateral non-injected eyes, it was discovered that in the high dose (2 × 10⁴ U)

Fig. 6a,b Permeability of the BRB to mannitol following intravitreal injection of 2×10^4 U of TNF-α. A monophasic increase in barrier permeability was observed, as shown by an increase in the R_t/R_p ratio, in the retina (a) and the vitreous (b) when compared to vehicle control. A significant increase in barrier permeability was also detected in the non-injected contralateral eyes. The R_t/R_p ratios from contralateral eyes increased from day 1 to 5 PI in the retina (c) and from 4 h to day 9 PI in the vitreous (d). *$P < 0.05$, **$P < 0.01$, ***$P < 0.001$
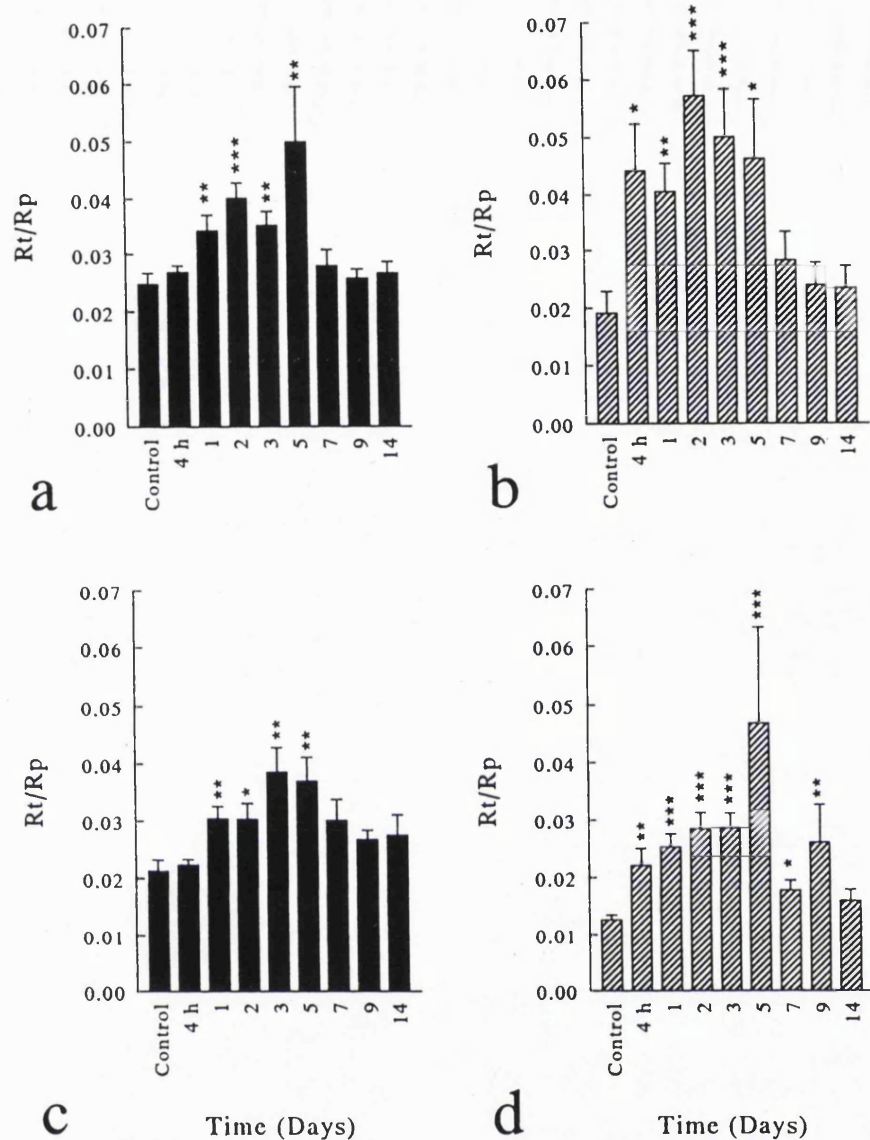
TNF-α-treated animals there was disruption of the contralateral BRB. The R_t/R_p values were significantly increased in the retina of the non-injected eyes from days 1 to 5 PI of the test eye ($P < 0.05$) before returning to control values at day 7 PI (Fig. 6c). The vitreous samples of the contralateral eyes also gave a significantly higher ^{14}C mannitol R_t/R_p ratio at time points corresponding to a PI time in the ipsilateral eye of 4 h to 9 days ($P < 0.05$; Fig. 6d).

The intravitreal administration of the cytokine IL-6 at a concentration of 1×10^3 U had no significant effect on BRB permeability to the small tracer ^{14}C mannitol from 4 h to 3 days PI (Fig. 7).

___

Discussion

The intravitreal injection of TNF-α in the Lewis rat causes a monophasic increase in BRB permeability ac-companied by a small but persistent infiltration of MN cells. This is in contrast to the effects seen in a previous study where a distinct biphasic opening of the BRB was seen following an intravitreal injection of IL-1β [2]. The initial increase in permeability following IL-1β injection was found to occur at 4 h PI and coincided with the appearance of both PMN and MN leucocytes adhering to the blood vessel endothelium. The permeability then declined but was accompanied by an increase in leucocyte infiltration. A second larger, and more prolonged, increase in BRB permeability occurred at 1–2 days PI and coincided with peak inflammatory cell infiltration. Unlike IL-1β studies, therefore, where leucocytes were seen in large numbers throughout the neuroretina, ciliary body and vitreous, the TNF-α-injected eyes only exhibited a small-scale MN infiltrate.

The mechanism by which TNF-α causes BRB breakdown is not clear. It is possible that TNF-α is acting directly upon the cells that form the BRB causing disruption
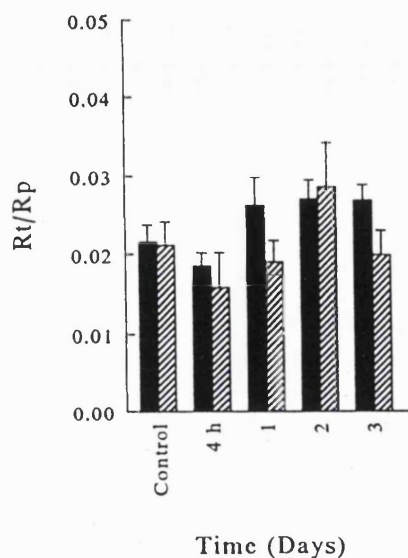
Fig. 7 Permeability of the BRB to mannitol following intravitreal injection of 1 × 10³ U of IL-6 into the right vitreous. No significant increase in mannitol extravasation was detected in the retina (*solid bars*) or vitreous (*hatched bars*) of the injected eyes

of the tight junctions, but this would seem unlikely as the effect is so prolonged. Alternatively, this cytokine may be acting on immunoresponsive tissue-resident cells such as the so-called perivascular cells and microglia. These cells, once activated, may release other vasoactive compounds leading to disruption of the BRB. A recent study has described the presence of CD18-positive cells in the rabbit retina following IL-1β injection that was thought to represent perivascular macrophages [11]. In an attempt to determine whether tissue-resident cells were being activated following TNF-α injection, we immuno-stained frozen sections of retina for various markers including MHC class II and the macrophage, monocyte, dendritic cell marker ED1. The results from these investigations demonstrated that there was a significant increase in the expression of both MHC class II- and ED1-positive cells, whereas the macrophage marker, ED2, only stained occasional cells. This suggests that a significant proportion of the MHC class II/ED1-positive cells are activated tissue-resident cells. Indeed, the observation that most of the cells lay in the ganglion cell/inner plexiform layers, just below the inner limiting membrane, where the inner plexus of retinal vessels lie, is also consistent with this area being an interface with the vitreous through which infectious agent may enter the retina. The presence of high concentrations of MHC class II-reactive cells has also been reported in other areas of the CNS where there exists the possibility of entry of infectious agents, such as the subarachnoid space and pial surface [4].

A further possible cause of BRB disruption is the induction of a MN cell infiltrate which followed a similar time-course to the duration of barrier opening. However, as the number of infiltrating cells was very small and as a similar number of leucocytes were observed following the injection of the lower dose of TNF-α, where no BRB disruption was detected, it is unlikely that this is the cause of barrier dysfunction.

Of particular interest was the observation that following an intravitreal injection of 2 × 10⁴ U of TNF-α there was a significant and prolonged disruption of the BRB in the contralateral non-injected eye. This leakage of the BRB, which did not occur with intraocular IL-1β administration [2], nor with the lower dose of TNF-α investigated, followed a similar time-course to that of the injected eye. Disruption of the contralateral blood-ocular barriers and cellular infiltration has also been reported following the intravitreal injection of IL-6 [21] and lipopolysaccharide, a method used to induce inflammation in the anterior chamber [17]. In these studies, however, the left eye served as an injected control and was therefore subject to a degree of trauma which may have resulted in the observed increase in leakage of protein into the aqueous humour [21], but was shown not to be responsible for the influx of cells [17]. In a further study, where IL-1 or IL-8 was injected into the rat eye, the contralateral non-injected eye yielded a cellular inflammatory response [14] although there was no indication of whether barrier disruption also occurred.

The mechanism responsible for the opening of the contralateral BRB is not clear but may be due to a variety of possible factors. It is most unlikely, however, that this is due to leakage of TNF-α from the vitreous into the systemic circulation as dilution in the blood would reduce the concentration delivered to the contralateral vasculature by several orders of magnitude. An alternative explanation may result from the observation that TNF-α injected into the vitreous of the mouse can induce morphological changes in the optic nerve [9] and cause both an increase in axonal transport of protein and demyelination of optic nerve fibres [24]. Whether this optic nerve damage can lead to perturbations of the contralateral retina, however, remains highly speculative. Indeed, we were unable to detect any structural damage or inflammatory reaction, as determined by increased expression of MHC class II or CD18 in the non-injected eye. A further possible explanation may be that TNF-α is acting centrally, involving the brain stem nuclei which may provoke dilatation of the contralateral ocular vasculature. It is well recognized that vasodilatation is associated with increased vascular leakage which may explain the observed disruption of the BRB. Whether this occurs is currently under investigation but the involvement of a reflex arc has previously been discussed as a likely mechanism [8, 17, 32]. At present, however, the exact cause of this effect remains unresolved.

Although 2 × 10⁴ U of TNF-α induced a significant and prolonged extravasation of mannitol, the large-molecular-weight tracer HRP was excluded from entering the neuroretina at 5 days PI. This would suggest that the size of the pores formed through the BRB by the action of TNF-α is small enough to allow the passage of mannitol but not HRP [27]. An alternative explanation may be that only isolated areas of the BRB are disrupted and that these were not the areas sampled for electron microscopy. This

explanation, however, is unlikely as no HRP reaction product was observed macroscopically in the retina during processing or in the semi-thin sections used for light microscopy. The HRP reaction product observed in the ciliary body of both the injected and non-injected eyes was expected as the vasculature in this region is leaky but the further spread of HRP was restricted by the tight junctions of the ciliary body non-pigmented epithelium.

Our results are consistent with a number of previous studies where TNF has been injected into the eye. The inflammatory consequences of intraocular TNF have been described as both mild and inconsistent [33] especially when compared with the effects of intraocular administration of either IL-1 [10, 30] or LPS [17]. In addition, this minimal inflammatory response to TNF-α in vivo has been reported in the skin of rabbits where an intradermal injection resulted in either a mild PMN infiltrate [35] or had no effect at all [36]. Intravitreal TNF has also been reported to have other effects upon the rabbit retina, apart from inflammation, such as inducing an increase in visual evoked potentials [5] and a transient increase in endothelial cell pinocytotic activity in the capillary bed [6]. However, some studies have shown a substantial inflammatory response to TNF but have employed very high concentrations of cytokine in doses ranging from 1,000 ng [16] to 10,000 ng [25], compared to the doses of 5.5 and 11 ng used in our study.

Following the intravitreal administration of IL-6 we were unable to detect any disruption to the BRB despite a small-scale leucocytic infiltration. Previous studies, however, have reported a more pronounced inflammatory response to intravitreal IL-6 [21, 22] accompanied by breakdown of the blood-aqueous barrier. This discrepancy may result from differences in the source of IL-6 as these studies employed human recombinant IL-6 injected into rat eyes. The lack of disruption to the BRB in our study despite the small-scale infiltration of MN and PMN cells would indicate that this level of infiltration, which was similar in scale to that induced by TNF-α, is not sufficient to elicit a detectable alteration in barrier integrity.

In this study we have shown that the intravitreal administration of TNF-α causes a monophasic and prolonged opening of the BRB in both the injected eye and the contralateral control eye. This disruption is not associated with a large-scale leucocyte infiltration as has previously been observed following the injection of IL-1β. In contrast, injection of the cytokine IL-6 into the vitreous had no detectable effect on the integrity of the BRB despite inducing a mild cellular infiltration.

References

1. Abbott NJ (1992) Comparitive physiology of the blood-brain barrier. In: Bradbury MWB (ed) Physiology and pharmacology of the blood-brain barrier. Handbook of experimental pharmacology, 103. Springer, New York Berlin Heidelberg, pp 371–396

2. Bamforth SD, Greenwood J, Lightman SL (1994) The effect of interleukin-1 on blood-retinal barrier permeability in the anaesthetized rat. J Physiol (Lond) 480:19–20P

3. Brett J, Gerlach H, Nawroth P, Steinberg S, Godman G, Stern D (1989) Tumour necrosis factor/cachectin increases permeability of endothelial cell monolayers by a mechanism involving regulatory G proteins. J Exp Med 169:1977–1991

4. Broadwell RD, Baker BJ, Hickey WF (in press) CNS transplants and the host immune response: the blood-brain barrier and immunological privilege within the mammalian brain. In: Greenwood J, Begley D, Segal M, Lightman S (eds) New concepts of a blood-brain barrier. Plenum Press, London

5. Brosnan CF, Litwak MS, Schroeder CE, Selmaj K, Raine CS, Arezzo JC (1989) Preliminary studies of cytokine-induced functional effects on the visual pathways in the rabbit. J Neuroimmunol 25:227–239

6. Brosnan CF, Claudio L, Tansey FA, Martiney J (1990) Mechanisms of autoimmune neuropathies. Ann Neurol 27:S75–S79

7. Burke-Gaffney A, Keenan AK (1993) Modulation of human endothelial cell permeability by combinations of the cytokines interleukin-1α/β, tumor necrosis factor-α and interferon-γ. Immunopharmacology 25:1–9

8. Butler JM, Unger WG, Hammond BR (1979) Sensory mediation of the ocular response to neutral formaldehyde. Exp Eye Res 28:577–589

9. Butt AM, Jenkins HG (1994) Morphological changes in oligodendrocytes in the intact mouse optic nerve following intravitreal injection of tumour necrosis factor. J Neuroimmunol 51:27–33

10. Claudio L, Martiney JA, Brosnan CF (1994) Ultrastructural studies of the blood-retina barrier after exposure to interleukin-1β or tumor necrosis factor-α. Lab Invest 70:850–861

11. Cuff C, Berman JW, Brosnan CF (1994) Perivascular cells of the rabbit retina are disrupted by IL-1-induced inflammation. J Neuroimmunol 154

12. De Boer JH, Haren MAC van, Vries-Knoppert WAEJ de, Baarsma GS, Jong PVTM de, Postema FJ, Rademakers AJJM, Kijlstra A (1992) Analysis of IL-6 levels in human vitreous fluid obtained from uveitis patients, patients with proliferative intraocular disorders and eye bank eyes. Curr Eye Res 11:181–186

13. De Vos AF, Klaren VNA, Kijlstra A (1994) Expression of multiple cytokines and IL-1RA in the uvea and retina during endotoxin-induced uveitis. Invest Ophthalmol Vis Sci 35:3873–3883

14. Ferrick MR, Thurau SR, Oppenheim MH, Herbort CP, Ni M, Zachariae CO, Matsushima K, Chan C (1991) Ocular inflammation stimulated by intravitreal interleukin-8 and interleukin-1. Invest Ophthalmol Vis Sci 32:1534–1539

15. Fleisher LN, Ferrell JB, McGahan MC (1990) Ocular inflammatory effects of intravitreally injected tumour necrosis factor-alpha and endotoxin. Inflammation 14:325–335

16. Fleisher LN, Ferrell JB, Smith MG, McGahan MC (1991) Lipid mediators of tumour necrosis factor-induced uveitis. Invest Ophthalmol Vis Sci 32:2393–2399

17. Forrester JV, Worgul BV, Merriam GR Jr (1980) Endotoxin-induced uveitis in the rat. Albrecht von Graefes Arch Clin Ophthalmol 213:221–233

18. Franks WA, Limb GA, Stanford MR, Ogilvie J, Wolstencroft RA, Chignell AH, Dumonde DC (1992) Cytokines in human intraocular inflammation. Curr Eye Res 11:187–191

19. Greenwood J (1992) Experimental manipulation of the blood-brain and blood-retinal barriers. In: Bradbury MWB (ed) Physiology and pharmacology of the blood-brain barrier. Handbook of experimental pharmacology, 103. Springer, New York Berlin Heidelberg, pp 460–486

20. Greenwood J, Howes R, Lightman S (1994) The blood-retinal barrier in experimental autoimmune uveoretinitis: leukocyte interactions and functional damage. Lab Invest 70:39–52

21. Hoekzema R, Murray PI, Haren MAC van, Helle M, Kijlstra A (1991) Analysis of interleukin-6 in endotoxin-induced uveitis. Invest Ophthalmol Vis Sci 32:88–95

22. Hoekzema R, Verhagen C, Haren M van, Kijlstra A (1992) Endotoxin-induced uveitis in the rat. The significance of intraocular interleukin-6. Invest Ophthalmol Vis Sci 33:532–539

23. Hooks JJ, Chan CC, Detrick B (1988) Identification of the lymphokines, interferon-gamma and interleukin-2, in inflammatory eye disease. Invest Ophthalmol Vis Sci 29:1444–1451

24. Jenkins HG, Ikeda H (1992) Tumour necrosis factor causes an increase in axonal transport of protein and demyelination in the mouse optic nerve. J Neurol Sci 99:104

25. Kulkarni PS, Srinivasan BD (1988) Cachectin: a novel polypeptide induces uveitis in the rabbit eye. Exp Eye Res 46: 631–633

26. Lightman S (1991) Vascular changes in the posterior segment in clinical and experimental ocular inflammatory disease. Eye 5:432–437

27. Lightman S, Greenwood J (1992) Effect of lymphocytic infiltration on the blood-retinal barrier in experimental autoimmune uveoretinitis. Clin Exp Immunol 88:473–477

28. Lightman SL, Palestine AG, Rapoport SI, Rechthand E (1987) Quantitative assessment of the permeability of the rat blood-retinal barrier to small water-soluble non-electrolytes. J Physiol (Lond) 389:483–490

29. Luthert PJ, Greenwood J, Lantos PL, Pratt OE (1986) The effect of dexamethasone on vascular permeability of experimental brain tumours. Acta Neuropathol (Berl) 69:288–294

30. Martiney JA, Berman JW, Brosnan CF (1992) Chronic inflammatory effects of interleukin-1 on the blood-retina barrier. J Neuroimmunol 41:167–176

31. Maruo N, Morita I, Shirao M, Murota S (1992) Il-6 increases endothelial permeability in vitro. Endocrinology 131:710–714

32. Perkins ES (1957) Influence of the fifth cranial nerve on the intra-ocular pressure of the rabbit eye. Br J Ophthalmol 41:257–300

33. Rosenbaum JT, Howes Jr, Rubin RM, Samples JR (1988) Ocular inflammatory effects of intravitreally-injected tumour necrosis factor. Am J Pathol 133:47–53

34. Samples JR, Boney RS, Rosenbaum JT (1993) Ocular inflammatory effects of intravitreally injected interleukin-2. Curr Eye Res 12:649–654

35. Wankowicz Z, Megyeri P, Issekutz A (1988) Synergy between tumour necrosis factor and interleukin-1 in the induction of polymorphonuclear leucocyte migration during inflammation. J Leukoc Biol 43:349–356

36. Watson ML, Lewis GP, Westwick J (1989) Increased vascular permeability and polymorphonuclear leucocyte accumulation in vivo in response to recombinant cytokines and supernatant from cultures of human synovial cells treated with interleukin 1. Br J Exp Pathol 70:93–101

37. Whitcup SM, Chan C, Li Q, Nussemblatt RB (1992) Expression of cell adhesion molecules in posterior uveitis. Arch Ophthalmol 110:662–666

38. Yoshida M, Yoshimura N, Hangai M, Tanihara H, Honda Y (1994) Interleukin-1α, interleukin-1β, and tumor necrosis factor gene expression in endotoxin-induced uveitis. Invest Ophthalmol Vis Sci 35:1107–1113